COMPARISON OF TRANSPORT EFFECTS OF PERFLUORINATED AND HYDROCARBON SURFACTANTS ON ENVIRONMENTAL CO-CONTAMINANTS

By

Rashad Najee Simmons

A DISSERTATION

Submitted to
Michigan State University
in partial fulfillment of the requirements
for the degree of

DOCTOR OF PHILOSOPHY

Chemistry – Environmental Toxicology

2011

ABSTRACT

COMPARISON OF TRANSPORT EFFECTS OF PERFLUORINATED AND HYDROCARBON SURFACTANTS ON ENVIRONMENTAL CO-CONTAMINANTS

By

Rashad Najee Simmons

The use of groundwater as drinking water justifies efforts for the prevention and remediation of groundwater contamination by environmental pollutants. The inclusion of hydrocarbon surfactants (HCSs), at high concentrations, in a groundwater system has been used for groundwater remediation, and is known to increase the transport of environmental pollutants. While much information is known about HCS, little to no information is available for the perfluorinated surfactants (PFSs). The overall objective of this research was to determine the transport effects of PFSs on known environmental contaminants, in comparison to the transport effects of HCSs. Polycyclic aromatic hydrocarbons, halogenated benzene compounds, and the BTEX series of compounds (benzene, toluene, ethylbenzene, and *p*-xylene) were used as representatives of important classes of hydrophobic neutral environmental pollutants. A series of aromatic amines was used as representatives of cationic environmental pollutants. Reversed-phase liquid chromatography (RPLC) was used to model the groundwater system.

Above their critical micelle concentration (CMC), surfactants form micelles that can act as partitioning mediums for hydrophobic neutral pollutants, increasing their transport. In the first study, the transport effects of HCSs and PFSs, above their CMC (> 20 mM), were compared in the RPLC system for representative neutral environmental pollutants. Transport effects were elucidated from retention factors, k, and the

equilibrium constant per micelle of the model pollutants. The resulting data suggest that the presence of HCSs and PFSs, above the CMC, increases the transport of co-contaminants in a groundwater system. However, PFSs (18 to 103 % increase) exhibit a lesser transport effect than HCSs (32 to 247 % increase).

Previous literature suggests that surfactants below their CMC have a negligible effect on the transport of hydrophobic neutral pollutants, while undergoing ion-pair formation with ionic pollutants and decreasing their transport. In the second and third studies, the transport effects of HCSs and PFSs, below their CMC (< 6 mM), were compared in the RPLC system. Transport effects were elucidated from retention factors, k, and selectivity factors, α, of the model pollutants. The resulting data suggest the presence of HCSs statistically decreases transport of neutral pollutants (4 to 13 %), while the presence of PFSs statistically increases their transport (5 to 16 %). Further results show that transport of cationic aromatic amines decreases with increasing concentration of both anionic HCSs and PFSs in RPLC system, with PFSs (99 to 100 % decrease) exhibiting a greater transport effect than HCSs (96 to 100 % decrease).

Due to the differences in chemical and physical properties, PFSs exhibit different transport effects in comparison to HCSs under the same conditions. The inclusion of anionic PFSs in a groundwater system will increase the transport of neutral environmental pollutants, while decreasing the transport of cationic pollutants. An unintentional release of PFSs can lead to an increase in groundwater contamination by neutral pollutants. However, the judicious use of PFSs can be used for remediation of cationic pollutants in groundwater.

To my family, immediate and extended, near and far, living and departed,

for your support and love through this process.

ACKNOWLEDGMENTS

"Intelligence plus character – that is the true goal of education. The complete education gives one not only power of concentration, but worthy objectives upon which to concentrate."

– Dr. Martin Luther King Jr.

At this time, I would like to thank all those that helped and contributed my overall education, and to the completion of this dissertation and the research contained within. First and foremost, I would like to thank God the Creator for giving me divine courage to pursue graduate school, strength to endure the tough road that it is, and wisdom to take advantage of the opportunities it has afforded me. I would like to thank my wife, Sheena Simmons, enduring this process with me, and strengthening me with her ever present faith. I would like to thank my family and friends for their many prayers, words of encouragement, and overall show of love towards me through this process.

To my advisor Dr. Victoria McGuffin, I would like to thank you for all of your guidance throughout these many years. Thank you for your always honest discussions with me, your patience, and your support. You have helped me to become a better researcher, while also allowing me to develop into the educator that I am today. I will take your words with me in life, wherever that may lead me.

To my esteemed committee members (Drs. Baker, Bruening, and Voice), I would like to thank you for all of the input (both scientific and general) you have given me over these many years. I have tried to soak up your knowledge, and follow your example of

how a good scientist should conduct oneself. In addition, thank you for all of your encouragement to finish this dissertation process; it was greatly appreciated.

I would like to thank the following individuals for their contributions to this research. Dr. Michael E. Mackay and Leslie Passeno, formerly of Michigan State University (MSU), for the use of their equipment and help with the densitometry measurements. Dr. James Jackson, MSU, for his discussions on the interactions of cationic amines. Dr. Kathy Severin, MSU, for the use of a UV detector during the duration of these studies. The East Asia and Pacific Summer Institutes and the National Institute of Advanced Industrial Science and Technology in Tsukuba, Japan for the opportunity to conduct research and gain experience in an international setting. The King, Chavez, Parks Future Faculty Fellowship (KCP-FFF), the Graduate School at MSU, and the Center for Water Science at MSU for funding to conduct the research.

Lastly, I would like to thank the Department of Chemistry and the Charles Drew Science Scholars Program for giving me the opportunity to increase my intelligence and character, through the education of MSU students.

TABLE OF CONTENTS

LIST OF TABLES

LIST OF FIGURES

CHAPTER 1: INTRODUCTION AND BACKGROUND

1.1 Introduction

One of the greatest resource of humanity is fresh drinking water. The human race's continuous survival is dependent on a recurrent source of clean and unpolluted drinkable water. It is estimated that 25 % of all freshwater used in the U.S. is groundwater, and that more than 40 % of the U.S. population utilizes groundwater as a source of drinking water [1]. The protection of all freshwater sources, such as lakes, rivers, groundwater aquifers, etc., from possible contamination is therefore of the utmost importance. Contamination of drinking water can take place via direct point sources (e.g. waste from industrial plants or treatment facilities) or nonpoint sources, such as rainwater runoff or leaching of organic pollutants from underground gasoline tanks [2]. The majority of research is focused on the detection, sources, and fates of persistent organic pollutants in the environment. The persistent organic pollutants of interest consist of aromatic hydrocarbons, halogenated compounds, and pesticides. However, little research is reported on the transport effects of organic compounds on afore mentioned environmental pollutants. Of the research that has been conducted, the main focus has been dedicated to the transport effects of hydrocarbon surfactants on selected organic pollutants, which has been reported in the literature [3-6]. For various reasons, the transport effects of other organic compounds, such as perfluorinated surfactants, are not readily researched, even though the use of perfluorinated surfactants grew from the 1950s to about 2000. However, due to their resistance to degradation perfluorinated surfactants were initially believed to be safe and non-toxic; thus little to no research was reported. The use of groundwater as drinking water justifies efforts for the prevention and/or

remediation of groundwater contamination by environmental pollutants. Thus the effects of perfluorinated surfactants on the transport of persistent organic pollutants, in a groundwater system, needs to be investigated. Chapter 1 seeks to give background information on surfactants, the transport of pollutants in the environment, and several classes of co-pollutants of environmental importance.

1.2 Surfactants

Surfactants are organic compounds consisting of at least one lyophilic (solvent-loving) and lyophobic (solvent-fearing) group [7]. Since the most commonly used solvent is water, the two groups are referred to as hydrophilic (i.e. the polar head group) and hydrophobic (i.e. the nonpolar tail group), respectively. As such, all further discussion of surfactants will be in terms of aqueous solutions. Surfactants are most known for the ability to exhibit surface activity and to form self-assembled aggregates (e.g. micelles, vesicles, bilayers, etc.) in liquids and aqueous solutions. The term surface activity refers to the ability of a surfactant to reduce the surface or interfacial excess free energy within a system [7]. The excess free energy per unit area (units of J m^{-2} or ergs cm^{-2}), which is equivalent to force per unit length (units of mN m^{-1} or dyne cm^{-1}), is referred to as the surface tension (γ) when the boundary is the air/liquid interface, and is referred to as the interfacial tension when the boundary is the liquid/liquid or liquid/solid interface. The addition of a surfactant can reduce the surface tension of water from 72 mN m^{-1} down to around 30 mN m^{-1} for hydrocarbon surfactants [8] and as low as 15 mN m^{-1} for fluorocarbon surfactants at 25 °C [9].

There are four main classes of surfactants, which are distinguished via the hydrophilic head group: anionic, cationic, nonionic, and zwitterionic (amphoteric).

Anionic surfactants contain a head group that has a negative charge when ionized in aqueous solutions. Common anionic head groups include sulfates ($-OSO_3^-$), sulfonates ($-SO_3^-$), carboxylates ($-COO^-$), and phosphates ($-OP(OR)_2O^-$). Cationic surfactants contain a head group that has a positive charge when ionized in aqueous solutions. Common cationic head groups include primary ($-N^+H_3$), secondary ($-N^+(R)H_2$), tertiary ($-N^+(R)_2H$), and quaternary ($-N^+(R)_3$) amines. Nonionic surfactants do not produce ions in aqueous solutions, but rather contain polar functional groups such as alcohols, amides, polyglucosides and glucamides, organosilicones, and ethoxylates. The most common nonionic head groups include alkyl alcohol ethoxylates ($-(OC_2H_4)_XOH$) or alkylphenol ethoxylates ($-C_6H_4(OC_2H_4)_XOH$). A zwitterionic surfactant has both a cationic portion and an anionic portion at the same time. The most common zwitterionic head groups usually include an amine and a carboxylate group ($-N^+(R)_2CH_2COO^-$). Anionic surfactants represent the most utilized and studied class of surfactants. As of 2000, in the United States and Canada, the most utilized surfactants were anionic (59 %), followed by nonionic (24 %), cationic (10 %), and zwitterionic (7 %) [10]. As such, all further discussion of surfactants will be in terms of anionic surfactants.

To a lesser extent, a surfactant can be classified based on the hydrophobic tail group. The hydrophobic tail group can either be a hydrocarbon chain, a fluorocarbon chain, a hydrocarbon/fluorocarbon chain mix, or silicone chains [11]. The majority of surfactants utilized in commercial and industrial applications have a hydrocarbon hydrophobic tail group [12]. As such, hydrocarbon surfactants are also the most studied form of surfactants. Over the years, there has been an emergence in the use of surfactants

with a fluorocarbon tail group in applications with conditions that preclude the use of hydrocarbon surfactants. Both hydrocarbon and fluorocarbon surfactants are discussed in further detail in the following sections.

1.2.1 Hydrocarbon Surfactants

Hydrocarbon surfactants (HCSs) are surfactants in which the hydrophobic tail group consists of alkyl groups, typically of chain lengths between $C_4 - C_{18}$. The hydrophobic tail groups of HCSs are also lipophilic, making them soluble in oils, organic, non-aqueous, or hydrocarbon liquids/phases. Common hydrophobic tail groups include alkylbenzene chains, saturated and unsaturated linear alkyl chains, and branched alkyl chains. Both the length and linearity of the hydrophobic tail group affect several properties of surfactants. As the length of the hydrophobic tail group increases, the solubility of HCSs decreases in water, while increasing in organic solvents. In addition, an increase in the hydrophobic tail chain length leads to an increase in the tendency of HCSs to adsorb at an interface/surface or to form aggregates (e.g. micelles). Also, it causes closer packing of HCSs at the surface and increases the sensitivity of ionic HCSs to precipitate from water due to counterions [10]. Branching in the hydrophobic tail group decreases toxicity and increases water solubility, while reducing both adsorption to surfaces and biodegradability. HCSs have a greater affinity for hydrocarbon/water interfaces in comparison to air/water interfaces [13]. This greater affinity is due to the more highly favorable interactions of the hydrocarbon chain with the hydrocarbon phase.

In aqueous systems, surfactant monomers (free or unassociated surfactant molecules) move towards surfaces and interfaces. Surfactants undergo various

interactions, within an aqueous system, with respect to changes in the total concentration of the surfactant. These interactions are represented in Figure 1.1.

At extremely low concentrations of surfactants (Region A), surfactant monomers will adsorb on a surface. There is little to no interaction between the adsorbed surfactant monomers within this region. As the concentration of the surfactant increases (Regions B and C), surfactant monomers begin to pack closer together at the surface and form a monolayer or bilayer depending on the type of surface. Surfactant monomers will continue to be adsorbed at the surface until surface saturation is reached. The change in slope between Regions B and C is due to the decrease in adsorption sites on the surface. As the concentration of surfactant increases (Region D), the excess surfactant monomers (in solution) can self-assemble into aggregates called micelles [14].

The surfactant interactions of Regions B – D will be examined in greater detail. In Regions B and C, the hydrophilic head group is oriented towards the polar phase (i.e. water) and the hydrophobic tail group is oriented towards the nonpolar phase (e.g. air or a surface). If the surface is a hydrophobic surface, then the surfactant monomer will adsorb tail down and form a monolayer; or the monomer will partition into the surface. If the surface is hydrophilic (i.e. charged as in soil) and has the same charge as the surfactant head group, then the surfactant monomer will adsorb tail down and form a monolayer. If the surface has the opposite charge as the surfactant head group, then the surfactant monomer will adsorb head down and form a hemimicelle/admicelle layer. A hemimicelle layer is a surfactant monolayer where the surfactant head group is adsorbed onto the surface (via electrostatic interactions), with the tail group oriented upward.

Figure 1.1

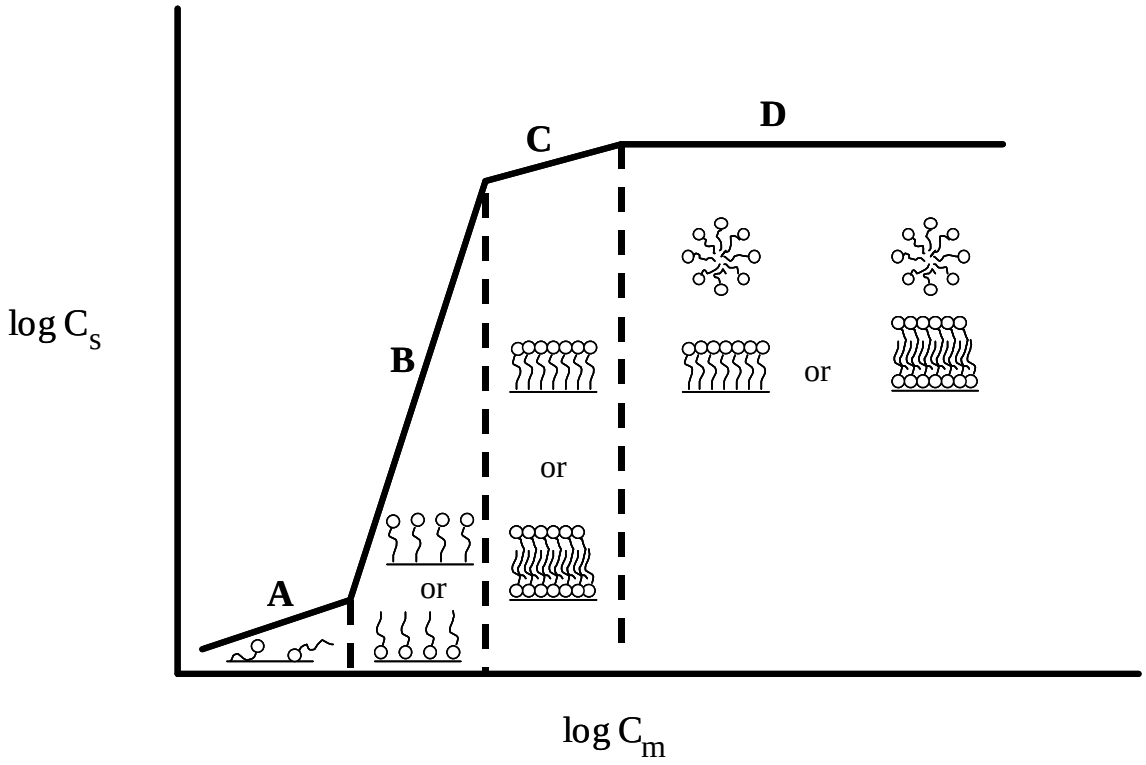

Figure 1.1: Graph of logarithmic concentration of surfactant in a mobile phase (C_m) versus the logarithmic concentration of surfactant adsorbed on a stationary phase (C_s). Region A: Very low surfactant concentration below the CMC. Regions B and C: Surfactant concentration below the CMC. Region D: Surfactant concentration above the CMC.

As the surfactant concentration increases, additional surfactant monomers adsorb (tail down) to the hemimicelle layer forming an admicelle (e.g. bilayer). A hemimicelle layer results in the surface becoming more hydrophobic, while an admicelle layer results in the surface gaining an overall opposite charge. In Region D, the excess surfactant monomers will typically aggregate into spherical shaped micelles in an aqueous system, with the hydrophilic head group in contact with water and the hydrophobic tail group forming the core of the micelle. The core of the micelle provides an environment for other hydrophobic species in an aqueous system. The concentration (or narrow concentration range) where the extensive aggregation of the surfactant monomers into micelles takes place is called the critical micelle concentration (CMC). If the concentration of the surfactant is significantly increased beyond this point, liquid crystal phases can begin to form (e.g. hexagonal or lamellar phases).

1.2.2 Fluorocarbon Surfactants

Fluorocarbon surfactants are surfactants in which hydrogen atoms of the tail group have been partially or completely replaced by fluorine atoms. The majority of commercially available fluorocarbon surfactants are based on a linear tail group ($-(CF_2)_nF$), where the value of n ranges from 4 – 13, but averages 8 [9]. Typical fluorocarbon surfactants are perfluorinated or may contain a few methylene groups, e.g. fluorotelomers or zonyl alcohol ($C_8F_{17}CH_2CH_2OH$). Perfluorinated surfactants (PFSs) are surfactants in which all of the hydrogen atoms on the hydrocarbon tail group have been substituted by fluorine atoms, e.g. perfluorooctanoic acid ($C_8F_{17}COOH$). PFSs are commercially prepared via two main processes: electrochemical fluorination or telomerization [9,15,16]. The electrochemical fluorination process was invented over 50

years ago by Joseph Simons and commercialized by the 3M Company [16]. The electrochemical fluorination process produces both odd- and even-numbered fluorocarbon chain surfactants, distributed in a 70:30 % ratio between linear and branched surfactants, respectively [17,18]. The telomerization process was commercially developed by the DuPont Company, and predominantly produces even-numbered, linear fluorocarbon chain surfactants (greater than 90 %) [19,20].

Partially fluorinated surfactants have greater solubility in conventional hydrocarbon solvents than perfluorinated surfactants, as well as lower toxicity by being more biodegradable [21]. Research has been conducted that studied the properties of PFSs [22-24], including electrical properties [25], phase structures [26], physicochemical properties [27], and properties such as Krafft points, CMCs, and surface tension [28]. In addition, the physiochemical properties of HCSs and PFSs have been compared [29]. In this study, Blanco *et al*. concluded that PFSs with a chain length 1.5 times shorter than the analogous HCSs would have similar CMCs and thermodynamic properties. In aqueous solutions, fluorocarbon surfactants typically behave similarly to hydrocarbon surfactants. PFSs form the same type of micelles and micellar phases as their hydrocarbon analogues [30,31], with the micelles retaining a globular shape even at high concentrations [32]. However, there are a few exceptions due to differences in physical and chemical properties. These differences in properties are often advantageously used in applications where conditions might be too harsh for HCSs, such as hydraulic fluids in aircraft, aqueous fire fighting foams, and electroplating baths [9,33].

The substitution of fluorine atoms onto the tail group makes PFSs more hydrophobic than HCSs in aqueous solutions [13]. In addition, the tail groups of PFSs

are also lipophobic (oil-fearing) [34], thus having a greater tendency to leave a water or water-oil environment and form a separate microphase. The tail groups of fluorocarbon surfactants are more rigid than HCSs [35]. As such, fluorocarbon surfactants tend to gather more at the air/water interface than HCSs. The substitution of fluorine atoms increases the surface activity, allowing fluorocarbon surfactants to greatly reduce the surface tension of water in comparison to analogous HCSs. Due to the higher average bond energy of the C-F bond (485 kJ mol^{-1}) compared to the C-H bond (413 kJ mol^{-1}), fluorocarbon surfactants are considered to be more thermally and chemically stable in the environment [36]. Fluorocarbon surfactants are stable to heat, acids and bases, and reducing and oxidizing agents [18,37]. Fluorocarbon surfactants typically have a much larger pH usage range than analogous HCSs, being tolerant to exposure to low pH (i.e. 1 – 2) [7]. There are several disadvantages of fluorinated surfactants. Fluorocarbon surfactants are more resistant to degradation, have a greater potential for bioaccumulation [38], and are more bioaccessible to humans and animals in the environment than HCSs. In addition, fluorinated surfactants are 2 – 3 orders of magnitude more expensive than HCSs for the same amount.

Since the year 2000, the numbers of peer-reviewed publications related to perfluorinated substances have dramatically increased [17]. A literature search of the phrases “perfluorinated surfactants” and “perfluorinated compounds” illustrates this increase (Figure 1.2). The search of “perfluorinated compounds” is a more total search, as the results include literature on PFSs as well.

Figure 1.2: Graph of number of publications versus the year of publication based on a literature search of the phrases: (■) perfluorinated compounds and (■) perfluorinated surfactants.

Figure 1.2

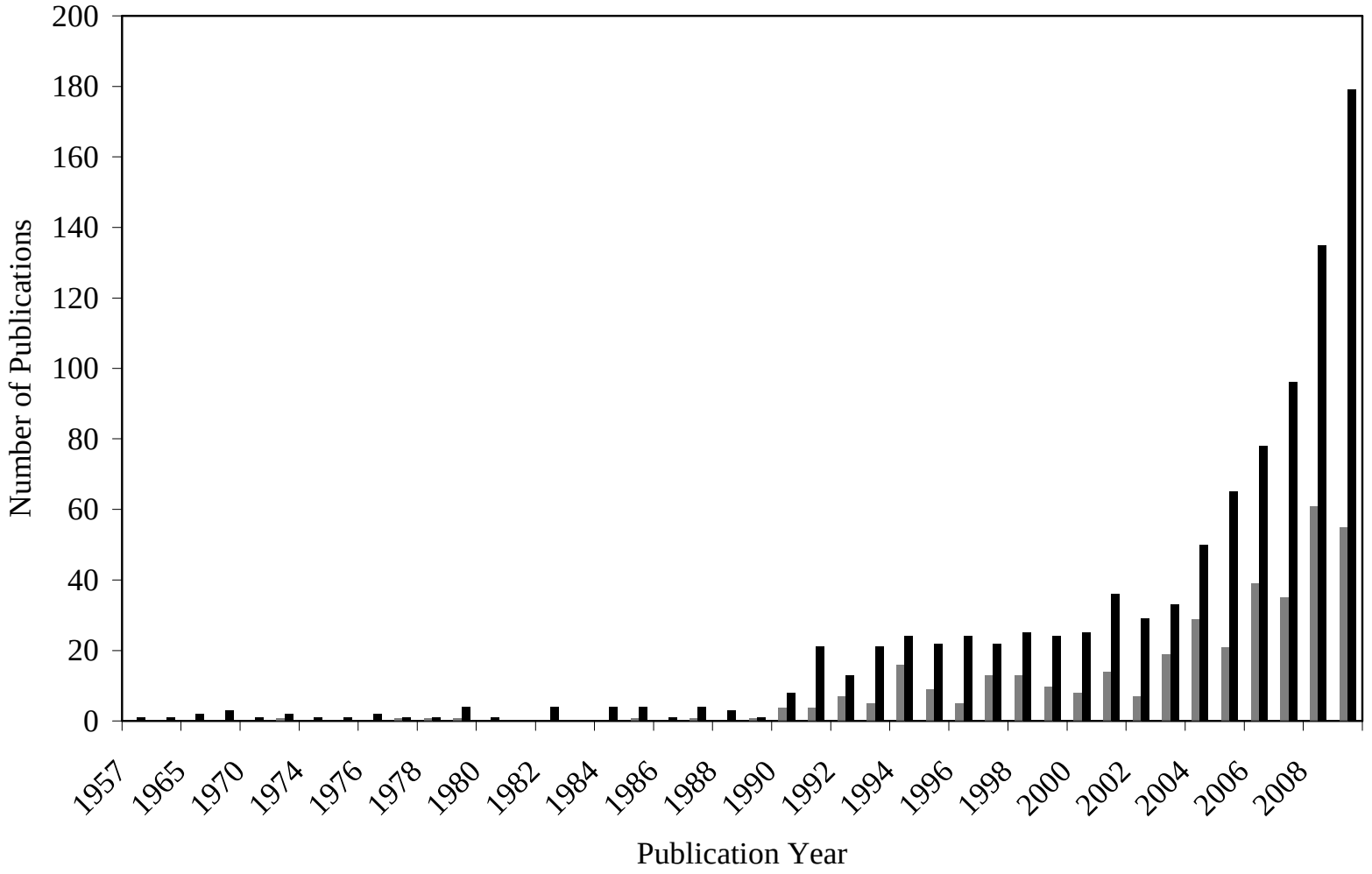
200
180
160
140
120
100
80
60
40
20
0
Number of Publications
1957
1965
1970
1974
1976
1978
1980
1982
1984
1986
1988
1990
1992
1994
1996
1998
2000
2002
2004
2006
2008
Publication Year

The main research areas in current literature consist of 1) detection of PFSs in environmental matrices, 2) toxicological effects of PFSs in humans and animals, and 3) sources and fates of PFSs in the environment.

PFSs have been detected using techniques such as nuclear magnetic resonance [39], fast atom bombardment/mass spectrometry [40], liquid chromatography with mass spectrometry or tandem mass spectrometry [37,41-45], quadrupole/time of flight mass spectrometry [46], gas chromatography [47-50], gas chromatography with electron impact mass spectrometry [51], and gas chromatography with chemical ionization mass spectrometry [52,53]. PFSs have also been detected within a wide variety of environmental matrices, with perfluorooctane sulfonate (PFOS) and perfluorooctanoic acid (PFOA) as the main two detected PFSs. These environmental matrices include house dust (PFOS 201 ng g^{-1}, PFOA 148 ng g^{-1}) [51], surface and subsurface water in China [54], surface and drinking water (PFOA in drinking water 519 ng L^{-1}, PFOA in surface water 33900 ng L^{-1}, PFOS in surface water 3160 ng L^{-1}) [55], groundwater [49,56,57], biota [58,59], and effluent from wastewater treatment plants [60,61]. Studies were conducted on the adsorption of PFOS onto sand and clay surfaces [62], as well as adsorption on sediments [63]. In the area of toxicological effects on humans and animals, studies have been conducted into the general toxicity of PFSs [64], toxicity of PFOS and PFOA in aquatic life (PFOS, LC_{50} = 45.2 μg L^{-1} for midges) [65], toxicity in rats [66], and in a zooplanktonic community [67]. The third area of interest has been the study of the sources and fates of PFSs in the environment. These include studies identifying the transport of PFSs via their volatile precursors [68,69].

1.3 Environmental Pollutant Transport

There are a variety of ways that organic pollutants can be transported through the environment depending on their chemical and physical properties. The transport of organic pollutants can take place in or between the atmosphere, water, and soil. Atmospheric transport of pollutants can consist of deposition of pollutant particulates and gases, precipitation (i.e. in rain or snow) of pollutant gases and aerosols, and adsorption of pollutants on particulate matter (i.e. dust, soot, etc.) with subsequent deposition. Water transport of pollutants can consist of volatilization from the water, sorption on sediment or suspended particulates, and uptake or release by biota. Soil transport of pollutants can consist of volatilization from soil or vegetation, uptake or release by biota or vegetation, adsorption of pollutants onto soil particulates and transport via runoff, and leaching into groundwater [70]. Volatile organic pollutants most readily undergo atmospheric transport, while transport via water or soil plays a larger role for semi-volatile, persistent organic pollutants. Since PFSs are nonvolatile persistent organic pollutants, an understanding of their transport in water and soil matrices is of utmost importance; however atmospheric transport may not be neglected.

Atmospheric transport of volatile precursors of PFSs has been studied as a means of environmental transport [68]. In the long range transport of PFSs to remote environments (e.g. polar icecaps), it is theorized that the volatile fluorotelomers are transported through the atmosphere and are later degraded into PFSs, such as PFOA or PFOS. As stated in Section 1.2.2, studies have been conducted that detected PFSs in various water matrices ranging from surface water to groundwater [49,54-57,60,61]. In water at low concentrations, monomers of PFSs will congregate either at the air/water

interface with the perfluorinated tail group oriented towards air, or adsorb at a water/soil surface with the perfluorinated tail group oriented towards soil. As the concentration of PFSs increases, the monomers pack closer together at the air/water or water/soil interfaces and form a monolayer. As surfactant concentration rises above the CMC, micelle formation takes place and the micelle is transported through the water. In a groundwater system, soil organic matter (SOM) is considered a key component in the accumulation of persistent organic pollutants; thus it will also play an important role in the transport process of PFSs. The transport of PFSs in groundwater can be retarded via sorption on SOM. SOM acts like micelles [71], providing a more favorable environment for hydrophobic organic pollutants than water in a groundwater system. The predominant sorption process is the partitioning of hydrophobic organic pollutants into SOM, however in soil with low carbon content, reactions with the underlying mineral surface can become important. Researchers have utilized several techniques to study the transport of organic pollutants, ranging from batch equilibration, leaching equilibration, solubility enhancement, and reversed-phase separation studies [72].

One of the most widely utilized methods for studying pollutant transport is the batch equilibration method [73-75]. In this method, a known mass of soil (or sediment) is placed in a vial with a known volume of solution that contains a known concentration of the solute (i.e. pollutant) in water. A known concentration of an electrolyte, such as sodium chloride, can be added to the solution in order to simulate the ionic strength of groundwater [76,77]. The vial is shaken over a timeframe long enough to reach equilibrium, then the vial is centrifuged, with the resulting phases separated and analyzed to determine the concentration of solute. The mass of solute sorbed per unit mass of soil

(or sediment) can be determined through the difference between the initial concentration of the solute and the final concentration of the solute after equilibrium was reached. This technique has been utilized to determine the sorption of selected organic compounds [78-82]. While this method has advantages, there are several disadvantages. A disadvantage is the loss of the pollutant through volatilization or degradation through reaction with the soil, leading to incorrect concentration values. The phases can have incomplete separation, leading to difficulties in concentration analysis. Most importantly, the length of time for the batch study might be insufficient for the system to reach equilibrium.

Another technique is the leaching equilibration method, or column method. In this method, a solution containing a known concentration of the solute (i.e. pollutant) dissolved in water is pumped through a column containing a sorbent (e.g. soil) at a known flow rate. The effluent is collected and analyzed for the concentration of the solute. Collection stops when the concentrations at the column inlet and outlet are equal, and equilibrium has been reached. This technique has been used to determine the sorption of organic compounds [77,83]. Disadvantages of this method can include poor packing of the sorbent in the column and length of time necessary to reach equilibrium. The sorption coefficients determined via batch and column methods have been correlated with octanol/water partition coefficients (K_{OW}) [84,85] and water solubility (S_W) [85,86]. In the study by Vowles and Mantoura, there was good correlation between the logarithmic sediment or soil-water partition coefficient (K_P) and the logarithmic K_{OW} ($R^2 = 0.961$) and the logarithmic S_W ($R^2 = 0.955$) for 14 hydrocarbons. In addition, the correlation increased upon examining a homologous series of hydrocarbons. The correlation between log K_P and log K_{OW} was $R^2 = 0.998$ and $R^2 = 0.996$ for a

homologous series of polycyclic aromatic hydrocarbon and alkylbenzenes, respectively. The correlation between log K_P and log S_W was $R^2 = 0.994$ for a homologous series of alkylbenzenes.

Reversed-phase separation via liquid chromatography has also been utilized to study the sorption constants and transport of organic compounds. The theory of reversed-phase liquid chromatography (RPLC) is analogous to the concept of partitioning in sorption [84,87]. In RPLC, the mobile phase represents a polar phase, while the stationary phase represents a non-polar phase. Typically, the polar mobile phase is either a pure solvent (e.g. methanol or water) or a solution (i.e. methanol/water mixture). The stationary phase typically consists of a totally porous octadecylsilica material. As non-polar organic compounds (i.e. pollutants) travel through a RPLC column, they partition between the mobile and stationary phases and are retained on the non-polar phase. The retention times of the compounds are used to calculate retention factors. The retention factors from RPLC studies for selected organic compounds have been correlated with sorption coefficients and, by extension, with environmental transport of the compounds [72,85,88,89]. In the study by Vowles and Mantoura, there is excellent correlation between log K_P and the logarithmic retention factors on octadecylsilane phase (log k'_{ODS}) for a homologous series of polycyclic aromatic hydrocarbons ($R^2 = 0.998$) and a homologous series of alkylbenzenes ($R^2 = 0.996$).

1.4 Environmental Pollutants

Environmental pollutants can be separated into several major types, each consisting of several subclasses of relevant chemicals and pollutants. Some of the major types of environmental pollutants include air, water, and soil contaminants [90]. These

types of pollution can arise from point sources (e.g. industrial plants and waste treatment facilities) and nonpoint sources (e.g. runoff and atmospheric deposition) [2]. The chemical properties, amount (i.e. concentration), and environmental persistence of a contaminant impact how it is classified as an environmental pollutant. Based on these criteria, organic compounds are types of environmental pollutants whose study is of utmost importance. The U.S. Environmental Protection Agency (EPA) currently regulates a list of 126 priority pollutants [91], which contains such environmental organic pollutants as polycyclic aromatic hydrocarbons (PAHs), polychlorinated biphenyls (PCBs), substituted benzene compounds, chlorinated organic compounds, and pesticides. Some of these organic pollutants have been listed as either *known to be human carcinogens* or *reasonably anticipated to be a human carcinogen* [92]. Persistent organic pollutants consist of a diverse group of organic compounds that are toxic, persistent, bioaccumulate, and prone to long-range transport [93]. Examples of persistent organic pollutants of concern include PAHs, polyhalogenated biphenyls (i.e. PCBs and polybrominated biphenyls), substituted benzene compounds (e.g. anilines or the BTEX compounds of toluene, ethylbenzene, and xylene), polyhalogenated dibenzodioxins and dibenzofurans (i.e. dioxins and furans, respectively), and organochlorine pesticides. New and emerging persistent organic pollutants include perfluorinated octyl sulfonamides and sulfonates. Some of these pollutants are produced as by-products during processes involving related organic compounds. For example, polybrominated dibenzodioxins and dibenzofurans can be produced during the pyrolysis [94] or recycling [95] of plastics coated with brominated flame retardants (such as polybrominated biphenyls) [96]. Due to the toxicity of some of the persistent organic pollutants, the use of model solutes is

preferred in this research described in Chapters 3 – 6. The backbone structure of a majority of the organic pollutants is based on substituted benzene compounds and PAHs; thus benzene, substituted benzene compounds, and PAHs make good model solutes. A brief discussion of these solutes is given in the following sections (Sections 1.4.1 and 1.4.2).

1.4.1 Substituted Benzene Compounds

Substituted benzene compounds are organic compounds in which hydrogen atoms on the benzene ring have been partially or completely replaced by a substituent atom or group. Typically, the substituent atom is a halogen atom (e.g. fluorine, chlorine, or bromine). Common organic pollutant substituent groups include hydroxyl (–OH), methyl ($–CH_3$), ethyl ($–C_2H_5$), amine ($–NH_2$), or nitro ($–NO_2$) groups. Replacing hydrogen atoms on the benzene ring with substituents can change various chemical and physical properties. In terms of halogen substituents, increasing the number of halogen atoms increases toxicity, octanol-water partition coefficients, soil sorption coefficients, and decreases water solubility [97]. In addition, the type of halogen substituent affects toxicity, such that brominated compounds are less toxic than chlorinated compounds [98]. In comparing halogen substituents to alkyl groups (i.e. methyl and ethyl), the compounds with the alkyl groups are slightly less toxic than those with the halogen substituents [99]. Increasing the number of alkyl substituents increases the hydrophobic characteristics (i.e. increased octanol-water partition coefficients, decreased water solubility, etc.). However, increasing the number of amine substituents increases the hydrophilic characteristics (i.e. decreased octanol-water partition coefficients, increased water solubility, etc.). The change in characteristics will lead to different interactions

within a groundwater system (both in the presence and absence of surfactants). Thus the use of these types of compounds as model analytes is justified. The compounds used as model analytes in Chapters 3 – 6 consisted of benzene, biphenyl, and various mono- and perhalogenated benzene compounds. The structures are shown in Figures 1.3 and 1.4.

1.4.2 Polycyclic Aromatic Hydrocarbons

Polycyclic aromatic hydrocarbons (PAHs) are a subclass of organic compounds, which contain two, or more, fused aromatic rings. PAHs can be distinguished from one another by the number of atoms in their member rings, ring number, and annelation structure. PAHs can consist of four-, five-, six-, or seven-member rings. PAHs containing only six-member rings, which are classified as alternant PAHs, are the most common and most studied PAHs in the environment. Ring number is used to identify the number of fused rings contained within a PAH. As the ring number increases, PAHs exhibit an increase in hydrophobic characteristics (e.g. decreased volatility, decreased water solubility, etc.) [97]. The term annelation structure refers to the degree of fusion between the rings within an individual PAH.

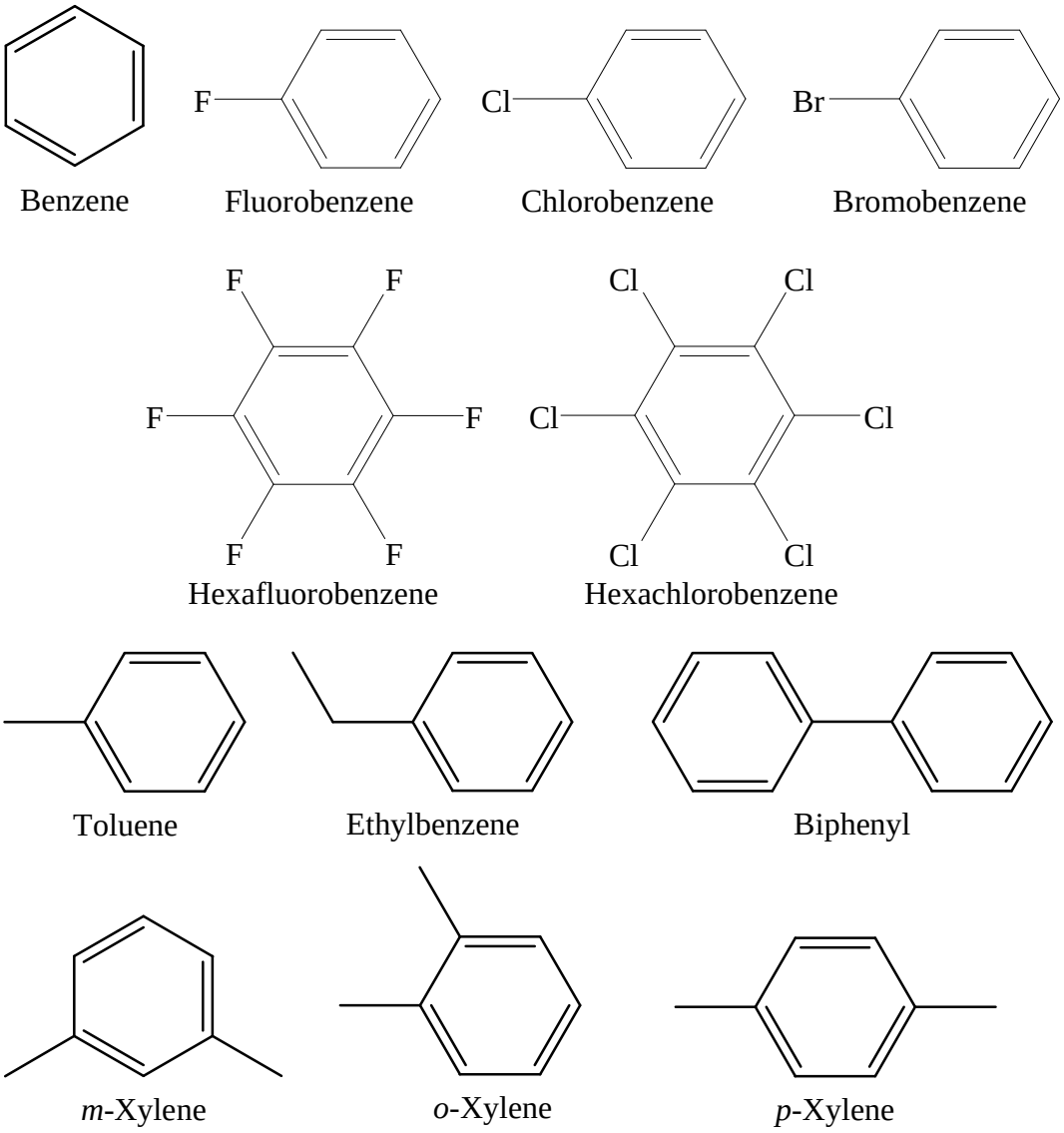

Figure 1.3: Structures of the substituted benzene compounds used as model analytes for environmental pollutants (e.g. polyhalogenated biphenyls, dioxins, and furans). The analytes are used in Chapters 3 – 4.

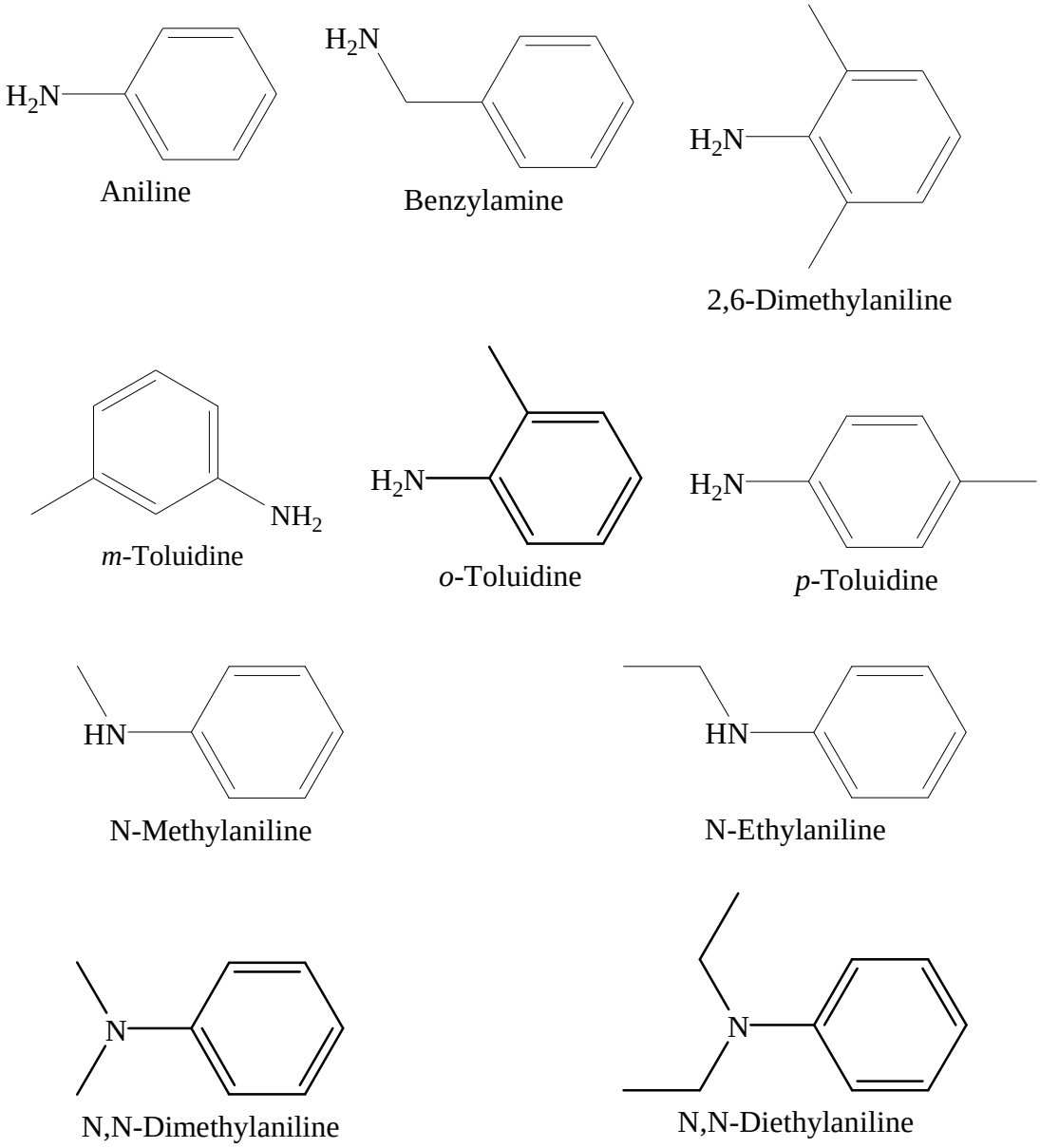

Figure 1.4: Structures of the amines used as analytes in Chapters 5 – 6.

Annelation structure can be divided into the following three categories: linearly fused, *ortho*-fused, and *peri*-fused. The *ortho*-fused (angularly-fused) PAHs are compounds in which two rings have two, and only two, atoms in common [100]. The *peri*-fused PAHs are compounds in which one ring contains two, and only two, atoms in common with each of two or more rings of a continuous series of rings [100]. The linearly fused PAHs are compounds in which all the rings are on a single axis in a continuous series. As the ring number increases for the linearly-fused PAHs, the stability decreases. This trend is not observed for the *ortho*-fused PAHs. The PAHs used as model analytes in Chapter 3 are of the alternant class, range in ring number from 2 – 4, and are of all three annelation categories. The structures of the PAHs are shown in Figure 1.5.

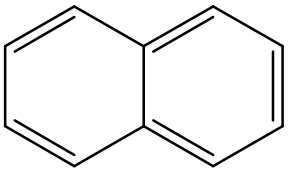

Naphthalene

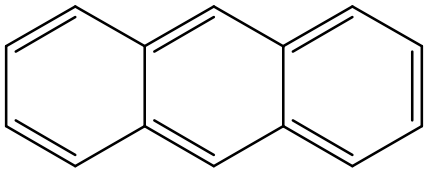

Anthracene

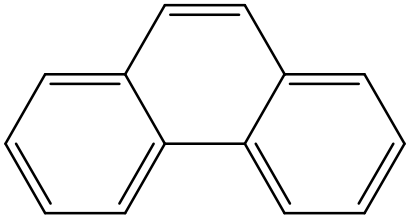

Phenanthrene

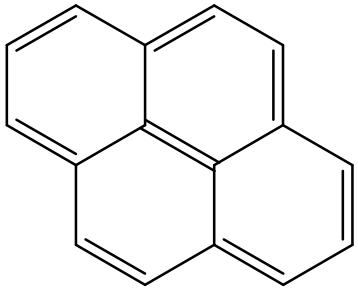

Pyrene

Figure 1.5: Structures of PAHs used as model analytes in Chapter 3.

1.5 Statement of Dissertation Objectives

It is believed that fluorocarbon surfactants behave like hydrocarbon surfactants in aqueous solutions. Like HCSs, literature has shown that PFSs can enhance the solubilization of PAHs [28,101,102]. However, fluorocarbon surfactants have been shown to solubilize fluorinated compounds better than HCSs [103]. Nevertheless, little to no research has been aimed at identifying what transport effects PFSs would have on environmental co-contaminants. As such, the overall objective of the research within this dissertation was to determine the transport effects of PFSs on known organic contaminants, in comparison to the transport effects of HCSs, in an environmental groundwater system. Several research objectives where established to be investigated; and are as follows:

- Develop a controllable analytical technique that can fundamentally resemble an environmental groundwater system, in which to study transport effects.
- Determine what transport effects the inclusion of a PFS, both above and below the CMC, in a groundwater system will have on neutral organic pollutants, and compare those effects to that of a HCS.
- Determine what transport effects the inclusion of an anionic PFS, below the CMC, in a groundwater system will have on cationic organic pollutants, and compare those effects to that of a HCS.
- Identify and quantify PFSs in environmentally relevant samples.

Chapter 2 of this dissertation addresses the first objective, and details the experimental methods and instrumentation used during the course of this research to model a groundwater system. Investigations to experimentally determine the CMC and

aggregation number of a PFS are detailed in Chapter 2, with the hopes of applying these experiments to emerging PFS. In addition, Chapter 2 details the investigation to determine the transport of surfactants within the experimental system using RPLC with refractive index detection. Chapters 3 and 4 address the second objective, and detail the research comparing the transport effects of PFSs and HCSs on neutral organic co-pollutants in a model groundwater system. Investigations are made both above (Chapter 3) and below (Chapter 4) the CMC, to compare the unknown transport effects of PFSs to the transport effects of HCSs (above and below the CMC, respectively). Chapter 5 addresses the third objective, and details the research comparing the transport effects of anionic PFSs and HCSs on cationic organic co-pollutants in a model groundwater system. Chapter 6 details the investigation of system peaks as markers of surfactant retention within the experimental system. Chapter 7 addresses the fourth objective, and details research performed at the National Institute of Advanced Industrial Science and Technology in Tsukuba, Japan, which uses a method to detect PFSs in environmental samples. Chapter 8 gives a summary of future directions within the field of study into the transport effects of PFSs.

REFERENCES

1.6 References

[1] I. Toro-Suarez, Reduced Transport of Organic Pollutants in Soil Modified with Hexadecyltrimethylammonium, Ph.D. Dissertation, Michigan State University, East Lansing, MI, 1994.

[2] U.S. Environmental Protection Agency, EPA's Polluted brochure, EPA-841-F-94-005, 1994.

[3] S.J. Grimberg, C.T. Miller, M.D. Aitken, Environ. Sci. Technol. 30 (1996) 2967-2974.

[4] J.S. Leithner, M.P. Mastumotom, Hazardous Industrial Wastes 28 (1996) 211-218.

[5] R.T. Kureja, D. Hodko, O.J. Murphy, Contam. Soils 2 (1997) 151-165.

[6] C. Madichie, G.M. Greenway, T. McCreedy, Anal. Chim. Acta 392 (1999) 39-46.

[7] R.J. Farn, Chemistry and Technology of Surfactants, Blackwell Publishing, Oxford, UK, 2006.

[8] M. Pabon, J.M. Corpart, J. Fluorine Chem. 114 (2002) 149-156.

[9] E. Kissa, Fluorinated Surfactants and Repellents, Marcel Dekker, New York, NY, 2001.

[10] M.J. Rosen, Surfactants and Interfacial Phenomena, 3rd ed., John Wiley and Sons, Inc., 2004.

[11] M.R. Porter, Handbook of Surfactants, 2nd ed., Chapman and Hall, New York, NY, 1994.

[12] M.R. Porter, Handbook of Surfactants, Chapman and Hall, New York, NY, 1991.

[13] P. Mukerjee, J. Am. Oil Chem. Soc. 59 (1982) 573-578.

[14] M.J. Schwuger, Ber. Bunsenges. Phys. Chem. 83 (1979) 1193-1205.

[15] H.C. Fielding, Organofluorine Chemicals and Their Industrial Applications, ed. R.E. Banks, Ellis Horwood, New York, NY, 1979.

[16] J.H. Simons, J. Electrochem. Soc. 95 (1949) 47-52.

[17] J.W. Martin, K. Kannan, U. Berger, P. de Voogt, J. Field, J. Franklin, J.P. Giesy, T. Harner, D.C.G. Muir, B. Scott, M. Kaiser, U. Järnberg, K.C. Jones, S.A. Mabury, H. Schroeder, M. Simcik, C. Sottani, B. van Bavel, A. Kärrman, G. Lindström, S. van Leeuwen, Environ. Sci. Technol. (2004) 248A-255A.

[18] E. Kissa, Fluorinated Surfactants: Synthesis, Properties, and Applications, Marcel Dekker, New York, NY, 1994.

[19] J. C. D'eon, S.A. Mabury, Environ. Sci. Technol. 41 (2007) 4799-4805.

[20] M.M. Schultz, D.F. Barofsky, J.A. Field, Environ. Eng. Sci. 20 (2003) 487-501.

[21] E.G. Shafrin, W.A. Zisman, J. Phys. Chem. 66 (1962) 740-748.

[22] E. Fisicaro, E. Pelizzetti, R. Bongiovanni, E. Borgarello, Colloid. Surface. 48 (1990) 259-275.

[23] R. Bongiovanni, E. Borgarello, F.M. Carlini, E. Fisicaro, E. Pellizzetti, Colloid. Surface. 48 (1990) 277-283.

[24] R. Bongiovanni, E. Borgarello, C. Carniani, C. Genova, Colloid. Surface. 54 (1991) 75-82.

[25] S. Erkoc, F. Erkoc, J. Mol. Struct. Theochem. 549 (2001) 289-293.

[26] K. Fontell, B. Lindman, J. Phys. Chem. 87 (1983) 3289-3297.

[27] K. Shinoda, M. Hato, T. Hayashi, J. Phys. Chem. 76 (1972) 909-914.

[28] H. Kunieda, K. Shinoda, J. Phys. Chem. 80 (1976) 2468-70.

[29] E. Blanco, A. González-Pérez, J.M. Ruso, R. Pedrido, G. Prieto, F. Sarmiento, J. Colloid. Interf. Sci. 288 (2005) 247-260.

[30] H. Hoffmann, J. Wurtz, J. Mol. Liq. 72 (1997) 191-230.

[31] V. Tomasic, A. Chittofratia, N. Kallay, Colloid. Surface. A 104 (1995) 95-99.

[32] R. Muzzalupo, G.A. Ranieri, C. La Mesa, Colloid. Surface. A 104 (1995) 327-336.

[33] G. Lewandowski, E. Meissner, E. Milchert, J. Hazard. Mater. 136 (2006) 385-391.

[34] P. Barthélémy, V. Tomao, J. Selb, Y. Chaudier, B. Pucci, Langmuir 18 (2002) 2557-2563.

[35] K. Matsuoka, Y. Moroi, Curr. Opin. Colloid In. 8 (2003) 227-235.

[36] E. Kissa, Fluorinated Surfactants, 2nd ed., Marcel Dekker, New York, NY, 2002.

[37] M. Villagrasa, M.L. De Alda, D. Barcelo, Anal. Bioanal. Chem. 386 (2006) 953-972.

[38] R. Renner, Environ. Sci. Technol. 36 (2002) 54A-55A.

[39] C.A. Moody, W.C. Kwan, J.W. Martin, D.C.G. Muir, S.A. Mabury, Anal. Chem. 73 (2001) 2200-2206.

[40] M.M. Schultz, D.F. Barofsky, J.A. Field, Chimia 57 (2003) 556-560.

[41] A-M. Weremiuk, S. Gerstmann, H. Frank, J. Sep. Sci. 29 (2006) 2251-2255.

[42] N. Yamashita, K. Kannan, S. Taniyasu, Y. Horii, T. Okazawa, G. Petrick, T. Gamo, Environ. Sci. Technol. 38 (2004) 5522-5528.

[43] D. Skutlarek, M. Exner, H. Faerber, Environ. Sci. Pollut. R. Int. 13 (2006) 299-307.

[44] R. Loos, J. Wollgast, T. Huber, G. Hanke, Anal. Bioanal. Chem. 387 (2007) 1469-1478.

[45] M. Murakami, K. Kuroda, N. Sato, T. Fukushi, S. Takizawa, H. Takada, Environ. Sci. Technol. 43 (2009) 3480-3486.

[46] L. Song, A.D. Wellman, H. Yao, J. Adcock, Rapid Commun. Mass Sp. 21 (2007) 1343-1351.

[47] P. Voogt, M. Sàez, Trends Anal. Chem. 25 (2006) 326-342.

[48] M. Joyce, M.J.A. Dinglasan, Y. Yun, E.A. Edwards, S.A. Mabury, Environ. Sci. Technol. 38 (2004) 2857-2864.

[49] C.A. Moody, J.A. Field, Environ. Sci. Technol. 33 (1999) 2800-2806.

[50] C.A. Moody, J.A. Field, Environ. Sci. Technol. 34 (2000) 3864-3870.

[51] M.J. Strynar, A.B. Lindstrom, Environ. Sci. Technol. 42 (2008) 3751-3756.

[52] J.W. Martin, D.C.G. Muir, C.A. Moody, D.A. Ellis, W.C. Kwan, K.R. Solomo, S.A. Mabury, Anal. Chem. 74 (2002) 584-590.

[53] R. Alzaga, J.M. Bayona, J. Chromatogr. A 1042 (2004) 155-162.

[54] X. Ju, Y. Jin, K. Sasaki, N. Saito, Environ. Sci. Technol. 42 (2008) 3538-3542.

[55] D. Skutlarek, M. Exner, H. Faerber, Environ. Sci. Pollut. Res. Int. 13 (2006) 299-307.

[56] M.M. Schultz, D.F. Barofsky, J.A. Field, Environ. Sci. Technol. 38 (2004) 1828-1835.

[57] C.A. Moody, G.N. Hebert, S.H. Strauss, J.A. Field, J. Environ. Monitor. 5 (2003) 341-345.

[58] C.A. Moody, J.W. Martin, W.C. Kwan, D.C.G. Muir, S.A. Mabury, Environ. Sci. Technol. 36 (2002) 545-551.

[59] K.S. Guruge, P.M. Manage, N. Yamanaka, S. Miyazaki, S. Taniyasu, N. Yamashita, Chemosphere 73 (2008) S210-S215.

[60] M.H. Plumlee, J. Larabee, M. Reinhard, Chemosphere 72 (2008) 1541-1547.

[61] B. Boulanger, J.D. Vargo, J.L. Schnoor, K.C. Hornbuckle, Environ. Sci. Technol. 39 (2005) 5524-5530.

[62] R.L. Johnson, A.J. Anschutz, J.M. Smolen, M.F. Simcik, R.L. Penn, J. Chem. Eng. Data 52 (2007) 1165-1170.

[63] C.P. Higgins, R.G. Luthy, Environ. Sci. Technol. 40 (2006) 7251-7256.

[64] C.M. Cooney, Environ. Sci. Technol. 42 (2008) 3486-3487.

[65] M.M. MacDonald, A.L. Warne, N.L. Stock, S.A. Mabury, K.R. Solomon, P.K. Sibley, Environ. Toxicol. Chem. 23 (2004) 2116-2123.

[66] J.L. Butenhoff, G.L. Kennedy, S.R. Frame, J.C. O'Connor, R.G. York, Toxicology 196 (2004) 95-116.

[67] H. Sanderson, T.M. Boudreau, S.A. Mabury, K.R. Solomon, Ecotox. Environ. Safe. 58 (2004) 68-76.

[68] U. Schenker, M. Scheringer, M. Macleod, J.W. Martin, I.T. Cousins, K. Hungerbühler, Environ. Sci. Technol. 42 (2008) 3710-3716.

[69] J.C. D'eon, S.A. Mabury, Environ. Sci. Technol. 41 (2007) 4799-4805.

[70] Y. Cohen, Environ. Sci. Technol. 20 (1986) 538-544.

[71] E. Heyse, D. Augustijn, P.S.C. Rao, J.J. Delfino, Crit. Rev. Env. Sci. Tec. 32 (2002) 337-397.

[72] A. D. Site, J. Phys. Chem. Ref. Data 30 (2001) 187-439.

[73] T.B. Stauffer, W.G. MacIntyre, D.C. Wickman, Environ. Toxicol. Chem. 8 (1989) 845-852.

[74] T.H. Dao, D. Bouchard, J. Mattice, T.L. Lavy, Soil Sci. 141 (1986) 26-30.

[75] N. Carmosin, L.S. Lee, Environ. Sci. Technol. 42 (2008) 6559-6565.

[76] G. Singh, W.F. Spencer, M.M. Cliath, M.T. van Genuchten, J. Environ. Qual. 19 (1990) 520-525.

[77] J.A. Johnson, W.J. Farmer, Soil Sci. 155 (1993) 92-99.

[78] C.T. Chiou, D.E. Kile, D.W. Rutherford, G. Sheng, S.A. Boyd, Environ. Sci. Technol. 34 (2000) 1254-1258.

[79] S. Sun, W.P. Inskeep, S.A. Boyd, Environ. Sci. Technol. 29 (1995) 903-913.

[80] D.E. Kile, C.T. Chiou, H. Zhou, H. Li, O. Xu, Environ. Sci. Technol. 29 (1995) 1401-1406.

[81] C.T. Chiou, S.E. McGroddy, D.E. Kile, Environ. Sci. Technol. 32 (1998) 264-269.

[82] G. Sheng, C.T. Johnston, B.J. Teppen, S.A. Boyd, J. Agr. Food Chem. 49 (2001) 2899-2907.

[83] L.W. Lion, T.B. Stauffer, W.G MacIntyre, J. Contam. Hydrol. 5 (1990) 215-234.

[84] C.T. Chiou, P.E. Porter, D.W. Schmedding, Environ. Sci. Technol. 17 (1983) 227-231.

[85] P.D. Vowles, R.F.C. Mantora, Chemosphere 16 (1987) 109-116.

[86] C.T. Chiou, L.J. Peters, V.H. Freed, Science 206 (1979) 831-832.

[87] C. Horvath, W.J. Melander, J. Chromat. Sci. 15 (1977) 393-404.

[88] K. Valkó, J. Chromatogr. A 1037 (2004) 299-310.

[89] H. Hong, L. Wang, S. Han, Z. Zhang, G. Zou, Chemosphere 34 (1997) 827-834.

[90] U.S. Environmental Protection Agency, http://www.epa.gov/ebtpages/pollutants.html http://www.epa.gov/ebtpages/pollutants.html#subtopics.

[91] U.S. Environmental Protection Agency, EPA-40-CFR-423, Appendix A, http://www.epa.gov/waterscience/methods/pollutants.htm.

[92] Report on Carcinogens, 11th ed., U.S. Department of Health and Human Services, Public Health Service, National Toxicology Program.

[93] R. Lohmann, K. Breivik, J. Dachs, D. Muir, Environ. Pollut. 150 (2007) 150-165.

[94] H. Thoma, G. Haushulz, E. Knorr, O. Hutzinger, Chemosphere 16 (1987) 277-285.

[95] J. Ebert, M. Bahadir, Environ. Int. 29 (2003) 711-716.

[96] B. Jansson, L. Asplund, M. Olsson, Chemosphere 16 (1987) 2343-2349.

[97] C.L. Yaws, Chemical Properties Handbook, McGraw-Hill Book Co., New York, NY, 1999.

[98] L.W.D. Weber, H. Greim, J. Toxicol. Env. Heal. A. 50 (1997) 195-216.

[99] T.W. Schultz, G.W. Riggin, Toxicol. Lett. 25 (1985) 47-54.

[100] A.D. McNaught, A. Wilkinson, IUPAC Compendium of Chemical Terminology, 2nd ed., Blackwell Scientific Publications, Oxford, UK, 1997.

[101] Y.J. An, E.R. Carraway, M.A. Schlautman, Water Res. 36 (2002) 300-308.

[102] Y.-J. An, S.-W. Jeong, J. Colloid Interf. Sci. 242 (2001) 419-424.

[103] T. Asakawa, T. Kitaguchi, S. Miyagishi, J. Surfactants Deterg. 1 (1998) 195-199.

CHAPTER 2: EXPERIMENTAL METHODS

2.1 Introduction

In order to study the transport effects of hydrocarbon and perfluorinated surfactants on co-contaminants in an environmental system, an analytical technique was required that could fundamentally resemble such a system, but whose parameters were controllable. For this purpose, reversed-phase liquid chromatography (RPLC) was used as a model for a flow-through groundwater system. The stationary phase packing material, as well as the instrumentation and treatment of the data for the various experimental measurements are explained in the following sections.

2.2 Chromatographic Measurements

2.2.1 Stationary Phase

The commercially available stationary phase chosen consisted of pellicular particles made of small, non-porous glass beads with a 5.0 μm diameter covered with chemically bonded porous octadecylsilica (ODS) with a 300 Å pore size, 2.1 μmol m^{-2} bonding density, 0.39 % carbon content, and 6.0 m^2 g^{-1} surface area. The pellicular material (Poroshell 300SB-C_{18}, Agilent) was selected because it is a well defined packing material, whose properties of carbon content and surface area are substantially lower than those of traditional, totally porous ODS materials routinely used in RPLC (12 – 18 %, 200 – 400 m^2 g^{-1} respectively). These properties of the pellicular material are within, and more closely resemble, the typical ranges of carbon content (0.11 – 6.09 %) and surface area (1.07 – 54.0 m^2 g^{-1}) for various soils, bed sediments, and suspended solids [1]. Based on these properties, it is believed that the pellicular material is more representative as a model for soil than traditional RPLC stationary phases.

2.2.2 Instrumentation

The liquid chromatography system, represented in Figure 2.1, was used to determine the chromatographic retention of the model analytes in aqueous surfactant mobile phases. The system consisted of a single-piston reciprocating pump (Beckman, Model 110B) operating with a maximum pressure limit of 4500 psi. Samples were introduced to the system via an injection valve (Valco, Model EC6W) with a 20 μL injection loop. Upon injection, the samples are carried through a commercially available analytical column (4.6 mm i.d. x 250 mm length) packed with the Poroshell material previously described (Section 2.2.1), whose outlet is connected to a commercially available ultraviolet-visible absorbance detector (Hitachi, Model L-4200). The UV absorbance wavelength of 254 nm was specific for the detection of the analytes, and did not incur any interference from the surfactants. The output signal from the UV-visible absorbance detector was either recorded on a chart recorder (Linear Cole-Parmer Instrument Company, Model 0555-0000) or converted to the digital domain (National Instruments, Model PCI-MIO-16XE-50) and stored via a user-defined software program (National Instruments, Labview v5.1) for further data analysis. All experiments were carried out at ambient temperature.

2.2.3 Data Analysis

The void time, t_0, was taken as the first positive deviation from the baseline arising from either residue methanol or lithium nitrate ($LiNO_3$) in each sample. The retention time, t_R, for each analyte was determined from the peak maximum, which was appropriate for the symmetric Gaussian peaks observed in these studies.

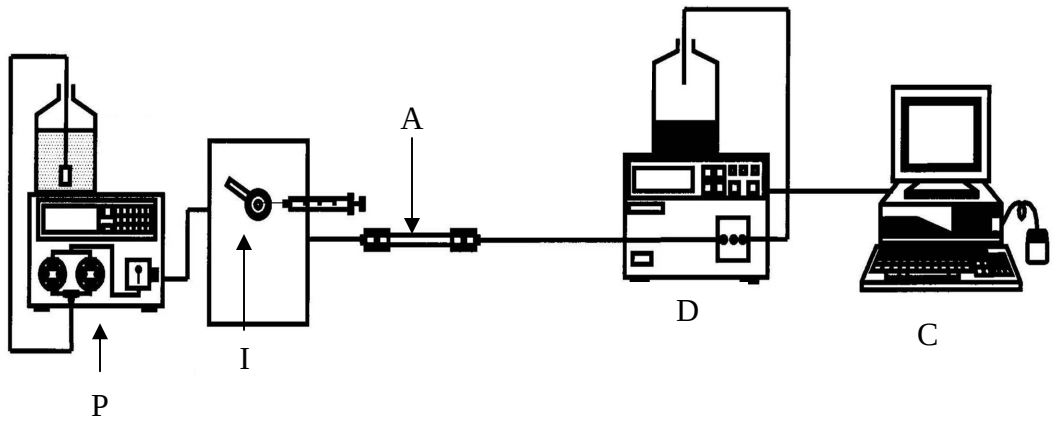

Figure 2.1: Schematic diagram of the liquid chromatography system used for the determination of transport effects of perfluorinated surfactants. System components: single-piston reciprocating pump (P), injection valve (I), analytical column with Poroshell stationary phase (A), UV-visible absorbance detector (D), and computer data acquisition system (C).

The retention factor, k, was then calculated by

$$k = \frac{t_R - t_0}{t_0} \qquad (2.1)$$

The k values (average of at least three trials) were used for the subsequent elucidation of transport effects (Chapters 3 – 5), the determination of equilibrium constants (Chapter 3), and selectivity factors (Chapters 4 – 5).

2.2.4 Refractive Index

RPLC with refractive index detection was investigated in an effort to experimentally determine the retention of the representative hydrocarbon and perfluorinated surfactants in the experimental system. Refractive index measurements were performed in tandem with UV-visible absorbance detection, with the UV-visible absorbance detector used as a secondary means to identify the carboxylic acids. The liquid chromatography system previously described (Section 2.2.2) was used with slight modification. The outlet of the analytical column was connected to a commercially available refractive index detector (Beckman, Model 156), whose sample outlet was connected, via a stainless steel connector, to the sample inlet of the UV-visible absorbance detector. The UV absorbance wavelength of 203 nm was chosen for the detection of carboxylic acids (with carbon chain lengths of $C_1 – C_4$, C_6, and C_8) and the representative surfactants. The output signal from both the refractive index and UV-visible absorbance detector was recorded on a chart recorder for further data analysis.

Injections of the various carboxylic acids were first performed to validate the sensitivity of refractive index detector. While peaks for the carboxylic acids were observed with the UV-visible detector, corresponding peaks were not observed with the

refractive index detector. The refractive index detector proved to have an inadequate sensitivity to accurately determine the retention of the carboxylic acids (at concentrations of 5.0 x 10^{-3} M). Thus, the retention of the surfactants within the chromatographic system could not be determined via this method. Consequently, an alternative approach based on the detection of system peaks via UV-visible absorbance was later employed (Chapter 6).

2.3 Conductivity Measurements

Capillary electrophoresis (CE) techniques have previously been used to determine the critical micelle concentration (CMC) of various surfactants [2-5]. Based on this previously reported literature, conductivity measurements of aqueous sodium dodecyl sulfate (SDS) and lithium perfluorooctane sulfonate (LiPFOS) solutions were performed via CE to experimentally determine the CMC of the surfactants.

2.3.1 Instrumentation

Conductivity measurements were experimentally performed using a CE system that had been constructed and utilized previously within the McGuffin research group [6]. The CE system was constructed of an incubation oven (Labline, Model 3500-DT), which was able to hold a constant temperature within the range of 5.0 – 50.0 ± 0.2 °C. The modified oven contained plexiglass inserts, which supported the various components of the system (e.g. buffer and sample vials, capillary, etc.) while electrically insulating the interior of the oven. The samples were carried through a fused-silica capillary (50.0 μm i.d., 360 μm o.d., 60.0 cm length) upon injection using an auto-reversing high-voltage power supply (Bertan High Voltage, Model 2341-A). The power supply was used in fixed voltage mode (20.0 kV ± 0.1 %) while monitoring the current. A user-defined

software program (National Instruments, Labview v5.1) was used to store data from the power supply that represented the current in fixed voltage mode.

2.3.2 Data Analysis

Prior to each set of SDS measurements, the CE system was rinsed with a 0.1 M sodium hydroxide solution for 10 minutes, deionized water for 10 minutes, and 1.0 mM SDS solution for at least two hours to equilibrate the capillary. Aqueous samples of SDS at various concentrations (1, 2, 4, 6, 8, 10, 20, 30, and 40 mM) were each injected into the system at five temperatures (ambient, 10 °C, 15 °C, 30 °C, and 35 °C), with the resulting current measured. It was observed that increasing the SDS concentration resulted in the current increasing. In addition, increasing the temperature of the system resulted in an increase in the current, which was more prominent at higher concentrations of SDS.

A graph of the current versus surfactant concentration, at each temperature, for SDS is shown in Figure 2.2. The graph displays an increasing linear trend with a break in the slope of the line, resulting in two distinct linear regions for SDS. The break in the slope represents the CMC of the surfactant solution at that temperature. Statistical treatment of the data for the two regions via linear regression resulted in two equations that were combined to determine the CMC of the surfactant at a specific temperature (Table 2.1). For SDS, the slope trends and general shape of the lines were similar at all temperatures. The experimentally determined CMC based on the data at ambient temperature (22 °C) was 8.41 mM, and was within 4.0 % error of the reported literature value of 8.1 mM (25 °C) [7].

Figure 2.2: Graph of the current versus the concentration of sodium dodecyl sulfate (SDS). Temperatures: (♦) ambient, (■) 10 °C, (▲) 15 °C, (x) 30 °C, (∗) 35 °C. Other experimental conditions as given in the text.

Figure 2.2

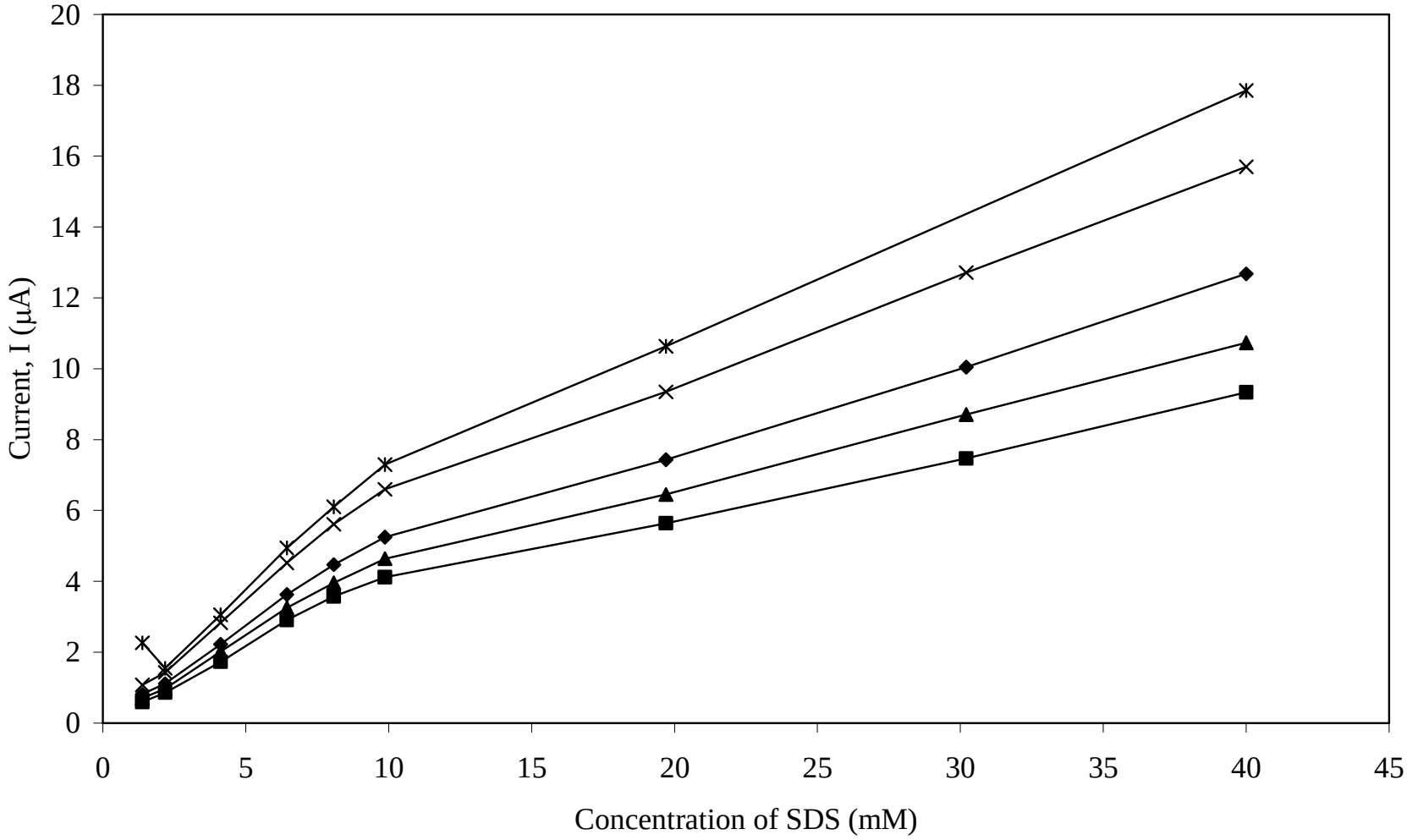
20
18
16
14
12
10
8
6
4
2
0
Current, I (μA)
0
5
10
15
20
25
30
35
40
45
Concentration of SDS (mM)

Table 2.1: Experimentally determined CMC values for SDS via conductivity measurements

Experimental Temperature	CMC (mM)	Linear Range	Slope ± std. error	Intercept ± std. error	R^2
10 °C	8.30	low	0.455 ± 0.012	−0.09 ± 0.06	0.9979
		high	0.176 ± 0.004	2.23 ± 0.11	0.9981
15 °C	8.39	low	0.501 ± 0.013	−0.05 ± 0.07	0.9978
		high	0.208 ± 0.005	2.41 ± 0.12	0.9984
22 °C	8.41	low	0.560 ± 0.014	−0.04 ± 0.07	0.9982
		high	0.251 ± 0.006	2.56 ± 0.15	0.9983
30 °C	8.58	low	0.692 ± 0.016	0.02 ± 0.08	0.9984
		high	0.311 ± 0.007	3.29 ± 0.17	0.9986
35 °C	8.64	low	0.779 ± 0.013	−0.14 ± 0.08	0.9994
		high	0.360 ± 0.011	3.48 ± 0.25	0.9982

Conductivity measurements of LiPFOS were performed after SDS measurements. Prior to LiPFOS measurements, the CE system was rinsed with a 0.1 M lithium hydroxide solution for 10 minutes, deionized water for 10 minutes, and a 6.5 mM LiPFOS solution for at least two hours to equilibrate the capillary. Aqueous samples of LiPFOS at various concentrations (1, 2, 4, 5, 6, 8, 10, 20, 30, and 40 mM) were each injected into the system at ambient temperatures (25 °C and 23 °C), with the resulting current measured.

A graph of the current versus surfactant concentration, at ambient temperature, for LiPFOS is shown in Figure 2.3. The graph displayed an initial decreasing trend at very low concentrations (1 – 4 mM), followed by an increasing trend (4 – 20 mM), and then a decreasing trend (20 – 40 mM). Due to the "S-curve" shape of the graph, a definitive break in the slope could not be identified, thus the CMC for LiPFOS could not be experimentally determined from this method. A possible explanation for this phenomenon could be the early formation of dimers or trimers of the fluorinated surfactant at low concentrations prior to the formation of micelles at higher concentrations. Due to the inability to determine the CMC of LiPFOS via this method, the accepted literature values for the CMC of SDS and LiPFOS (8.1 mM and 6.5 mM respectively) [7,8] were used in the calculations for the above CMC studies (Chapter 3).

Figures 2.3A-B: Graphs of current versus the concentration of lithium perfluorooctane sulfonate (LiPFOS). Temperatures: (A) 25 °C, (B) 23 °C. Other experimental conditions as given in text.

Figure 2.3A

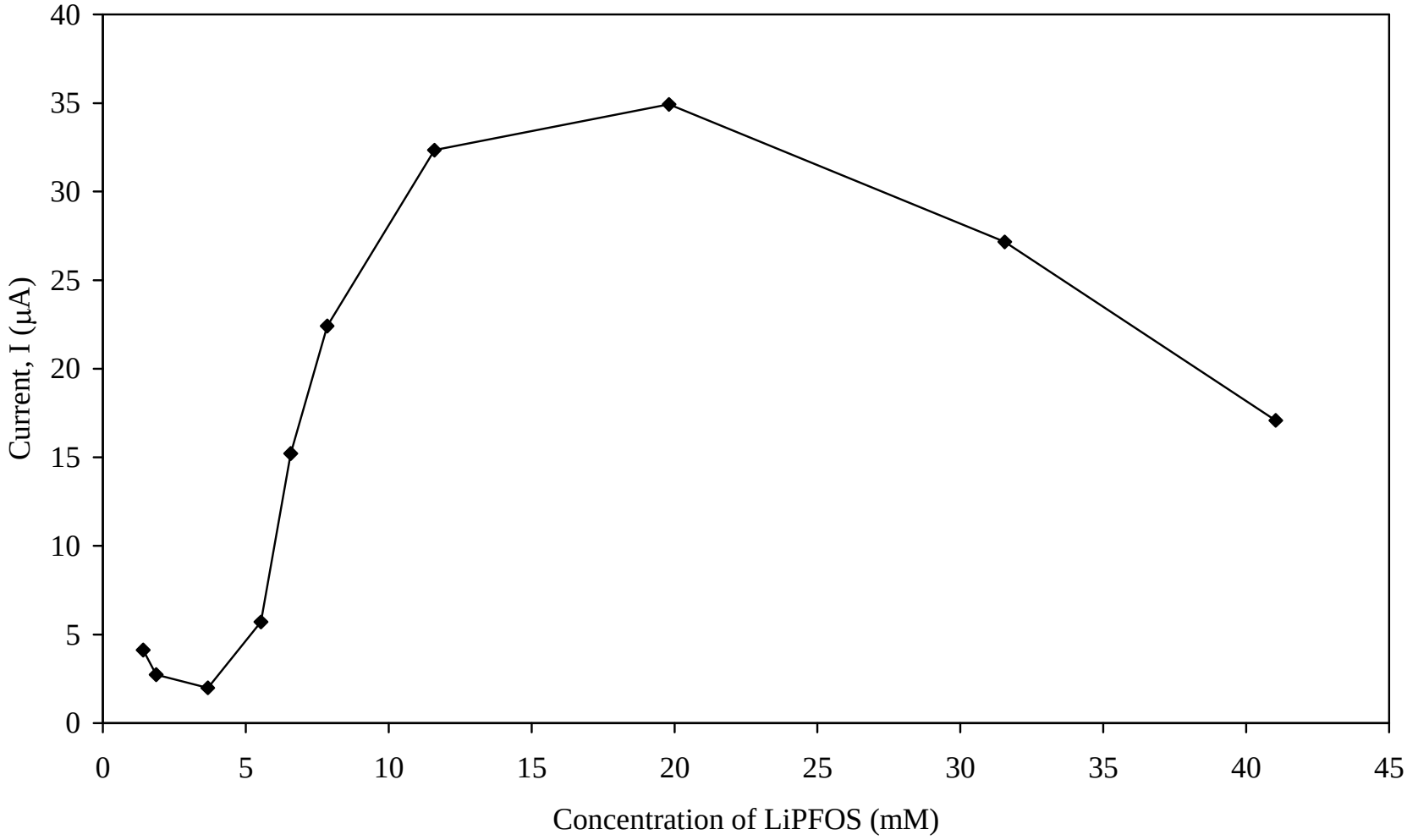
40
35
30
25
20
15
10
5
0
Current, I (μA)
0
5
10
15
20
25
30
35
40
45
Concentration of LiPFOS (mM)

Figure 2.3B

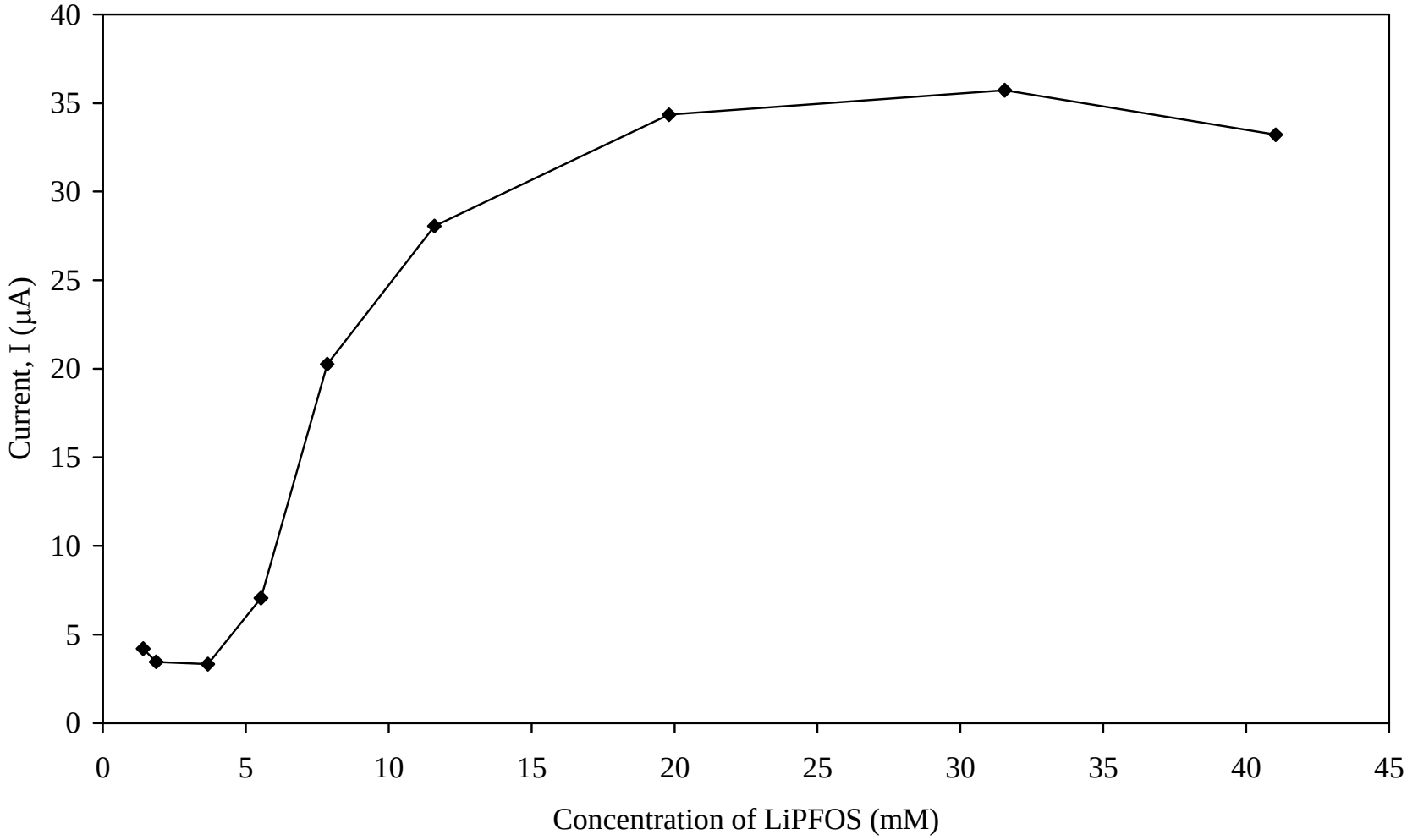
Current, I (μA)
0
5
10
15
20
25
30
35
40
0
5
10
15
20
25
30
35
40
45
Concentration of LiPFOS (mM)

2.4 Densitometry Measurements

Several techniques, such as positron annihilation lifetime spectroscopy [9], small angle neutron scattering [10], or light scattering techniques [11,12], have been used to determine the aggregation number of surfactants. However, it can be difficult to obtain reliable data by these methods for some surfactant solutions whose surfactant carbon chain length approaches 1.0 nm. For this study, the aggregation number for the representative hydrocarbon and perfluorinated surfactants were experimentally determined via densitometry measurements.

2.4.1 Instrumentation

The density of aqueous SDS and LiPFOS solutions, within the concentration range of 0.02 – 0.1 M, were measured by using a calculating digital density meter (Anton PAAR, Model DMA 45 SI), which was held at a temperature of 25 °C by a PolyScience temperature controller (VWR-Scientific Products, Model 1166).

2.4.2 Data Analysis

The density of a surfactant solution (ρ) can be expressed as

$$\rho = w_1\rho_1 + w_2\rho_2 \qquad (2.2)$$

where ρ_1 and ρ_2 are the densities and w_1 and w_2 are the weight percents of the surfactant and water, respectively. Since $w_2 = 1 - w_1$, equation 2.2 can be expressed as

$$\rho = \left(\rho_1 - \rho_2\right) w_1 + \rho_2 \qquad (2.3)$$

A graph of the density of the surfactant solution versus the weight percent of the surfactant yields a linear correlation, where the sum of the slope and the intercept

provides a quantitative estimate of the density of the surfactant. The density of the surfactant is related to the volume of the surfactant monomer, v, by

$$\rho_1 = \frac{MW}{(N_a v)} \tag{2.4}$$

where MW is the molecular weight of the surfactant, and N_a is Avogadro's number. The volume of the surfactant is then related to the aggregation number, N, by

$$N = \frac{4\pi R^3}{3v} \tag{2.5}$$

where R is the radius of the spherical micelle, which is equivalent to the length of the linear surfactant monomer [13]. The length of LiPFOS (1.17 nm) and SDS (1.67 nm) were calculated by using the PyMOL™ molecular modeling software (DeLano Scientific, version 0.09).

The aggregation number of SDS determined from these experimental data (65 ± 8) was in good agreement with the literature value (62) [7,14]. Based on this good agreement, the experimentally determined aggregation numbers for SDS and LiPFOS (11 ± 3) were used in the calculations for the above CMC studies (Chapter 3).

2.5 Summary

The use of a well-defined experimental system, experimentally accurate physical data, and robust data treatment is necessary in order to study the transport effects of perfluorinated surfactants on co-contaminants. This chapter detailed the experimental system and data analysis procedures that were used to collect and analyze the desired data for the experiments performed in Chapters 3 – 5.

REFERENCES

2.6 References

[1] D.E. Kile, C.T. Chiou, H. Zhou, H. Li, O. Xu, Environ. Sci. Technol. 29 (1995) 1401-1406.

[2] A. Cifuentes, J.L. Bernal, J.C. Diez-Masa, Anal. Chem. 69 (1997) 4271-4274.

[3] M. Schwing, Bulletin de l'Union des Physiciens 97 (2003) 323-328.

[4] C.-E. Lin, J. Chromatogr. A 1037 (2004) 467-478.

[5] H. Liu, Y. Gao, Z. Hu, J. Anal. Chem. 62 (2007) 176-178.

[6] C.I.D. Newman, Capillary Electrophoresis for Thermodynamic and Kinetic Studies, Ph.D. Dissertation, Michigan State University, East Lansing, MI, 2006.

[7] D.W. Armstrong, Sep. Purif. Methods 14 (1985) 213-304.

[8] K. Shinoda, M. Hato, T. Hayashi, J. Phys. Chem. 76 (1972) 909-914.

[9] F. Bockstahl, G. Duplatre, Phys Chem Chem Phys 2 (2000) 2401-2405.

[10] H. Hoffmann, J. Kalus, H. Thurn, Colloid Polymer Sci 261 (1983) 1043-1049.

[11] Z.J. Yu, R.D. Neuman, Langmuir 8 (1992) 2074-2076.

[12] C. Thevenot, B. Grassl, G. Bastiat, W. Binana, Colloid Surface Physicochem Eng Aspects 252 (2005) 105-111.

[13] J.N. Israelachvili, Intermolecular and Surface Forces: With Applications to Colloidal and Biological Systems, Academic Press, San Diego, CA, 1989, p. 250.

[14] M. Arunyanart, L.J. Cline Love, Anal. Chem. 56 (1984) 1557-1561.

CHAPTER 3: COMPARISON OF TRANSPORT EFFECTS ABOVE THE CRITICAL MICELLE CONCENTRATION

3.1 Introduction

The ability of hydrocarbon surfactants to affect the transport, sorption, and solubility of neutral hydrophobic organic compounds has been reported in the literature [1-6]. Further studies have examined the effect of hydrocarbon surfactants on the sorption of organic compounds in a soil-water system [7-9].

In addition to these environmental studies, hydrocarbon surfactants have been used as mobile phase modifiers in many analytical separation techniques, such as ion-pair chromatography, micellar liquid chromatography (MLC), and micellar electrokinetic capillary chromatography [10,11]. The addition of a hydrocarbon surfactant at low concentrations has been widely used for ion-pair chromatography in order to enhance the separation of oppositely charged ions in solution. Although surfactant monomers have also been shown to enhance the solubility of neutral hydrophobic organic compounds, their general effectiveness is substantially less than that of surfactant aggregates formed above the critical micelle concentration (CMC) [1,2,9]. In a micellar solution, neutral compounds can partition into the micelle, thus increasing the solubility and transport in the aqueous system [1-6,10,11].

Compared to hydrocarbon surfactants, perfluorinated surfactants have characteristics that impart greater chemical and thermal stability, as well as the ability to form micelles at lower concentrations [12-20]. These properties make the commercial and industrial use of perfluorinated surfactants highly appealing. Throughout the last three decades, the production and use of perfluorinated surfactants for commercial and industrial applications increased. However, in response to growing concerns, the major

US manufacturer of perfluorinated surfactants, 3M, voluntarily ceased production of surfactants based on perfluorooctane sulfonate (PFOS) chemistry in May 2000 [21]. In March 2006, 3M, DuPont, and six other companies voluntarily agreed to reduce emissions of perfluorooctanoic acid (PFOA) and related compounds [22,23]. Based on numerous studies, perfluorinated surfactants are globally distributed and persistent in the environment. These chemicals also bioaccumulate, thereby posing a significant health risk in humans and animals [24-26]. Studies have been conducted to understand the physicochemical properties [27] as well as the structural and electronic properties [28]. Additional studies have focused on the bioaccumulation and global distribution of perfluorinated surfactants [29-33], as well as the ability of perfluorinated surfactants to enhance the solubilization of polycyclic aromatic hydrocarbons [34]. Despite these important studies, relatively little information is available regarding the effects of perfluorinated surfactants on the transport of other environmental contaminants.

The main focus of this study is to compare the effects of perfluorinated and hydrocarbon surfactants above their CMC on the transport of environmental contaminants in a groundwater system. Reversed-phase micellar liquid chromatography is used as a model for the groundwater system, with lithium perfluorooctane sulfonate and sodium dodecyl sulfate as representatives of the two classes of surfactants. Various halogenated benzenes and polycyclic aromatic hydrocarbons are used as models of the environmental contaminants. The results of this study yield information concerning the retention factor and equilibrium constant of the model contaminant between water and the micelle. These values can be used in modeling programs to elucidate the transport of

pollutants that might leach from waste disposal or other contaminated sites into an aquifer.

3.2 Experimental Methods

3.2.1 Mobile Phase and Analytes

The hydrocarbon surfactant, sodium dodecyl sulfate (SDS), was obtained from Aldrich and was used as received. The perfluorinated surfactant, lithium perfluorooctane sulfonate (LiPFOS), was prepared by dissolving the appropriate amounts of heptadecafluorooctane sulfonic acid (TCI America) and lithium hydroxide monohydrate (99.95 %, Aldrich) in deionized, distilled water. The micellar solutions were prepared by dissolving the appropriate amount of surfactant in deionized, distilled water (Corning Mega-Pure, Models D2 and MP-3A) and gently stirring the solution overnight to allow equilibrium to be reached. The solutions were then filtered through a cellulose acetate membrane (Alltech) with a 0.45 μm pore size. The analytes benzene, biphenyl, naphthalene, anthracene, phenanthrene, pyrene, fluorobenzene, chlorobenzene, and bromobenzene (Aldrich), as well as hexafluorobenzene, hexachlorobenzene, and hexabromobenzene (TCI America) were used as received. Stock solutions (1.0×10^{-3} M) of the analytes were prepared in high-performance liquid chromatography-grade methanol (Spectrum Chemical), except hexabromobenzene, which was prepared in dichloromethane (Spectrum Chemical). Analytical samples were prepared by diluting the proper amount of stock solution with the surfactant solution to acquire the working concentrations. The working concentrations were benzene (2.25×10^{-4} M), biphenyl (2.00×10^{-6} M), naphthalene (3.80×10^{-5} M), anthracene (4.99×10^{-7} M), phenanthrene (4.99×10^{-7} M), pyrene (3.80×10^{-5} M), fluorobenzene (3.23×10^{-4} M), chlorobenzene

(2.98 x 10^{-4} M), bromobenzene (3.45 x 10^{-4} M), hexafluorobenzene (1.31 x 10^{-3} M), hexachlorobenzene (2.22 x 10^{-4} M), and hexabromobenzene (5.00 x 10^{-5} M).

3.2.2 Experimental System

The experimental chromatographic methods, as detailed in Section 2.2, are briefly recapped in this section. The commercial analytical column (4.6 mm i.d. x 250 mm length) was packed with Poroshell 300SB-C_{18} pellicular particles (Agilent) of 5.0 μm diameter and 6.0 m^2 g^{-1} surface area, with an octadecylsilica stationary phase of 2.1 μmol m^{-2} bonding density and 0.39 % carbon content. The pellicular particles consist of solid silica glass beads coated with a 300 Å layer of porous octadecylsilica. The MLC system consisted of a single-piston reciprocating pump (Beckman, Model 110B), an injector with a 20 μL injection loop (Valco, Model EC6W), an analog interface module, and a UV-visible absorbance detector (Beckman, Models 406 and 166, respectively). The UV absorbance wavelength of 254 nm was specific for the detection of the analytes, and did not incur any interference from the surfactants. Chromatograms were recorded on a chart recorder (Linear Cole-Parmer Instrument Company, Model 0555-0000). All experiments were carried out at ambient temperature with a maximum pressure limit of 4500 psi. The flow rate was 1.0 mL min^{-1} during the SDS experiments and 0.5 mL min^{-1} during the LiPFOS experiments. The lower flow rate was used for the LiPFOS experiments due to higher back pressure in the RPLC system during measurements. The void time was taken as the first positive deviation from the baseline arising from the residual methanol in each sample.

3.2.3 Data Analysis

In order to elucidate meaningful information regarding the transport effects of perfluorinated surfactants in a groundwater system, an analytical technique was used that could fundamentally resemble such a system, but whose parameters were controllable. Reversed-phase MLC was used to model a groundwater system, in which the octadecylsilica stationary phase represents soil and the aqueous micellar mobile phase represents groundwater that contains a surfactant above its CMC.

In the paper by Arunyanart and Cline Love [6], MLC is described by three competing reversible equilibria, which are treated as binding phenomena instead of the more traditional partitioning phenomena. Treating the equilibria in this manner eliminates the need for prior information pertaining to the concentration of analytes in solution, the volume of the stationary phase, or the partial specific volume of the micelle aggregate. The first equilibrium is expressed as

$$A + S \underset{}{\overset{K_1}{\rightleftharpoons}} AS \tag{3.1}$$

which represents the analyte in the bulk mobile phase, A, binding to a stationary phase site, S, to form a complex, AS. The second equilibrium is

$$A + M \overset{K_2}{\rightleftharpoons} AM \tag{3.2}$$

which represents the analyte in the bulk mobile phase, A, binding to a surfactant micelle in the bulk mobile phase, M, to form a micellar complex, AM. The third equilibrium is

$$AM + S \overset{K_3}{\rightleftharpoons} AS + M \tag{3.3}$$

which represents the transfer of the analyte from the surfactant micelle in the bulk mobile phase, AM, to a stationary phase site, S. Among these equilibria, only two are

independent and the other dependent. For example, the third equilibrium constant can be expressed as the ratio of the first and second equilibrium constants. For this reason, we may consider the retention mechanism to be controlled by the first and second equilibria [11,35].

The retention factor, k, can be defined from the molar concentrations of the free and bound analyte as

$$k = \frac{\phi[AS]}{\left([A] + [AM]\right)} \tag{3.4}$$

where ϕ is the phase ratio, which is the ratio of the volumes of the stationary and mobile phases. The value for k is experimentally determined by

$$k = \frac{t_R - t_0}{t_0} \tag{3.5}$$

where t_R and t_0 are the chromatographic retention time of the analyte and the void time of the column, respectively. By combining Equations 3.1, 3.2, and 3.4, an expression can be obtained that relates k to the binding constants of the two controlling equilibria, K_1 and K_2, as well as the concentration of the surfactant micelle

$$k = \frac{\phi[S]K_1}{\left(1 + K_2[M]\right)} \tag{3.6}$$

By taking the reciprocal of Equation 3.6, the following expression is obtained

$$\frac{1}{k} = \frac{K_2}{\phi[S]K_1}[M] + \frac{1}{\phi[S]K_1} \tag{3.7}$$

where [M] is the molar concentration of surfactant in the micellar form, which is equal to the total concentration minus the CMC.

By graphing the inverse of k versus [M], a linear correlation is obtained. From the ratio of the slope to the y-intercept, a quantitative value for K_2 can be calculated. This value of K_2 represents the binding constant of the analyte between the bulk mobile phase and the micelle, expressed per monomer of surfactant in Equation 3.2. Upon multiplying K_2 by the aggregation number of the surfactant, the equilibrium constant per micelle, K_{eq}, is obtained. The aggregation numbers used in this study for both SDS and LiPFOS were experimentally determined during this study by means of densitometry measurements, as previously described in Section 2.4.

3.3 Results and Discussion

The experimental conditions for this study were selected, insofar as possible, to model a groundwater system. The Poroshell stationary phase was chosen because of its low carbon content (0.39 %) and surface area (6.0 $m^2\ g^{-1}$), which more closely resembles the properties of soil than a traditional octadecylsilica stationary phase (12 – 18 %, 200 – 400 $m^2\ g^{-1}$). In addition, this phase allows for the complete elution of all analytes even at very low concentration of surfactants.

Sodium dodecyl sulfate (SDS) was chosen as the representative hydrocarbon surfactant because it is commonly used in commercial products and has been detected in the environment. Moreover, there is a large volume of information on SDS in the literature [36,37]. Perfluorooctane sulfonate (PFOS) was chosen as the representative perfluorinated surfactant because it is used commercially and has been detected in the environment [29-33,38]. The lithium salt (LiPFOS) has a low Krafft point that allows it to form micelles at room temperature [32] and has a CMC of the same magnitude as SDS

[11,21, Table 3.1]. In a study by Hu and Haddad [39], it was shown that surfactant monomers could adsorb onto the surface of the stationary phase, thereby changing the physical and chemical properties. To control this effect, it was desirable to maintain the SDS and LiPFOS monomers at similar concentrations. In solutions where the total surfactant concentration is above the CMC, the concentration of monomers is equal to the CMC and, hence, is similar for SDS and LiPFOS.

Finally, the analytes chosen for this study represent important classes of environmental contaminants. The polycyclic aromatic hydrocarbons (PAHs) are known human carcinogens and environmental pollutants. Biphenyl and the halogenated benzene compounds serve as models for polychlorinated biphenyls and polychlorinated and polybrominated dibenzodioxins and dibenzofurans. Moreover, all of these analytes can be used to examine how their differences in physical and chemical characteristics influence the transport effects of hydrocarbon and perfluorinated surfactants.

3.3.1 Transport Effects of Sodium Dodecyl Sulfate

In preliminary studies, the experimental system and data analysis methods were validated by using SDS mobile phases (0.02 – 0.1 M). Hexabromobenzene exhibited limited solubility in the SDS mobile phase and, consequently, was excluded from further studies. All other test analytes were soluble and eluted from the column at each surfactant concentration, with the exception of hexachlorobenzene at the lowest concentration. The elution order for the analytes in SDS was as follows: benzene < fluorobenzene < hexafluorobenzene < chlorobenzene < bromobenzene < naphthalene < biphenyl < phenanthrene < anthracene < pyrene < hexachlorobenzene.

Table 3.1: Physical data of representative hydrocarbon and perfluorinated surfactants used in this study.

Surfactant	Chemical Formula	Critical Micelle Concentration (M)	Aggregation Number [c]	Krafft Point (°C) [b]
SDS	$C_{12}H_{25}OSO_3^-Na^+$	8.1×10^{-3} [a]	65 ± 8	16
LiPFOS	$C_8F_{17}SO_3^-Li^+$	6.5×10^{-3} [b]	11 ± 3	<0

[a] Reference 11
[b] Reference 32
[c] This study, Section 2.4
[a] The critical micelle concentration is the point (or narrow concentration range) where extensive aggregation of the surfactant monomers takes place.
[a] The aggregation number is the average number of monomer surfactant molecules per micelle.
[a] The Krafft point is the temperature (or narrow temperature range) above which the solubility of a surfactant becomes equal to the critical micelle concentration.

This elution order was identical to that observed for the analytes in methanol/water mobile phases on the same stationary phase.

The chromatographic retention times of the model analytes were used to calculate the retention factors, k, according to Equation 3.5. The retention factors are summarized in Table 3.2. It is noteworthy that the retention factors determined in this study were an order of magnitude lower than those determined by Arunyanart and Cline Love [6] for comparable analytes and concentrations of SDS. This discrepancy is believed to be due to differences in the stationary phases, specifically carbon content, used in the two studies. In comparing the retention factors in 0.1 M SDS to that in pure water (Table 3.2), the values decreased by 39 to 80 % for benzene and the monohalogenated benzenes. Correspondingly, the linear velocities increased by 32 to 247 %. It is apparent that SDS increases chromatographic transport of benzene and the substituted benzenes and, by implication, increases environmental transport as well.

Graphs of the inverse retention factor (k^{-1}) versus the concentration of SDS in the micelle (M) are shown in Figure 3.1. Statistical treatment of these graphs via linear regression demonstrated that there was a linear relationship between k^{-1} and M, where the R^2 values were all greater than 0.97 (Table 3.3). For the more retained analytes, the slope of the line became shallower and the intercept approached zero. From the graphs in Figure 3.1, the overall effect was that the retention of the analytes decreased as the concentration of SDS increased.

Table 3.2: Summary of retention factors[a] of analytes for several mobile phases.

Analyte	Pure Water	0.1 M SDS	0.1 M LiPFOS
Benzene	1.57 ± 0.01	0.953 ± 0.004	1.17 ± 0.02
Fluorobenzene	1.95 ± 0.01	1.04 ± 0.03	1.31 ± 0.02
Chlorobenzene	5.70 ± 0.03	1.58 ± 0.03	2.83 ± 0.02
Bromobenzene	8.47 ± 0.03	1.73 ± 0.03	3.66 ± 0.02
Hexafluorobenzene	N/A	1.41 ± 0.01	1.90 ± 0.03
Hexachlorobenzene	N/A	4.96 ± 0.04	D/E
Naphthalene	N/A	2.03 ± 0.06	7.2 ± 0.2
Biphenyl	N/A	2.70 ± 0.02	14.9 ± 0.2
Phenanthrene	N/A	3.33 ± 0.02	47.5 ± 0.6
Anthracene	N/A	3.50 ± 0.07	36.3 ± 1.6
Pyrene	N/A	4.25 ± 0.11	66.9 ± 2.8

[a] Retention factors are an average of at least three injections.
N/A… Analyte was not included in this mobile phase due to excessive retention.
D/E… Analyte exhibited excessive retention.

Figure 3.1: Plot of inverse retention factor versus the concentration of sodium dodecyl sulfate (SDS) in the micelle. Analytes: (♦) benzene, (■) fluorobenzene, (▲) hexafluorobenzene, (x) chlorobenzene, (∗) bromobenzene, (●) naphthalene, (○) biphenyl, (◊) phenanthrene, (□) anthracene, (Δ) pyrene, (+) hexachlorobenzene. Other experimental conditions as given in the text.

Figure 3.1

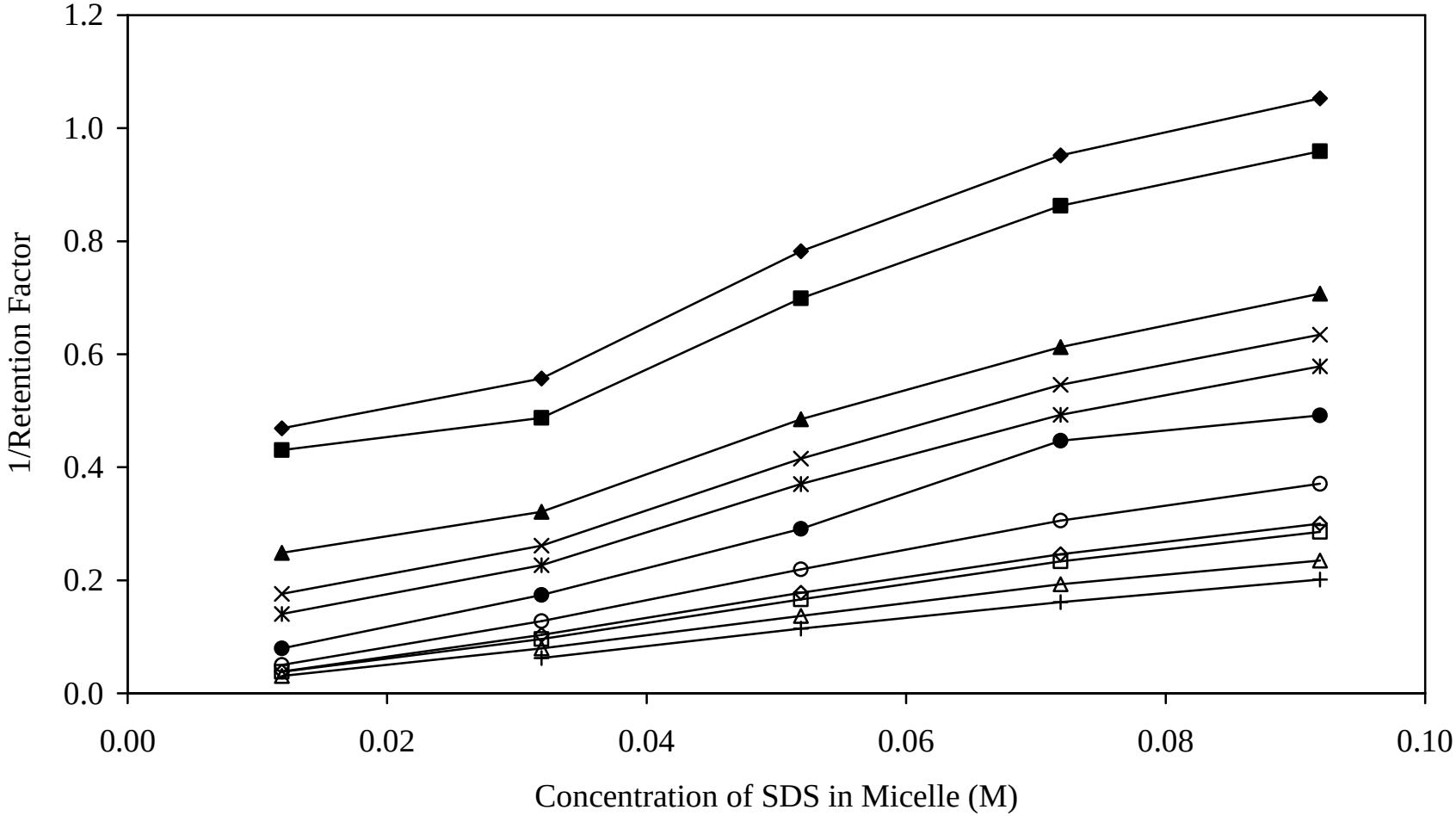
1.2
1.0
0.8
0.6
0.4
0.2
0.0
1/Retention Factor
0.00
0.02
0.04
0.06
0.08
0.10
Concentration of SDS in Micelle (M)

The equilibrium constants, K_{eq}, for the transfer of each analyte from water to the SDS micelle are summarized in Table 3.3. For several of the comparable analytes, such as benzene, the values were of the same magnitude as those reported by Arunyanart and Cline Love [6]. In order to understand the accuracy of these values, it is useful to examine the propagation of error. According to Equation 3.7, the uncertainty in K_{eq} values is determined by the uncertainty in the slope and intercept. For benzene, the monohalogenated benzenes, and hexafluorobenzene, the uncertainty in the intercept was low, resulting in small error in K_{eq}. For the highly retained analytes, i.e. hexachlorobenzene and the PAHs, there was large uncertainty in the intercept, even resulting in negative values for several of the analytes. Due to this uncertainty, K_{eq} values for highly retained analytes were not reliably obtained via this method. This is most notably evident from the negative K_{eq} values acquired for three of the analytes, anthracene, pyrene, and hexachlorobenzene. However, the retention factors (Table 3.2) appear to be roughly correlated with the K_{eq} values (Table 3.3), such that transport trends of the analytes can be elucidated. For the series of monohalogenated benzenes, the K_{eq} values increased with the size and polarizability of the halogen substituent. Additionally, the K_{eq} values increased as the number of halogen substituents increased from one to six. For the series of PAHs, the K_{eq} values increased with the number of aromatic rings. Moreover, the annelation structure of the PAHs appears to affect the K_{eq} value. For example, the fused-ring aromatic structure of naphthalene had a lower K_{eq} value than the non-fused-ring structure of biphenyl.

Table 3.3: Equilibrium constants of analytes from water to the SDS micelle.

Analyte	SDS					
	Method One[a]		Method Two[b]		Method Three[c]	
	K_{eq} (10^3 M^{-1})	R^2	K_{eq} (10^3 M^{-1})	R^2	K_{eq} (10^3 M^{-1})	R^2
Benzene	1.38 ± 0.18	0.981	1.28 ± 0.19	0.969	1.29 ± 0.23	0.970
Fluorobenzene	1.43 ± 0.23	0.974	1.22 ± 0.25	0.946	1.24 ± 0.29	0.949
Chlorobenzene	3.99 ± 0.85	0.991	3.19 ± 0.43	0.988	3.32 ± 0.56	0.988
Bromobenzene	5.5 ± 1.4	0.993	4.31 ± 0.57	0.991	4.50 ± 0.75	0.992
Hexafluorobenzene	2.35 ± 0.37	0.988	1.95 ± 0.30	0.976	2.02 ± 0.38	0.977
Hexachlorobenzene	−17 ± 12	0.997	−9.87 ± 1.9	0.999	DNC	0.980
Naphthalene	29 ± 63	0.980	17 ± 4	0.997	18 ± 5	0.997
Biphenyl	110 ± 370	0.997	120 ± 72	0.999	130 ± 88	0.999
Phenanthrene	330 ± 3100	0.997	−250 ± 250	0.999	DNC	0.999
Anthracene	−510 ± 6700	0.998	120 ± 91	0.999	140 ± 120	0.999
Pyrene	−230 ± 1400	0.998	490 ± 1300	0.999	800 ± 3400	0.999

[a] Data calculated via linear regression of Equation 3.7.
[b] Data calculated via nonlinear regression of Equation 3.7.
[c] Data calculated via nonlinear regression of Equation 3.6
DNC… Regression did not converge.

In addition, the angular *ortho*-condensed structure of phenanthrene had a lower K_{eq} value than the corresponding linear *ortho*-condensed structure of anthracene. These trends provide important insight into the transport effects of SDS in environmental systems as well.

3.3.2 Transport Effects of Lithium Perfluorooctane Sulfonate

Initial studies were performed in order to obtain information on retention factors and the elution order of the model analytes in the perfluorinated surfactant solution, since this information was not available. The experimental k values for each analyte in 0.1 M LiPFOS are summarized in Table 3.2. The elution order for the analytes was similar to that in 0.1 M SDS, with the notable exception that phenanthrene eluted after anthracene.

In comparing the retention factors in 0.1 M LiPFOS to that in pure water (Table 3.2), the values decreased by 25 to 57 % for benzene and the monohalogenated benzenes. Correspondingly, the linear velocities increased by 18 to 103 %. It is apparent that LiPFOS increases chromatographic transport of benzene and the substituted benzenes and, by implication, increases environmental transport as well.

While the retention factors of the analytes decreased in both surfactant solutions, LiPFOS exhibited a lesser effect than SDS. In comparing the experimental results in 0.1 M LiPFOS to that in 0.1 M SDS, the k values increased by 23 to 112 % for benzene, the monohalogenated benzenes, and hexafluorobenzene, and by 255 to 1470 % for hexachlorobenzene and the PAHs. Correspondingly, the linear velocities decreased by 10 to 41 % for the substituted benzenes and by 63 to 92 % for the PAHs. It is apparent that LiPFOS induces less chromatographic and environmental transport than does SDS for these analytes.

Based on the data obtained in this initial study, further studies with LiPFOS were separated into two concentration ranges. For analytes with k values less than 10 in Table 3.2, the concentration range of 0.02 – 0.1 M LiPFOS was utilized. For analytes with k values greater than 10, the concentration range of 0.1 – 0.3 M LiPFOS was utilized. Graphs of the inverse retention factor (k^{-1}) versus the concentration of LiPFOS in the micelle (M) are shown in Figures 3.2 and 3.3. Statistical treatment of these graphs via linear regression demonstrated that there was a linear relationship between k^{-1} and M, where the R^2 values were all greater than 0.90 (Table 3.4). From the graphs in Figures 3.2 and 3.3, the overall effect was that the retention of the analytes decreased as the concentration of LiPFOS increased. In comparing the results for hexafluorobenzene (Figures 3.1 and 3.2), the slope of the line was shallower in LiPFOS than in SDS over the same concentration range. The line for hexafluorobenzene crossed those for chlorobenzene and bromobenzene in LiPFOS, but not in SDS.

Figures 3.2 & 3.3: Plot of inverse retention factor versus the concentration of lithium perfluorooctane sulfonate (LiPFOS) in the micelle. Analytes: (♦) benzene, (■) fluorobenzene, (▲) hexafluorobenzene, (x) chlorobenzene, (∗) bromobenzene, (●) naphthalene, (○) biphenyl, (◊) phenanthrene, (□) anthracene, (Δ) pyrene, (+) hexachlorobenzene. Other experimental conditions as given in the text.

Figure 3.2

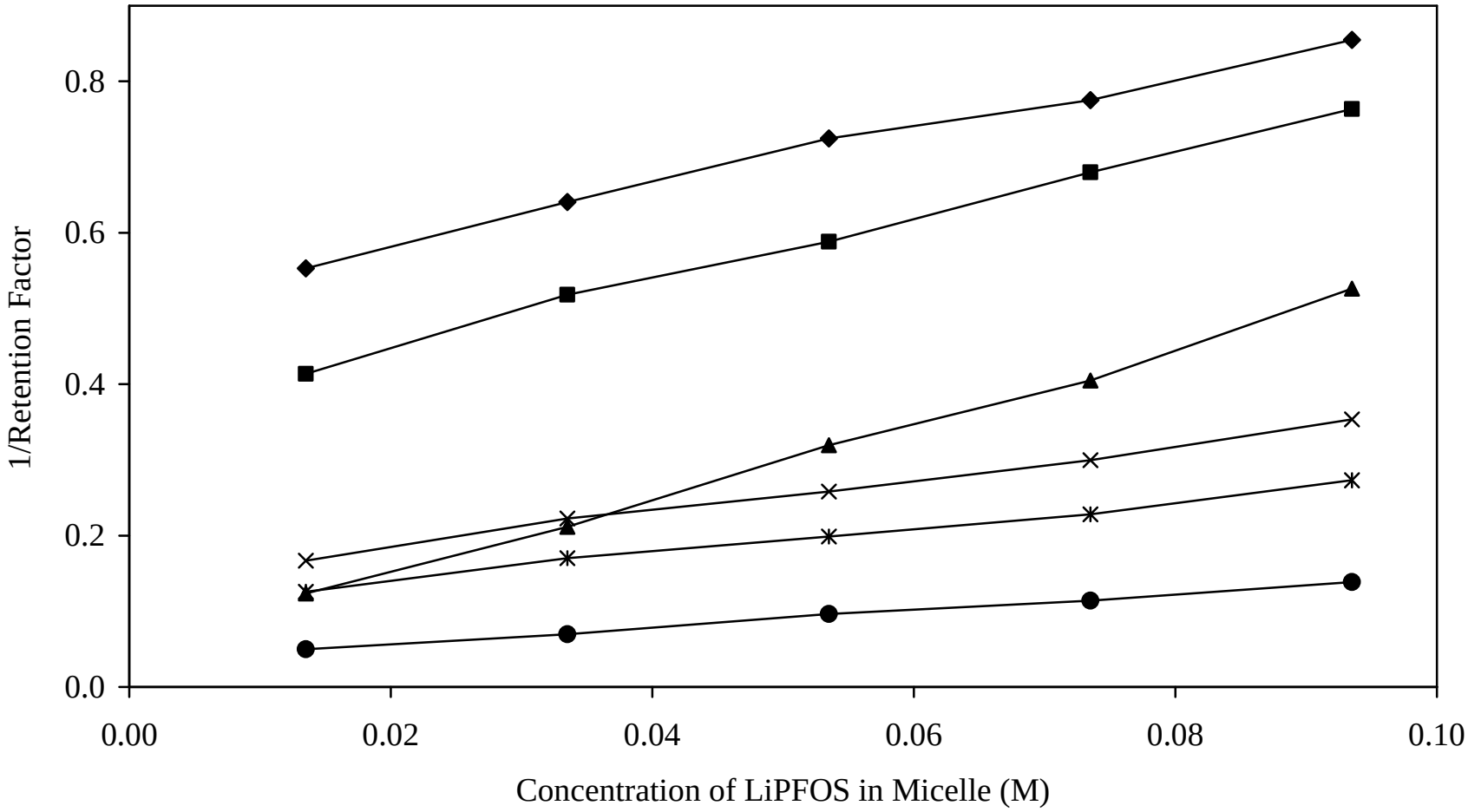
0.8
0.6
0.4
0.2
0.0
1/Retention Factor
0.00
0.02
0.04
0.06
0.08
0.10
Concentration of LiPFOS in Micelle (M)

Figure 3.3

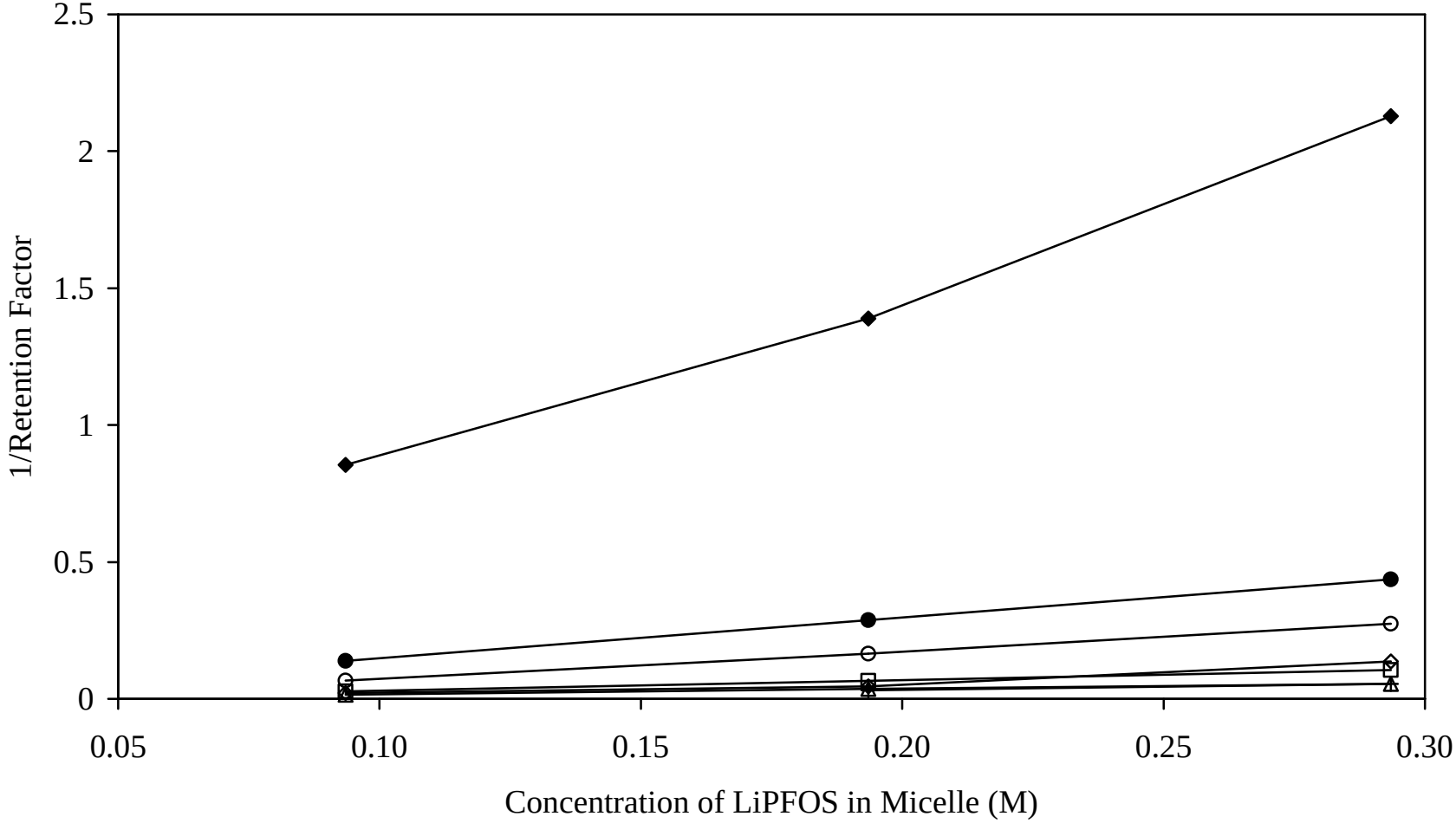
2.5
2
1.5
1
0.5
0
1/Retention Factor
0.05
0.10
0.15
0.20
0.25
0.30
Concentration of LiPFOS in Micelle (M)

Table 3.4: Equilibrium constants of analytes from water to the LiPFOS micelle.

Analyte	LiPFOS					
	Method One[a]		Method Two[b]		Method Three[c]	
	K_{eq} (10^3 M^{-1})	R^2	K_{eq} (10^3 M^{-1})	R^2	K_{eq} (10^3 M^{-1})	R^2
Benzene	0.079 ± 0.004	0.993	0.096 ± 0.009	0.989	0.100 ± 0.010	0.988
Fluorobenzene	0.131 ± 0.005	0.997	0.136 ± 0.006	0.996	0.136 ± 0.008	0.996
Chlorobenzene	0.177 ± 0.011	0.994	0.184 ± 0.011	0.993	0.184 ± 0.014	0.993
Bromobenzene	0.185 ± 0.014	0.992	0.194 ± 0.013	0.992	0.195 ± 0.017	0.992
Hexafluorobenzene	1.1 ± 0.2	0.997	0.869 ± 0.049	0.999	0.876 ± 0.065	0.999
Hexachlorobenzene	[d] −0.187 ± 0.000	1.000	N/A	N/A	N/A	N/A
Naphthalene	0.356 ± 0.025	0.997	0.358 ± 0.021	0.997	0.366 ± 0.027	0.997
Biphenyl	−0.36 ± 0.14	0.999	−0.417 ± 0.045	0.999	DNC	0.973
Phenanthrene	−0.15 ± 0.14	0.901	−0.823 ± 3.12	0.952	DNC	0.933
Anthracene	−0.486 ± 0.003	0.999	−0.488 ± 0.001	0.999	DNC	0.981
Pyrene	−0.673 ± 0.400	0.998	−0.499 ± 0.087	0.999	DNC	0.981

[a] Data calculated via linear regression of Equation 3.7.
[b] Data calculated via nonlinear regression of Equation 3.7.
[c] Data calculated via nonlinear regression of Equation 3.6.
[d] Values for hexachlorobenzene in LiPFOS were calculated from data at two concentrations.
DNC… Regression did not converge.

These two observations suggest that hexafluorobenzene has a high affinity for the perfluorinated surfactant, due to the similarity in their basic structure. This may imply that any highly fluorinated analyte may be selectively transported by LiPFOS in environment systems.

The equilibrium constants, K_{eq}, for the transfer of each analyte from water to the LiPFOS micelle are summarized in Table 3.4. From the K_{eq} values, similar trends are observed for LiPFOS and SDS. As the size, polarizability, and number of halogen substituents increased, so too did the K_{eq} values of the analyte. In addition, the K_{eq} values increased as the number of aromatic rings increased. However, upon more detailed comparison, several differences are observable. The K_{eq} value for hexafluorobenzene was on the same order of magnitude in both LiPFOS and SDS surfactants. The K_{eq} value for monofluorobenzene was an order of magnitude lower in LiPFOS than in SDS, whereas benzene and the other monohalogenated benzenes were more than an order of magnitude lower. These observations suggest that the perfluorinated surfactant maintains some degree of selectivity for analytes with one or more fluorine substituents. The K_{eq} value for naphthalene was two orders of magnitude lower in LiPFOS than in SDS. The lower K_{eq} values show that the analytes exhibit a weaker binding to LiPFOS than to SDS, which results in decreased transport in the perfluorinated surfactant compared to the hydrocarbon surfactant solutions.

The K_{eq} values for the remaining PAHs and hexachlorobenzene could not be reliably determined, due in large part to the uncertainty in the intercept. This uncertainty resulted in negative intercepts and K_{eq} values for these analytes. A possible explanation for this phenomenon is that, for highly retained analytes, the binding constant of the analyte between the bulk mobile phase and the stationary phase, K_1, has a greater impact on transport effects than the binding constant of the analyte between the bulk mobile phase and the surfactant micelle, K_2. According to Equation 3.7, the larger the values of K_1 compared to K_2, the smaller the slope and the closer the intercept to zero. Under these conditions, small imprecision in the retention data can lead to uncertainty in the slope and even larger uncertainty in the intercept. An alternative explanation for this phenomenon is that, for highly retained analytes, the binding constant of the analyte between the surfactant micelle in the mobile phase and the stationary phase, K_3, cannot be considered negligible. This causes the treatment of the retention mechanism using Equations 3.1 and 3.2, substituted into Equation 3.4, to be unreliable. However, treatment using Equations 3.1 and 3.3 or Equations 3.2 and 3.3 yields similarly unreliable results. Hence, it appears that equilibrium constants for highly retained analytes must be determined by other non-chromatographic methods.

3.4 Summary

The overall trend was that an increase in surfactant concentration above the CMC resulted in an increase in transport, relative to that in the system devoid of any surfactant. In general, the transport in the model groundwater system was less in the perfluorinated surfactant solution than in the hydrocarbon surfactant solution. The transport trends of

the individual analytes were similar for the perfluorinated and hydrocarbon surfactants, based on the size, polarizability, and number of halogen substituents on the aromatic compound. Transport trends for large, highly retained analytes could not be reliably elucidated from the equilibrium constants, due to large uncertainty. A more detailed understanding of the retention mechanism of highly retained analytes in reversed-phase micellar liquid chromatography is needed. In addition, studies are needed to further characterize transport effects of perfluorinated surfactants on environmental pollutants, based on different structures of the surfactant.

REFERENCES

3.5 References

[1] D.E. Kile, C.T. Chiou, Environ. Sci. Technol. 23 (1989) 832-838.

[2] D.A. Edwards, R.G. Luthy, Z. Liu, Environ. Sci. Technol. 25 (1991) 127-133.

[3] Y. Moroi, K. Mitsunobu, T. Morisue, Y. Kadobayashi, M. Sakai, J. Phys. Chem. 99 (1995) 2372-2376.

[4] D.J Luning Prak, P.H. Pritchard, Water Res. 36 (2002) 3463-3472.

[5] C.L. Chun, J.-J. Lee, J.-W. Park, Environ. Pollut. 118 (2002) 307-313.

[6] M. Arunyanart, L.J. Cline Love, Anal. Chem. 56 (1984) 1557-1561.

[7] S. Sun, W.P. Inskeep, S.A. Boyd, Environ. Sci. Technol. 29 (1995) 903-913.

[8] C.T. Jafvert, Environ. Sci. Technol. 25 (1991) 1039-1045.

[9] S.-O. Ko, M.A. Schlautman, E.R. Carraway, Environ. Sci. Technol. 32 (1998) 2769-2775.

[10] M.G. Khaledi, J. Chromatogr. A 780 (1997) 3-40.

[11] D.W. Armstrong, Sep. Purif. Methods 14 (1985) 213-304.

[12] B.D. Key, R.D. Howell, C.S. Criddle, Environ. Sci. Technol. 31 (1997) 2445-2454.

[13] K.J. Hansen, L.A. Clemen, M.E. Ellefson, H.O. Johnson, Environ. Sci. Technol. 35 (2001) 766-770.

[14] C. Damas, R. Naejus, R. Coudert, C. Frochot, A. Brembilla, M.-L. Viriot, J. Phys. Chem. B 102 (1998) 10917-10924.

[15] E. Kissa, Fluorinated Surfactants: Synthesis, Properties, and Applications, Marcel Dekker, New York, NY, 1994.

[16] R.E. Banks, B.E. Smart, J.C. Tatlow, Organofluorine Chemistry: Principles and Commercial Applications, Plenum Press, New York, NY, 1994.

[17] P. Varughese, M.E. Gangoda, R.K. Gilpin, J. Chromatogr. Sci. 26 (1988) 401-405.

[18] C.A. Moody, J.A. Field, Environ. Sci. Technol. 34 (2000) 3864-3870.

[19] C.A. Moody, W.C. Kwan, J.W. Martin, D.C.G. Muir, S.A. Mabury, Anal. Chem. 73 (2001) 2200-2206.

[20] C.A. Moody, J.W. Martin, W.C. Kwan, D.C.G. Muir, S.A. Mabury, Environ. Sci. Technol. 36 (2002) 545-551.

[21] A. Tullo, Chem. Eng. News 78(21) (2006) 9-10.

[22] C. Hogue, Chem. Eng. News 84(5) (2006) 8.

[23] C. Hogue, Chem. Eng. News 84(11) (2006) 10.

[24] S.K. Ritter, Chem. Eng. News 82(24) (2004) 44-45.

[25] C. Hogue, Chem. Eng. News 82(35) (2004) 17-19.

[26] S.K. Ritter, Chem. Eng. News 84(5) (2006) 37-40.

[27] K. Shinoda, M. Ható, T. Hayashi, J. Phys. Chem. 76 (1972) 909-914.

[28] Ş. Erkoç, F. Erkoç, J. Molecular Structure (Theochem) 549 (2001) 289-293.

[29] J.P. Giesy, K. Kannan, Environ. Sci. Technol. (2002) 148A-152A.

[30] J.P. Giesy, K. Kannan, Environ. Sci. Technol. 35 (2001) 1339-1342.

[31] K. Kannan, J. Koistinen, K. Beckmen, T. Evans, J.F. Gorzelany, K.J. Hansen, P.D. Jones, E. Helle, M. Nyman, J.P. Giesy, Environ. Sci. Technol. 35 (2001) 1593-1598.

[32] K. Kannan, J.C. Franson, W.W. Bowerman, K.J. Hansen, P.D. Jones, J.P. Giesy, Environ. Sci. Technol. 35 (2001) 3065-3070.

[33] S. Taniyasu, K. Kannan, Y. Horii, N. Yamashita, Organohalogen Compd. 59 (2002) 105-108.

[34] Y.-J. An, E.R. Carraway, M.A. Schlautman, Water Res. 36 (2002) 300-308.

[35] W.L. Hinze, S.G. Weber, Anal. Chem. 63 (1991) 1808-1811.

[36] D. Myers, Surfactant Science and Technology, 3rd Ed., John Wiley and Sons, Hoboken, NJ, 2006, p. 35.

[37] M.M. Singer, R.S. Tjeerdema, Rev. Environ. Contam. Toxicol. 133 (1993) 95-149.

[38] United States Environmental Protection Agency, Prevention, Pesticides and Toxic Substances (7505C), EPA-730-F-99-009, 1999.

[39] W. Hu, P.R. Haddad, Anal. Commun. 35 (1998**)** 191-194.

CHAPTER 4: COMPARISON OF TRANSPORT EFFECTS OF PERFLUORINATED AND HYDROCARBON SURFACTANTS BELOW THE CRITICAL MICELLE CONCENTRATION: NEUTRAL ANALYTES

4.1 Introduction

The addition of certain reagents (e.g. amphiphilic ions, surfactants, etc.) to the mobile phase in a reversed-phase liquid chromatography system can be used to adjust the separation of oppositely charged metal ions and ionic compounds in solution [1]. This technique has been given many different names throughout the years such as ion interaction chromatography [2], soap chromatography [3], ion-exchange chromatography [4], and ion-pair chromatography [5]. It has been postulated that the inclusion of an ion interaction reagent could either increase (through partition) or decrease (through competition for adsorption sites) the retention of a neutral compound [6,7]. However, the change in retention of neutral compounds is so small that an apparent lack of retention dependence on surfactant has been claimed [8]. This correlates with information in the literature that states the effectiveness of the surfactant monomers to enhance the solubility of neutral hydrophobic organic compounds is substantially less than that of surfactant aggregates formed above the critical micelle concentration (CMC) [9-11].

Perfluorinated surfactants, which have different physical and chemical characteristics than hydrocarbon surfactants, have been detected in the environment at concentrations lower than their CMC [12-15]. Previous studies of perfluorinated surfactants have focused on their bioaccumulation and global distribution [16-20], their ability to enhance the solubilization of polycyclic aromatic hydrocarbons [21], and transport effects above their CMC on neutral hydrophobic compounds [22]. Despite these important studies, relatively little information is available regarding the effects of

low levels of perfluorinated surfactants on the transport of other environmental contaminants.

The main focus of this study is to compare the effects of perfluorinated and hydrocarbon surfactants below their CMC on the transport of neutral hydrophobic environmental contaminants in a groundwater system. Reversed-phase liquid chromatography (RPLC) is used as a model for the groundwater system, with lithium perfluorooctane sulfonate and sodium dodecyl sulfate as representatives of the two classes of surfactants. Benzene, toluene, ethylbenzene, and *p*-xylene are chosen as representatives of the BTEX compounds. In addition, several monohalogenated benzenes were chosen as models of halogenated environmental pollutants. The results of this study yield information concerning the retention factors and several selectivity factors of the model pollutants. These values can be used to elucidate the transport effects of perfluorinated surfactants on pollutants that might leach from waste disposal, underground gas tanks, or other contaminated sites into an aquifer.

4.2 Experimental Methods

4.2.1 Mobile Phase and Analytes

The hydrocarbon surfactant, sodium dodecyl sulfate (SDS), was obtained from Aldrich and was used as received. The perfluorinated surfactant, lithium perfluorooctane sulfonate (LiPFOS), was prepared by dissolving the appropriate amounts of heptadecafluorooctane sulfonic acid (TCI America) and lithium hydroxide monohydrate (99.95 %, Aldrich) in deionized, distilled water (Corning Mega-Pure, Models D2 and MP-3A). The aqueous surfactant solutions were prepared by dissolving the appropriate amount of surfactant in deionized, distilled water. The solutions were then filtered

through a cellulose acetate membrane (Alltech) with a 0.45 μm pore size. The surfactant mobile phase solutions were adjusted to pH 4.00 ± 0.10 with hydrochloric acid. An aqueous stock solution of lithium nitrate (1.0×10^{-1} M, Spectrum Chemical) was prepared in deionized, distilled water. The analytes fluorobenzene, chlorobenzene, bromobenzene, benzene, toluene, ethylbenzene, and *p*-xylene (Aldrich) were used as received. Stock solutions of 9.0×10^{-1} M for the monohalogenated benzenes, 5.0×10^{-2} M for benzene, and 1.0×10^{-1} M for the remaining BTEX compounds were prepared in high-performance liquid chromatography-grade methanol (Spectrum Chemical). Analytical samples were prepared by diluting the proper amount of stock solution and aqueous lithium nitrate ($LiNO_3$) solution with the surfactant solution to acquire the working concentrations in a 2 mL final volume. Where necessary, the stock solutions were evaporated with nitrogen, such that the residual concentration of methanol was less than 1 % (v/v) in the final analytical sample. The working concentrations in the analytical samples were $LiNO_3$ (1.00×10^{-2} M), fluorobenzene (5.82×10^{-4} M), chlorobenzene (5.37×10^{-4} M), bromobenzene (5.18×10^{-4} M), benzene (5.00×10^{-4} M), toluene (5.03×10^{-4} M), ethylbenzene (5.03×10^{-4} M), and *p*-xylene (5.03×10^{-4} M).

4.2.2 Experimental System

The experimental chromatographic methods, as detailed in Section 2.2, are briefly recapped in this section. The analytical column (4.6 mm i.d. x 250 mm length) was packed with Poroshell 300SB-C_{18} pellicular particles (Agilent) of 5.0 μm diameter and 6.0 $m^2\ g^{-1}$ surface area, with an octadecylsilica stationary phase of 2.1 μmol m^{-2} bonding

density and 0.39 % carbon content. The liquid chromatography system consisted of a single-piston reciprocating pump (Beckman, Model 110B), an injector with a 20 μL injection loop (Valco, Model EC6W), and a UV-visible absorbance detector (Hitachi, Model L-4200). The UV absorbance wavelength of 254 nm was specific for the detection of the analytes, and did not incur any interference from the surfactants. Chromatograms were recorded on a chart recorder (Linear Cole-Parmer Instrument Company, Model 0555-0000). All experiments were carried out at ambient temperature with a maximum pressure limit of 4500 psi. The flow rate was 1.0 mL min^{-1} during the SDS experiments and 0.5 mL min^{-1} during the LiPFOS and pure water experiments. The void time, t_0, was taken as the first positive deviation from the baseline arising from $LiNO_3$ in each sample. The retention time, t_R, for each analyte was determined from the peak maximum, which is appropriate for the symmetric Gaussian peaks observed in this study. The retention factor, k, was then calculated by

$$k = \frac{t_R - t_0}{t_0} \tag{4.1}$$

The k values (average of at least three trials) were used for the subsequent elucidation of transport effects and determination of selectivity factors as described in the following section.

4.2.3 Data Analysis

4.2.3.1 Retention Factor Measurements

In order to elucidate meaningful information regarding the transport effects of perfluorinated surfactants in an environmental system, an analytical technique was used that could fundamentally resemble such a system, but whose parameters were

controllable. Reversed-phase liquid chromatography (RPLC) was used to model the environmental system, in which the octadecylsilica stationary phase represents soil and the aqueous mobile phase represents groundwater. When a surfactant is added to the system below its CMC, the monomers distribute or partition between the mobile and stationary phases. These surfactant monomers have the potential to alter the retention of the analytes (pollutants).

In the RPLC system, the retention of a neutral analyte is mainly controlled by a partitioning phenomenon, where the analyte is in equilibrium between the mobile and stationary phases. The equilibrium constant, K, can be defined as

$$K = \frac{a_S}{a_M} = \frac{\gamma_S C_S}{\gamma_M C_M} \tag{4.2}$$

where a_S and a_M represent the activities, γ_S and γ_M represent the activity coefficients, and C_S and C_M represent the analytical concentrations of the analyte in the stationary (S) and mobile (M) phases, respectively. Assuming the activity coefficients are equal to unity, Equation 4.2 indicates that the equilibrium constant is directly related to the ratio of the analyte concentrations in the stationary and mobile phases. This equilibrium constant represents all interactions between the analyte, stationary phase, mobile phase, and surfactant monomers. However, the determination of this equilibrium constant is difficult because of the inability to directly measure the concentrations of the analyte in the mobile and stationary phases.

The retention factor, k, is defined as

$$k = K\phi \tag{4.3}$$

where ϕ is the phase ratio, defined as

$$\phi = \frac{V_S}{V_M} \tag{4.4}$$

where V_M and V_S are the volumes of the mobile and stationary phase, respectively. Assuming that the phase ratio is constant, the value for k is proportional to K. Consequently, the trends in retention factor are consistent with and can be used to predict the trends in equilibrium constant. In particular, an increase in the retention factor implies an increase in the concentration of the analyte in the stationary phase relative to the mobile phase, according to Equation 4.2.

4.2.3.2 Selectivity Factor Calculations

In addition to the retention factors, several selectivity factors are also compared to elucidate transport effects. Each selectivity factor provides different information concerning the various interactions between the analytes and the surfactants.

The first selectivity factor, α_1, is defined as the ratio of the retention factor of an analyte to that of benzene, while all other experimental conditions remain constant.

$$\alpha_1 = \frac{k_{analyte}}{k_{benzene}} \tag{4.5}$$

The value for α_1 is related to the effect of the addition of a substituent group to the benzene structure on the transport of the model analytes. As α_1 increases, the additional substituent group leads to increasing interaction of the neutral analyte with the stationary phase.

The second selectivity factor, α_2, is defined as the ratio of the retention factor of an analyte in a surfactant mobile phase to that of the same analyte in pure water, while all other experimental conditions remain constant.

$$\alpha_2 = \frac{k_{surfactant}}{k_{water}} \quad (4.6)$$

The value for α_2 is related to the effect of the surfactant monomers on the transport of the model analytes. As α_2 increases, the neutral analyte exhibits a preference of interaction with the surfactant monomers in the stationary phase.

The third selectivity factor, α_3, is defined as the ratio of the retention factor of an analyte in LiPFOS mobile phase to that of the same analyte in SDS mobile phase, while all other experimental conditions remain constant.

$$\alpha_3 = \frac{k_{LiPFOS}}{k_{SDS}} \quad (4.7)$$

The value for α_3 is related to the affinity of the model analyte for LiPFOS compared to SDS. As α_3 increases, the neutral analyte exhibits a greater preference for interaction with LiPFOS than with SDS in the stationary phase.

4.3 Results and Discussion

The rationale behind the choice of stationary phase and surfactants has been discussed in Section 2.2.1 and a previous report [22]. The Poroshell stationary phase was selected because its carbon content (0.39 %) and surface area (6.0 $m^2 g^{-1}$) are within the typical ranges for various soils, bed sediments, and suspended solids [23]. Sodium dodecyl sulfate (SDS) and lithium perfluorooctane sulfonate (LiPFOS) were chosen as representative surfactants because they are used commercially and have been detected in the environment [15-20,24-27]. The analytes represent important classes of environmental contaminants. The BTEX compounds are suspected human carcinogens, which have entered the environment from spills and leakage of underground fuel tanks.

In addition, these analytes can be used to examine if their differences in physical and chemical characteristics influence the transport effects of hydrocarbon and perfluorinated surfactants.

4.3.1 Transport Effects in Water

In order to be able to compare the transport effects of the surfactant monomers, the retention of the neutral analytes was determined in a water mobile phase devoid of surfactants. Three water studies were performed, with the first study taking place before any surfactant was introduced, the second after the SDS study, and the third after the LiPFOS study. In all cases, the elution order for the analytes in the water mobile phase was as follows: benzene < fluorobenzene < toluene <chlorobenzene < bromobenzene < ethylbenzene < *p*-xylene. The retention order followed what is expected for a partition mechanism. The retention factors for the analytes are shown in Table 4.1. A student's t-test was performed at the 95 % confidence level (C.L.), which revealed that the retention factors were statistically different between the first and second studies, but statistically the same between the second and third studies. Based on these results, each surfactant study will be compared with the preceding water study, as described in the following sections.

Table 4.1: Retention factors of analytes in pure water.[a]

Analyte	Retention Factors (k)		
	Study 1[b]	Study 2[c]	Study 3[d]
Benzene	1.94 ± 0.04	1.59 ± 0.04	1.56 ± 0.02
Fluorobenzene	2.43 ± 0.02	1.96 ± 0.03	1.95 ± 0.02
Chlorobenzene	6.82 ± 0.00	5.75 ± 0.09	5.70 ± 0.04
Bromobenzene	10.0 ± 0.0	8.54 ± 0.13	8.47 ± 0.04
Toluene	6.28 ± 0.02	5.38 ± 0.09	5.26 ± 0.00[e]
Ethylbenzene	18.1 ± 0.0	16.2 ± 0.1	15.6 ± 0.1
p-Xylene	20.9 ± 0.1	18.0 ± 0.2	———

[a] Retention factors are an average of at least three injections. Experimental conditions as given in the text.
[b] Measurements in pure water were performed before the SDS mobile phase study.
[c] Measurements in pure water were performed before the LiPFOS mobile phase study.
[d] Measurements in pure water were performed after the LiPFOS mobile phase study.
[e] Single injection of toluene.

4.3.2 Transport Effects of Sodium Dodecyl Sulfate

Injections of the analytes were performed in SDS mobile phases within the concentration range of 1.0 – 5.0 mM. The elution order for the analytes in SDS was identical to that observed in a water mobile phase on the same stationary phase. These results imply that the addition of the surfactant monomers to the system does not change the fundamental partitioning mechanism of the RPLC system, in relation to a pure water system.

The experimental retention factors for the BTEX compounds and the monohalogenated benzenes are summarized in Table 4.2. In comparing the k values in 1.0 mM SDS to those in pure water, the values increased by 2 to 15 %. A larger increase of 8 to 34 % was observed upon comparing the k values in 5.0 mM SDS to those in pure water. Statistical treatment of the data via a t-test at the 95 % C.L. shows that the overall increase in k values with an increase in SDS concentration is statistically significant in all cases. Consistently, fluorobenzene displayed a relatively small increase, whereas chlorobenzene and bromobenzene displayed the largest increases.

A graph of the logarithmic retention factor versus the concentration of SDS is shown in Figure 4.1. Statistical treatment of these graphs via linear regression demonstrated that there was an increasing linear relationship between k and surfactant concentration, where the R^2 values were greater than 0.91 for chlorobenzene, bromobenzene, and toluene. The R^2 values were between 0.46 – 0.75 for fluorobenzene, ethylbenzene, benzene, and *p*-xylene. Although several R^2 values were less than 0.90, the slope of each line was statistically greater than zero when tested at the 95 % C.L.

Table 4.2: Retention and selectivity factors of analytes in pure water and SDS mobile phases.[a]

Analyte	Retention Factors (k)			Selectivity Factors (α)	
	Pure Water[b]	1.0 mM SDS	5.0 mM SDS	α_1[c]	α_2[d]
Benzene	1.94 ± 0.04	2.02 ± 0.04	2.19 ± 0.04	1.00 ± 0.03	1.13 ± 0.03
Fluorobenzene	2.43 ± 0.02	2.51 ± 0.08	2.66 ± 0.08	1.21 ± 0.04	1.09 ± 0.04
Chlorobenzene	6.82 ± 0.00	7.75 ± 0.12	9.01 ± 0.07	4.11 ± 0.08	1.32 ± 0.01
Bromobenzene	10.0 ± 0.0	11.5 ± 0.2	13.4 ± 0.1	6.13 ± 0.12	1.34 ± 0.01
Toluene	6.28 ± 0.02	6.58 ± 0.03	7.09 ± 0.08	3.23 ± 0.07	1.13 ± 0.01
Ethylbenzene	18.1 ± 0.0	19.0 ± 0.2	20.1 ± 0.2	9.17 ± 0.19	1.11 ± 0.01
p-Xylene	20.9 ± 0.1	21.4 ± 0.0	22.5 ± 0.5	10.2 ± 0.3	1.07 ± 0.02

[a] Retention and selectivity factors are an average of at least three injections. Experimental conditions as given in the text.
[b] Measurements in pure water were performed before the SDS mobile phase study.
[c] Selectivity factors calculated between analyte and benzene in 5.0 mM SDS (Equation 4.5).
[d] Selectivity factors calculated for analyte between 5.0 mM SDS and pure water (Equation 4.6).

Figure 4.1: Graph of the logarithmic retention factor versus the concentration of sodium dodecyl sulfate (SDS) in the micelle. Analytes: (♦) benzene, (■) fluorobenzene, (x) chlorobenzene, (∗) bromobenzene, (▲) toluene, (○) *p*-xylene, (●) ethylbenzene. Other experimental conditions as given in the text.

Figure 4.1

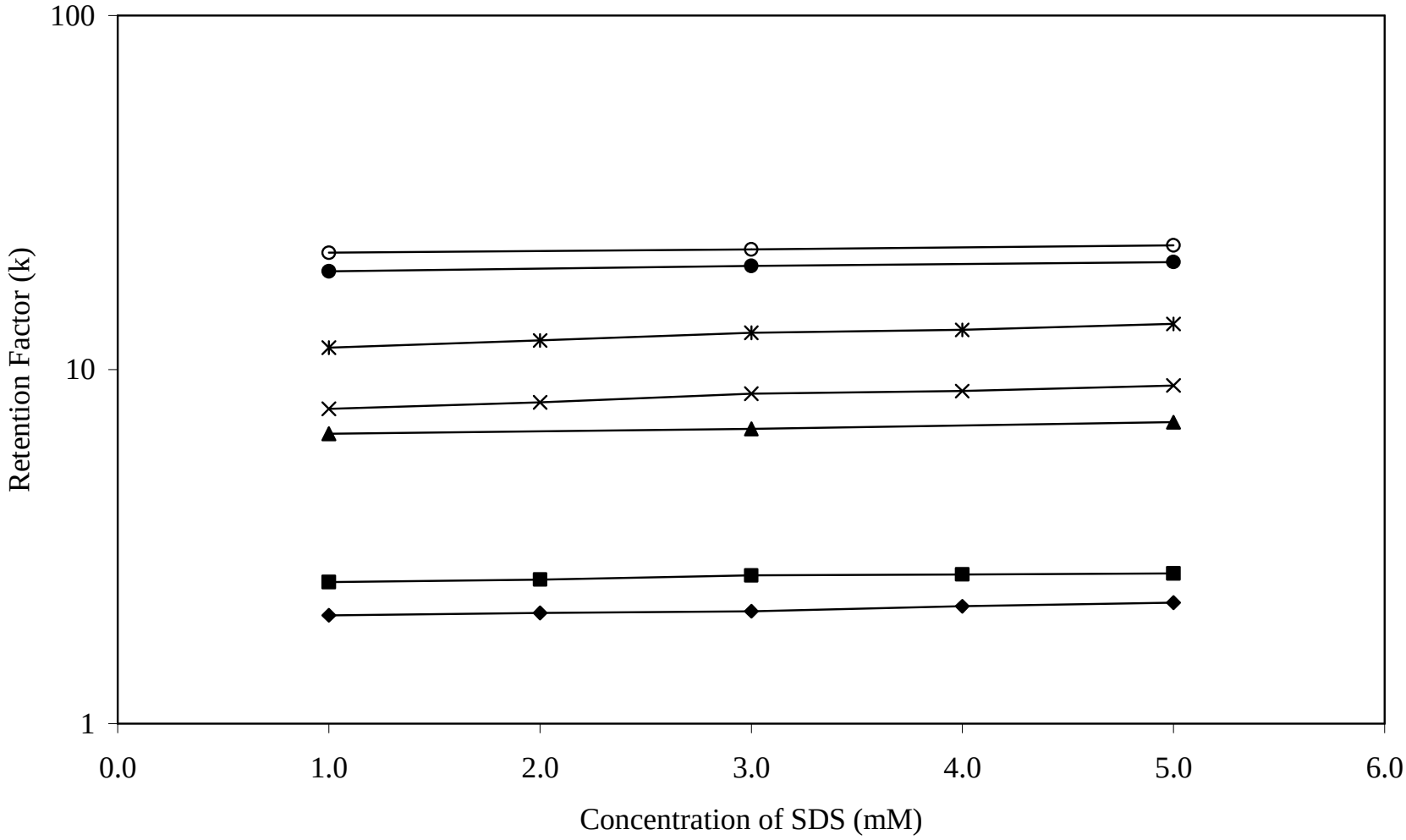
100
10
1
Retention Factor (k)
0.0
1.0
2.0
3.0
4.0
5.0
6.0
Concentration of SDS (mM)

Based on these results, the overall effect was that the retention of the analytes increased as the concentration of SDS increased. Consequently, SDS decreases chromatographic transport of benzene and the substituted benzenes and, by implication, decreases environmental transport as well.

The selectivity factor α_1 was calculated from the average retention factors of the analyte and benzene (Equation 4.5), with representative data summarized in Table 4.2. All α_1 values were greater than or equal to unity, which suggests that all substituents increased the analyte interaction with the stationary phase. It was observed that α_1 values increased as the size of the substituent increased for the series of monohalogenated benzenes and the BTEX compounds. For example, the α_1 values increased from 1.2 to 6.1 as the size of the halogen substituent increased from fluorine to bromine (Table 4.2). The α_1 data were statistically treated via linear regression and a t-test at the 95 % C.L. These results demonstrated that there is an increasing linear trend between α_1 values and increasing SDS concentration for chlorobenzene and bromobenzene. For the remaining analytes, the α_1 values were either statistically invariant (toluene, ethylbenzene, and fluorobenzene) or statistically decreasing (*p*-xylene) with increasing SDS concentration. This result suggests that the inclusion of chlorine and bromine substituents increases the interaction of a pollutant with in the stationary phase as the SDS concentration increases. In contrast, fluorine and short-chain alkyl substituents have little or no interaction.

The selectivity factor α_2 was calculated from the average retention factors of the analyte in surfactant and water mobile phases (Equation 4.6), with representative data summarized in Table 4.2. All α_2 values were greater than unity at each SDS mobile

phase concentration. It was observed that α_2 values were consistently the highest for chlorobenzene and bromobenzene, while relatively low for fluorobenzene. The α_2 values for the remaining analytes were grouped within a similar range. Statistical treatment shows that there is an increasing linear trend between α_2 values and increasing SDS concentration for all analytes. These results suggest that chlorobenzene and bromobenzene have increased interaction with SDS surfactant monomers in the stationary phase, compared to a system devoid of surfactant. The interaction of the remaining analytes with SDS monomers is of similar but smaller magnitude.

4.3.3 Transport Effects of Lithium Perfluorooctane Sulfonate

Injections of the analytes were performed in LiPFOS mobile phases over the same concentration range as SDS (1.0 – 5.0 mM). The elution order for the analytes in LiPFOS was identical to that observed in pure water and SDS mobile phases on the same stationary phase. These results imply that the addition of the perfluorinated surfactant does not change the fundamental partitioning mechanism of the RPLC system, in relation to a system devoid of a surfactant or containing a hydrocarbon surfactant.

The experimental k values for each analyte in LiPFOS mobile phases are summarized in Table 4.3. In comparing 1.0 mM LiPFOS to pure water, the k values increased by 2 to 18 % for the BTEX and the monohalogenated benzenes, except for bromobenzene which decreased by 3 %. In comparing 5.0 mM LiPFOS to pure water, the majority of analytes displayed a decrease in k values (3 to 18 %), with the exceptions of benzene, toluene, and fluorobenzene. Statistical treatment of the data via a t-test at the 95 % C.L. shows that the overall decrease in k values with an increase in LiPFOS concentration is statistically significant in all cases.

Table 4.3: Retention and selectivity factors of analytes in pure water and LiPFOS mobile phases.[a]

Analyte	Retention Factors (k)			Selectivity Factors (α)		
	Pure Water[b]	1.0 mM LiPFOS	5.0 mM LiPFOS	α_1[c]	α_2[d]	α_3[e]
Benzene	1.59 ± 0.04	1.76 ± 0.04	1.62 ± 0.09	1.00 ± 0.08	1.02 ± 0.06	0.74 ± 0.04
Fluorobenzene	1.96 ± 0.03	2.31 ± 0.01	2.16 ± 0.12	1.31 ± 0.11	1.10 ± 0.07	0.81 ± 0.05
Chlorobenzene	5.75 ± 0.09	5.99 ± 0.02	5.19 ± 0.25	3.20 ± 0.24	0.90 ± 0.05	0.58 ± 0.03
Bromobenzene	8.54 ± 0.13	8.31 ± 0.06	7.01 ± 0.29	4.33 ± 0.31	0.82 ± 0.04	0.52 ± 0.02
Toluene	5.38 ± 0.09	5.96 ± 0.15	5.40 ± 0.10	3.33 ± 0.20	1.00 ± 0.03	0.76 ± 0.02
Ethylbenzene	16.2 ± 0.1	16.6 ± 0.1	15.3 ± 0.1	9.41 ± 0.54	0.94 ± 0.01	0.76 ± 0.01
p-Xylene	18.0 ± 0.2	19.7 ± 0.6	17.5 ± 0.1	10.8 ± 0.6	0.97 ± 0.02	0.78 ± 0.02

[a] Retention factors are an average of at least three injections. Experimental conditions as given in the text.
[b] Measurements in pure water were performed before the LiPFOS mobile phase study.
[c] Selectivity factors calculated between analyte and benzene in 5.0 mM LiPFOS (Equation 4.5).
[d] Selectivity factors calculated for analyte between 5.0 mM LiPFOS and pure water (Equation 4.6).
[e] Selectivity factors calculated for analyte between 5.0 mM LiPFOS and 5.0 mM SDS (Equation 4.7).

Consistently, fluorobenzene displayed the smallest decrease, whereas chlorobenzene and bromobenzene displayed the largest decrease.

Overall, the retention factors for each analyte were lower in LiPFOS than those in SDS mobile phases of identical concentrations. With regard to 1.0 mM LiPFOS (Table 4.3) and 1.0 mM SDS (Table 4.2), the k values decreased by 8 to 13 % for the BTEX analytes and by 8 to 28 % for the monohalogenated benzenes. The difference in k values became more pronounced at concentrations of 5.0 mM for both surfactants, as the decrease in k values almost doubles or triples in some cases. It is apparent that LiPFOS induces less retention and, hence more transport, than does SDS for these analytes.

A graph of the logarithmic retention factor versus the concentration of LiPFOS is shown in Figure 4.2. Statistical treatment of these graphs via linear regression demonstrated that there was a decreasing linear relationship between k and surfactant concentration, where the R^2 values were between 0.85 – 0.96 for *p*-xylene, chlorobenzene, bromobenzene, and ethylbenzene. The R^2 values were between 0.31 – 0.54 for toluene, benzene, and fluorobenzene. Although several R^2 values were less than 0.90, the slope of each line was statistically less than zero when tested at the 95 % C.L. Based on these results, the overall effect was that the retention of the analytes decreased as the concentration of LiPFOS increased. Consequently, LiPFOS increases chromatographic transport of benzene and the substituted benzenes and, by implication, increases environmental transport as well.

Figure 4.2: Graph of logarithmic retention factor versus the concentration of lithium perfluorooctane sulfonate (LiPFOS) in the micelle. Analytes: (♦) benzene, (■) fluorobenzene, (x) chlorobenzene, (∗) bromobenzene, (▲) toluene, (○) *p*-xylene, (●) ethylbenzene. Other experimental conditions as given in the text.

Figure 4.2

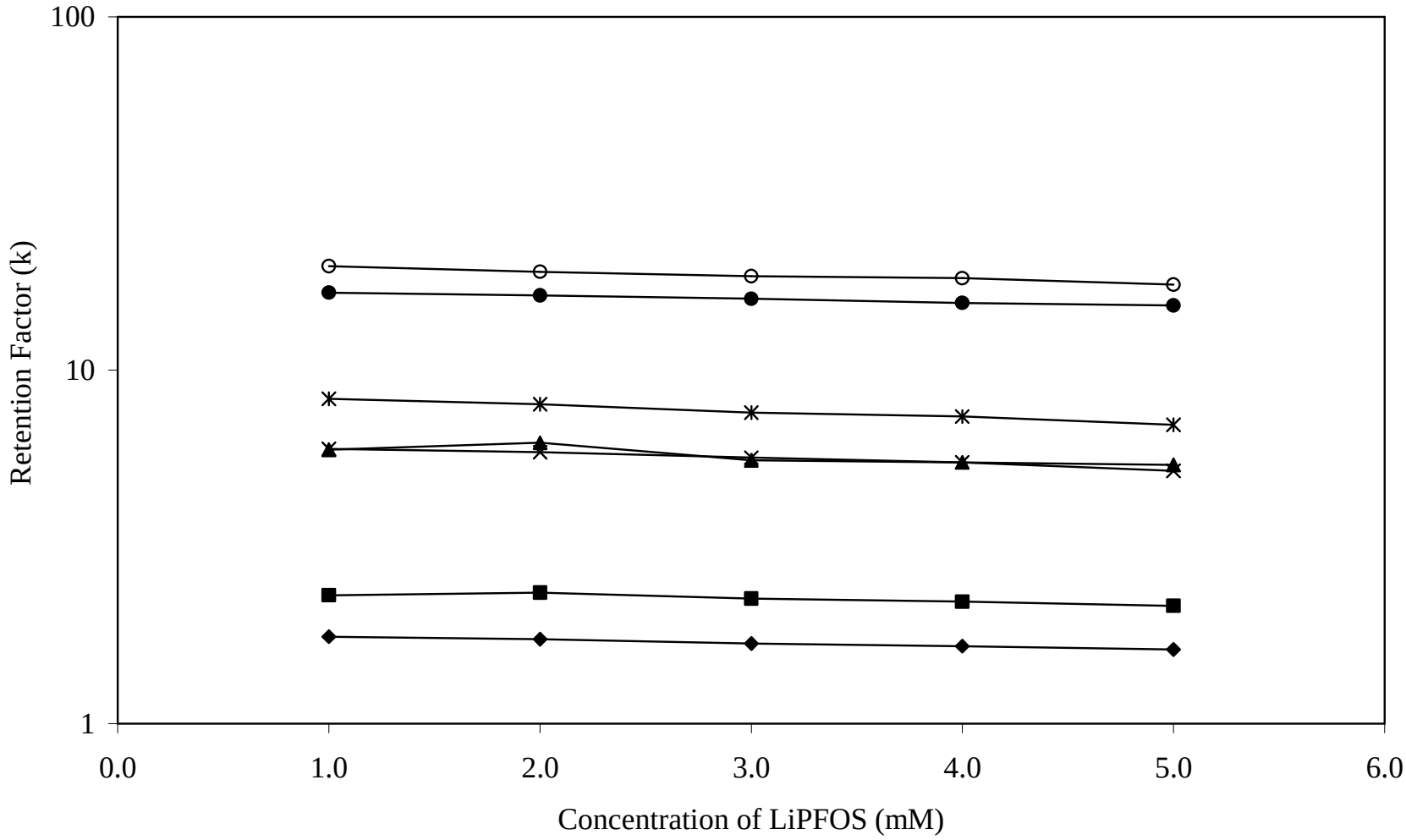
100
10
1
Retention Factor (k)
0.0
1.0
2.0
3.0
4.0
5.0
6.0
Concentration of LiPFOS (mM)

The selectivity factor α_1 was calculated from the average retention factors of the analyte and benzene (Equation 4.5), with representative data summarized in Table 4.3. All α_1 values were greater than or equal to unity, as observed previously for SDS. The α_1 values were greater in LiPFOS (Table 4.3) than SDS (Table 4.2) for all analytes, with the exception of chlorobenzene and bromobenzene. Identical in trend to SDS, the α_1 values increased as the size of the substituent increased for the series of monohalogenated benzenes and the BTEX compounds. The α_1 data were statistically treated via linear regression and a t-test at the 95 % C.L. These results demonstrated that there is a decreasing linear trend between α_1 values and increasing LiPFOS concentration for chlorobenzene, bromobenzene, and *p*-xylene. For the remaining analytes, the α_1 values were statistically invariant (toluene, ethylbenzene, and fluorobenzene) with increasing LiPFOS concentration. This suggests that the inclusion of the chlorine and bromine substituents decreases the interaction of a pollutant with LiPFOS monomers in the stationary phase.

The selectivity factor α_2 was calculated from the average retention factors of the analytes in surfactant and water mobile phases (Equation 4.6), with representative data summarized in Table 4.3. The α_2 values were slightly greater than or equal to unity at all mobile phase concentrations for benzene, fluorobenzene, and toluene. The α_2 values were less than unity at all mobile phase concentrations for bromobenzene. The α_2 values for chlorobenzene and ethylbenzene were slightly greater than unity at low concentrations (1.0 – 2.0 mM LiPFOS) and less than unity at higher concentrations (3.0 – 5.0 mM LiPFOS). It was observed that α_2 values were the lowest for chlorobenzene,

bromobenzene, and ethylbenzene, while fluorobenzene had the highest α_2 values at all LiPFOS concentrations. Statistical treatment of the α_2 data shows that there is a decreasing linear trend between α_2 values and increasing LiPFOS concentration for all analytes. These results suggest that chlorobenzene and bromobenzene have decreased interaction with the LiPFOS surfactant monomers adsorbed on the stationary phase. However, fluorobenzene, which is more chemically similar to LiPFOS than the other analytes, displayed an increased interaction with LiPFOS surfactant monomers adsorbed on the stationary phase. These results are consistent with those for α_1 summarized above.

The selectivity factor α_3 was calculated from the average retention factors of the analytes in LiPFOS and SDS mobile phases (Equation 4.7), with representative data summarized in Table 4.3. All α_3 values were less than unity, which suggests that all analytes had a greater affinity for SDS surfactant in the stationary phase than for LiPFOS. It was observed that α_3 values were the lowest for chlorobenzene and bromobenzene and highest for fluorobenzene at all surfactant concentrations. These results are consistent with those for α_2 summarized above, which indicate that chlorobenzene and bromobenzene have the least interaction with LiPFOS, and fluorobenzene has the greatest interaction. Statistical treatment of the α_3 data shows that there is a decreasing linear trend between α_3 values and increasing surfactant concentration for all analytes. Hence, the affinity of the analytes for SDS relative to LiPFOS becomes more pronounced with increasing surfactant concentration. From these results, it is apparent that increasing SDS concentration induces more retention and, hence less chromatographic and environmental transport, than does increasing LiPFOS concentration.

4.3.4 Effect of Ionic Surfactant on the Polarity of the System

In a RPLC system, analyte retention can be described by a partition mechanism. Partitioning occurs as the analyte distributes between a polar mobile phase and a non-polar stationary phase. Neutral, non-polar analytes are more likely to partition into the stationary phase and be retained. The addition of a surfactant monomer to the RPLC system can lead to a change in polarity of the system, which can lead to a change in retention compared to a pure water system.

The retention factor of an analyte in a RPLC system can be related to the Hildebrand solubility parameter (δ) [28] by the following equation

$$\ln k = \frac{V_i}{RT}\left[\left(\delta_i - \delta_M\right)^2 - \left(\delta_i - \delta_S\right)^2\right] - \ln \phi \qquad (4.8)$$

where V_i is the molar volume of the analyte, R is the gas constant, T is the absolute temperature, and δ_i, δ_M, and δ_S are the solubility parameters of the analyte, mobile phase, and stationary phase, respectively [29,30]. In RPLC, the analytes are often intermediate in polarity, such that $\delta_M > \delta_i > \delta_S$. For a given analyte, the balance of interactions with the mobile phase ($\delta_i - \delta_M$) and stationary phase ($\delta_i - \delta_S$) controls the retention factor. Upon the addition of a surfactant to the RPLC system, the monomers can partition into the octadecylsilica stationary phase. The SDS surfactant (δ_{SDS} = 29 $MPa^{1/2}$ [31]) will cause the overall δ_S of the stationary phase to increase, leading to an increase in retention factors according to Equation 4.8. However, the fluoroalkyl chain of LiPFOS ($\delta_{C8F18} \approx$ 11.7 $MPa^{1/2}$ [31]) is much less polar than the alkyl chain of SDS ($\delta_{C12H26} \approx$ 16.1 $MPa^{1/2}$ [31]). Thus, the LiPFOS surfactant will cause the overall δ_S of the stationary phase to

decrease, leading to a decrease in retention factors according to Equation 4.8. The results observed in this study are consistent with the general predictions of this model, thus leading to the conclusion that the change in analyte retention arises from the change in polarity of the system.

4.3.5 Effect of Ionic Surfactant on the Solubility of the Analytes

It has been reported in the literature that the addition of ionic species to pure water can change the solubility of neutral non-polar analytes [32,33]. Therefore, it is possible that this is the origin of the change in retention, rather than the change in polarity of the stationary phase as described above. To examine this possibility, a study was conducted to evaluate whether changes in the analyte retention were due to "salting out" (hydrophobic effect) caused by the addition of the ionic surfactant. In order to simulate the effects at the highest surfactant concentration used in this study, a 5.0 mM aqueous lithium nitrate ($LiNO_3$) mobile phase was used. The retention factors of the BTEX compounds (excluding *p*-xylene) and the monohalogenated benzenes were calculated, with representative data summarized in Table 4.4. Statistical treatment via a t-test at the 95 % C.L. demonstrated that the k values were statistically the same as those determined in pure water mobile phase.

Table 4.4: Retention and selectivity factors of analytes in pure water and $LiNO_3$ mobile phases.[a]

Analyte	Retention Factors (k)		Selectivity Factors (α)
	Pure Water[b]	5.0 mM $LiNO_3$	α_4[c]
Benzene	1.56 ± 0.02	1.55 ± 0.04	0.99 ± 0.03
Fluorobenzene	1.95 ± 0.02	1.96 ± 0.06	1.00 ± 0.03
Chlorobenzene	5.70 ± 0.04	5.72 ± 0.15	1.00 ± 0.03
Bromobenzene	8.47 ± 0.04	8.48 ± 0.22	1.00 ± 0.03
Toluene	5.26 ± 0.00[d]	5.27 ± 0.03	1.00 ± 0.01
Ethylbenzene	15.6 ± 0.1	15.5 ± 0.2	0.99 ± 0.01

[a] Retention factors are an average of at least three injections, except as noted below. Experimental conditions as given in the text.
[b] Measurements in pure water were performed before the $LiNO_3$ mobile phase study.
[c] Selectivity factors calculated for analyte between 5.0 mM LiPFOS and pure water (equation 9).
[d] Single injection of toluene.

The fourth selectivity factor, α_4, is defined as the ratio of the retention factor of an analyte in a 5.0 mM $LiNO_3$ mobile phase to that of the same analyte in pure water, while all other experimental conditions remain constant.

$$\alpha_4 = \frac{k_{LiNO_3}}{k_{water}} \tag{4.9}$$

The value for α_4 is related to the hydrophobic effect of the $LiNO_3$ salt in the RPLC system on the transport of the analytes. As the values of α_4 are statistically equal to unity (Table 4.4), there is no hydrophobic effect caused by the addition of the ionic salt at the concentration of 5.0 mM. These results lend credibility to the claim that the addition of the ionic surfactants (within the same experimental concentration range) does not induce a hydrophobic effect on the analytes in the aqueous mobile phases used in this study.

4.4 Summary

During this study, the effects of a hydrocarbon and perfluorinated surfactant below their CMC were determined on the transport of environmental contaminants in a model groundwater system. The overall trend was that an increase in surfactant concentration below the CMC resulted in a statistically significant change in the transport relative to that in the system devoid of any surfactant. The addition of the hydrocarbon surfactant below the CMC statistically decreased transport of the analytes in the model groundwater system, while the addition of the perfluorinated surfactant statistically increased transport. It is postulated that the adsorption of the hydrocarbon surfactant to the stationary phase lead to increased analyte interaction, which caused the decrease in analyte transport. The transport trends of the individual analytes were similar based on size of the substituent in both surfactants. Transport trends of chlorobenzene and

bromobenzene were opposite that of fluorobenzene in both the hydrocarbon and perfluorinated surfactant. The fluorinated analyte displayed a greater interaction with the perfluorinated surfactant below the CMC. Further studies are needed to characterize transport effects of perfluorinated surfactants on environmental pollutants, based on different carbon chain lengths ($C_4 – C_8$) and head group (sulfonate, carboxylate, etc.) of the surfactant.

REFERENCES

4.5 References

[1] J. Ståhlberg, J. Chromatogr. A 855 (1999) 3-55.

[2] B.A. Bidlingmeyer, S.N. Deming, W.P. Price Jr., B. Sachok, M. Petrusek, J. Chromatogr. 186 (1979) 420-434.

[3] J.H. Knox, G.R. Laird, J. Chromatogr. 122 (1976) 17-34.

[4] J.C Kraak, K.M. Jonker, J.F.K. Huber, J. Chromatogr. 142 (1977) 671-688.

[5] B. Fransson, K.G. Wahlund, I.M. Johansson, G. Schill, J. Chromatogr. 125 (1976) 327-344.

[6] T. Cecchi, F. Pucciarelli, P. Passamonti, Chromatographia 53 (2001) 27-34.

[7] J.R. Jezorek, K.A. Wagner, J. Chromatogr. A 776 (1997) 221-231.

[8] C. Sarzanini, M.C. Bruzzoniti, G. Sacchero, E. Mentasti, Anal. Chem. 68 (1996) 4494-4500.

[9] D.E. Kile, C.T. Chiou, Environ. Sci. Technol. 23 (1989) 832-838.

[10] D.A. Edwards, R.G. Luthy, Z. Liu, Environ. Sci. Technol. 25 (1991) 127-133.

[11] S.O. Ko, M.A. Schlautman, E.R. Carraway, Environ. Sci. Technol. 32 (1998) 2769-2775.

[12] C.A. Moody, J.A. Field, Environ. Sci. Technol. 34 (2000) 3864-3870.

[13] C.A. Moody, W.C. Kwan, J.W. Martin, D.C.G. Muir, S.A. Mabury, Anal. Chem. 73 (2001) 2200-2206.

[14] C.A. Moody, J.W. Martin, W.C. Kwan, D.C.G. Muir, S.A. Mabury, Environ. Sci. Technol. 36 (2002) 545-551.

[15] United States Environmental Protection Agency, Prevention, Pesticides and Toxic Substances (7505C), EPA-730-F-99-009, 1999.

[16] J.P. Giesy, K. Kannan, Environ. Sci. Technol. (2002) 148A-152A.

[17] J.P. Giesy, K. Kannan, Environ. Sci. Technol. 35 (2001) 1339-1342.

[18] K. Kannan, J. Koistinen, K. Beckmen, T. Evans, J.F. Gorzelany, K.J. Hansen, P.D. Jones, E. Helle, M. Nyman, J.P. Giesy, Environ. Sci. Technol. 35 (2001) 1593-1598.

[19] K. Kannan, J.C. Franson, W.W. Bowerman, K.J. Hansen, P.D. Jones, J.P. Giesy, Environ. Sci. Technol. 35 (2001) 3065-3070.

[20] S. Taniyasu, K. Kannan, Y. Horii, N. Yamashita, Organohalogen Compd. 59 (2002) 105-108.

[21] Y.J. An, E.R. Carraway, M.A. Schlautman, Water Res. 36 (2002) 300-308.

[22] R.N. Simmons, V.L. McGuffin, Anal. Chimica Acta 603 (2007) 93-100.

[23] D.E. Kile, C.T. Chiou, H. Zhou, H. Li, O. Xu, Environ. Sci. Technol. 29 (1995) 1401-1406.

[24] K. Heinig, C. Vogt, Electrophoresis 290 (1999) 3311-3328.

[25] J.A. Field, M. Schultz, D. Barofsky, Chimia 57 (2003) 556-560.

[26] M.N. Khan, U. Zareen, J. Hazard. Mater. 133 (2006) 269-275.

[27] S. Martinez-Barrachina, J. Alonso, L. Matia, R. Prats, M. del Valle, Anal. Chem. 71 (1999) 3684-3691.

[28] A.F.M. Barton, Chem. Rev. 75 (1975) 731-754.

[29] R. Tijssen, H.A.H. Billiet, P.J. Schoenmakers, J. Chromatogr. 122 (1976) 185-203.

[30] P.J. Schoenmakers, H.A.H. Billiet, L. de Galan, Chromatographia 15 (1982) 205-214.

[31] A.F.M. Barton, Handbook of Solubility Parameters and Other Cohesion Parameters, 2nd Ed., CRC Press, Boca Raton, FL, 1991.

[32] C.F. Poole, S.K. Poole, Chromatography Today, Elsevier Science Publishers, Amsterdam, 1991, Chapter 4.

[33] C. Tanford, The Hydrophobic Effect: Formation of Micelles and Biological Membranes, John Wiley and Sons, New York, NY, 1980.

CHAPTER 5: COMPARISON OF TRANSPORT EFFECTS BELOW THE CRITICAL MICELLE CONCENTRATION: CATIONIC AROMATIC AMINES

5.1 Introduction

Perfluorinated surfactants, such as perfluorooctane sulfonate, have different physical and chemical characteristics than hydrocarbon surfactants [1-2]. They have been detected in the environment at concentrations substantially lower than their critical micelle concentration (CMC) [3-6]. Previous studies of perfluorinated surfactants have focused on their bioaccumulation and global distribution [7-11], their ability to enhance the solubilization of polycyclic aromatic hydrocarbons [12], and transport effects above and below their CMC on neutral hydrophobic compounds [13-14]. However, relatively little information is available regarding the effects of low levels of perfluorinated surfactants on the transport of ionic environmental contaminants.

One way to elucidate this information is the use of reversed-phase liquid chromatography (RPLC) with surfactants. The addition of surfactants to the mobile phase in a RPLC system has been used to adjust the separation of oppositely charged metal ions, ionic and neutral compounds in solution [15]. This technique has been given different names throughout the years [16-17], and is currently referred to as ion-pair chromatography [18] and ion interaction chromatography [19-20]. These terms are all characterized by the use of a reversed-phase stationary phase and an interaction reagent in the mobile phase, regardless of the presence of a pH buffer or an organic modifier [21].

In a RPLC system devoid of any surfactant, analyte retention is controlled either via a partition or adsorption mechanism. However, the inclusion of an ionic surfactant in the mobile phase also allows for the retention to be controlled either via the ion-pair or ion interaction mechanism [21-22], as well as those previously mentioned. The addition

of a surfactant allows for the possibility of ion interactions such as ion-induced dipole, ion-dipole, and/or ion-ion. Moreover, perfluorinated surfactants have greater polarizability than hydrocarbon surfactants, which can potentially increase induced dipole-induced dipole and dipole-induced dipole interactions. Any one or combination of these interactions will have an effect on the transport of ionic environmental contaminants.

The main focus of this study is to compare the effects of anionic perfluorinated and hydrocarbon surfactants below their CMC on the transport of cationic environmental contaminants in a model groundwater system. Lithium perfluorooctane sulfonate and sodium dodecyl sulfate are used as representatives of the two classes of anionic surfactants. Pyridine, 4-aminopyridine, aniline, and substituted anilines are used as models of cationic environmental pollutants. The results of this study yield information concerning the retention factors and several selectivity factors of the model pollutants. These values can be used to elucidate the transport effects of perfluorinated surfactants on pollutants that might leach into water systems or aquifers.

5.2 Experimental Methods

5.2.1 Mobile Phase and Analytes

The hydrocarbon surfactant, sodium dodecyl sulfate (SDS), was obtained from Aldrich and was used as received. The perfluorinated surfactant, lithium perfluorooctane sulfonate (LiPFOS), was prepared by dissolving the appropriate amounts of heptadecafluorooctane sulfonic acid (TCI America) and lithium hydroxide monohydrate (99.95 %, Aldrich) in deionized, distilled water (Corning Mega-Pure, Models D2 and MP-3A). The surfactant solutions were prepared by dissolving the appropriate amount of

surfactant (1.0 – 4.0 mM) and *β*-alanine (10 mM, Aldrich) as buffer in various ratios of methanol and deionized, distilled water (20 – 55 % v/v). The solutions were then filtered through a cellulose acetate membrane (Alltech) with a 0.45 μm pore size. The resulting buffered solutions were adjusted to pH 4.0 ± 0.1 with hydrochloric acid.

The aromatic amines pyridine, 4-aminopyridine, aniline, benzylamine, *o*-, *m*-, and *p*-toluidine, N-methylaniline, N,N-dimethylaniline, N-ethylaniline, N,N-diethylaniline, and 2,6-dimethylaniline (Aldrich) were used as received. Stock solutions (1.0×10^{-3} M) of the analytes were prepared in high-performance liquid chromatography-grade methanol (Spectrum Chemical). Analytical samples were prepared via dilution of the proper amount of stock solutions. First, the stock solutions were evaporated with nitrogen, such that the residual concentration of methanol from the stock solutions would be less than 1 % (v/v) in the final analytical sample. Next, the sample was diluted with the surfactant solution and 1.2 μL of aqueous lithium nitrate solution (2.00×10^{-1} M $LiNO_3$) to acquire the working concentrations in a 25.0 mL final volume. The working concentration in the analytical samples was 5.00×10^{-5} M for the analytes and 9.60×10^{-6} M for $LiNO_3$.

5.2.2 Experimental System

The experimental chromatographic methods, as detailed in Section 2.2, are briefly recapped in this section. The commercial analytical column (4.6 mm i.d. x 250 mm length) was packed with Poroshell 300SB-C_{18} pellicular particles (Agilent) of 5.0 μm diameter and 6.0 $m^2\ g^{-1}$ surface area, with an octadecylsilica stationary phase of 2.1 μmol m^{-2} bonding density and 0.39 % carbon content. The liquid chromatography

system consisted of a single-piston reciprocating pump (Beckman, Model 110B), an injector with a 20 μL injection loop (Valco, Model EC6W), and a UV-visible absorbance detector (Hitachi, Model L-4200). The UV absorbance wavelength of 205 nm was specific for the detection of the aromatic amines, and did not incur any interference from the surfactants. The signal from the UV-visible absorbance detector was converted to the digital domain (Model PCI-MIO-16XE-50, National Instruments) and stored via a user-defined software program (Labview v5.1, National Instruments). All experiments were carried out at ambient temperature with a maximum pressure limit of 4500 psi. The flow rate was 1.0 mL min^{-1} during the SDS experiments and 0.5 mL min^{-1} during the LiPFOS and pure water experiments. The void time, t_0, was taken as the first positive deviation from the baseline arising from $LiNO_3$ in each sample. The retention time, t_R, for each analyte was determined from the peak maximum, which is appropriate for the symmetric Gaussian peaks observed in this study. The retention factor, k, was then calculated by

$$k = \frac{t_R - t_0}{t_0} \qquad (5.1)$$

The k values (average of at least three trials) were used for the subsequent elucidation of transport effects and determination of selectivity factors as described in the following section.

5.2.3 Data Analysis

5.2.3.1 Retention Factor Measurements

In order to elucidate meaningful information regarding the transport effects of anionic perfluorinated surfactants on ionic analytes (e.g. cationic aromatic amines) in an environmental system, an analytical technique was used that could fundamentally

resemble such a system, but whose parameters were controllable. Reversed-phase liquid chromatography was used to model an environmental system, in which the octadecylsilica stationary phase represents soil and the aqueous mobile phase represents groundwater. When a surfactant is added to the RPLC system below its CMC, the monomers distribute or partition between the mobile and stationary phases. These ionic surfactant monomers have the potential to alter the retention of ionic analytes (pollutants) through ion interactions, as described in Section 5.1.

The equilibrium constant, K, which includes ion interactions can be defined as

$$K = \frac{a_S}{a_M} = \frac{\gamma_S C_S}{\gamma_M C_M} \tag{5.2}$$

where a_S and a_M represent the activities, γ_S and γ_M represent the activity coefficients, and C_S and C_M represent the analytical concentrations of the analyte in the stationary (S) and mobile (M) phases, respectively. Assuming the activity coefficients are equal to unity, Equation 5.2 indicates that the equilibrium constant is directly related to the ratio of the analyte concentrations in the stationary and mobile phases. This equilibrium constant represents all interactions between the analyte, stationary phase, mobile phase, and surfactant monomers. The equilibrium constant is a vital piece of information needed to model environmental systems. However, the determination of this equilibrium constant is difficult because of the inability to directly measure the concentrations of the analyte in the environmental mobile and stationary phases.

The retention factor, k, is defined as

$$k = K\phi \tag{5.3}$$

where ϕ is the phase ratio, defined as

$$\phi = \frac{V_S}{V_M} \tag{5.4}$$

where V_M and V_S are the volumes of the mobile and stationary phase, respectively. Assuming that the phase ratio is constant, the value for k is proportional to K. Consequently, the trends in retention factor are consistent with and can be used to predict the trends in equilibrium constant. In particular, an increase in the retention factor implies an increase in the concentration of the analyte in the stationary phase relative to the mobile phase, according to Equation 5.2.

5.2.3.2 Linear Solvent Strength Model

When the determination of the analyte retention factor in solvent A (e.g. aqueous surfactant solution) is impractical due to excessive retention, a stronger organic co-solvent B (e.g. methanol) can be added to the mobile phase to decrease the analyte retention. The linear solvent strength (LSS) model relates the analyte retention as a function of the percent composition of the organic solvent (% B) in the mixed mobile phase [23], via the following equation

$$\log k = -S(\%B) + \log k_0 \tag{5.5}$$

where S is the slope and k_0 is the analyte retention factor in pure solvent A (i.e. % B = 0). Linear regression is performed on the logarithmic k values measured at various % B. The k_0 value of the analyte at a given surfactant concentration is determined from the logarithmic y-intercept value.

The weighted mean [24] value for k_0 is defined by

$$\bar{k} = \frac{\sum_i \left(\frac{k_{0,i}}{\sigma_i^2} \right)}{\sum_i \left(\frac{1}{\sigma_i^2} \right)} \tag{5.6}$$

where $k_{0,i}$ is the extrapolated analyte retention factor at a given surfactant concentration and σ_i is the standard deviation of that individual extrapolated retention factor. The weighted standard deviation [24] of this mean value is defined by

$$\bar{\sigma} = \sqrt{\frac{1}{\sum_i \left(\frac{1}{\sigma_i^2} \right)}} \tag{5.7}$$

The value $\bar{k} \pm \bar{\sigma}$ represents the retention factor of the cationic analyte in an aqueous surfactant mobile phase. The retention factor of the aromatic amine determined in this manner is vital information needed for elucidation of transport effects.

5.2.3.3 Selectivity Factor Calculations

In addition to the weighted mean of the extrapolated retention factors determined from Equation 5.6, several selectivity factors are also compared to elucidate transport effects. Each selectivity factor provides different information concerning the various interactions between the analytes and the surfactants.

The first selectivity factor, α_1, is defined as the ratio of the retention factor of the analyte to that of the base aromatic amine (aniline or pyridine), while all other experimental conditions remain constant.

$$\alpha_{1A} = \frac{\bar{k}_{analyte}}{\bar{k}_{aniline}} \text{ or } \alpha_{1B} = \frac{\bar{k}_{analyte}}{\bar{k}_{pyridine}} \tag{5.8}$$

The value for α_1 is related to the effect of the addition of a substituent group to the base aromatic amine structure on the transport of the model analytes. As α_1 increases, the additional substituent group leads to increasing interaction of the ionic analyte with the stationary phase or with the surfactant monomers in the stationary phase.

The second selectivity factor, α_2, is defined as the ratio of the retention factor of an analyte in a surfactant mobile phase to that of the same analyte in pure water, while all other experimental conditions remain constant.

$$\alpha_2 = \frac{\bar{k}_{surfactant}}{\bar{k}_{water}} \tag{5.9}$$

The value for α_2 is related to the effect of the surfactant monomers on the transport of the model analytes. As α_2 increases, the ionic analyte exhibits a preference for interaction with the surfactant monomers in the stationary phase.

The third selectivity factor, α_3, is defined as the ratio of the retention factor of an analyte in LiPFOS mobile phase to that of the same analyte in SDS mobile phase, while all other experimental conditions remain constant.

$$\alpha_3 = \frac{\bar{k}_{LiPFOS}}{\bar{k}_{SDS}} \tag{5.10}$$

The value for α_3 is related to the affinity of the model analyte for LiPFOS compared to SDS. As α_3 increases, the ionic analyte exhibits a greater preference for interaction with LiPFOS than with SDS in the stationary phase.

5.3 Results and Discussion

The rationale behind the choice of stationary phase and surfactants has been discussed in Section 2.2.1 and a previous report [13], respectively. The Poroshell

stationary phase was selected because its carbon content (0.39 %) and surface area (6.0 $m^2\ g^{-1}$) are within the typical ranges for various soils, bed sediments, and suspended solids [25]. Sodium dodecyl sulfate (SDS) and lithium perfluorooctane sulfonate (LiPFOS) were chosen as representative surfactants because they are used commercially and have been detected in the environment [6-11,26-29]. The analytes represent important classes of environmental contaminants that are suspected human carcinogens. Aromatic amines, such as anilines and pyridines, are used in the manufacture of drugs, dyes and pigments, urethanes, and pesticides (e.g. herbicides, fungicides, insecticides, etc.) [30-31]. Commercial uses of the compounds can lead to direct or indirect exposure in the environment. Moreover, all of these analytes can be used to examine how their differences in physical and chemical characteristics influence the transport effects of hydrocarbon and perfluorinated surfactants.

5.3.1 Transport Effects in Water

In order to be able to compare the transport effects caused by the different surfactant monomers, the retention and elution order of the analytes were first determined in a water mobile phase devoid of surfactants. The retention factors of the analytes are shown in Table 5.1. It should be noted that the retention factors for most of the analytes were less than unity (Table 5.1), signifying that the analytes were not strongly retained. The retention factors for N,N-dimethylaniline, N-ethylaniline, N,N-diethylaniline, and 2,6-dimethylaniline were greater than unity but less than 10. The elution order for the analytes in the water mobile phase was as follows: 4-aminopyridine < pyridine < aniline < benzylamine < *p*-toluidine ≈ N-methylaniline < *m*-toluidine ≈ *o*-toluidine < N,N-dimethylaniline < N-ethylaniline < N,N-diethylaniline < 2,6-dimethylaniline.

Table 5.1: Retention and selectivity factors of cationic aromatic amines in pure water mobile phase.

Aromatic Amines	pK_a	Retention Factor $(\bar{k})$ [a]	Selectivity Factor (α)	
			α_{1A} [b]	α_{1B} [b]
pyridine	5.23	0.20 ± 0.01	0.72 ± 0.04	1.00 ± 0.00
4-aminopyridine	9.17	0.14 ± 0.01	0.51 ± 0.04	0.71 ± 0.04
aniline	4.60	0.27 ± 0.02	1.00 ± 0.00	1.39 ± 0.08
benzylamine	9.35	0.42 ± 0.01	1.55 ± 0.09	———
o-toluidine	4.45	0.93 ± 0.01	3.43 ± 0.19	———
m-toluidine	4.69	0.93 ± 0.02	3.43 ± 0.20	———
p-toluidine	5.08	0.78 ± 0.02	2.88 ± 0.17	———
N-methylaniline	4.85	0.82 ± 0.03	3.02 ± 0.19	———
N,N-dimethylaniline	5.07	1.41 ± 0.01	5.19 ± 0.28	———
N-ethylaniline	5.12	1.45 ± 0.01	5.33 ± 0.29	———
N,N-diethylaniline	6.57	3.25 ± 0.12	11.95 ± 0.78	———
2,6-dimethylaniline	3.89	3.70 ± 0.04	13.60 ± 0.76	———

[a] Retention factors are an average of three trials (Equation 5.1). Experimental conditions as given in the text.
[b] Selectivity factors calculated between (A) analyte and aniline or (B) analyte and pyridine (Equation 5.8).

A student's t-test was performed at the 95 % confidence level (C.L.), which revealed that the retention factors of *p*-toluidine and N-methylaniline as well as of *m*-toluidine and *o*-toluidine were statistically indistinguishable. The retention order of the amines in the water mobile phase followed what is expected for a partition mechanism. The addition of a methylene ($-CH_2-$) or methyl ($-CH_3$) substituent increased the non-polar characteristic of the analyte, and lead to increased retention. The addition of a polar amine substituent to the pyridine aromatic ring increased the polarity of the analyte, thus decreasing retention. The inclusion of nitrogen in the aromatic ring, as opposed to an amine substituent on the ring, decreased the retention of the analyte.

The selectivity factor α_1 was calculated from the $\bar{k}$ values of substituted aromatic amines and a base aromatic amine (Equation 5.8), with the data shown in Table 5.1. In relation to aniline, most of the α_{1A} values were greater than unity (Table 5.1), signifying that the addition of the substituent increased analyte interaction with the stationary phase. The α_{1A} values of pyridine and 4-aminopyridine were less than unity, suggesting the inclusion of nitrogen in the ring decreased analyte interaction with the stationary phase. It is observed that addition of a methyl substituent, regardless of position on the ring, contributed approximately the same amount to analyte interaction. The α_1 values increased with both the size (e.g. methyl versus ethyl) and number of substituents for the series of anilines. In relation to pyridine, the α_{1B} value was less than unity for 4-aminopyridine (0.71 ± 0.04) and greater than unity for aniline (1.39 ± 0.08). This suggests that the inclusion of a polar amine group decreased the interaction of pyridine with the stationary phase, thus increasing environmental transport.

5.3.2 Transport Effects of Sodium Dodecyl Sulfate

In preliminary experiments, the aromatic amines were examined in an aqueous SDS mobile phase (1.0 mM). The amines displayed excessive retention in this mobile phase, and retention factors could not be accurately determined. The LSS method (described in Section 5.2.3.2) was used for the remainder of this study. Retention factors, k, of the amines were determined in varying mobile phase compositions of aqueous SDS (1.0 – 4.0 mM) and methanol (20 – 50 % v/v). The retention of the analytes increased with increasing SDS concentration, which is in accordance with ion-pair chromatography and ion interaction theory [19].

Graphs of the logarithmic retention factor for each analyte versus the methanol composition (% B) are shown in Figures 5.1A-D. Statistical treatment of these graphs via linear regression demonstrated a linear relationship between log k and % B, where the square of the correlation coefficient, R^2, values were all greater than 0.970. The linear relationship observed is consistent with predictions of the LSS method. The aromatic amines N-ethylaniline, N,N-diethylaniline, and 2,6-dimethylaniline displayed excessive retention at low percentages of methanol in the 1.0 mM SDS mobile phase (Figure 5.1). As a result, the aforementioned amines were excluded from further study. The retention factors of the amines in aqueous surfactant mobile phases (k_0) were extrapolated at each SDS concentration using linear regression of Equation 5.5.

A graph of the logarithmic extrapolated retention factor for each analyte versus the concentration of SDS is shown in Figure 5.2. There is a significant increase in analyte retention from 0.0 to 1.0 mM SDS; however retention remains relatively constant from 1.0 to 4.0 mM SDS.

Figures 5.1A-D: Graphs of the logarithmic retention factor versus methanol composition (% B) in: (A) 1.0 mM aqueous sodium dodecyl sulfate (SDS), (B) 2.0 mM SDS, (C) 3.0 mM SDS, (D) 4.0 mM SDS. Analytes: (♦) pyridine, (■) 4-aminopyridine, (▲) aniline, (**x**) benzylamine, (∗) *o*-toluidine, (●) *m*-toluidine, (○) *p*-toluidine, (◊) N-methylaniline, (□) N,N-dimethylaniline, (Δ) N-ethylaniline, (**—**) N,N-diethylaniline, (+) 2,6-dimethylaniline. Other experimental conditions as given in the text.

Figure 5.1A

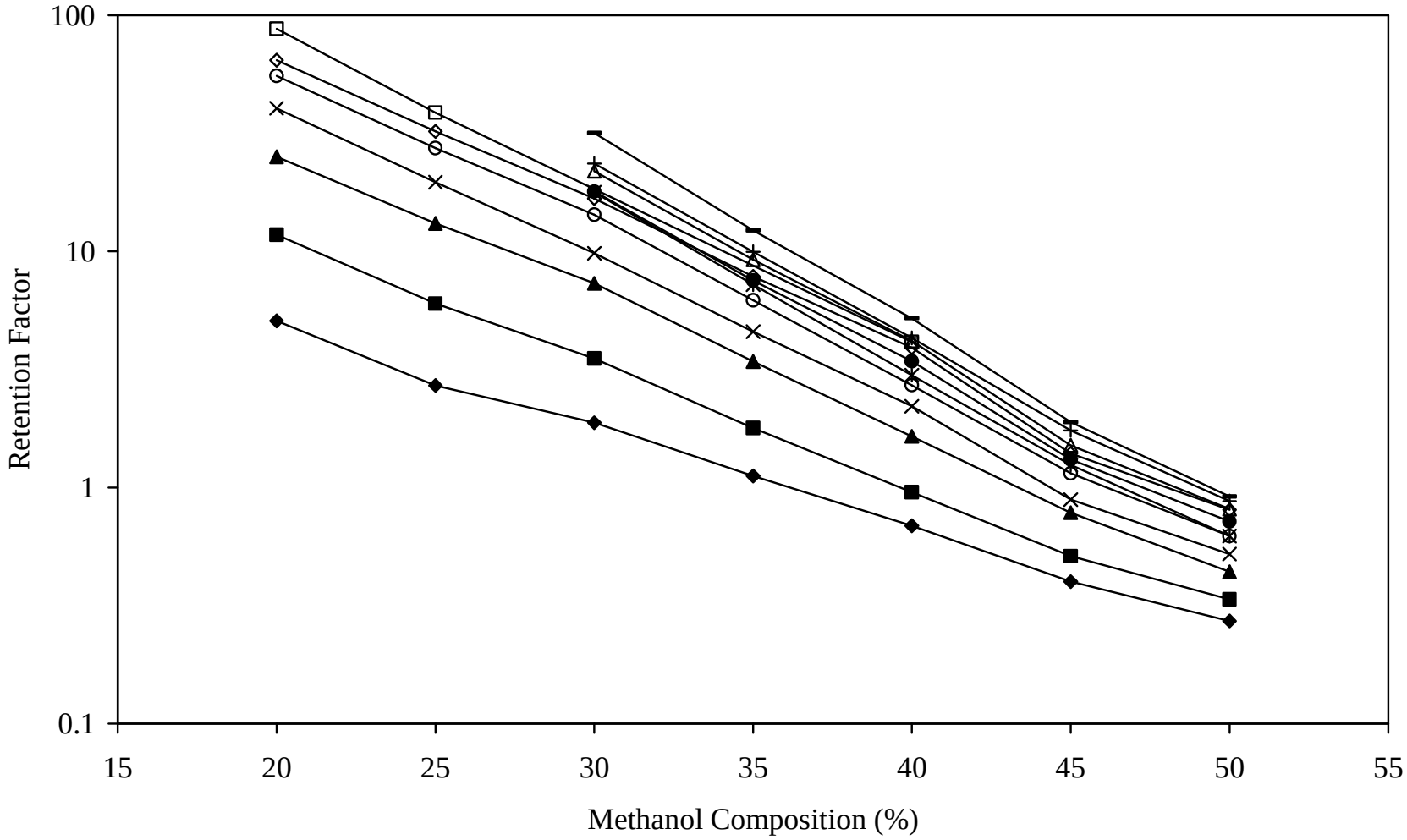
100
10
1
0.1
Retention Factor
15
20
25
30
35
40
45
50
55
Methanol Composition (%)

Figure 5.1B

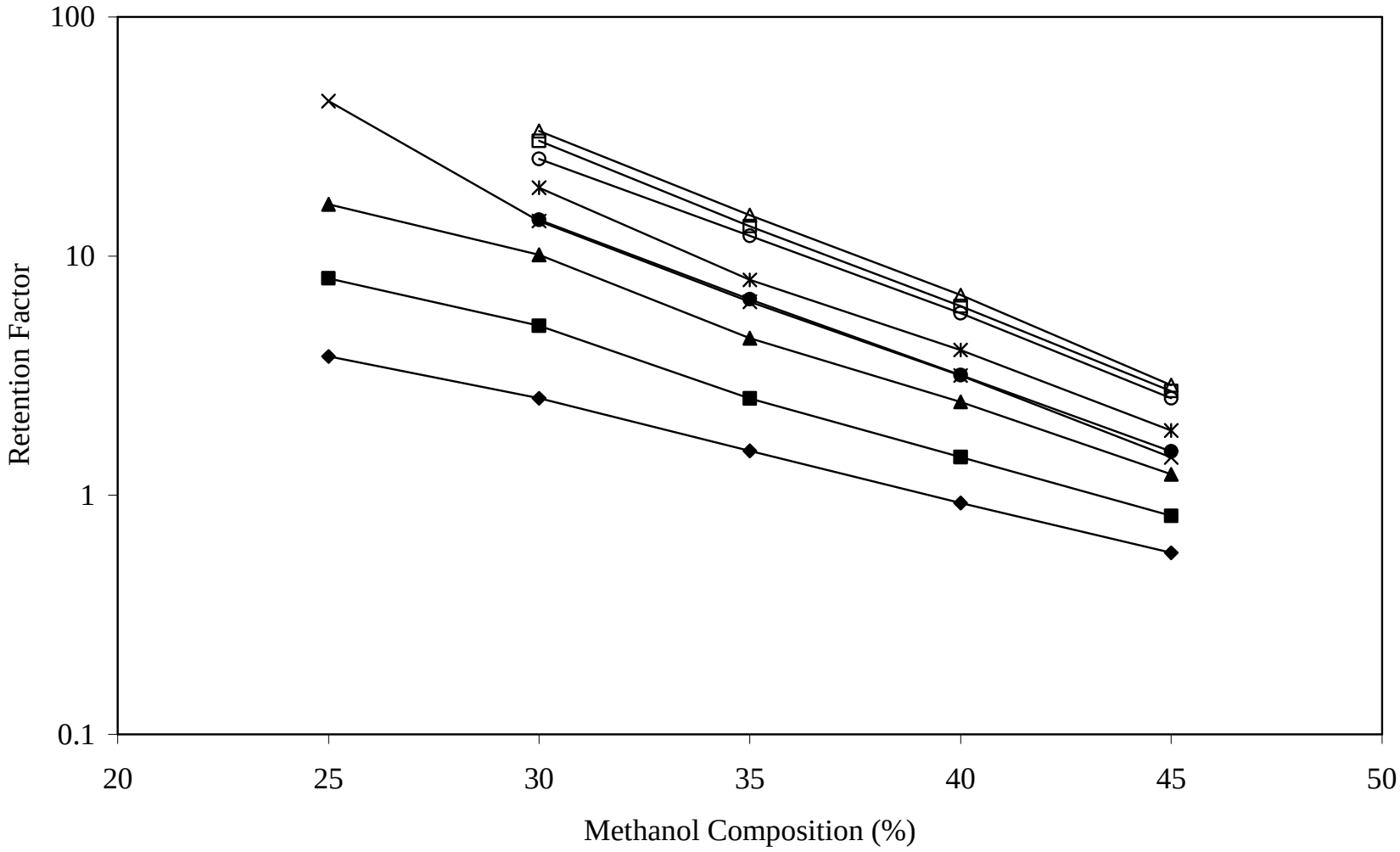
100
10
1
0.1
Retention Factor
20
25
30
35
40
45
50
Methanol Composition (%)

Figure 5.1C

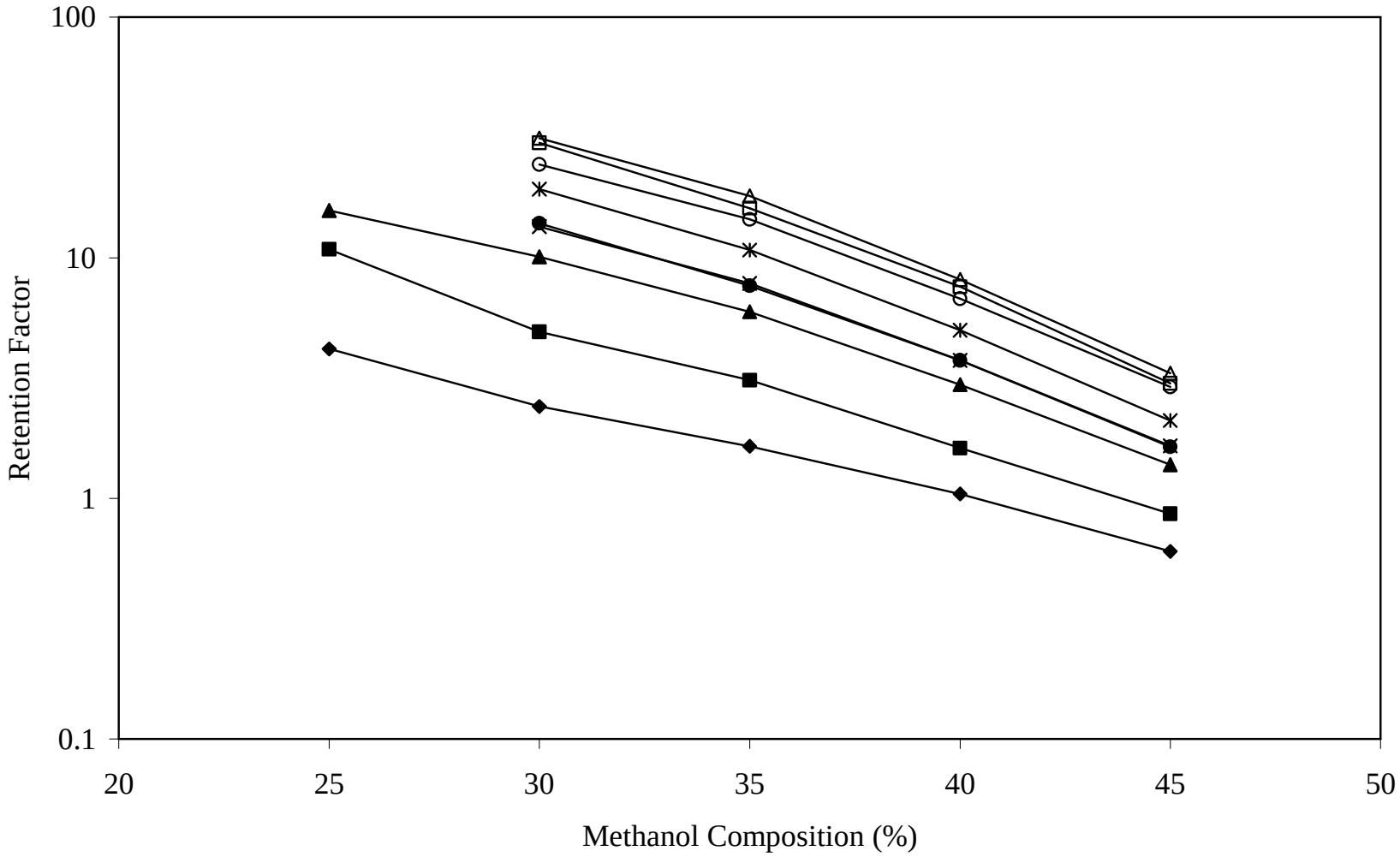
100
10
1
0.1
Retention Factor
20
25
30
35
40
45
50
Methanol Composition (%)

Figure 5.1D

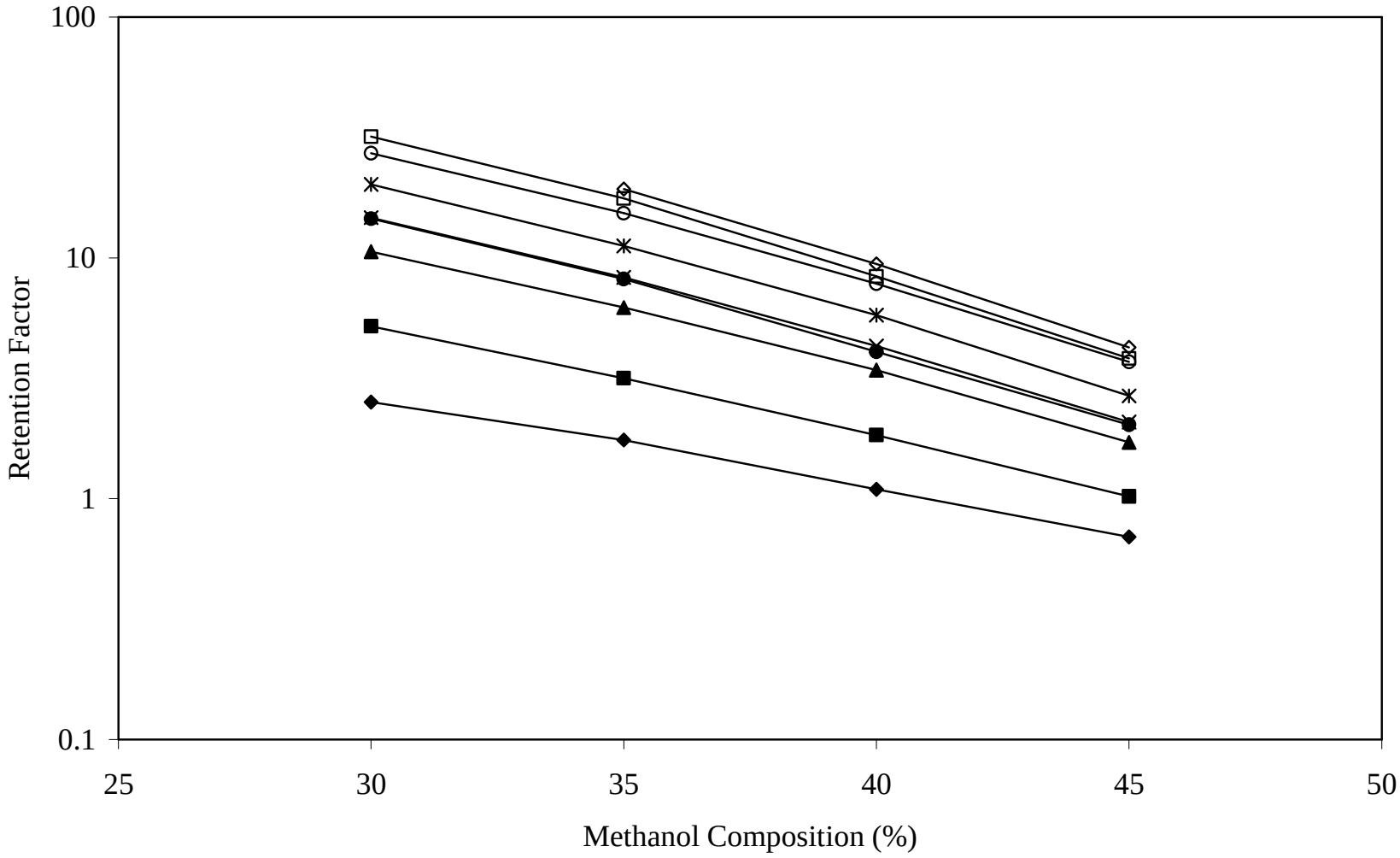
100
10
1
0.1
Retention Factor
25
30
35
40
45
50
Methanol Composition (%)

Figure 5.2: Graph of the logarithmic extrapolated retention factor for each analyte versus the concentration of SDS. Analytes: (♦) pyridine, (■) 4-aminopyridine, (▲) aniline, (**x**) benzylamine, (∗) *o*-toluidine, (●) *m*-toluidine, (○) *p*-toluidine, (◊) N-methylaniline, (□) N,N-dimethylaniline. Other experimental conditions as given in the text.

Figure 5.2

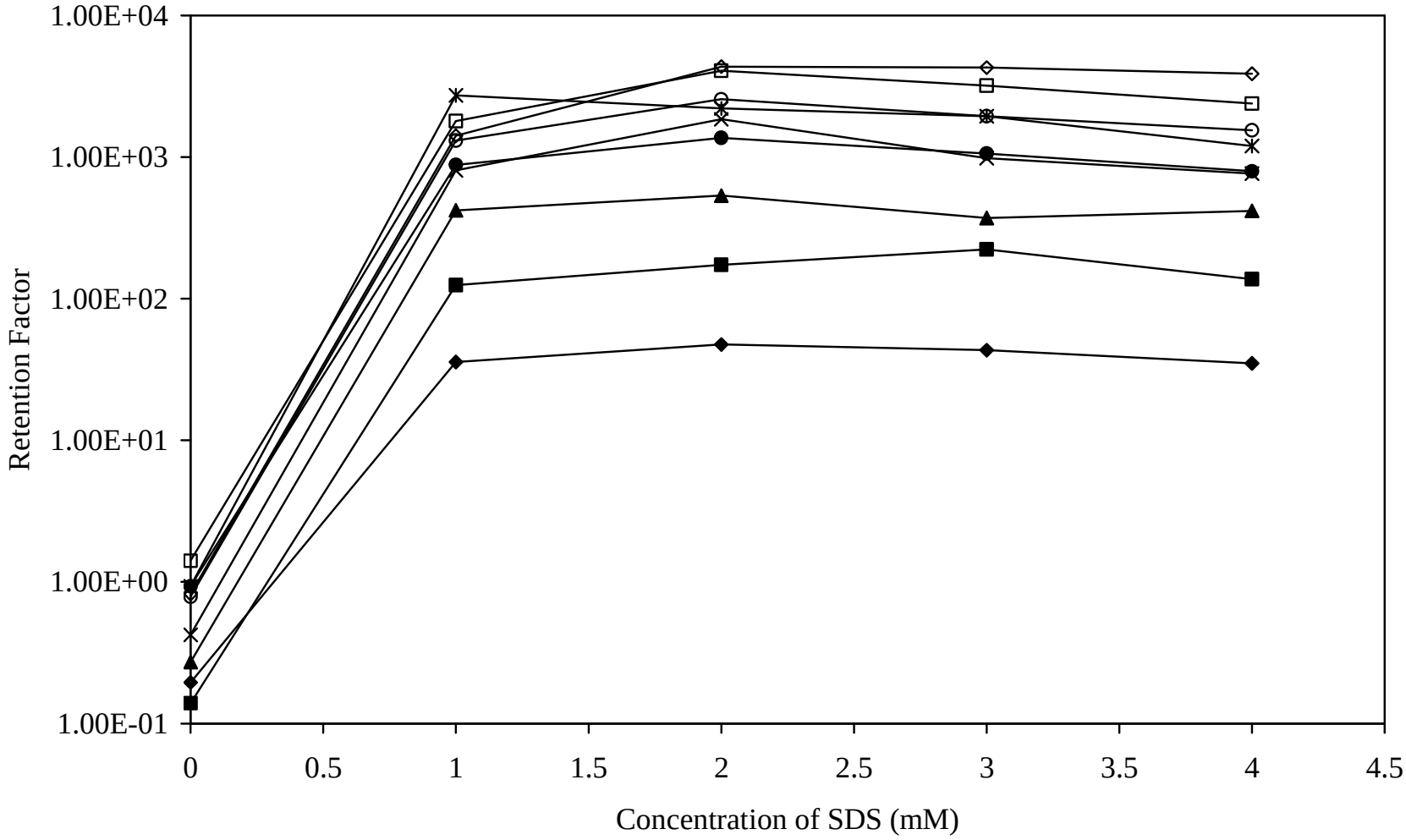
1.00E+04
1.00E+03
1.00E+02
1.00E+01
1.00E+00
1.00E-01
Retention Factor
0
0.5
1
1.5
2
2.5
3
3.5
4
4.5
Concentration of SDS (mM)

A t-test at the 95 % C.L. confirmed that the slope of this graph (within 1.0 – 4.0 mM SDS range) was indistinguishable from zero. Based on this information, the weighted mean of the extrapolated retention factors was used to elucidate transport effects.

The weighted mean retention factors ($\bar{k}$, calculated via Equation 5.6) and standard deviations ($\bar{\sigma}$, calculated via Equation 5.7) for the analytes are shown in Table 5.2. The relative standard deviations (RSDs) were all less than 8.0 %, which indicates the good precision of the individual extrapolated retention values. Most of the $\bar{k}$ values were greater than 100, signifying that the analytes were highly retained. The overall elution order was as follows: pyridine < 4-aminopyridine < aniline < benzylamine < *m*-toluidine < *o*-toluidine ≈ *p*-toluidine < N-methylaniline ≈ N,N-dimethylaniline. Statistical treatment of the $\bar{k}$ values via a t-test at the 95 % C.L. revealed that the retention factors of *o*-toluidine and *p*-toluidine as well as of N-methylaniline and N,N-dimethylaniline were statistically the same. Overall, the elution order follows the trend of a partition mechanism. A note of interest is that the retention order of 4-aminopyridine and pyridine reversed for all SDS mobile phases relative to pure water. It is believed that the protonated amine substituent on 4-aminopyridine has a greater interaction with the SDS in the stationary phase, thus leading to enhanced retention. In comparing the $\bar{k}$ values in SDS (Table 5.2) to those in pure water (Table 5.1), a large increase of 2 to 4 orders-of-magnitude is observed. It is apparent that the presence of SDS decreases chromatographic transport of the amines and, by implication, decreases environmental transport as well.

Table 5.2: Retention and selectivity factors of cationic aromatic amines in SDS mobile phase.

Aromatic Amines	Retention Factor $\left(\bar{k}\right)$ [a]	Selectivity Factor (α)		
		α_{1A} [b]	α_{1B} [b]	α_2 [c]
pyridine	39.32 ± 1.52	0.093 ± 0.004	1.00 ± 0.00	201.6 ± 34.4
4-aminopyridine	141.2 ± 6.0	0.33 ± 0.01	3.59 ± 0.19	1016 ± 607
aniline	422.6 ± 18.8	1.00 ± 0.00	10.75 ± 0.59	1554 ± 700
benzylamine	824.8 ± 40.9	1.95 ± 0.10	———	1954 ± 318
o-toluidine	1695 ± 117	4.01 ± 0.28	———	1815 ± 208
m-toluidine	937.7 ± 62.3	2.22 ± 0.15	———	1004 ± 172
p-toluidine	1700 ± 67	4.02 ± 0.16	———	2169 ± 392
N-methylaniline	2303 ± 107	5.45 ± 0.26	———	2799 ± 560
N,N-dimethylaniline	2468 ± 176	5.84 ± 0.42	———	1748 ± 157

[a] Retention factors calculated as the weighted mean of the extrapolated retention factors within the experimental concentration range, 1.0 – 4.0 mM (Equation 5.6). Experimental conditions as given in the text.

[b] Selectivity factors calculated between (A) analyte and aniline or (B) analyte and pyridine (Equation 5.8).

[c] Selectivity factors calculated for analyte between SDS and pure water (Equation 5.9).

The selectivity factor α_1 was calculated from the $\bar{k}$ values of substituted aromatic amines and a base aromatic amine (Equation 5.8), with the results shown in Table 5.2. Most of the α_1 values are greater than unity, signifying that the addition of the substituent increased analyte interaction with SDS in the stationary phase. The addition of a methyl substituent at the *meta*- position increased the interaction of the amine with the SDS monomers in the stationary phase by a factor of two. In contrast, the addition of the methyl substituent at either the *ortho*- or *para*- position led to a four-fold increase. The addition of a methyl group to the nitrogen of an amine substituent contributed to analyte retention by a five-fold increase. The addition of a second methyl group to the nitrogen resulted in the same increase. The addition of methyl or N-alkyl substituents increases the basicity and inductive effect of aniline. These results suggest the addition of methyl substituents to the analytes increased interaction with the SDS monomers in the stationary phase. In relation to aniline, the α_{1A} values of pyridine and 4-aminopyridine were less than unity (Table 5.2). This result suggests that the inclusion of nitrogen in the ring structure of an aromatic amine reduced interaction with the SDS monomers in the stationary phase.

The selectivity factor α_2 was calculated from the $\bar{k}$ values of the aromatic amines in SDS and pure water mobile phases (Equation 5.9), with the results shown in Table 5.2. Most of the α_2 values are greater than 1000, implying that the ion-pairing mechanism with SDS has a large contribution to the retention of the analytes when compared with partition alone. Although the α_2 value of pyridine (201.6 ± 34.4) is less than 1000, it still suggests that SDS ion-pairing is the major contributor to retention.

These results suggest that all of the cationic aromatic amines have strong interactions with SDS monomers in the stationary phase. This interaction causes the amines to display a significant decrease in environmental transport when compared to a system devoid of any surfactant. Based on these results, there is potential for SDS in environmental remediation of cationic aromatic amines

5.3.3 Transport Effects of Lithium Perfluorooctane Sulfonate

Retention factors, k, of the amines were determined in varying mobile phase compositions of aqueous LiPFOS (1.0 – 4.0 mM) and methanol (25 – 55 % v/v). Similar to SDS, analyte retention increased with increasing LiPFOS concentration in accordance with ion interaction theory [19].

Graphs of the logarithmic retention factor for each analyte versus the methanol composition (% B) are shown in Figure 5.3A-D. Statistical treatment of these graphs via linear regression demonstrated a linear relationship between log k and % B, where R^2 values were greater than 0.976. The linear relationship observed is consistent with predictions of the LSS method. The retention factors of the amines in aqueous surfactant mobile phases (k_0) were extrapolated at each LiPFOS concentration using linear regression of Equation 5.5.

Figures 5.3A-D: Graphs of the logarithmic retention factor versus methanol composition (% B) in: (A) 1.0 mM aqueous lithium perfluorooctane sulfonate (LiPFOS), (B) 2.0 mM LiPFOS, (C) 3.0 mM LiPFOS, (D) 4.0 mM LiPFOS. Analytes: (♦) pyridine, (■) 4-aminopyridine, (▲) aniline, (x) benzylamine, (∗) *o*-toluidine, (●) *m*-toluidine, (○) *p*-toluidine, (◊) N-methylaniline, (□) N,N-dimethylaniline. Other experimental conditions as given in the text.

Figure 5.3A

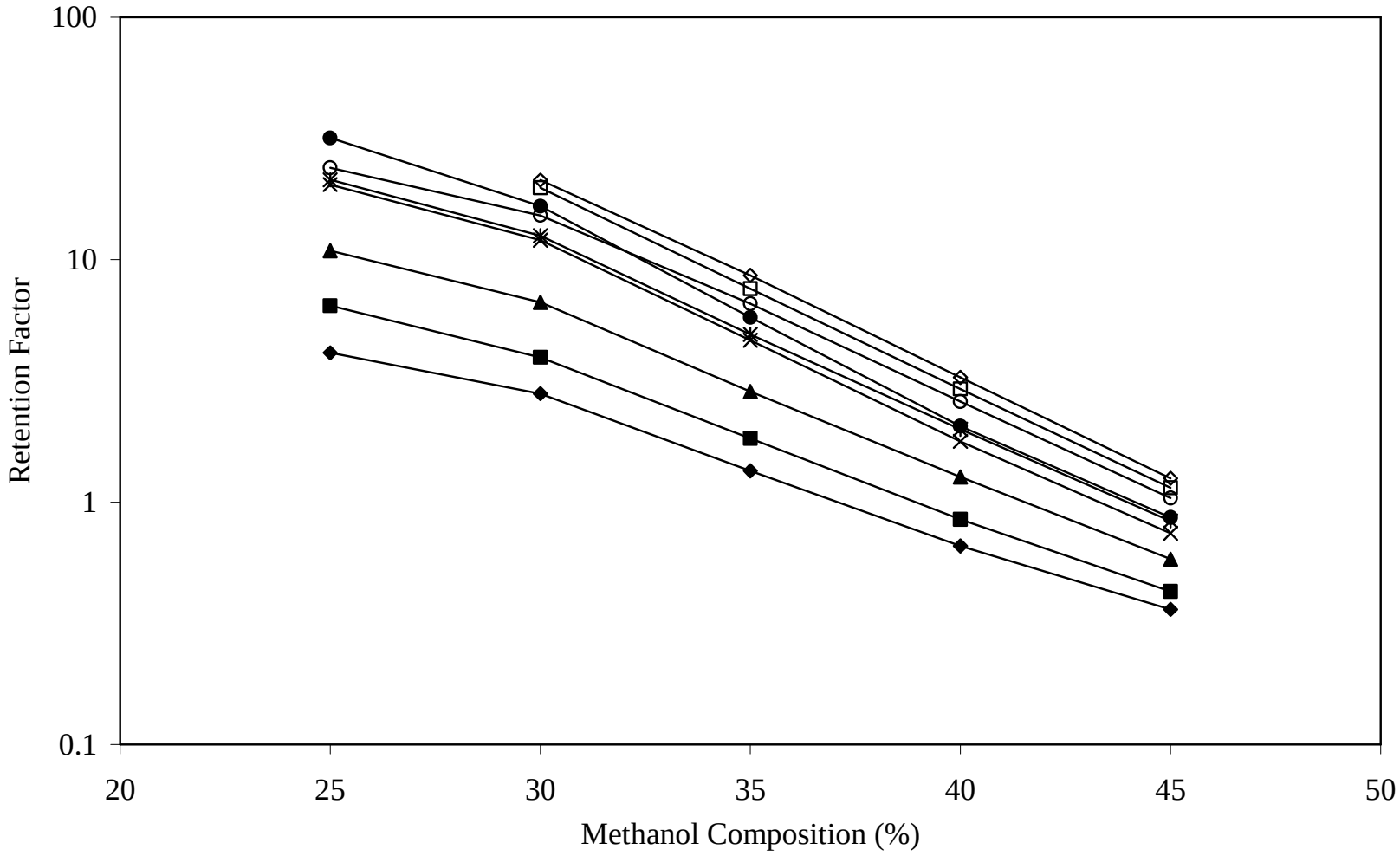
100
10
1
0.1
Retention Factor
20
25
30
35
40
45
50
Methanol Composition (%)

Figure 5.3B

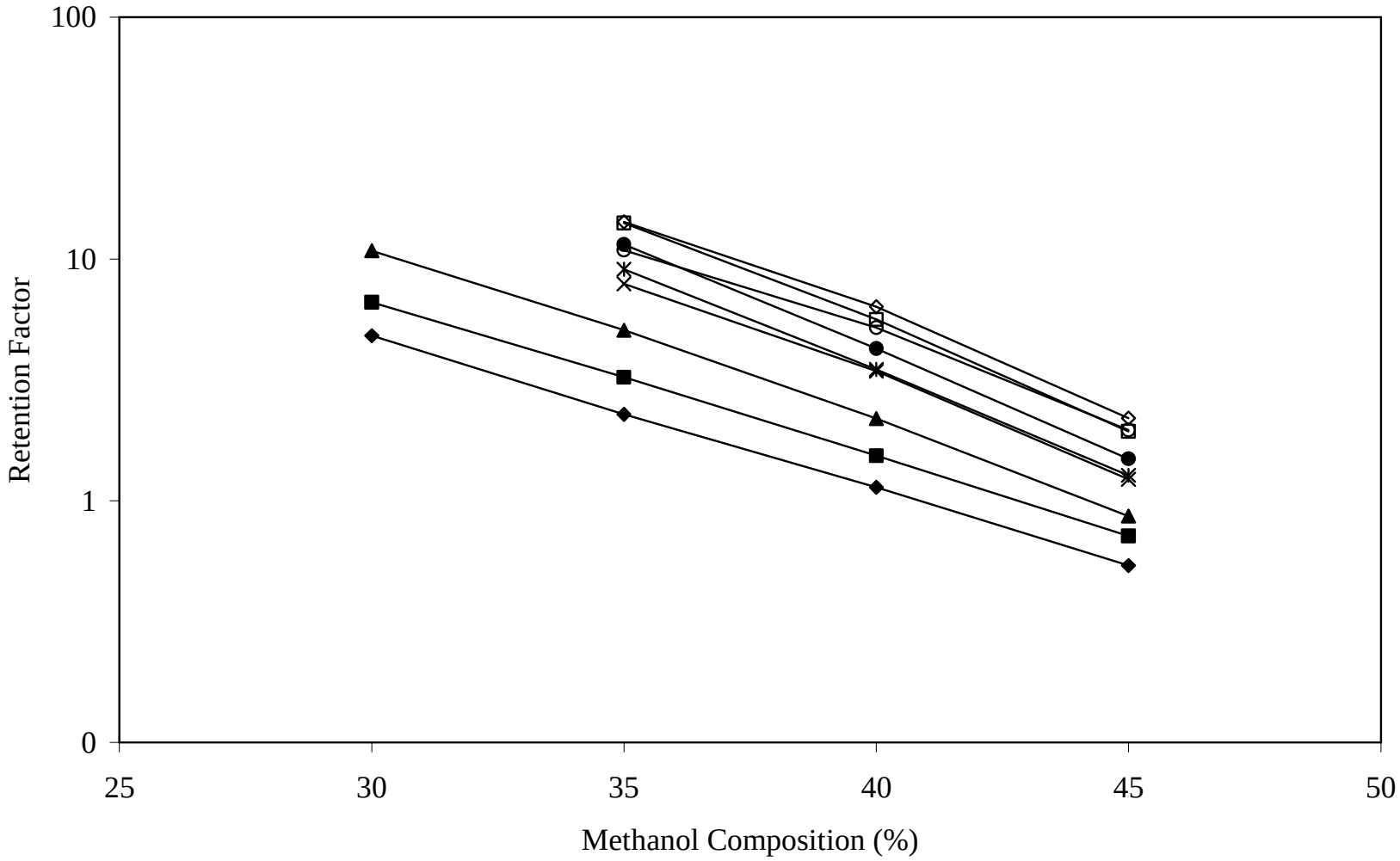
100
10
1
0
Retention Factor
25
30
35
40
45
50
Methanol Composition (%)

Figure 5.3C

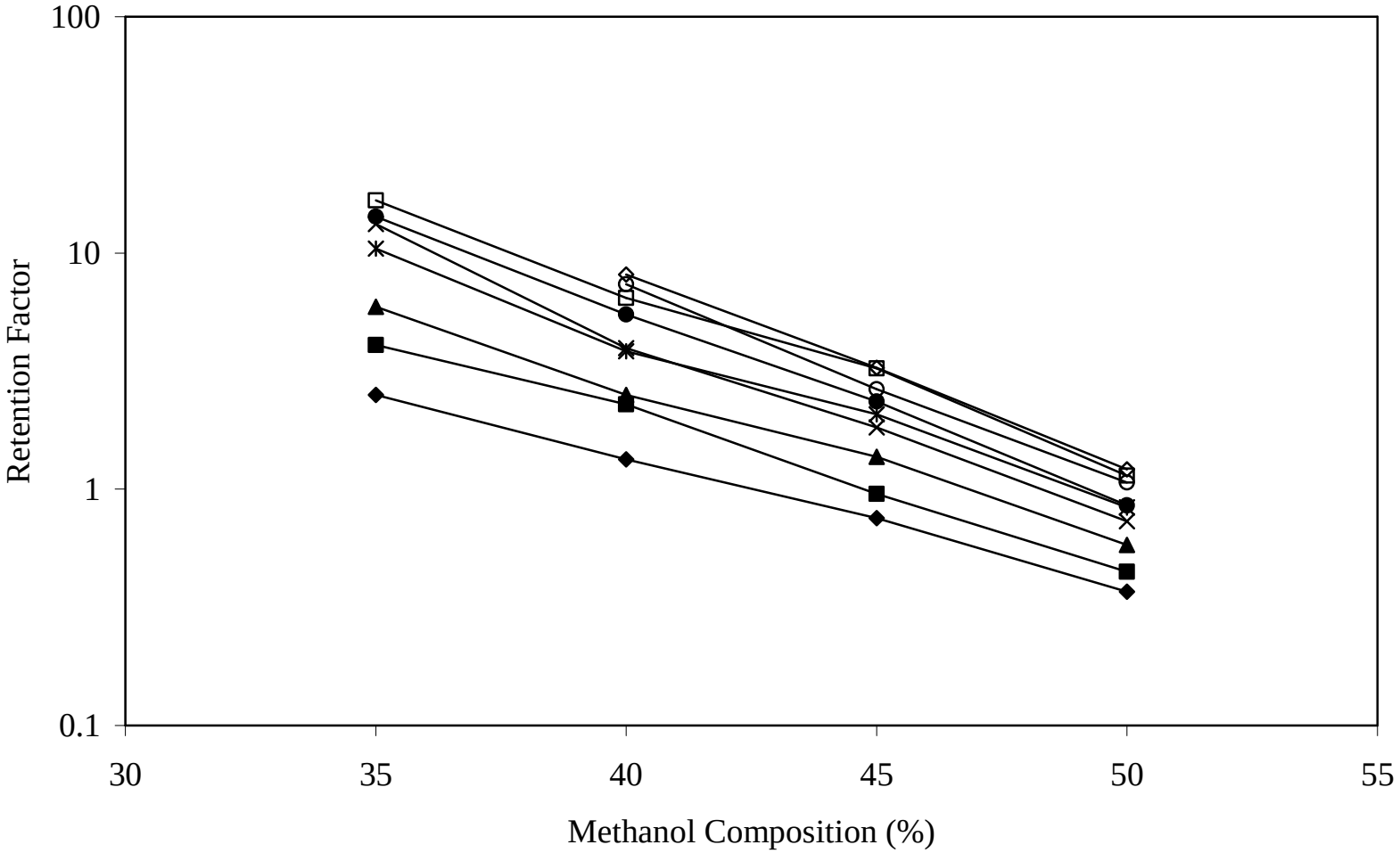
100
10
1
0.1
Retention Factor
30
35
40
45
50
55
Methanol Composition (%)

Figure 5.3D

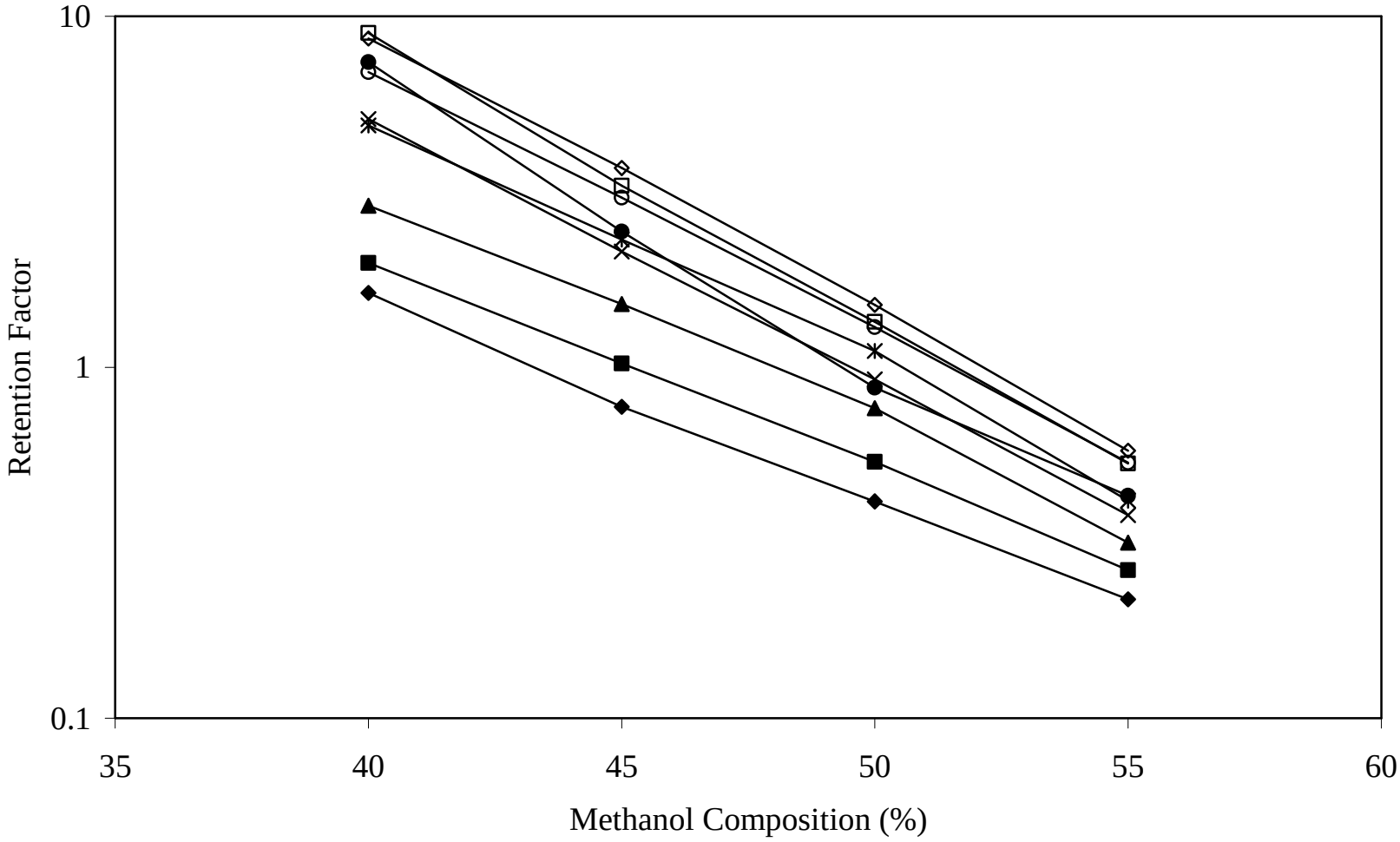
10
1
0.1
Retention Factor
35
40
45
50
55
60
Methanol Composition (%)

A graph of the logarithmic extrapolated retention factor for each analyte versus the concentration of LiPFOS is shown in Figure 5.4. Similar to SDS, there is a significant increase in analyte retention from 0.0 to 1.0 mM LiPFOS; however retention remains relatively constant from 1.0 to 4.0 mM LiPFOS. A t-test at the 95 % C.L confirmed that the slope of this graph (within 1.0 – 4.0 mM LiPFOS) was indistinguishable from zero. Based on this information, the weighted mean of the extrapolated retention factors was used to elucidate transport effects.

The weighted mean retention factors ($\bar{k}$, calculated via Equation 5.6) and standard deviations ($\bar{\sigma}$, calculated via Equation 5.7) for the analytes are shown in Table 5.3. The RSDs of the $\bar{k}$ values in LiPFOS were all less than 12.2 %, indicating that there is good precision in the extrapolated retention values. The slightly higher RSDs denotes a greater spread in the LiPFOS data than in SDS. All of the $\bar{k}$ values were greater than 100, signifying that the analytes were highly retained. The overall elution order was as follows: pyridine < 4-aminopyridine < aniline < *o*-toluidine < *p*-toluidine ≈ benzylamine < N,N-dimethylaniline < N-methylaniline < *m*-toluidine. Statistical treatment of the $\bar{k}$ values via a t-test at the 95 % C.L. revealed that the retention factors of *p*-toluidine and benzylamine were statistically the same. The elution order follows the general trend of a partition mechanism. Similar to the SDS results, 4-aminopyridine and pyridine reversed elution order for all LiPFOS mobile phases relative to pure water. While the trend in elution order was similar between LiPFOS and SDS, it is noteworthy that *m*-toluidine eluted after N,N-dimethylaniline in LiPFOS.

Figure 5.4: Graph of the logarithmic extrapolated retention factor for each analyte versus the concentration of LiPFOS. Analytes: (♦) pyridine, (■) 4-aminopyridine, (▲) aniline, (**x**) benzylamine, (∗) *o*-toluidine, (●) *m*-toluidine, (○) *p*-toluidine, (◊) N-methylaniline, (□) N,N-dimethylaniline. Other experimental conditions as given in the text.

Figure 5.4

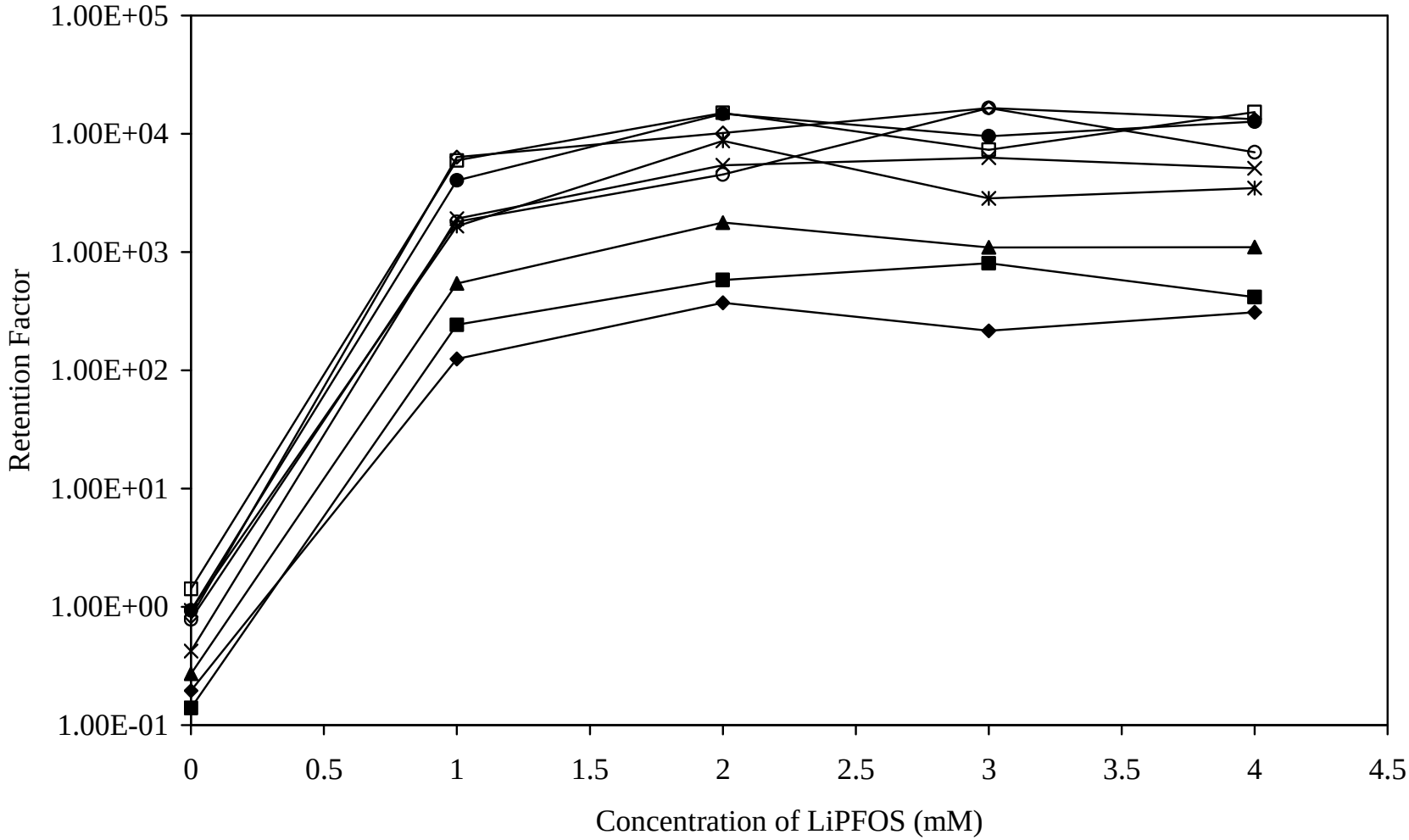
1.00E+05
1.00E+04
1.00E+03
1.00E+02
1.00E+01
1.00E+00
1.00E-01
Retention Factor
0
0.5
1
1.5
2
2.5
3
3.5
4
4.5
Concentration of LiPFOS (mM)

Table 5.3: Retention and selectivity factors of cationic aromatic amines in LiPFOS mobile phase.

Aromatic Amines	Retention Factor $(\bar{k})$ [a]	Selectivity Factor (α)			
		α_{1A} [b]	α_{1B} [b]	α_2 [c]	α_3 [d]
Pyridine	217.1 ± 11.0	0.32 ± 0.02	1.00 ± 0.00	1113 ± 198	5.52 ± 0.33
4-aminopyridine	339.3 ± 19.7	0.50 ± 0.03	1.56 ± 0.09	2442 ± 1462	2.40 ± 0.15
Aniline	683.9 ± 61.2	1.00 ± 0.00	3.15 ± 0.29	2515 ± 1150	1.62 ± 0.15
Benzylamine	2553 ± 256	3.73 ± 0.38	———	6047 ± 1116	3.10 ± 0.31
o-toluidine	2098 ± 212	3.07 ± 0.31	———	2246 ± 307	1.24 ± 0.13
m-toluidine	7224 ± 530	10.56 ± 0.78	———	7739 ± 1347	7.70 ± 0.57
p-toluidine	2394 ± 292	3.50 ± 0.43	———	3054 ± 656	1.41 ± 0.17
N-methylaniline	6612 ± 347	9.68 ± 0.52	———	8036 ± 1621	2.87 ± 0.15
N,N-dimethylaniline	6093 ± 220	8.91 ± 0.34	———	4316 ± 284	2.47 ± 0.09

[a] Retention factors calculated as the weighted mean of the extrapolated retention factors within the experimental concentration range, 1.0 – 4.0 mM (Equation 5.6). Experimental conditions as given in the text.

[b] Selectivity factors calculated between (A) analyte and aniline or (B) analyte and pyridine (Equation 5.8).

[c] Selectivity factors calculated for analyte between LiPFOS and pure water (Equation 5.9).

[d] Selectivity factors calculated for analyte between LiPFOS and SDS (Equation 5.10).

While the author does not have a definitive explanation for this phenomenon, it can be postulated that steric hindrance of N-alkyl substituted anilines with the sulfonate head group of LiPFOS contributes to this elution order. Other possible explanations for why *m*-toluidine eluted after N,N-dimethylaniline are postulated by the author in the Appendix 5.6. In comparing the $\bar{k}$ values in LiPFOS (Table 5.3) to those in pure water (Table 5.1), a large increase of 3 to 4 orders-of-magnitude in amine retention is observed. It is observed that the $\bar{k}$ values in LiPFOS (Table 5.3) are greater than in SDS (Table 5.2), with several of the values being an order of magnitude greater. It is apparent that the presence of LiPFOS dramatically decreases chromatographic transport of the analytes and, by implication, decreases environmental transport as well.

The selectivity factor α_1 was calculated from the $\bar{k}$ values of substituted aromatic amines and a base aromatic amine (Equation 5.8), with the results shown in Table 5.3. Most of the α_1 values are greater than unity, signifying that the addition of the substituent increased analyte interaction with LiPFOS in the stationary phase. The addition of a methyl substituent at the *meta*- position resulted in a ten-fold increase in the interaction of the amine with the LiPFOS monomers in the stationary phase. In contrast, the addition of the methyl substituent at either the *ortho*- or *para*- position led to a three-fold increase in the interaction. In relation to aniline, the α_{1A} values of pyridine and 4-aminopyridine were less than unity (Table 5.3). These results suggest that, similar to the trends in SDS, the inclusion of nitrogen in the ring structure of an aromatic amine reduced interaction with the LiPFOS monomers in the stationary phase. Also, the addition of a methyl substituent to the aromatic ring increased interaction with the LiPFOS monomers in the stationary phase.

The selectivity factor α_2 was calculated from the $\bar{k}$ values of the aromatic amines in LiPFOS and pure water mobile phases (Equation 5.9), with the results shown in Table 5.3. All of the α_2 values are greater than 1000, implying that the ion-pairing mechanism with LiPFOS has a large contribution to the retention of the analytes compared with partition alone. This result suggests that, similar to SDS, all of the cationic aromatic amines have strong interactions with LiPFOS monomers in the stationary phase. This interaction causes the amines to display a substantial decrease in environmental transport when compared to a system devoid of any surfactant. In addition, all α_2 values were greater in LiPFOS than in SDS.

The selectivity factor α_3 was calculated from the $\bar{k}$ values of the aromatic amines in LiPFOS and SDS mobile phases (Equation 5.10), with the results shown in Table 5.3. All α_3 values are greater than unity, implying that the analytes have stronger interactions with LiPFOS than SDS monomers in the stationary phase. Furthermore, the fact that α_3 values ranged from 1.2 – 7.7 suggests that the ion-pairing mechanism with LiPFOS will have selective interactions with certain cationic amines compared with SDS. Based on these results, there is potential for the use of LiPFOS in environmental remediation of cationic aromatic amines since the interactions are more pronounced in a LiPFOS than a SDS mobile phase. Although perfluorinated surfactants are more expensive than their hydrocarbon analogous, they are chemically and thermally more stable.

5.4 Summary

During this study, the effects of a hydrocarbon and perfluorinated surfactant on the transport of environmental contaminants (e.g. cationic aromatic amines) in a model

groundwater system were determined. The overall trend was that the addition of either an anionic hydrocarbon or anionic perfluorinated surfactant below the CMC substantially decreased the transport of cationic aromatic amines, in relation to transport in the system devoid of any surfactant. It is noteworthy that the amines displayed a decrease in transport when the perfluorinated and hydrocarbon surfactants were compared. Furthermore, an increase in surfactant concentration below the CMC resulted in a statistically invariant change in transport, within the concentration range tested in this study (1.0 – 4.0 mM). The individual amines displayed different transport trends between surfactant and pure water mobile phases. In the pure water system, transport was controlled via partitioning of the cationic aromatic amines between the polar mobile phase and the non-polar stationary phase. However, both partitioning and ion interactions impacted the transport of the amines in the presence of anionic surfactant monomers in the stationary phase.

These results and conclusions have important implications for the environmental transport or remediation of cationic aromatic amines. In particular, several of the cationic aromatic amines exhibit selective interaction with the perfluorinated surfactant compared to the hydrocarbon surfactant. Further studies are needed to characterize transport effects of perfluorinated surfactants, particularly in relation to their head group (sulfonate, carboxylate, etc.) and carbon chain length (C_4 – C_8), because of their importance to commercial procedures or possible application in environmental remediation clean-up techniques.

APPENDIX

5.5 Appendix

As stated in Section 5.3.3, while the elution order of the analytes was similar between SDS and LiPFOS, an exception was that *m*-toluidine eluted after N,N-dimethylaniline in LiPFOS. Two ideas are postulated as to the cause of this deviation in elution order.

First, through conversations with Dr. James Jackson of Michigan State University, it was postulated that a different elution order might appear if *m*-toluidine was protonated a site other than on the nitrogen. Dr. Jackson used a high level of ab initio calculation to determine the gas-phase relative energies, ΔH_{rel}, of the toluidines at various carbon protonation sites. The results showed that the C4-protonated isomer of *m*-toluidine has a lower relative energy ($\Delta H_{rel} = -2.3$ kcal mol^{-1}) than the N-protonated structure, while other isomers, such as the C2- and C6-protonated isomers, are higher in energy ($\Delta H_{rel} = +3.4$ kcal mol^{-1} and +1.7 kcal mol^{-1}, respectively). If the C4-protonated isomer played a significant role during the separation within the mobile phase, then it is possible the isomer could behave substantially different than the N-protonated toluidines, thus leading to the longer elution time of *m*-toluidine seen in this experiment.

Secondly, it has been reported in literature [32,33], that the pK_a of substituted anilines vary depending on the solvent. It is therefore postulated that the addition of the co-solvent methanol altered the pK_a of *m*-toluidine, affecting the protonation of *m*-toluidine in the mobile phase (pH 4.0). The variation in protonation could lead to substantially different interactions within the experimental system, thus leading to the different elution order and longer retention times for *m*-toluidine observed in this study.

REFERENCES

5.6 References

[1] E. Kissa, Fluorinated Surfactants: Synthesis, Properties, and Applications, Marcel Dekker, New York, NY, 1994.

[2] R.E. Banks, B.E. Smart, J.C. Tatlow, Organofluorine Chemistry: Principles and Commercial Applications, Plenum Press, New York, NY, 1994.

[3] C.A. Moody, J.A. Field, Environ. Sci. Technol. 34 (2000) 3864-3870.

[4] C.A. Moody, W.C. Kwan, J.W. Martin, D.C.G. Muir, S.A. Mabury, Anal. Chem. 73 (2001) 2200-2206.

[5] C.A. Moody, J.W. Martin, W.C. Kwan, D.C.G. Muir, S.A. Mabury, Environ. Sci. Technol. 36 (2002) 545-551.

[6] United States Environmental Protection Agency, Prevention, Pesticides and Toxic Substances (7505C), EPA-730-F-99-009, 1999.

[7] J.P. Giesy, K. Kannan, Environ. Sci. Technol. (2002) 148A-152A.

[8] J.P. Giesy, K. Kannan, Environ. Sci. Technol. 35 (2001) 1339-1342.

[9] K. Kannan, J. Koistinen, K. Beckmen, T. Evans, J.F. Gorzelany, K.J. Hansen, P.D. Jones, E. Helle, M. Nyman, J.P. Giesy, Environ. Sci. Technol. 35 (2001) 1593-1598.

[10] K. Kannan, J.C. Franson, W.W. Bowerman, K.J. Hansen, P.D. Jones, J.P. Giesy, Environ. Sci. Technol. 35 (2001) 3065-3070.

[11] S. Taniyasu, K. Kannan, Y. Horii, N. Yamashita, Organohalogen Compd. 59 (2002) 105-108.

[12] Y.J. An, E.R. Carraway, M.A. Schlautman, Water Res. 36 (2002) 300-308.

[13] R.N. Simmons, V.L. McGuffin, Anal. Chimica Acta 603 (2007) 93-100.

[14] R.N. Simmons, V.L. McGuffin, Anal. Chimica Acta, *manuscript submitted*.

[15] J. Ståhlberg, J. Chromatogr. A 855 (1999) 3-55.

[16] J.H. Knox, G.R. Laird, J. Chromatogr. 122 (1976) 17-34.

[17] J.C Kraak, K.M. Jonker, J.F.K. Huber, J. Chromatogr. 142 (1977) 671-688.

[18] B. Fransson, K.G. Wahlund, I.M. Johansson, G. Schill, J. Chromatogr. 125 (1976) 327-344.

[19] B.A. Bidlingmeyer, S.N. Deming, W.P. Price Jr., B. Sachok, M. Petrusek, J. Chromatogr. 186 (1979) 420-434.

[20] B.A. Bidlingmeyer, J. Chromatogr. 18 (1980) 525-539.

[21] M.C. Gennaro, Advances in Chromatography, Ed. By P.R. Brown and E. Grushka, Marcel Dekker, New York, NY, 1995, p. 343-381.

[22] S. Ahuja, Selectivity and Detectability Optimizations in HPLC, John Wiley and Sons, New York, NY, 1989.

[23] L.R. Snyder, J.W. Dolan, Advances in Chromatography, Ed. By P.R. Brown and E. Grushka, Marcel Dekker, New York, NY, 1998, p. 115-187.

[24] S.L. Meyer, Data Analysis for Scientists and Engineers, John Wiley and Sons, New York, NY, 1975, p. 28.

[25] D.E. Kile, C.T. Chiou, H. Zhou, H. Li, O. Xu, Environ. Sci. Technol. 29 (1995) 1401-1406.

[26] K. Heinig, C. Vogt, Electrophoresis 290 (1999) 3311-3328.

[27] J.A. Field, M. Schultz, D. Barofsky, Chimia 57 (2003) 556-560.

[28] M.N. Khan, U. Zareen, J. Hazard. Mater. 133 (2006) 269-275.

[29] S. Martinez-Barrachina, J. Alonso, L. Matia, R. Prats, M. del Valle, Anal. Chem. 71 (1999) 3684-3691.

[30] United States Environmental Protection Agency, Pollution Prevention and Toxics (7407), EPA-749-F-95-002a, 1994.

[31] Allied Chemical Corporation, National Aniline Division, Aniline, Allied Chemical Corporation, New York, NY, 1964.

[32] T.V Kashik, B.V. Prokop'ev, G.V. Rassolova, S.M. Ponomareva, Russ. Chem. B+ 20 (1971) 1847-1850.

[33] H.C. Brown, D.H. McDaniel, O. Häfliger, Ed. By E.A. Braude, F.C. Nachod, Determination of Organic Structures by Physical Methods, Academic Press, New York, 1955.

CHAPTER 6: USE OF SYSTEM PEAKS FOR THE DETERMINATION OF THE RETENTION OF FLUORINATED AND HYDROCARBON SURFACTANTS IN THE EXPERIMENTAL SYSTEM

6.1 Introduction

As described in Chapter 5, amine mixtures were analyzed in a pure water mobile phase (Figures 6.1A-C) and in methanol/aqueous surfactant mobile phases (of various compositions). During the course of these experiments, several extra peaks were observed in the chromatograms of the surfactant mobile phases (Figures 6.2A-B), which were not associated with any of the amine analytes. These peaks, which are classified as system peaks, are related to the components of the mobile phase and were not observed in the pure water mobile phase chromatograms (Figures 6.1A-C). System peaks can occur in a chromatographic system when 1) the mobile phase contains more than one component [1], 2) the component is distributed between the mobile phase and the stationary phase [2], and 3) the injection sample has a slightly different composition than the mobile phase. System peaks can be observed providing the detector in use is sensitive to those components. These peaks are often regarded as annoyances, and chromatographers try to eliminate them from chromatograms. Several studies have been conducted on various aspects of system peaks, such as their origin, formation, and importance in chromatographic techniques [1,3-4], their relationship to adsorption isotherms in the column [5], and their use for indirect detection [6] and quantitative analysis [7]. System peaks are relaxation products after the column equilibrium has been perturbed via an injection sample plug [1]. As such, system peaks are believed to provide information about the interactions within the chromatographic system.

Figures 6.1A-C: Representative chromatograms of amines in water mobile phase. Mobile phase: 10.0 mM *β*-alanine aqueous mobile phase. Flowrate: 0.5 mL min^{-1}. Analytes: (0) lithium nitrate, (1) 4-aminopyridine, (2) pyridine, (3) aniline, (4) benzylamine, (5) *p*-toluidine, (6) N-methylaniline, (7) *m*-toluidine, (8) *o*-toluidine, (9) N,N-dimethylaniline, (10) N-ethylaniline, (11) N,N-diethylaniline. Other experimental conditions as given in the text.

Figure 6.1A

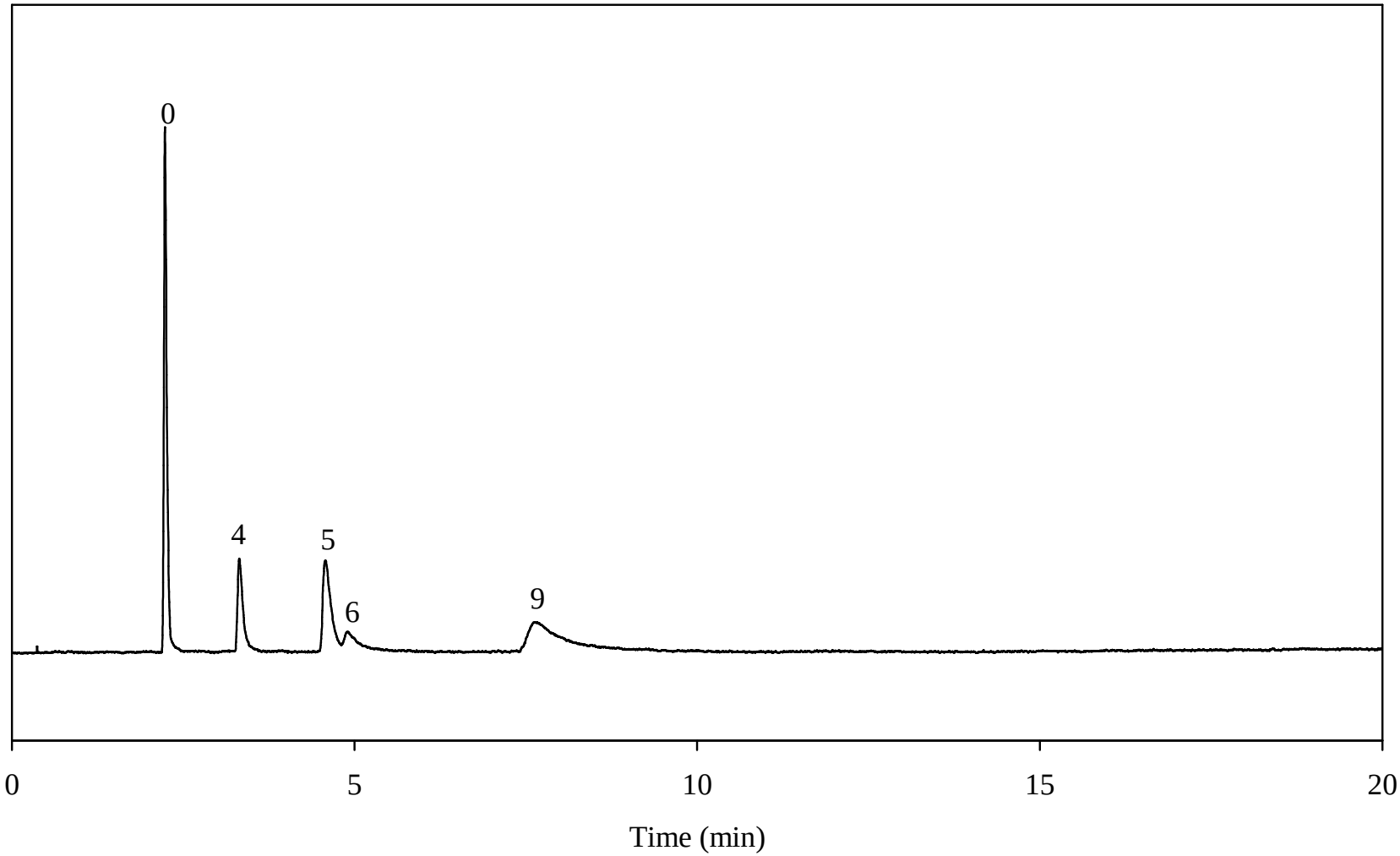

Figure 6.1B

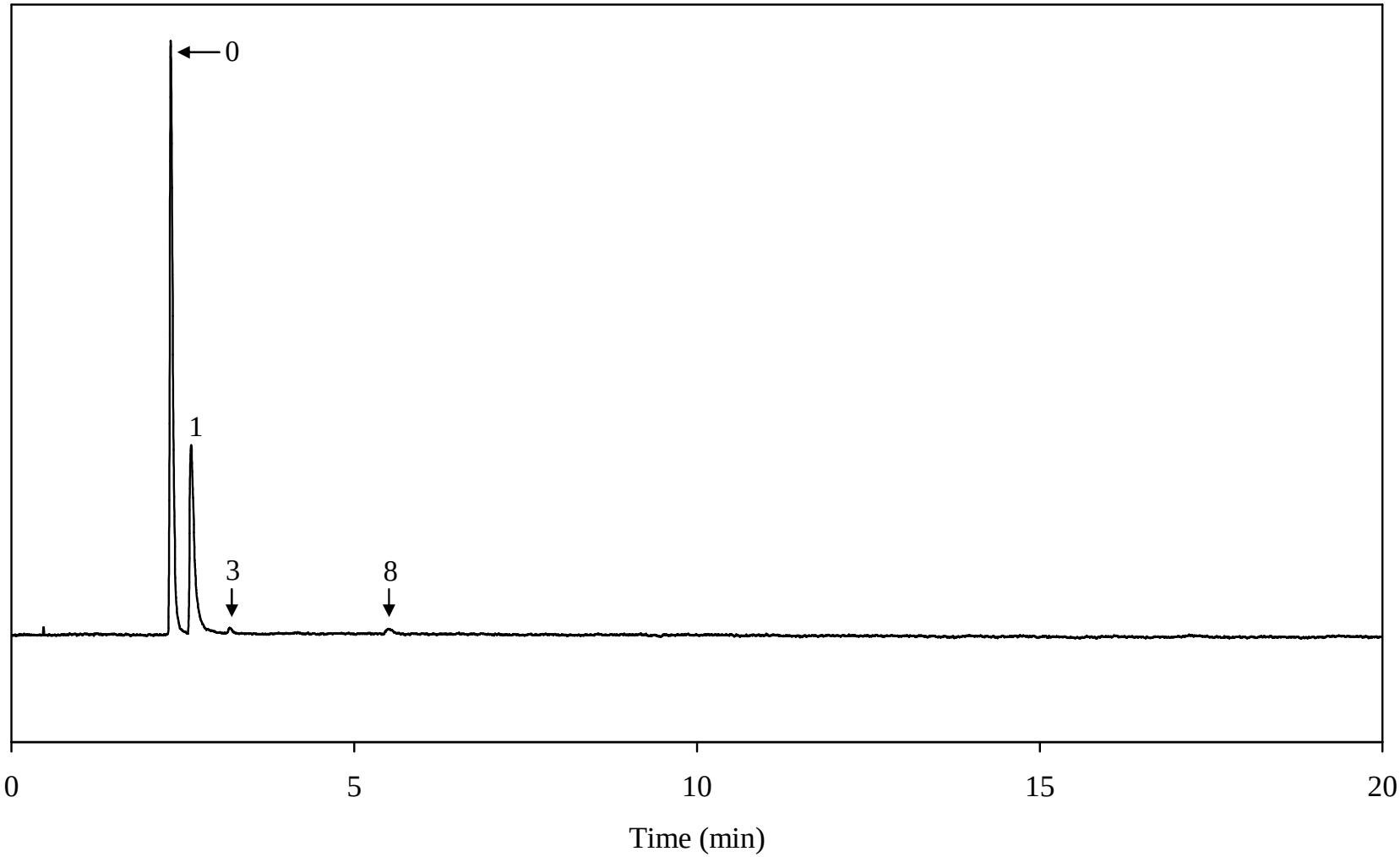

Figure 6.1C

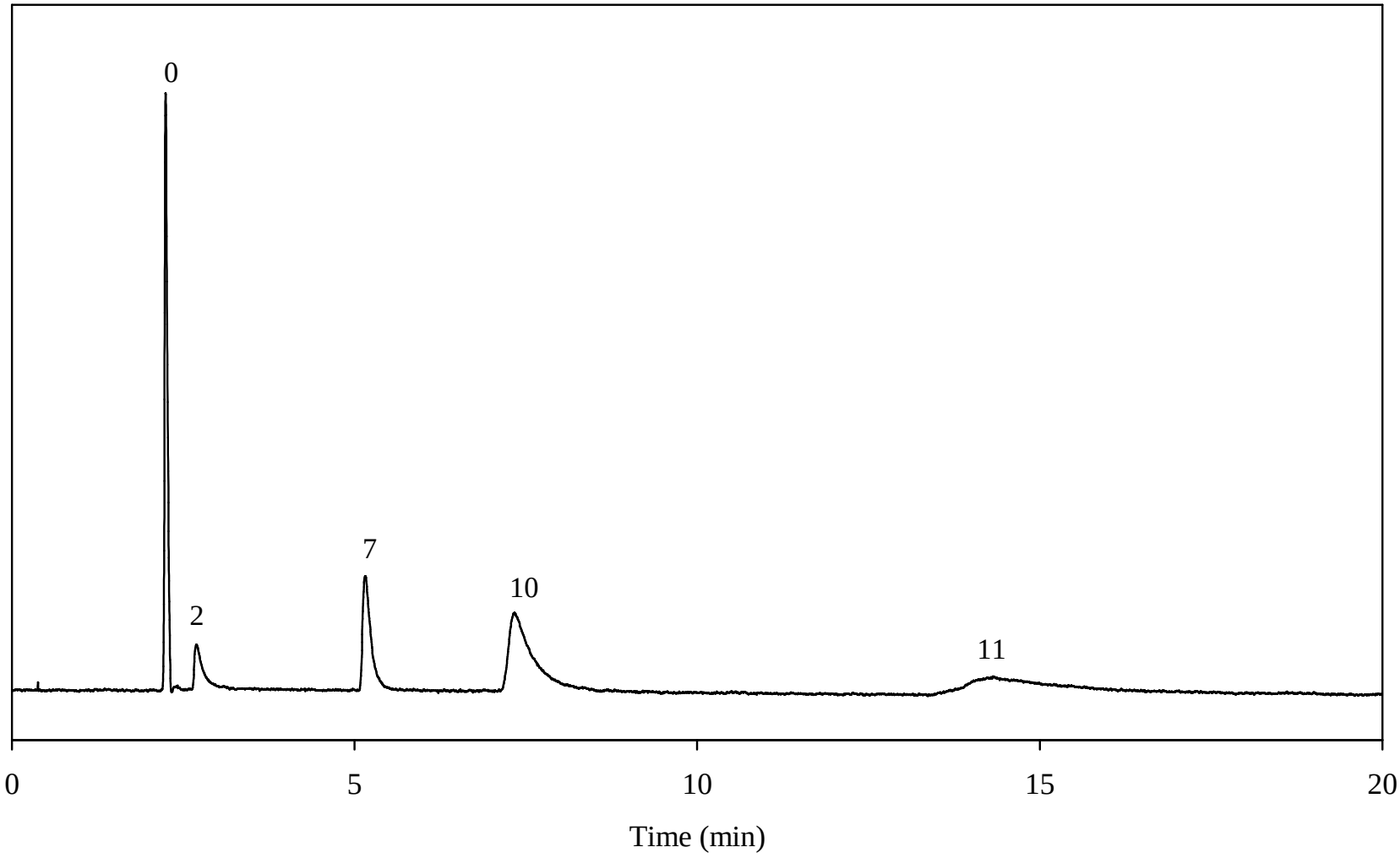

Figures 6.2A-B: Representative chromatograms of amines in surfactant mobile phases. (A) Mobile phase: 45:55 methanol/2.0 mM aqueous sodium dodecyl sulfate (SDS). Flowrate: 1.0 mL min^{-1}. (B) Mobile phase: 45:55 methanol/2.0 mM aqueous lithium perfluorooctane sulfonate (LiPFOS). Flowrate: 0.3 mL min^{-1}. Analytes: (0) lithium nitrate, (4) benzylamine, (5) *p*-toluidine, (6) N-methylaniline, (∗) unidentified system peak. Other experimental conditions as given in the text.

Figure 6.2A

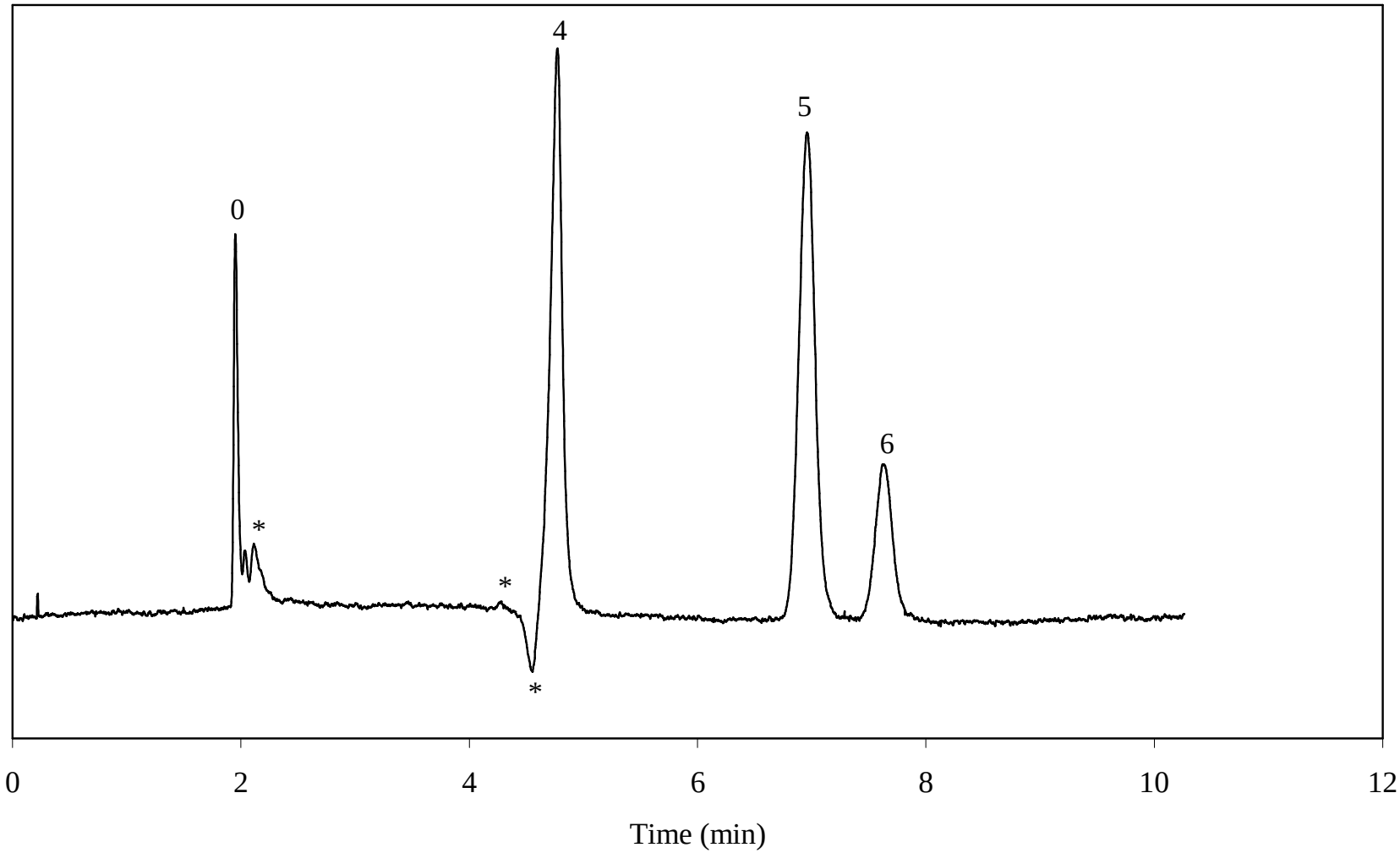

Figure 6.2B

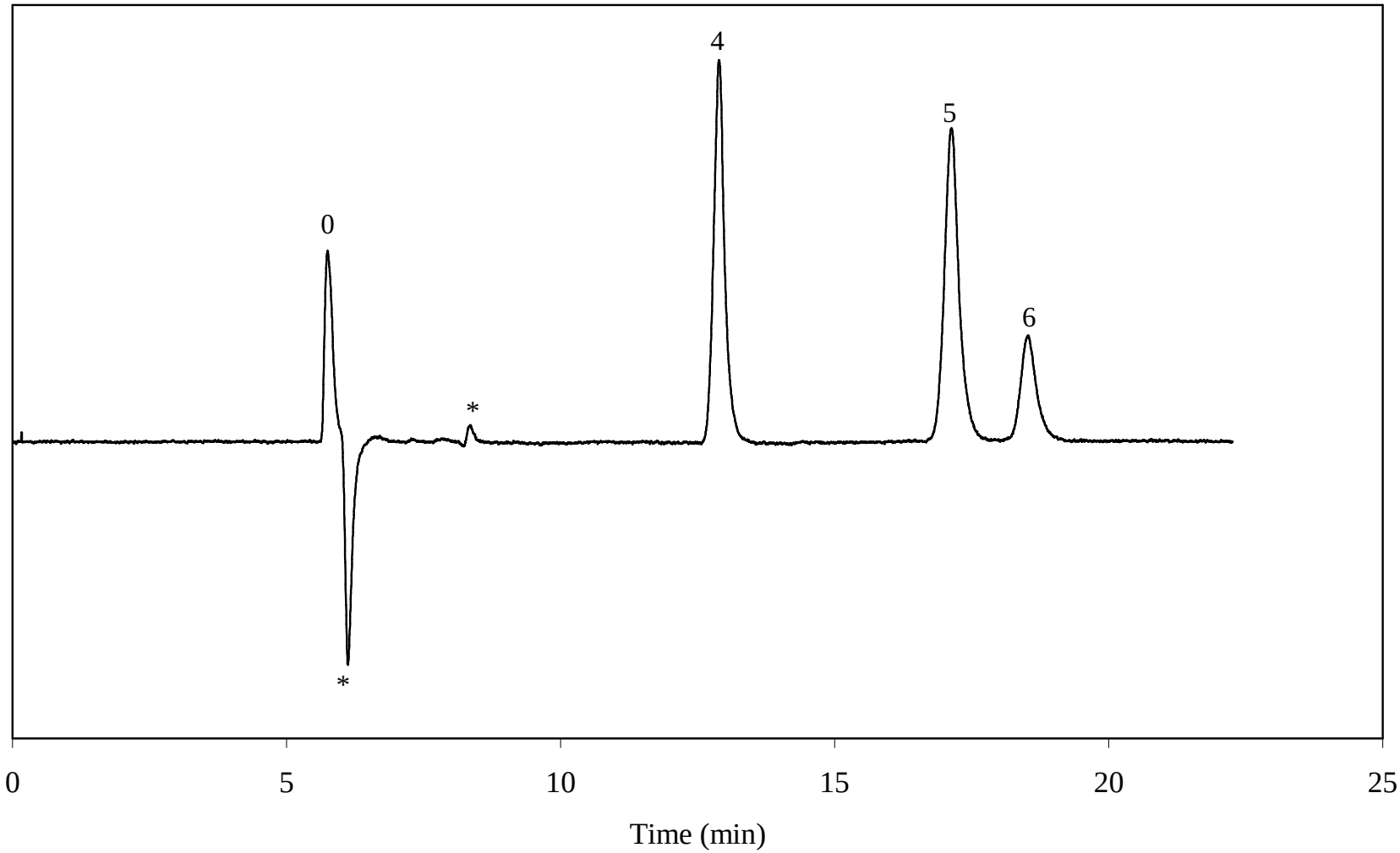

As described in Chapter 2 (Section 2.2.4), refractive index measurements were unsuccessful in determining the retention of the surfactants in the experimental system. It was therefore surmised that if the system peaks were related to the surfactants, then they could be used to determine surfactant retention within the chromatographic system. Thus, the main goal of this experiment was to determine the retention of the surfactants within the experimental chromatographic system based on the retention and identification of the system peaks. These retention values can be used to elucidate information about the environmental transport of the surfactants themselves through a groundwater system, which can have an impact on the transport of co-contaminants.

6.2 Experimental Methods

6.2.1 Mobile Phase and Analytes

The mobile phases and amine mixtures were the same as used in Chapter 5, and the preparation of which was previously described in Section 5.2.1.

6.2.2 Experimental System

The analytical column, liquid chromatography system, and detection system were the same as used in Chapter 5. All details are the same as described in Section 5.2.2, including the UV absorbance wavelength of detection (205 nm). All experiments were carried out at ambient temperature with a maximum pressure limit of 4500 psi. The flow rate was 1.0 mL min^{-1} during the sodium dodecyl sulfate (SDS) experiments and varied between 1.0 mL min^{-1} and 0.3 mL min^{-1} during the lithium perfluorooctane sulfonate (LiPFOS) experiments.

6.2.3 Data Analysis and Calculations

6.2.3.1 Retention Factor Measurements

As stated in previous chapters, reversed-phase liquid chromatography (RPLC) is used to model an environmental system in which the octadecylsilica stationary phase represents soil and the aqueous mobile phase represents groundwater. When a surfactant is added to the RPLC system below its critical micelle concentration (CMC), the surfactant monomers distribute or partition between the mobile and stationary phases. When the surfactant mobile phase in the column is allowed to reach equilibrium, this equilibrium is maintained as long as the chromatographic system is not disturbed, either by 1) changing the mobile phase or 2) injection of a sample plug.

The equilibrium constant, K, is directly related to the ratio of the surfactant monomer concentrations in the stationary and mobile phases. This equilibrium constant represents all interactions between the surfactant monomers, stationary phase, and mobile phase. The equilibrium constant is a vital piece of information needed to model environmental systems. However, the determination of this equilibrium constant is difficult because of the inability to directly measure the concentrations of the surfactant monomers in the environmental mobile and stationary phases.

The retention factor, k, is defined as

$$k = K\phi \tag{6.1}$$

where ϕ is the phase ratio. Assuming that the phase ratio is constant, the value for k is proportional to K. Consequently, the retention factor of the system peak can be used to elucidate information about the interactions of the surfactants in the experimental chromatographic system.

When a pure solvent is injected, the sample at the column head is relatively devoid of the other mobile phase components. This causes a perturbation of the column equilibrium, which the system tries to reestablish. Consequently, any mobile phase component adsorbed on the stationary phase surface is extracted into the injected volume [5]. The reestablishment of the column equilibrium results in the appearance of system peaks corresponding to each component. In order to identify which system peak is attributed to the surfactants in the experiment system, injections of pure methanol and the mobile phase were performed. Representative chromatograms of injections of pure methanol are located in Figures 6.3A and B for SDS and LiPFOS, respectively. For the methanol injections, the retention factor, k, was calculated by

$$k = \frac{t_R - t_0}{t_0} \qquad (6.2)$$

where the void time, t_0, was taken as the first positive deviation from the baseline arising from methanol, and the retention time, t_R, for the system peaks was determined from the negative peak minimum, which is appropriate for the peaks observed in this study. The k values were used for the subsequent elucidation of surfactant retention.

Figures 6.3A-B: Representative chromatograms of pure methanol in surfactant mobile phases. (A) Mobile phase: 45:55 methanol/2.0 mM aqueous SDS. (B) Mobile phase: 45:55 methanol/2.0 mM aqueous LiPFOS. Flowrate: 1.0 mL min^{-1}. Analytes: (0) methanol, (∗) unidentified system peak, (∗S) SDS system peak, (∗L) LiPFOS system peak. Other experimental conditions as given in the text.

Figure 6.3A

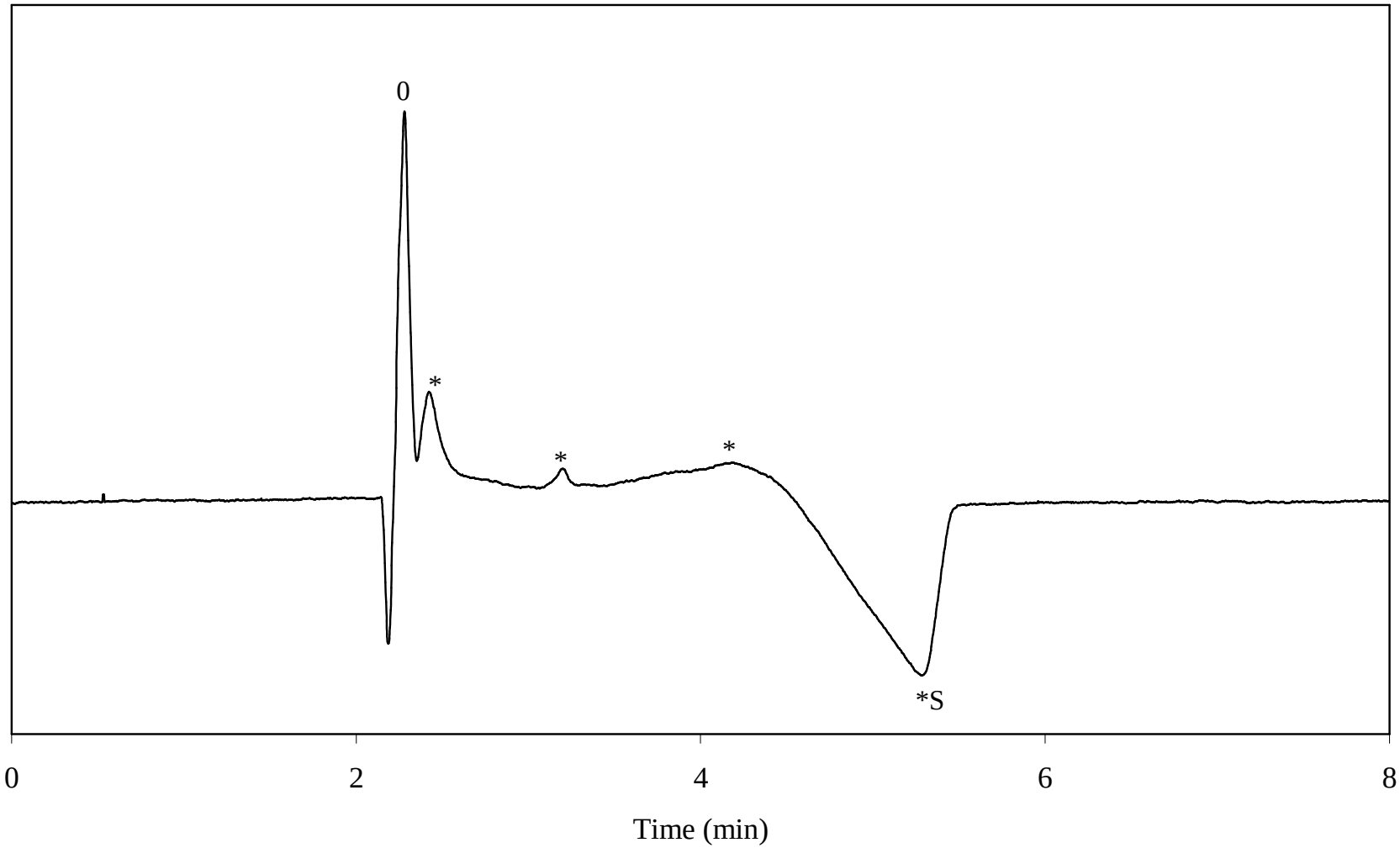

Figure 6.3B

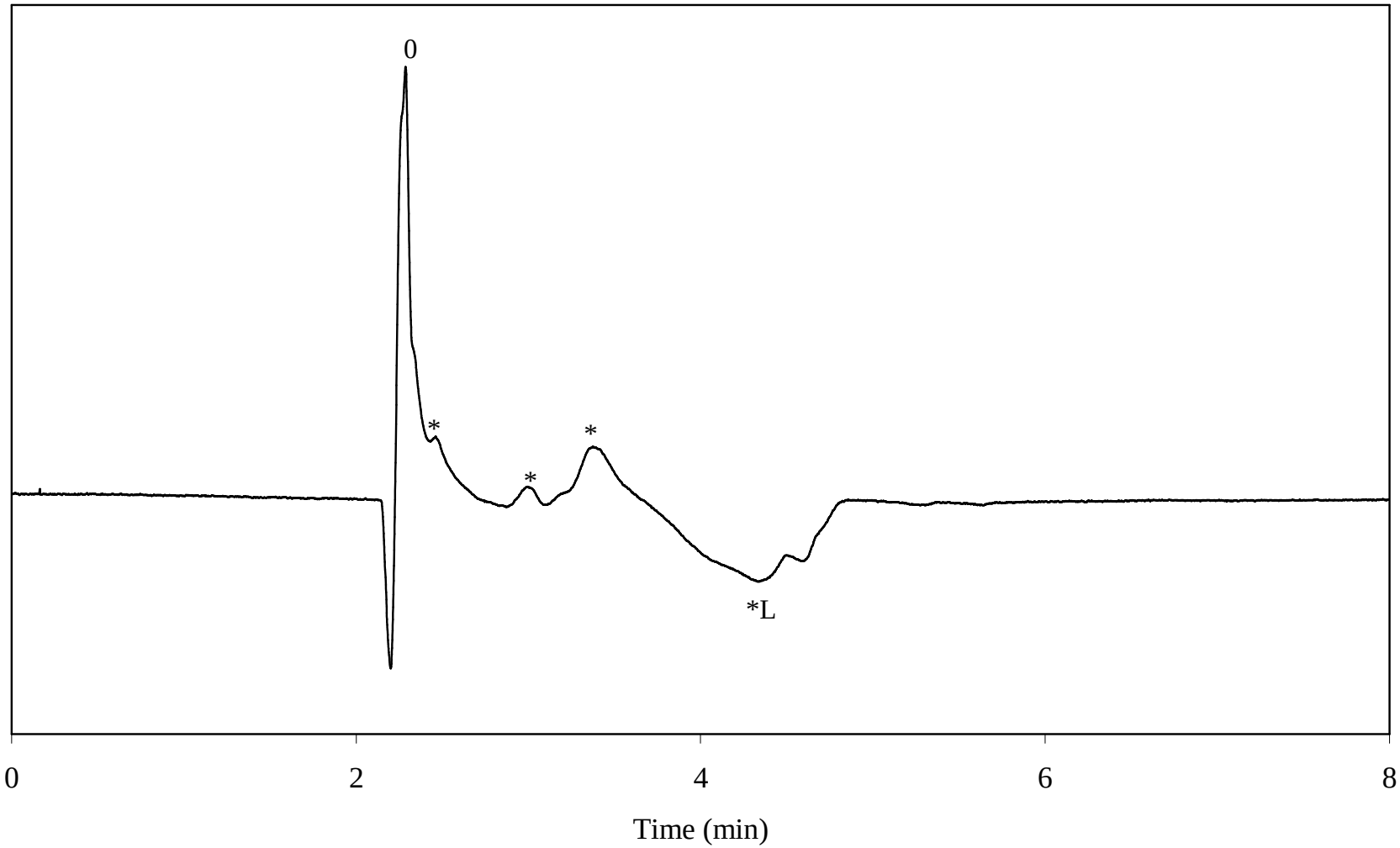

6.2.3.2 Linear Solvent Strength Model

Because the determination of surfactant retention factors in solvent A (e.g. aqueous surfactant solution) is impractical due to excessive retention, a stronger organic co-solvent B (e.g. methanol) was added to the mobile phase to decrease retention. The linear solvent strength (LSS) model relates the surfactant retention as a function of the percent composition of the organic solvent (% B) in the mixed mobile phase [8], via the following equation

$$\log k = -S(\%B) + \log k_0 \qquad (6.3)$$

where S is the slope and k_0 is the surfactant retention factor in pure solvent A (i.e. % B = 0). Linear regression is performed on the logarithmic k values measured at various % B. The k_0 value of the analyte at a given surfactant concentration is determined from the logarithmic y-intercept value.

6.3 Results and Discussion

The rationale behind the choice of stationary phase, surfactants, and analytes has been discussed in Chapters 2 and 5. In order to identify the system peaks, injections of surfactant mobile phases and pure methanol were performed, and the chromatograms collected concurrently with the amine analyte mixtures from Chapter 5.

6.3.1 System Peaks

System peaks can be characterized by having constant k values (irrespective of the sample injected), positive or negative peaks (relative to the detector base line), and peak areas that depend on the nature of the injected solutes [1]. In order to utilize this information, several injections and observations were made in both the SDS and LiPFOS mobile phases.

6.3.2 System Peaks in Sodium Dodecyl Sulfate Mobile Phases

As described in Section 6.1, several peaks were observed in the chromatograms that were not associated with any amine analytes. Representative chromatograms of amines in SDS mobile phases are shown in Figures 6.4A-C. It was observed that the retention times of several of the unidentified peaks did not change, regardless of the analyte mixture injected. This phenomenon is a characteristic of system peaks. Injections of pure solvents (methanol and mobile phase) were performed in an effort to correctly identify the system peak due to SDS.

Representative chromatograms of pure methanol in SDS mobile phases are shown in Figures 6.5A-D, and of the mobile phase in SDS mobile phases are shown in Figure 6.6. In comparing the chromatograms of Figures 6.4, 6.5, and 6.6, the large negative system peak, which is present in the chromatograms arising from the injections of amines and pure methanol, is absent in the chromatograms arising from the injections of the SDS mobile phase itself. In addition, as the concentration of SDS in the mobile phase increases, the peak area of the negative peak changes. Based on these observations, the negative system peak is attributed to the SDS component of the mobile phase.

Figures 6.4A-C: Representative chromatograms of amines in SDS mobile phases. Mobile phase: 45:55 methanol/2.0 mM aqueous SDS. Flowrate: 1.0 mL min^{-1}. Analytes: (0) lithium nitrate, (1) 4-aminopyridine, (2) pyridine, (3) aniline, (4) benzylamine, (5) *p*-toluidine, (6) N-methylaniline, (7) *m*-toluidine, (8) *o*-toluidine, (9) N,N-dimethylaniline, (∗) unidentified system peak. Other experimental conditions as given in the text.

Figure 6.4A

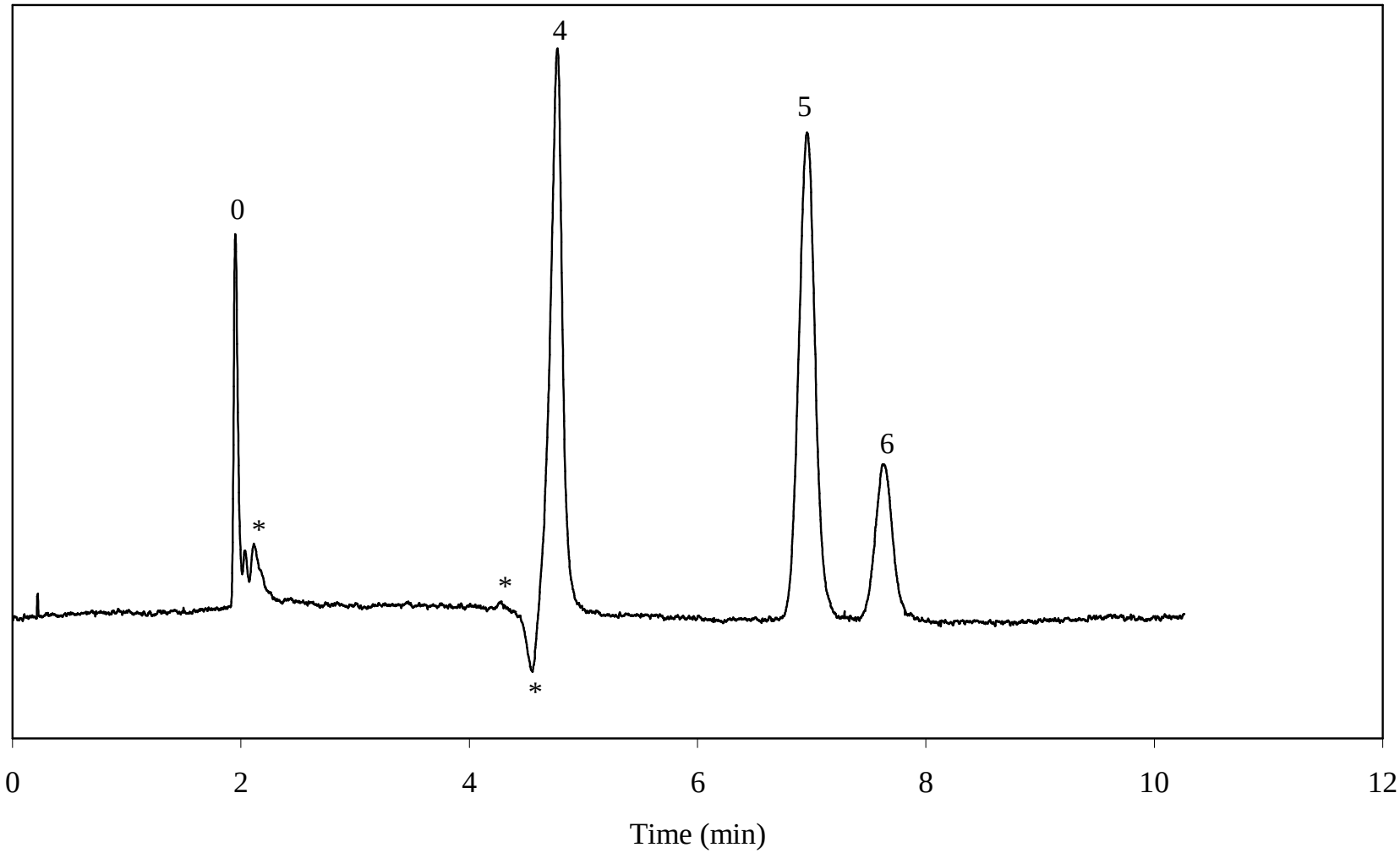

Figure 6.4B

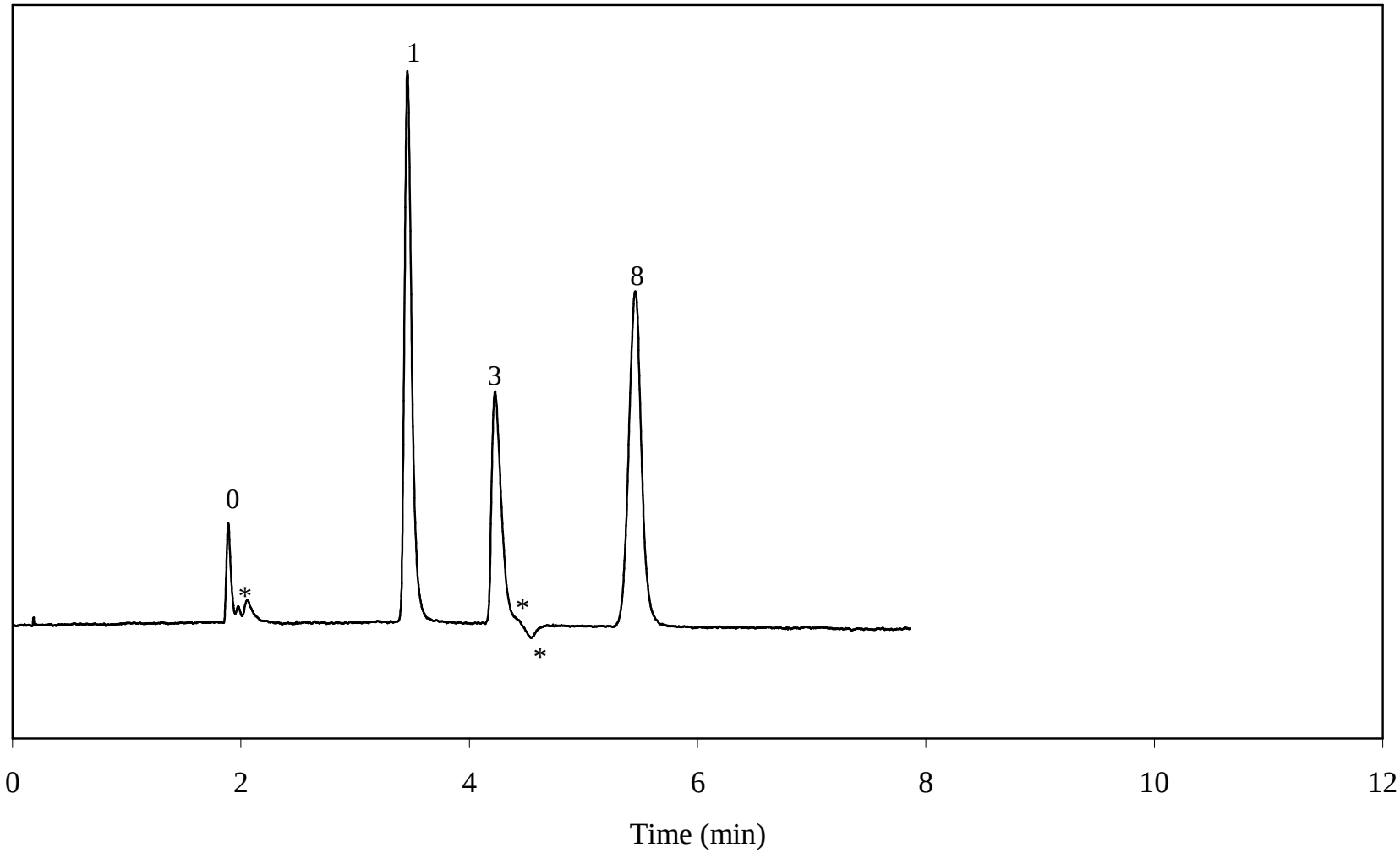

Figure 6.4C

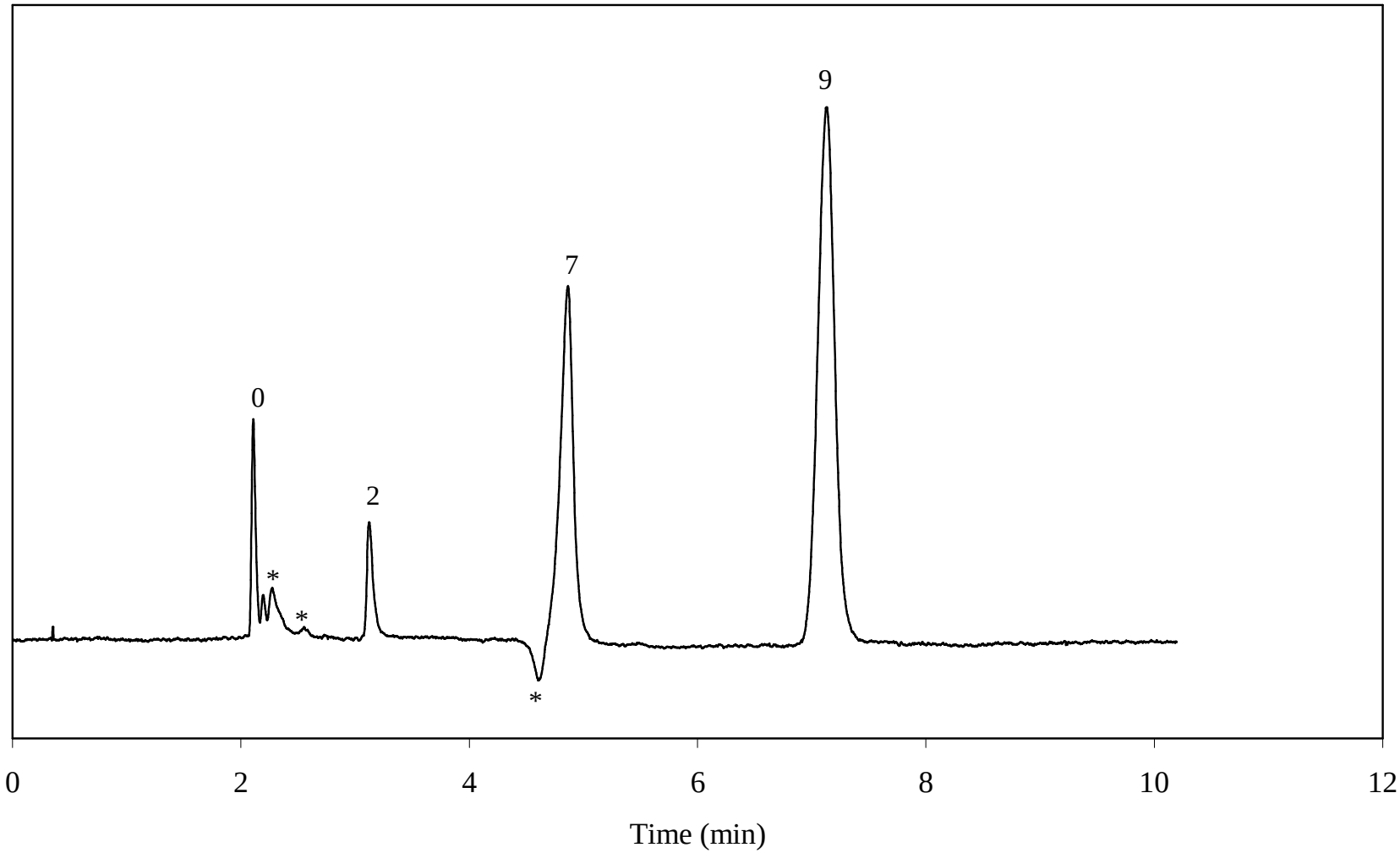

Figures 6.5A-D: Representative chromatograms of pure methanol in SDS mobile phases. Mobile phase: 45:55 methanol/aqueous SDS. (A) 1.0 mM SDS, (B) 2.0 mM SDS, (C) 3.0 mM SDS, (D) 4.0 mM SDS. Flowrate: 1.0 mL min^{-1}. Analytes: (0) methanol, (∗) unidentified system peak, (∗S) SDS system peak. Other experimental conditions as given in the text.

Figure 6.5A

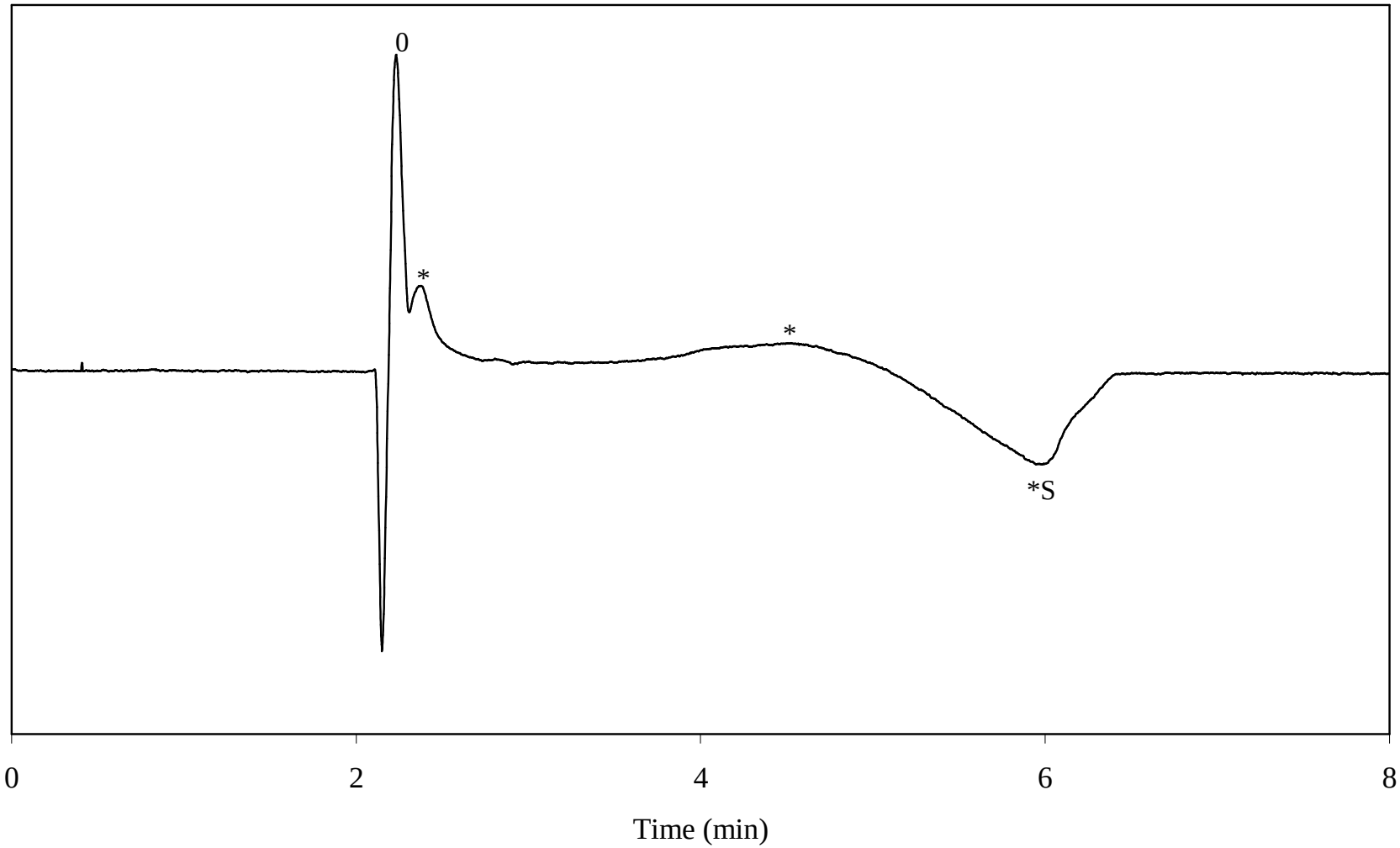

Figure 6.5B

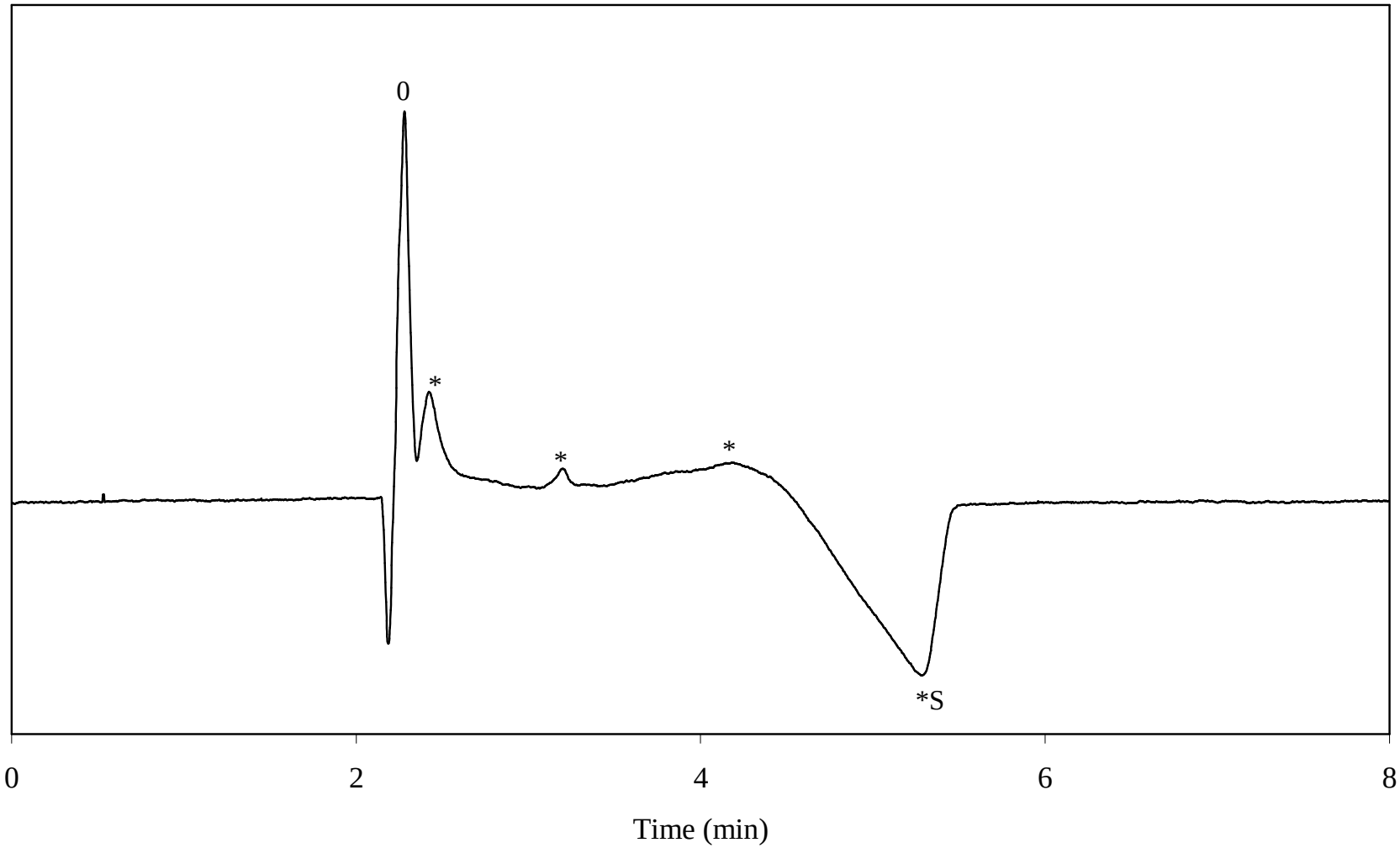

Figure 6.5C

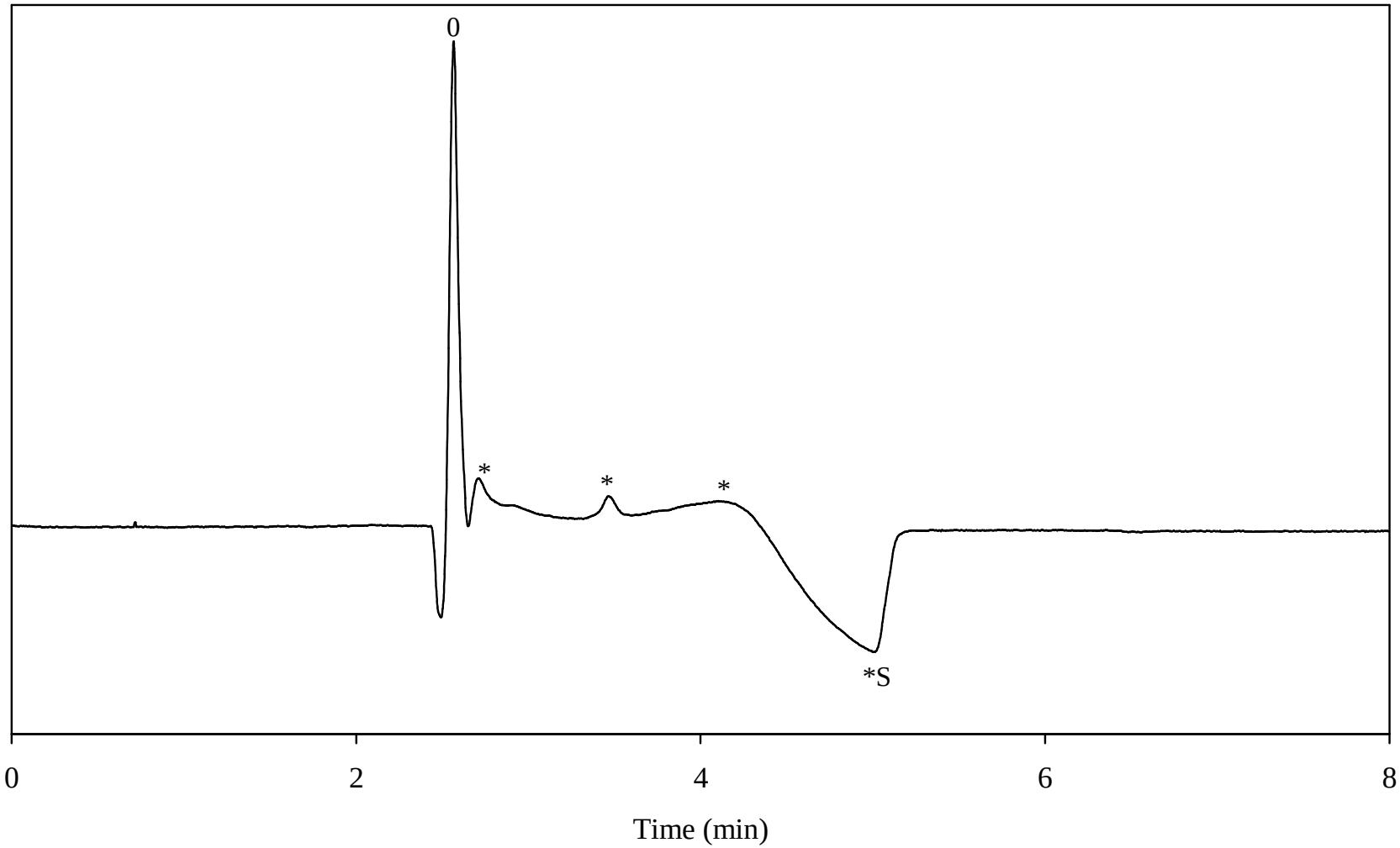

Figure 6.5D

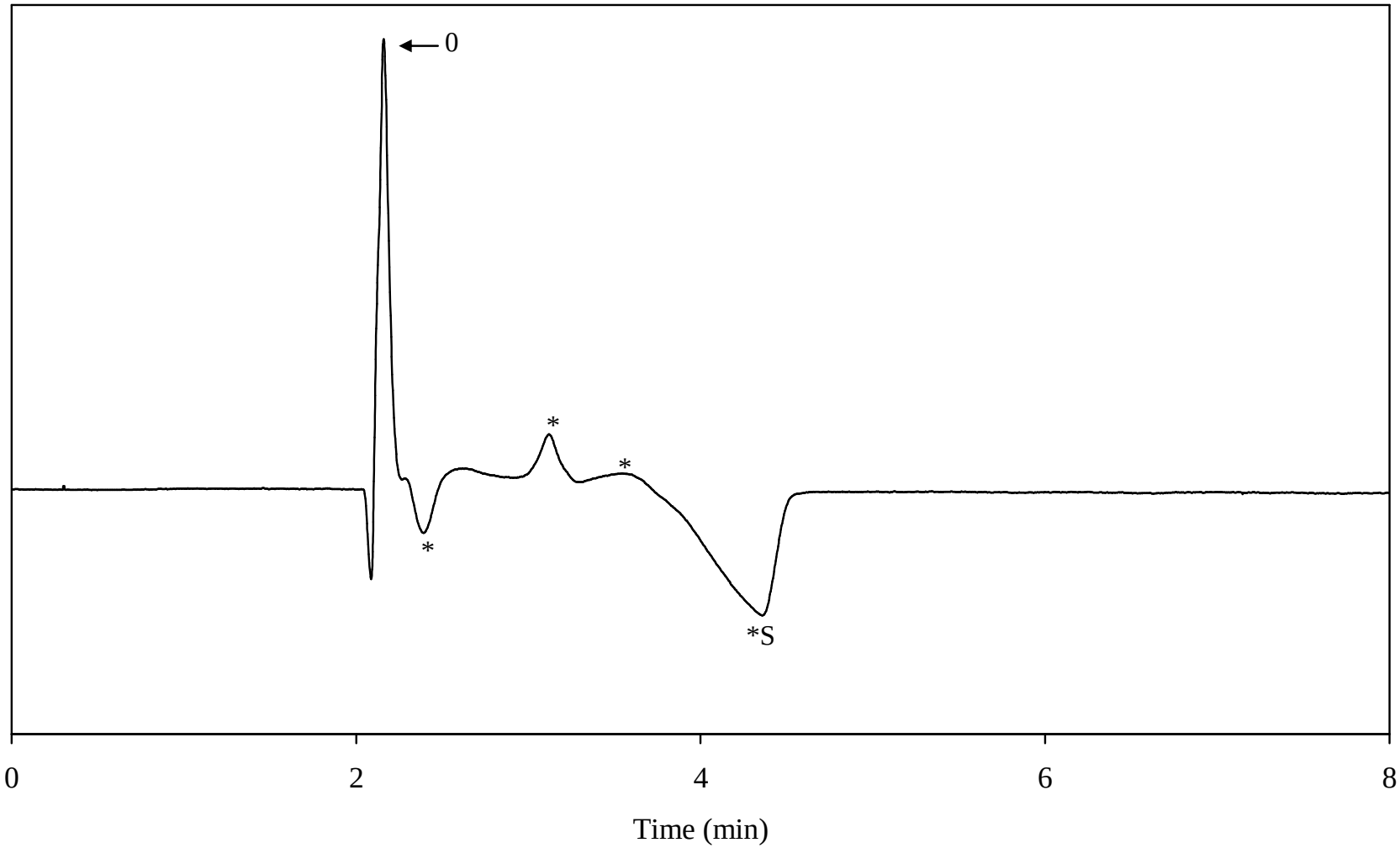

Figure 6.6: Representative chromatogram of mobile phase in SDS mobile phases. Mobile phase: 45:55 methanol/2.0 mM aqueous SDS. Flowrate: 1.0 mL min^{-1}. Analytes: (∗) unidentified system peak. Other experimental conditions as given in the text.

Figure 6.6

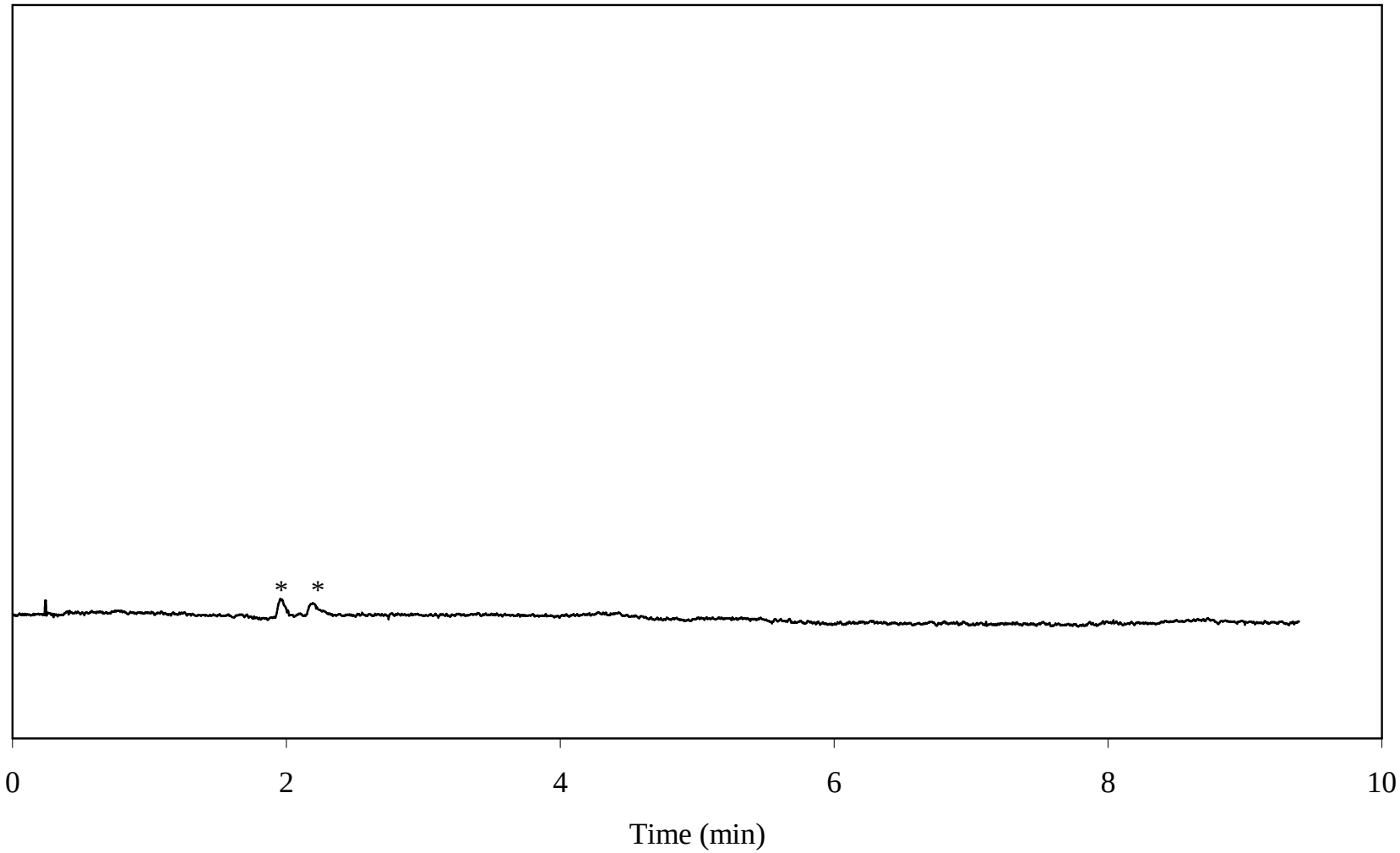

Retention factors, k, of the SDS system peaks were determined in varying mobile phase compositions of aqueous SDS (1.0 – 4.0 mM) and methanol (20 – 50 % v/v), during injections of pure methanol. A graph of the retention factor for the SDS system peak versus the methanol composition (% B) of the mobile phase is shown in Figure 6.7. Statistical treatment of these data via linear regression demonstrated a linear relationship between log k and % B, where the square of the correlation coefficient, R^2, values were all greater than 0.892, except for the 4.0 mM SDS concentration (0.655). It was observed that the logarithmic retention factor of the SDS system peak decreased with increasing methanol composition, which is consistent with predictions of the LSS method. In addition, the retention factor of the SDS system peak decreased with increasing surfactant concentration in the mobile phase, at each methanol composition.

The retention factor of the SDS system peak in an aqueous surfactant mobile phase (k_0) was determined by extrapolation at each SDS concentration using linear regression of Equation 6.3. A graph of the extrapolated retention factor for the SDS system peak versus the concentration of SDS is shown in Figure 6.8, where the error bars represent the standard deviation (±) of the individual extrapolated retention factors. There is a significant decrease in the SDS system peak retention from 1.0 to 2.0 mM SDS; however retention remains relatively constant from 2.0 to 4.0 mM SDS. The higher extrapolated retention factor at 1.0 mM SDS (32) than for 2.0 – 4.0 mM SDS (all below 10), suggests that the SDS surfactant monomers have saturated the stationary phase at a surfactant concentration of 2.0 mM and above. It has been shown in literature that parameters, such as retention factor and loading factor, are concentration dependent and will decrease with increasing concentration [9].

Figure 6.7: Graph of retention factor for SDS system peaks versus methanol composition (%) in: (♦) 1.0 mM SDS, (■) 2.0 mM SDS, (▲) 3.0 mM SDS, (**x**) 4.0 mM SDS. Other experimental conditions as given in the text.

Figure 6.7

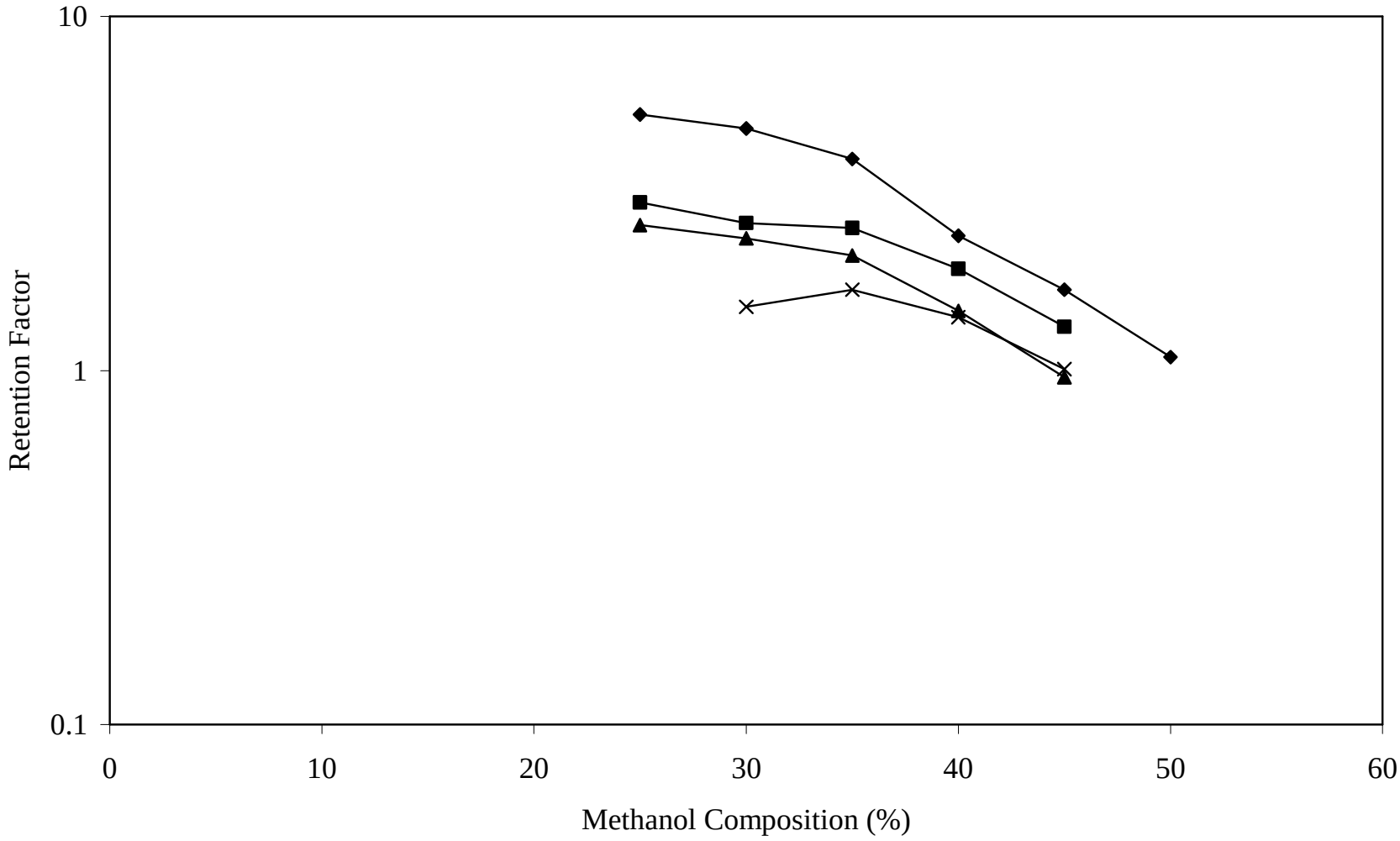
10
1
0.1
Retention Factor
0
10
20
30
40
50
60
Methanol Composition (%)

Figure 6.8: Graph of extrapolated retention factor for SDS system peaks versus the concentration of SDS. Other experimental conditions as given in the text.

Figure 6.8

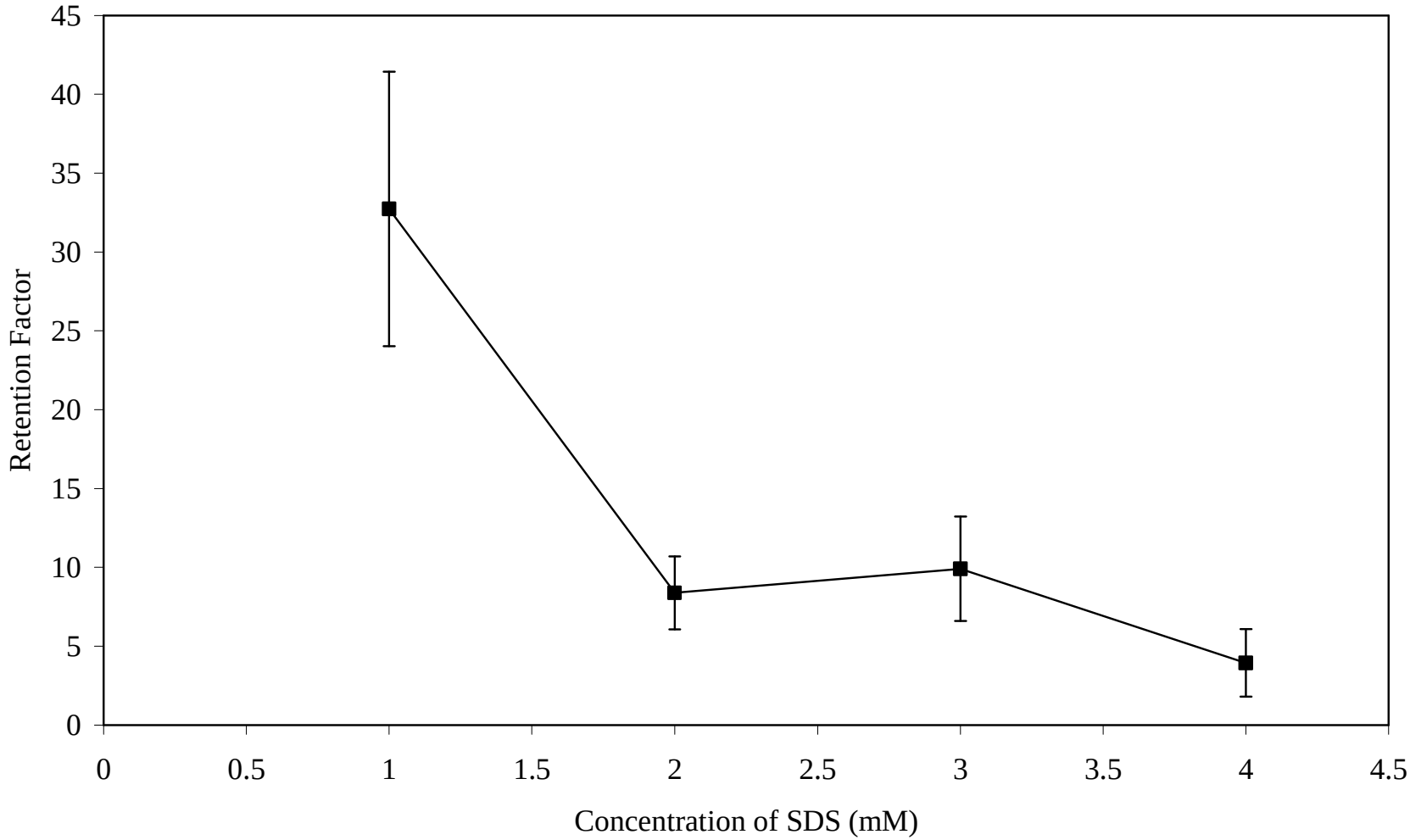
45
40
35
30
25
20
15
10
5
0
Retention Factor
0
0.5
1
1.5
2
2.5
3
3.5
4
4.5
Concentration of SDS (mM)

The phenomenon seen in this experiment suggests a simple Langmuir isotherm for the chromatographic system with SDS, as the retention of SDS in the system decreases with an increase in the concentration of SDS (in the mobile phase) from 1.0 to 2.0 mM, and remains constant thereafter.

6.3.3 System Peaks in Lithium Perfluorooctane Sulfonate Mobile Phases

Representative chromatograms of the amines in LiPFOS mobile phases are shown in Figures 6.9A-C. Similar to SDS, it was observed that the retention times of several of the unidentified peaks did not change, regardless of the analyte mixture injected. However, not all of the same peaks were observed in the LiPFOS mobile phases that were seen in the SDS mobile phases, or observed at the same relative position. Injections of pure solvents (methanol and mobile phase) were performed in an effort to correctly identify the system peak due to LiPFOS.

Representative chromatograms of the pure methanol in LiPFOS mobile phases are shown in Figures 6.10A-D, and of the mobile phase in LiPFOS mobile phases are shown in Figure 6.11. In comparing the chromatograms of Figures 6.9, 6.10, and 6.11, the large negative system peak, which is present in the chromatograms arising from the injections of pure methanol, is absent in the chromatograms arising from the injections of the LiPFOS mobile phase itself. Similar to SDS, as the concentration of LiPFOS in the mobile phase increases, the peak area of the negative peak changes. In comparing the shape of the negative system peak in LiPFOS to SDS, it is seen that the peak has less of a triangular shape, thus leading to a less pronounced peak minimum.

Figures 6.9A-C: Representative chromatograms of amine injections in LiPFOS mobile phases. Mobile phase: 45:55 methanol/2.0 mM aqueous LiPFOS. Flowrate: 0.3 mL min^{-1}. Analytes: (0) lithium nitrate, (1) 4-aminopyridine, (2) pyridine, (3) aniline, (4) benzylamine, (5) *p*-toluidine, (6) N-methylaniline, (7) *m*-toluidine, (8) *o*-toluidine, (9) N,N-dimethylaniline, (∗) unidentified system peak. Other experimental conditions as given in the text.

Figure 6.9A

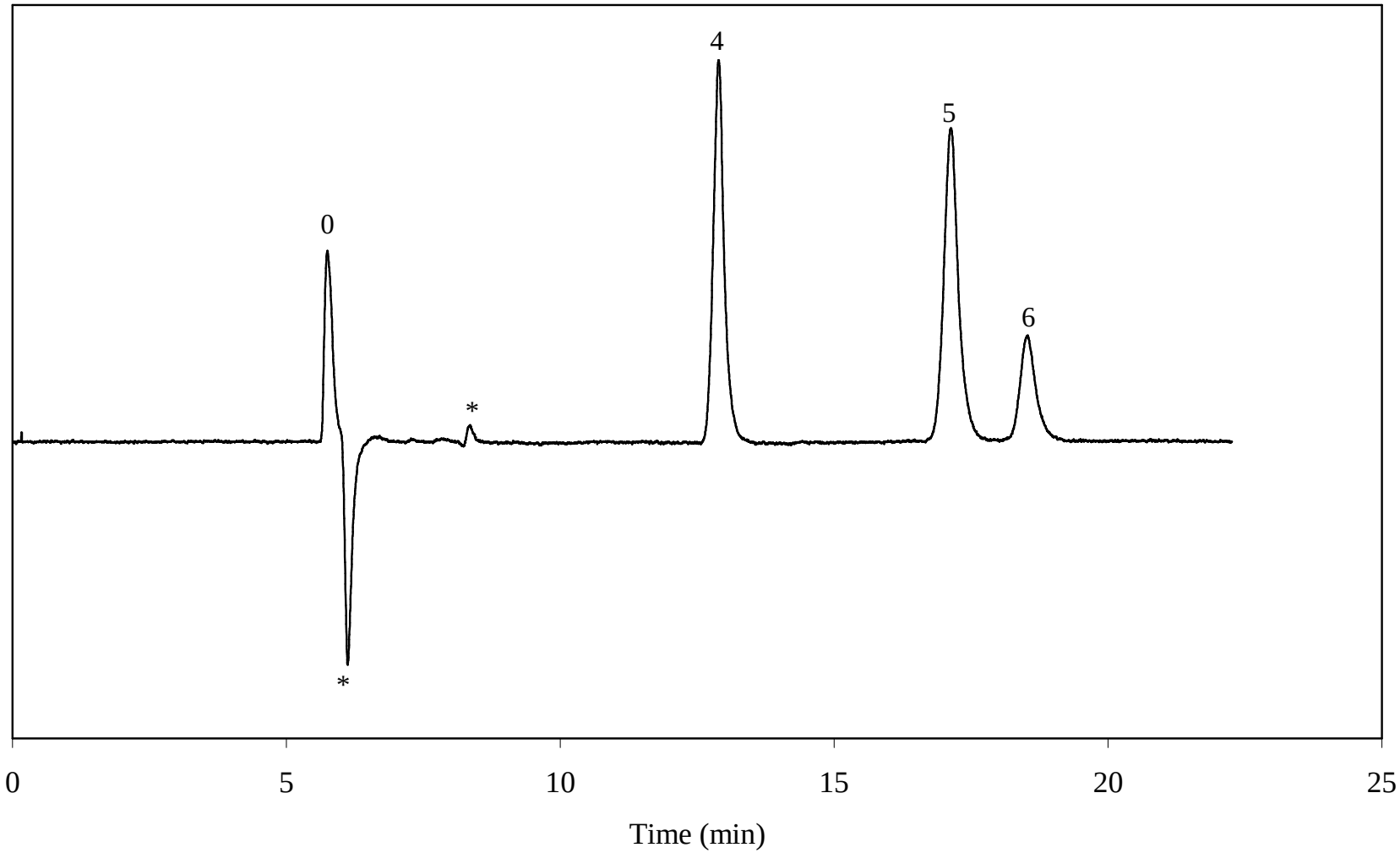

Figure 6.9B

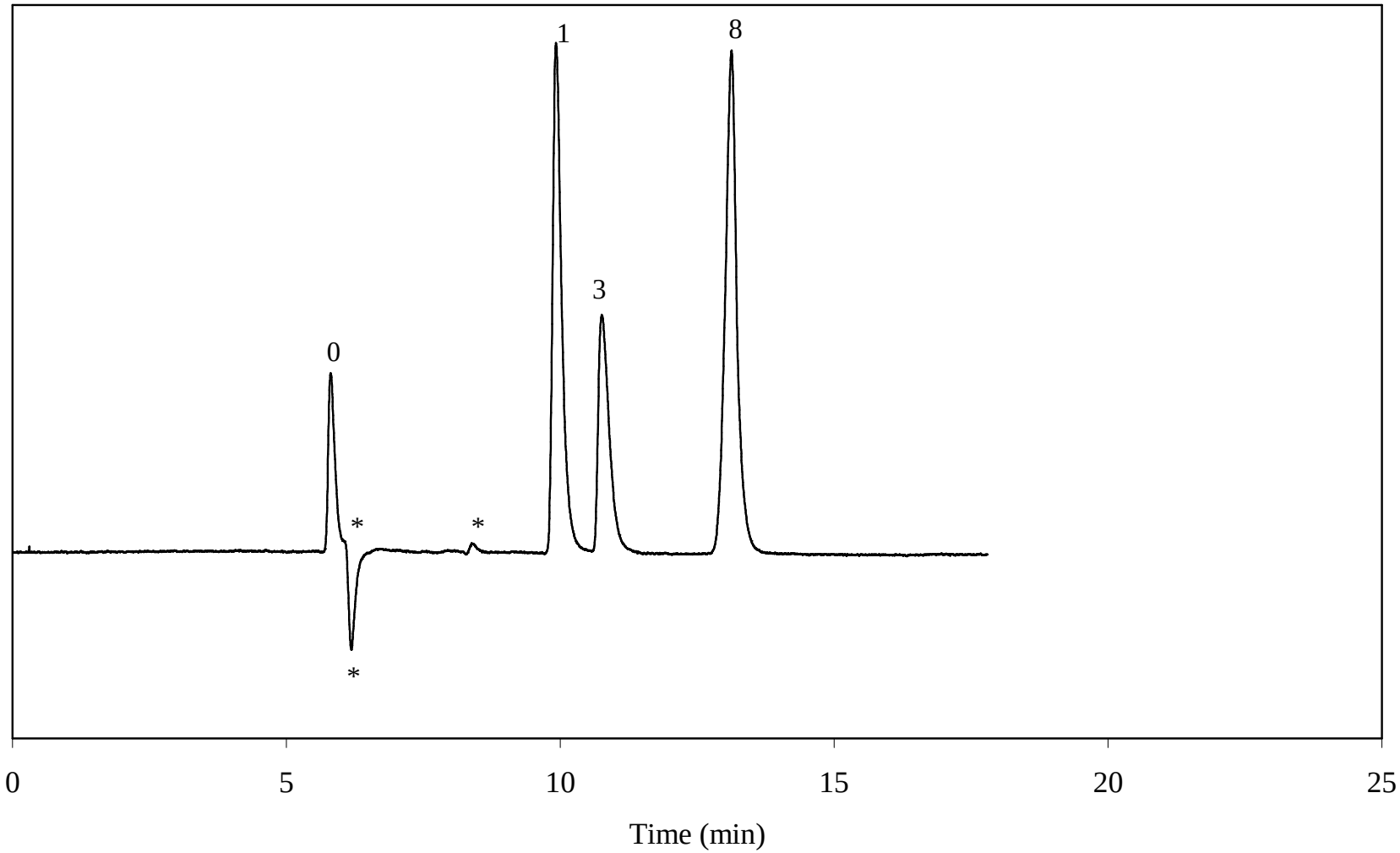

Figure 6.9C

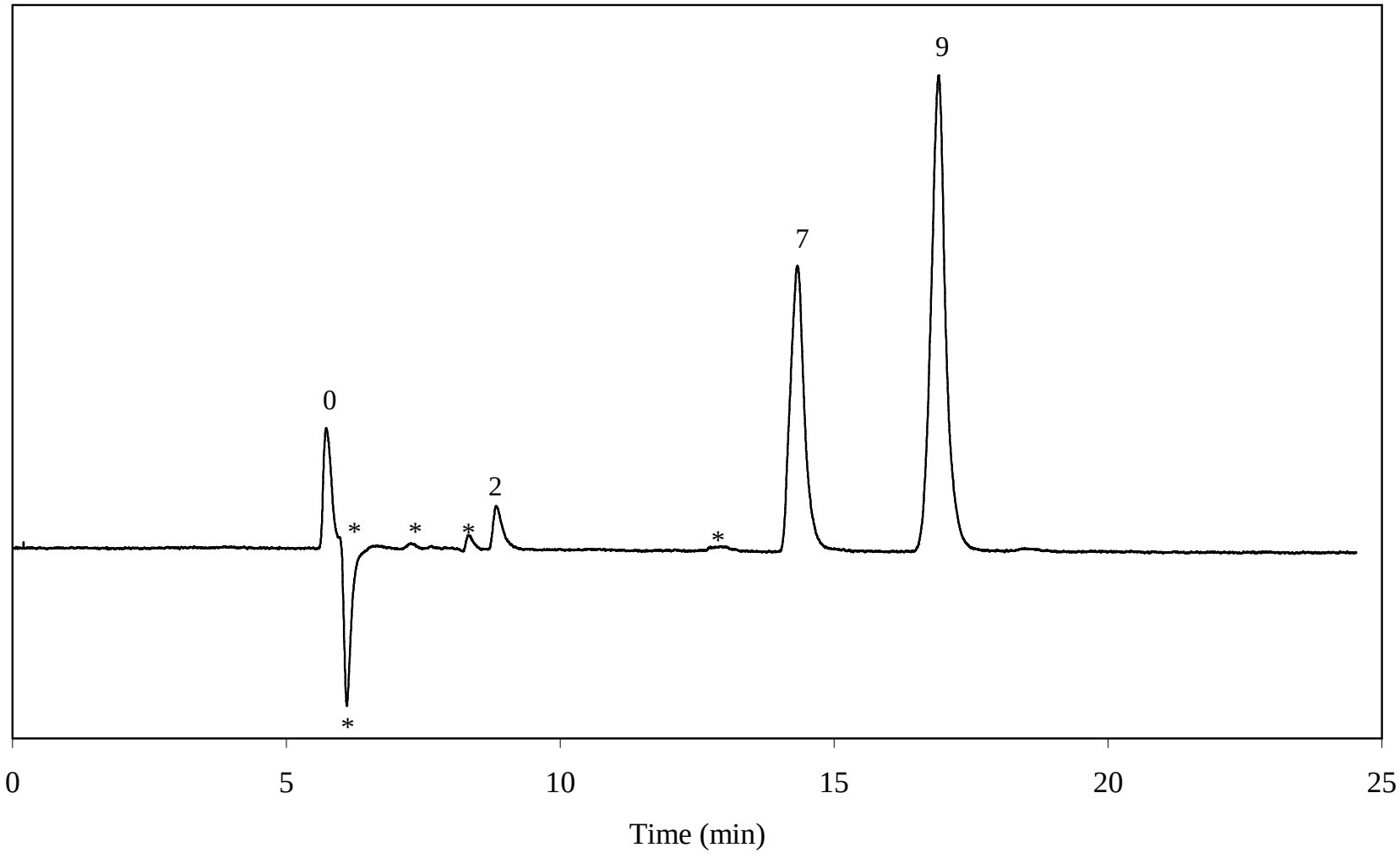

Figures 6.10A-D: Representative chromatograms of pure methanol injections in LiPFOS mobile phases. Mobile phase: 45:55 methanol/aqueous LiPFOS. (A) 1.0 mM LiPFOS, (B) 2.0 mM LiPFOS, (C) 3.0 mM LiPFOS, (D) 4.0 mM LiPFOS. Flowrate: 1.0 mL min^{-1}. Analytes: (0) methanol, (∗) unidentified system peak, (∗L) LiPFOS system peak. Other experimental conditions as given in the text.

Figure 6.10A

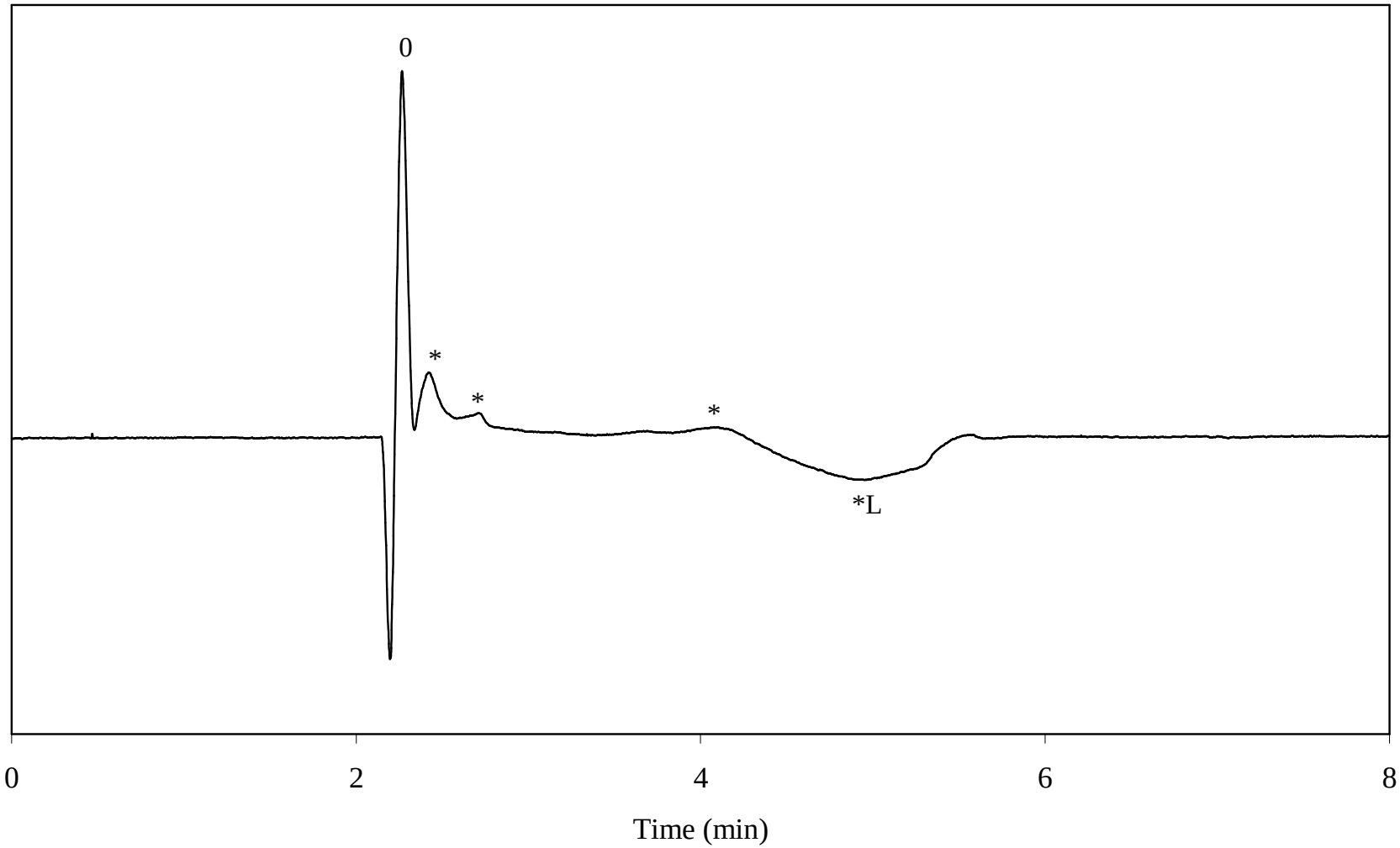

Figure 6.10B

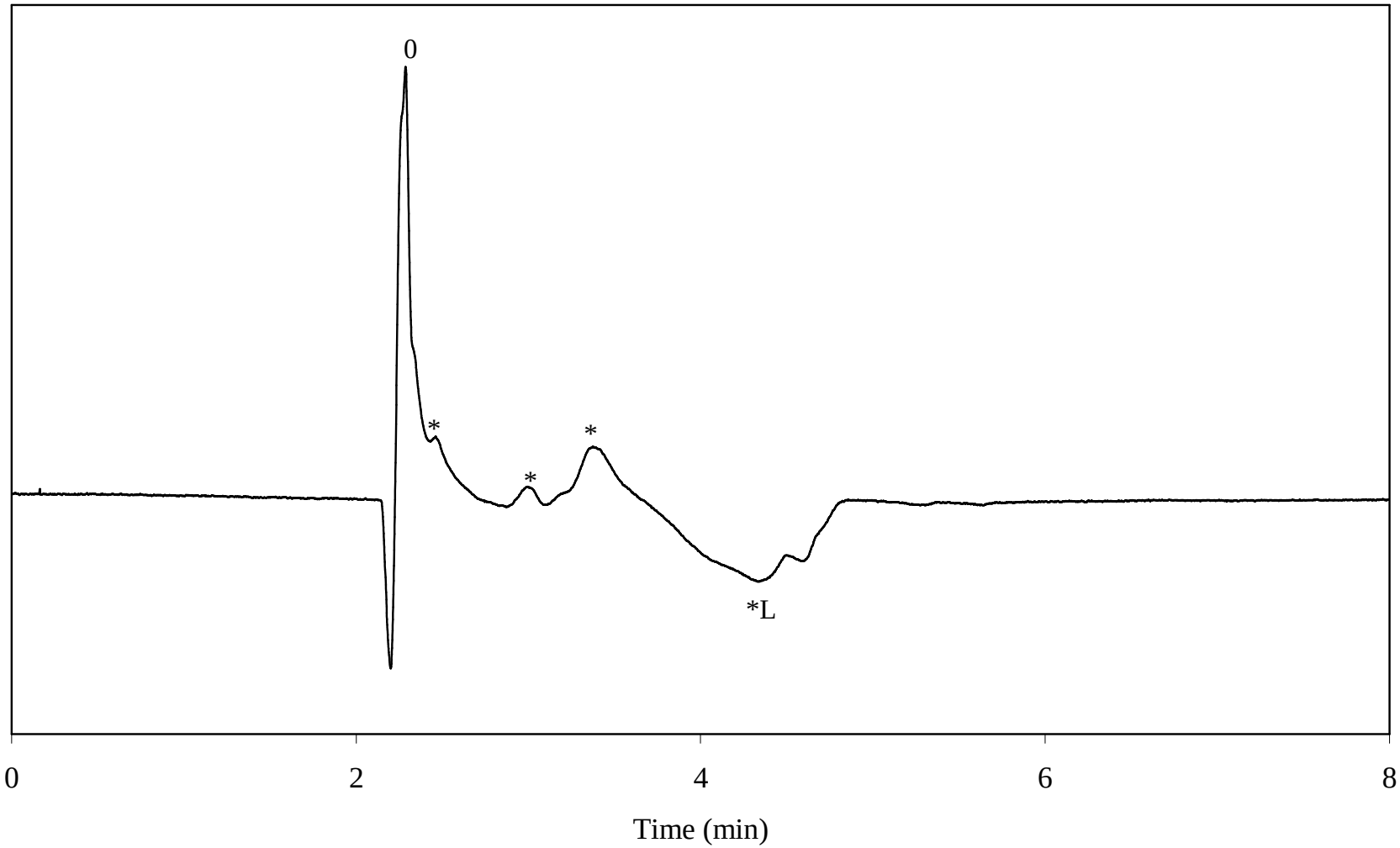

Figure 6.10C

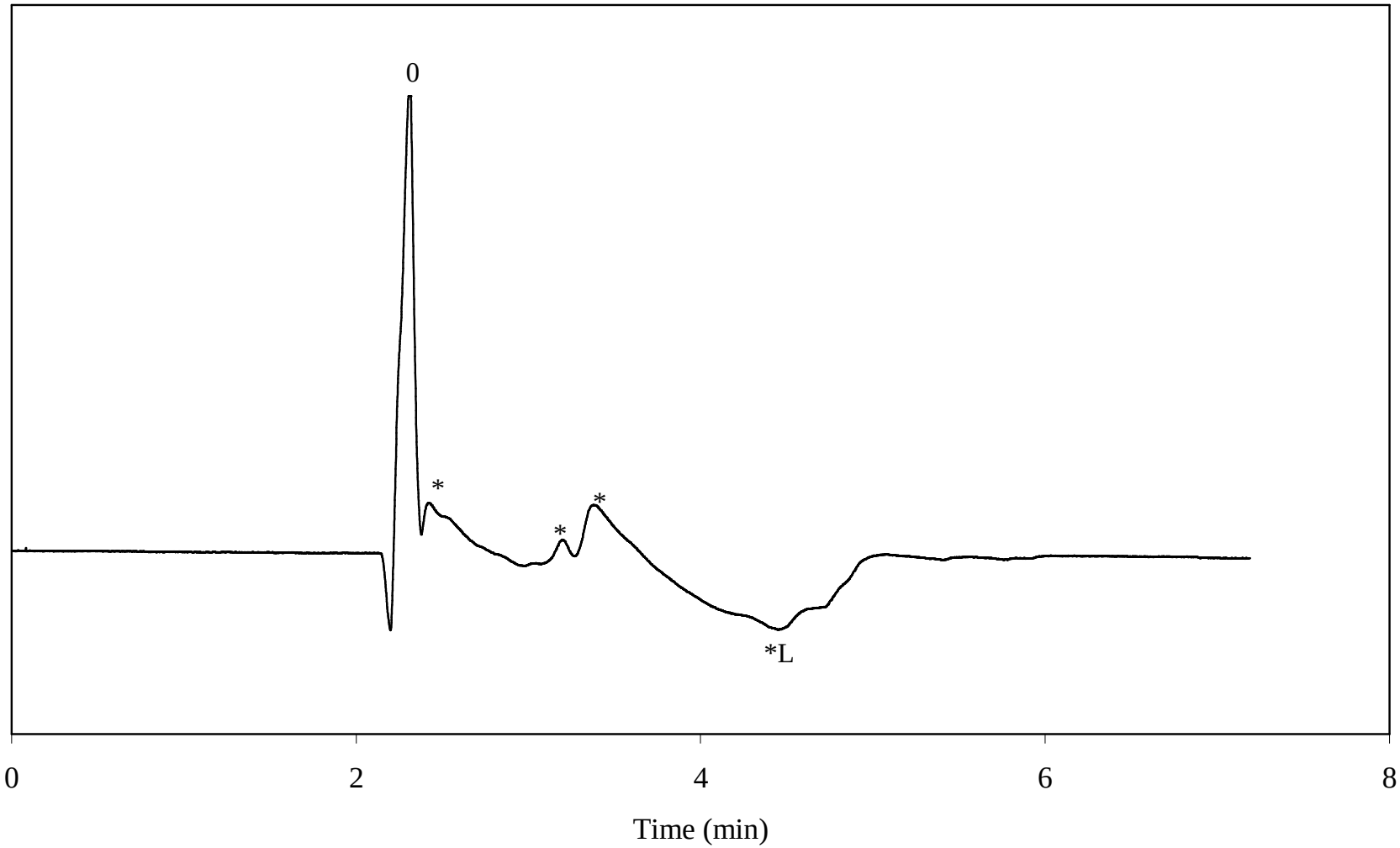

Figure 6.10D

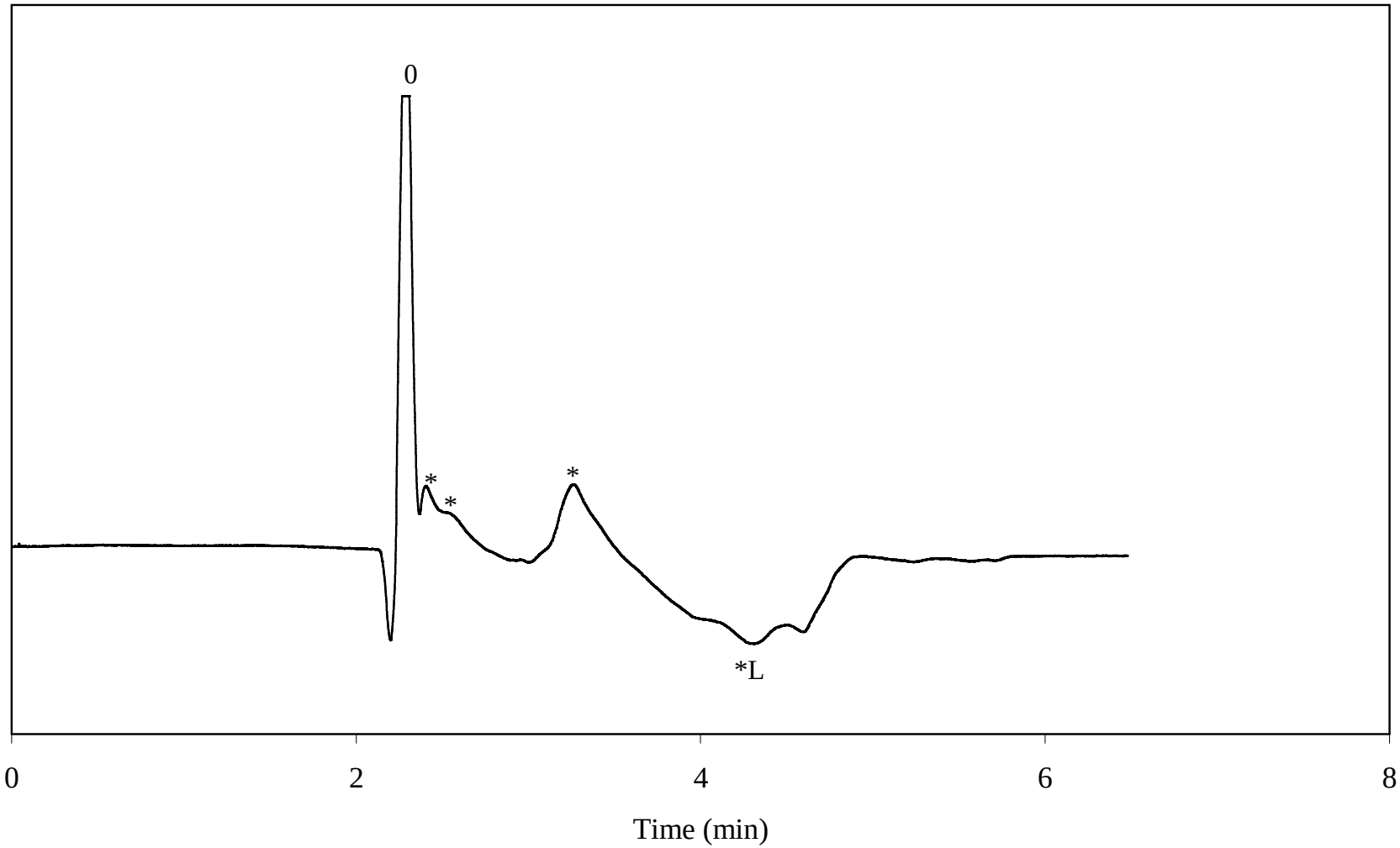

Figure 6.11: Representative chromatogram of mobile phase injection in LiPFOS mobile phases. Mobile phase: 45:55 methanol/2.0 mM aqueous LiPFOS. Flowrate: 0.3 mL min^{-1}. Analytes: (∗) unidentified system peak. Other experimental conditions as given in the text.

Figure 6.11

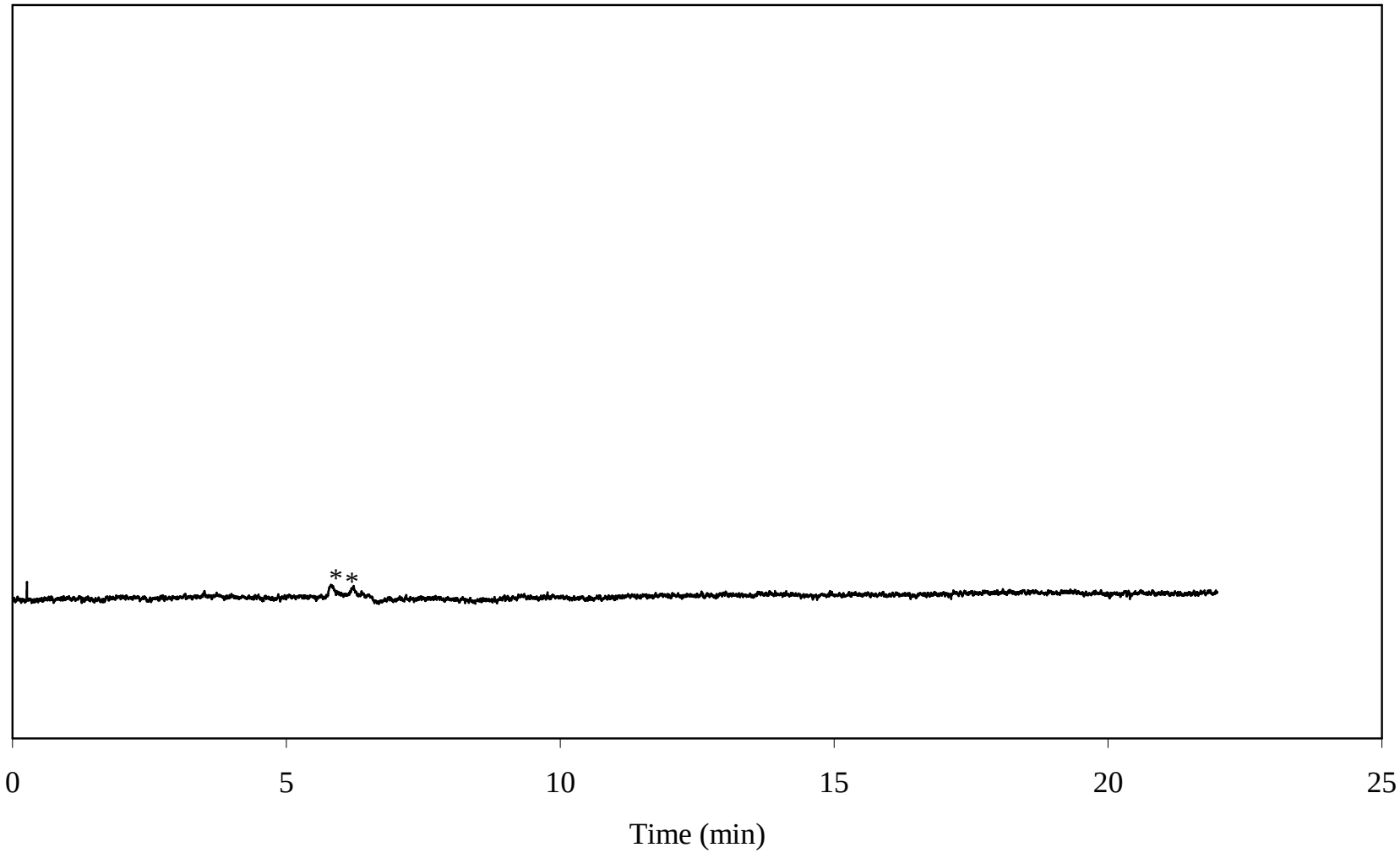

The triangular peak shape for SDS is typical for a simple Langmuir isotherm, while the strange peak shape for LiPFOS suggests that a simple isotherm is not taking place, but the possible formation of dimers and trimers. The lack of a simple isotherm is consistent with conductivity measurements (Section 2.3). Based on these observations, the negative system peak is attributed to the LiPFOS component of the mobile phase.

Retention factors, k, of the LiPFOS system peaks were determined in varying mobile phase compositions of aqueous LiPFOS (1.0 – 4.0 mM) and methanol (25 – 55 % v/v), during injections of pure methanol. A graph of the retention factor for the LiPFOS system peak versus the methanol composition (% B) of the mobile phase is shown in Figure 6.12. Statistical treatment of these data via linear regression demonstrated a linear relationship between log k and % B, where the square of the correlation coefficient, R^2, values were all greater than 0.918. It was observed that the logarithmic retention factor of the LiPFOS system peak decreased with increasing methanol composition, which is consistent with predictions of the LSS method. In addition, the retention factor of the LiPFOS system peak decreased with increasing surfactant concentration in the mobile phase, at each methanol composition. It is noteworthy to mention that at the higher compositions of methanol the LiPFOS system peak retention factors begin to converge to values <1.0 for all surfactant concentrations in the mobile phase.

Figure 6.12: Graph of retention factor versus methanol composition (%) in: (♦) 1.0 mM LiPFOS, (■) 2.0 mM LiPFOS, (▲) 3.0 mM LiPFOS, (**x**) 4.0 mM LiPFOS. Other experimental conditions as given in the text.

Figure 6.12

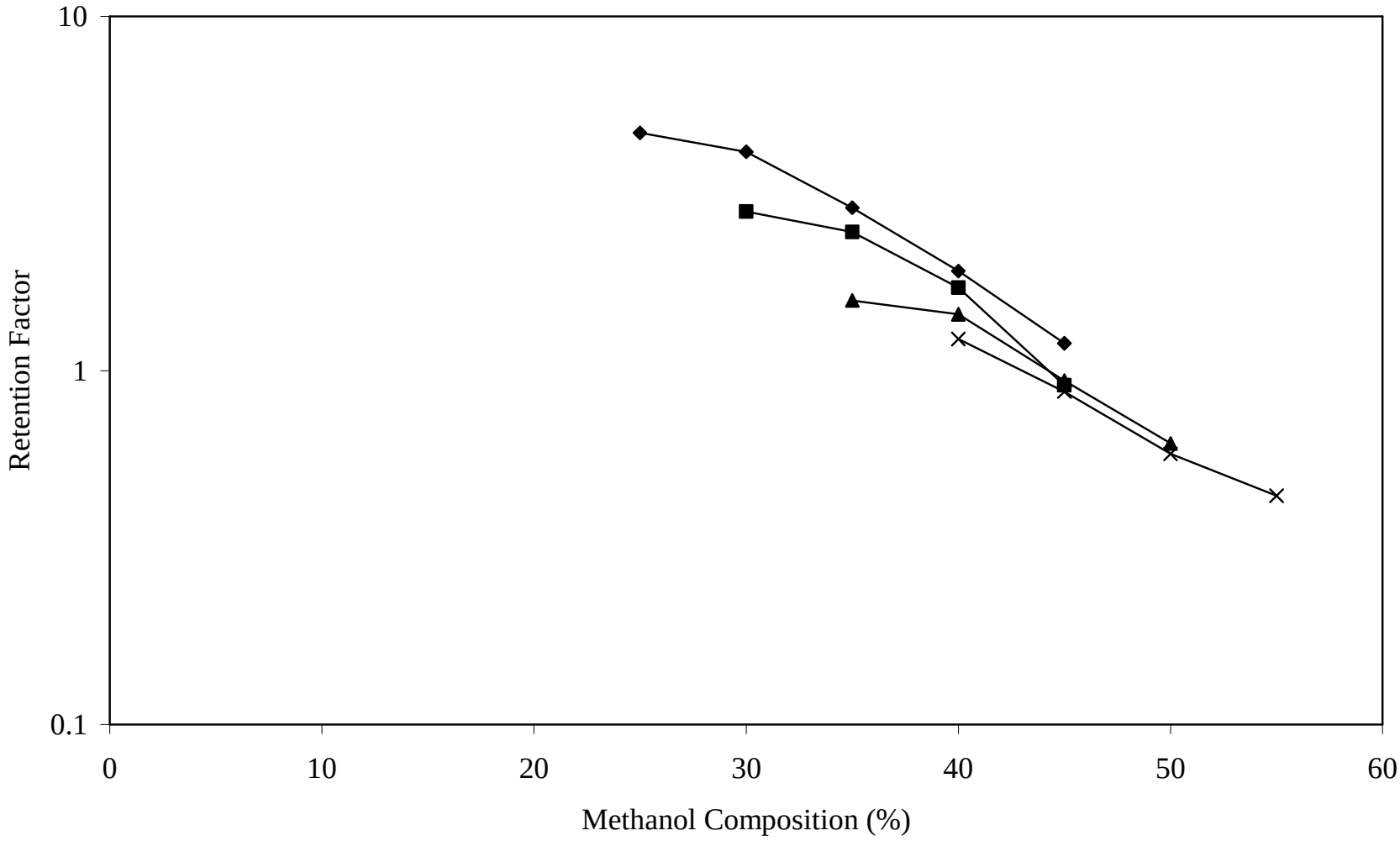
10
1
0.1
Retention Factor
0
10
20
30
40
50
60
Methanol Composition (%)

The retention factor of the LiPFOS system peak in an aqueous surfactant mobile phase (k_0) was determined by extrapolation at each LiPFOS concentration using linear regression of Equation 6.3. A graph of the extrapolated retention factor for the LiPFOS system peak versus the concentration of LiPFOS is shown in Figure 6.13, where the error bars represent the standard deviation (±) of the individual extrapolated retention factor. There appears to be a decrease in the LiPFOS system peak retention from 1.0 to 4.0 mM LiPFOS. However, upon taking the standard deviations into consideration, the retention remains relatively constant from 1.0 to 3.0 mM LiPFOS. This variability in the data suggests that the LiPFOS surfactant is experiencing slightly different interactions in the experimental chromatographic system, such as the possible formation of dimers and trimers. In comparing the extrapolated retention factors of LiPFOS (Figure 6.13) to SDS (Figure 6.8), it is observed that the retention factors are the same at 1.0 mM surfactant concentration but lower in SDS than in LiPFOS at the higher surfactant concentrations (2.0 – 4.0 mM).

Figure 6.13: Graph of extrapolated retention factor for LiPFOS system peaks versus the concentration of LiPFOS. Other experimental conditions as given in the text.

Figure 6.13

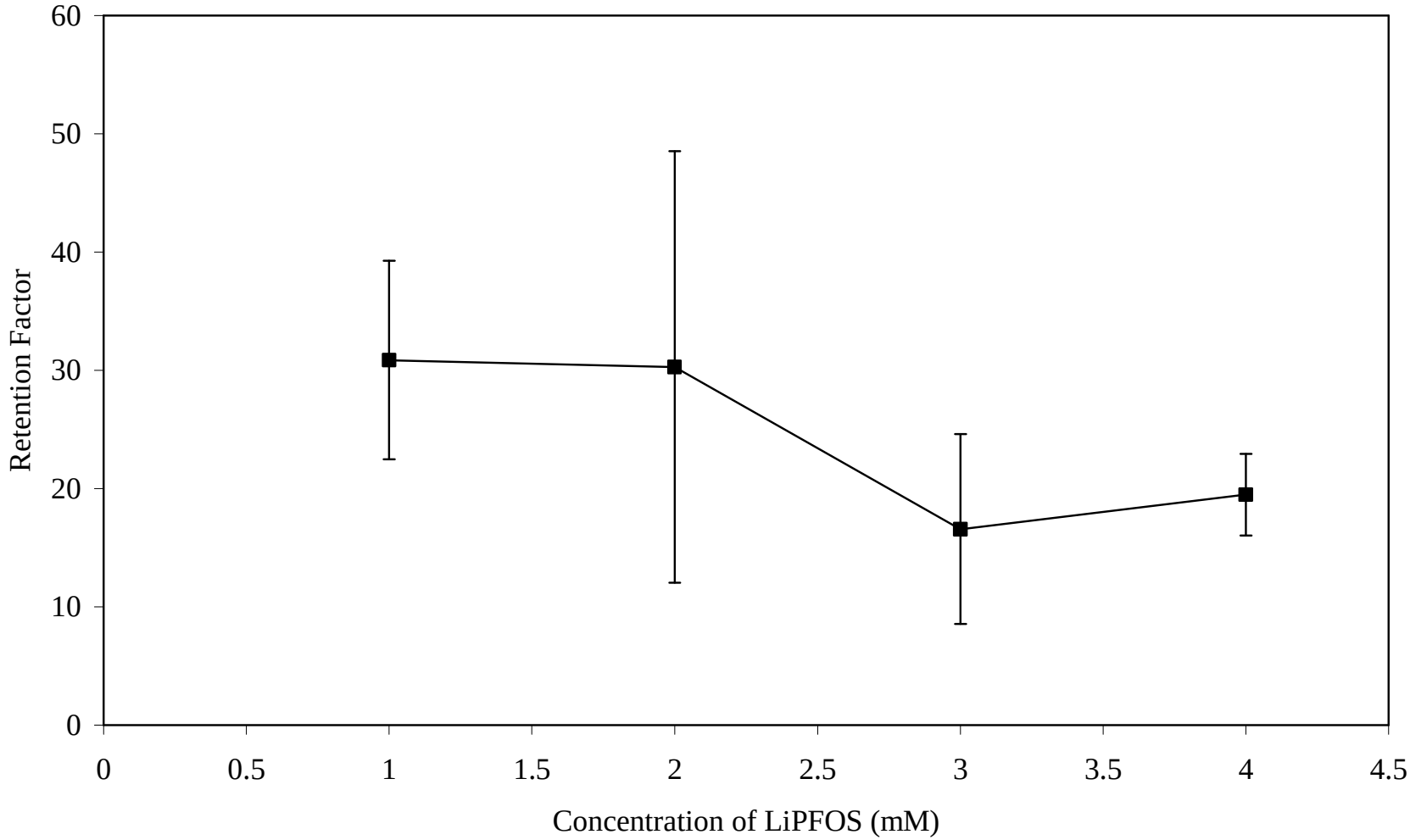
60
50
40
30
20
10
0
Retention Factor
0
0.5
1
1.5
2
2.5
3
3.5
4
4.5
Concentration of LiPFOS (mM)

6.4 Summary

During this study, the retention of anionic hydrocarbon and perfluorinated surfactants (SDS and LiPFOS) within the experimental chromatographic system was determined based on the identification and retention factors of system peaks. From injections of pure methanol and the mobile phase, the system peak attributed to each surfactant could be identified. The overall trend was that the retention factors of both surfactant system peaks decreased as the concentration of the surfactant in the mobile phase increased, below the CMC. It is noteworthy that the perfluorinated surfactant is less retained in the experimental chromatographic system than the hydrocarbon surfactant. Furthermore, an increase in surfactant concentration below the CMC resulted in a decrease in the retention of the surfactants (extrapolated to pure water), within the concentration range tested in this study. However, there was more variability in the perfluorinated surfactant data than the hydrocarbon surfactant data, a similar occurrence that was seen in the results of Chapter 5.

These results and conclusions have important implications for the study of the transport effects of perfluorinated surfactants on co-contaminants. In particular, the perfluorinated surfactant exhibited decreased interaction within the experimental chromatographic system, as compared to the hydrocarbon surfactant. In addition, a difference in isotherms between the perfluorinated and hydrocarbon surfactant systems was observed. Further studies are needed to characterize the retention of the surfactants within the experimental system. The use of current analytical detection techniques, such as mass spectrometry, coupled with liquid chromatography might lead to a better understanding of the interactions of the surfactants within the experimental system.

REFERENCES

6.5 References

[1] S. Levin, E. Grushka, Anal. Chem. 58 (1986) 1602-1607.

[2] S. Levin, E. Grushka, Anal. Chem. 61 (1989) 2428-2433.

[3] J. Srbek, P. Coufal, Z. Bosakova, E. Tesarova, J. Separation Sci. 28 (2005) 1263-1270.

[4] K. Kalikova, V. Hruska, J. Svobodova, R. Chudoba, B. Gas, E. Tesarova, J. Separation Sci. 32 (2009) 2864-2870.

[5] S. Levin, E. Grushka, Anal. Chem. 59 (1987) 1157-1164.

[6] J.Stahlberg, M. Almgren, Anal. Chem. 61 (1989) 1109-1112.

[7] N.Mizrotsky, L. Kristol, E. Grushka, J. Chromatogr. A. 691 (1995) 21-27.

[8] L.R. Snyder, J.W. Dolan, Advances in Chromatography, Ed. By P.R. Brown and E. Grushka, Marcel Dekker, New York, NY, 1998, p. 115-187.

[9] S. Golshan-Shirazi, G. Guiochon, J. Chromatogr. 603 (1992) 1-11.

CHAPTER 7: DETERMINATION OF FLUORINATED SURFACTANTS IN WASTEWATER SAMPLES BY HIGH-PERFORMANCE LIQUID CHROMATOGRAPHY WITH TANDEM MASS SPECTROMETRY

7.1 Introduction

Fluorinated organic compounds (FOCs) have been used as aerosol propellants, refrigerants, adhesives, surfactants, fire retardants, plastics, herbicides, pesticides, plant growth regulators, anesthetics, medicines, and even as blood substitutes [1-2]. A major class of FOCs is the perfluorinated compounds (PFCs), with more and more reports of the concentrations of the primary PFCs appearing in literature [3]. Due to the ubiquitous nature of some PFCs, it becomes necessary to have a reliable methodology for their detection and quantation in environmental samples. The acquisition of reliable concentration data can prove useful in understanding the transport and fate of PFCs.

During the term of the 2006 East Asia and Pacific Summer Institutes (EAPSI) program, the author received training on a specially modified high-performance liquid chromatography with tandem mass spectrometry (LC-MS/MS) system at the National Institute of Advanced Industrial Science and Technology (AIST) in Tsukuba, Japan. The LC-MS/MS system permits detection and quantitation of fluorinated surfactants down to the part-per-quadrillion level. Water samples, which were previously collected from the treatment tanks at an industrial manufacturing site and from the effluent in a nearby stream, were analyzed. The levels of 28 anionic fluorinated surfactants were quantitated in samples that had been collected, before and during a production cycle, over a period of four days.

7.2 Experimental Methods

7.2.1 Fluorinated Surfactants

Some of the most commercially utilized PFCs are the classes of fluorinated surfactant, in particular the anionic perfluorinated surfactants [4-5]. In addition, some perfluorinated surfactants are byproducts in fluorinated telomer alcohols and carboxylic acids (fluorotelomers) production [6], with some fluorotelomers believed to environmentally degrade into perfluorinated surfactants [7-9]. For these reasons, pure analytical standards of these classes of compounds are necessary for any detection method.

Mixtures of 28 anionic fluorinated surfactant standards, which were supplied by the Yamashita research group at AIST, were used as external standards (for construction of calibration curves) and internal standards (for spiking of recovery samples). A summary of the names, abbreviations, and structures for each fluorinated surfactant is located in Table 7.1.

Table 7.1: Summary of names, abbreviations, and structures for the perfluorinated compounds (PFCs).

Name	Abbreviation	Structure
Perfluoroalkyl sulfonates (PFAS):		
Perfluoroethane sulfonic acid	PFEtS	$F(CF_2)_2SO_3^-$
Perfluoropropane sulfonic acid	PFPrS	$F(CF_2)_3SO_3^-$
Perfluorobutane sulfonic acid	PFBS	$F(CF_2)_4SO_3^-$
Perfluorohexane sulfonic acid	PFHxS	$F(CF_2)_6SO_3^-$
Perfluorooctane sulfonic acid	PFOS	$F(CF_2)_8SO_3^-$
1H,1H,2H,2H-perfluorooctane sulfonic acid	THPFOS	$F(CF_2)_6(CH_2)_2SO_3^-$
Perfluoroalkyl carboxylic acids (PFCA):		
Perfluorobutyric acid	PFBA	$F(CF_2)_3COO^-$
Perfluoropentanoic acid	PFPeA	$F(CF_2)_4COO^-$
Perfluorohexanoic acid	PFHxA	$F(CF_2)_5COO^-$
Perfluoroheptanoic acid	PFHpA	$F(CF_2)_6COO^-$
Perfluorooctanoic acid	PFOA	$F(CF_2)_7COO^-$
Perfluorononanoic acid	PFNA	$F(CF_2)_8COO^-$
Perfluorodecanoic acid	PFDA	$F(CF_2)_9COO^-$
Perfluoroundecanoic acid	PFUnDA	$F(CF_2)_{10}COO^-$
Perfluorododecanoic acid	PFDoDA	$F(CF_2)_{11}COO^-$
Perfluorotetradecanoic acid	PFTeDA	$F(CF_2)_{13}COO^-$
Perfluorohexadecanoic acid	PFHxDA	$F(CF_2)_{15}COO^-$
Perfluorooctadecanoic acid	PFODA	$F(CF_2)_{17}COO^-$
^{13}C labeled Perfluorooctanoic acid	^{13}C-PFOA	$F(CF_2)_8{}^{13}CF_2{}^{13}COO^-$
Fluorinated telomer alcohols and carboxylic acids (FTOH and FTCA):		
1H,1H,2H,2H-perfluoro-1-decanol	8:2 FTOH	$F(CF_2)_8(CH_2)_2O^-$
1H,1H,2H,2H-perfluoro-1-dodecanol	10:2 FTOH	$F(CF_2)_{10}(CH_2)_2O^-$
1H,1H-perfluoro-1-octanol	7:1 FTOH	$F(CF_2)_7CH_2O^-$
1H,1H-perfluoro-1-undecanol	10:1 FTOH	$F(CF_2)_{10}CH_2O^-$
8:2 fluorotelomer acid	8:2 FTCA	$F(CF_2)_8CH_2COO^-$
8:2 fluorotelomer unsaturated acid	8:2 FTUCA	$F(CF_2)_7CF{=}CHCOO^-$
Fluorooctane sulfonamides (FOSA):		
Perfluorooctane sulfonamide	PFOSA	$F(CF_2)_8SO_2NH^-$
N-ethylperfluorooctane sulfonamidoacetate	*N*-EtFOSAA	$F(CF_2)_8SO_2N(C_2H_5)CH_2COO^-$
N-ethylperfluorooctane sulfonamide	*N*-EtFOSA	$F(CF_2)_8SO_2N(C_2H_5)^-$

7.2.2 Wastewater Samples

The Yamashita research group at AIST provided representative waste water samples for this study. The waste water samples had been previously collected from a perfluorooctane sulfonate (PFOS) manufacturing plant in Japan, prior to the arrival of the author. Multiple samples were taken from inside two waste water treatment tanks (sites A0 – A3 and B0 – B3), as well as one location from a stream adjacent to the facility (sites G1 – G2) into which the waste water was discharged. Due to the hydrophobic and hydrophilic nature of surfactants, a higher concentration of surfactants is expected at the water/air interface [10]. Based on this information, waste water samples were taken at depths between 0.0 – 50.0 cm from the surface. Samples were collected one day prior to production (J23) and three subsequent days (J24 – J26) during production of PFOS. The waste water samples were stored in 1.0 L polypropylene containers with screw tops, and were kept in a refrigerator at a temperature of $4 \pm 2\ ^{\circ}C$ before extraction.

7.2.3 Sample Extraction and Preparation

For the purpose of this study, the waste water samples were separated into smaller aliquots for extraction. The stored 1.0 L samples were allowed to equilibrate to room temperature and mixed by inversion, to insure accurate sampling. After inversion, two 100 mL aliquots of stored waste water samples (for sites B0 – B3 and G1 – G2) were placed into two clean polypropylene containers with screw tops. After inversion, two 1.0 mL aliquots of A0 – A3 samples were placed into two clean polypropylene containers with screw tops, and diluted to 50 mL with methanol. The water samples were kept refrigerated over the course of the study.

All water samples were extracted utilizing the standard methods of the Yamashita group [11]. Prior to extraction, the water samples were allowed to equilibrate to room temperature and mixed within the bottles by inversion. Next, the samples were treated by solid-phase extraction using weak anion-exchange cartridges (Waters Oasis® WAX) in order to isolate any extractable anionic fluorinated surfactants. Prior to loading a water sample, the cartridge was preconditioned by washing with 4.0 mL of 0.1 % NH_4OH in methanol, 4.0 mL methanol, and 4.0 mL of Milli-Q water at a rate of 2 drops s^{-1}. The waste water sample (50 – 100 mL) was then loaded onto the cartridge at a rate of 1 drop s^{-1}. The cartridge was prevented from drying out during the preconditioning and water loading phases. After the water loading, the cartridge was subsequently washed with 4.0 mL of 25 mM acetate buffer (pH 4.0) and then dried via a vacuum pump. To elute the target fraction, the cartridge was eluted first with 4.0 mL methanol and then with 4.0 mL of 0.1 % NH_4OH in methanol at a rate of 1 drop s^{-1}, and the target fraction was collected in a 10.0 mL graduated polypropylene vial. The column was eluted a second time with 4.0 mL of 0.1 % NH_4OH in methanol and the eluant was collected in a separate polypropylene vial; to ensured the elution of all target compounds. Diluted extract samples were prepared by taking 0.1 mL of the extracted fractions and diluting to 10.0 mL with methanol in a graduated polypropylene vial. The extracted fractions and diluted extract samples were kept refrigerated at 4 ± 2 °C until they could be analyzed. Prior to analysis, 100 μL aliquots of the extracted samples were transferred to polypropylene LC autosampler vials.

7.2.4 Experimental System

The water samples were analyzed using high-performance liquid chromatography with tandem mass spectrometry (LC-MS/MS). The LC-MS/MS system used in this study was specially modified to replace all components that could potentially introduce interferences (e.g. fluorinated polymers, Teflon tubing, etc.), thereby permitting reliable detection of PFCs down to the picogram (pg) level [12]. Samples (10 μL) were injected, via an autosampler, into the liquid chromatography system (Agilent, Model HP1100) and onto a Keystone Betasil C_{18} reversed-phase octadecylsilica column (2.1 mm i.d. x 50 mm length, 5.0 μm particle size). The mobile phase consisted of a 2.0 mM aqueous ammonium acetate buffer with a 10 – 100% methanol gradient at 300 μL min^{-1}. The LC effluent was directed via an electrospray interface to a Micromass Quattro II tandem mass spectrometer (Waters). The MS/MS system was operated in the negative ion mode with fixed MS/MS transitions to detect the individual PFCs.

Five functions were used for the detection of the characteristic MS/MS transitions for the individual PFCs, which had been previously utilized by the Yamashita research group at AIST. The total ion chromatogram (TIC) for each function, during a PFC standard mixture injection, is shown in Figure 7.1. The TIC for each function is comprised of chromatograms for multiple MS/MS transitions. For brevity, only the individual chromatograms for the PFCs detected within function #3 are shown in Figure 7.2.

Figure 7.1: Total ion chromatogram (TIC) for the five detection functions during a PFC standard mixture injection. Detection functions: #1 (A), #2 (B), #3 (C), #4 (D), #5 (E). For interpretation of the references to color in this and all other figures, the reader is referred to the electronic version of this dissertation.

Figure 7.1

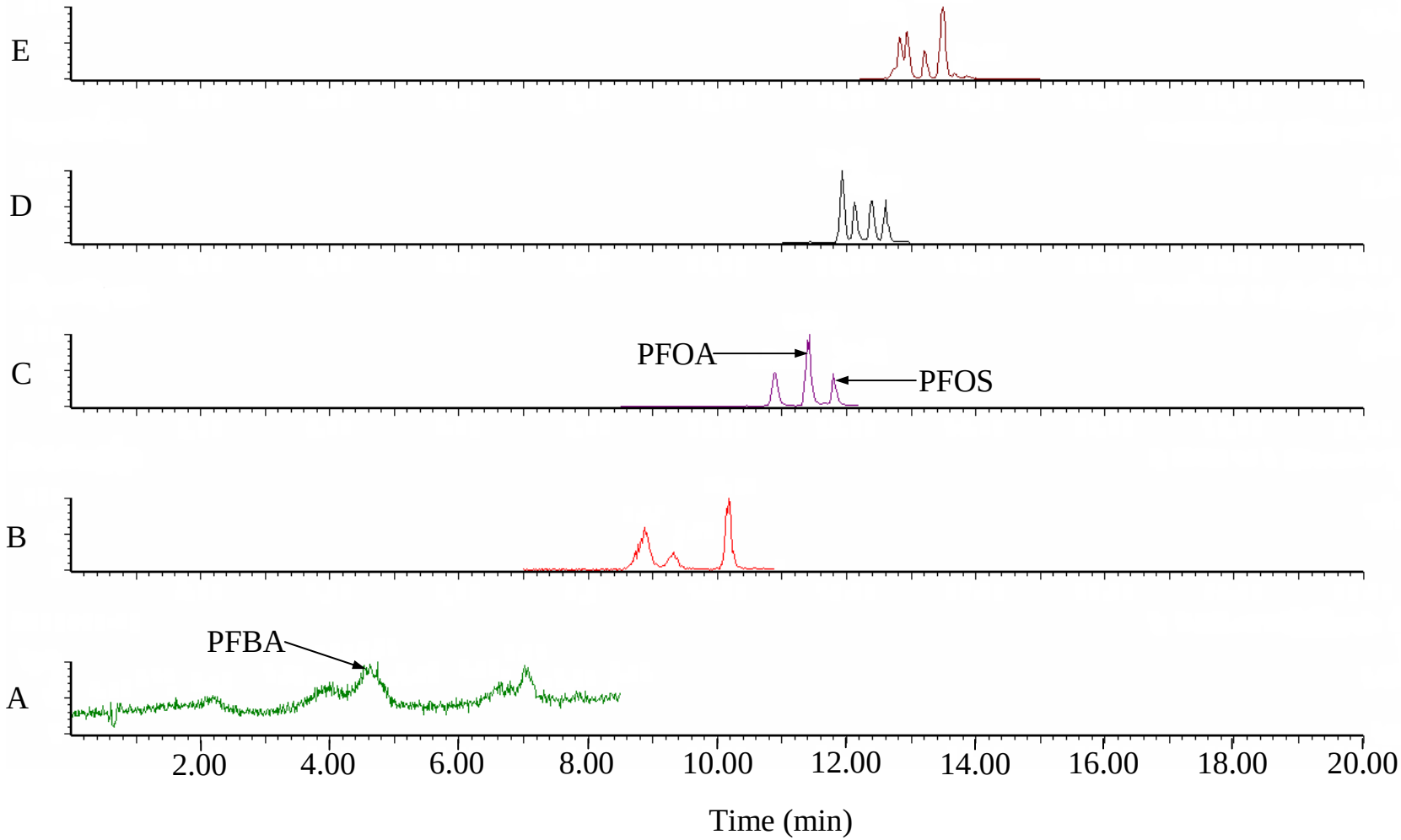
E
D
C
PFOA
PFOS
B
A
PFBA
2.00
4.00
6.00
8.00
10.00
12.00
14.00
16.00
18.00
20.00
Time (min)

Figure 7.2

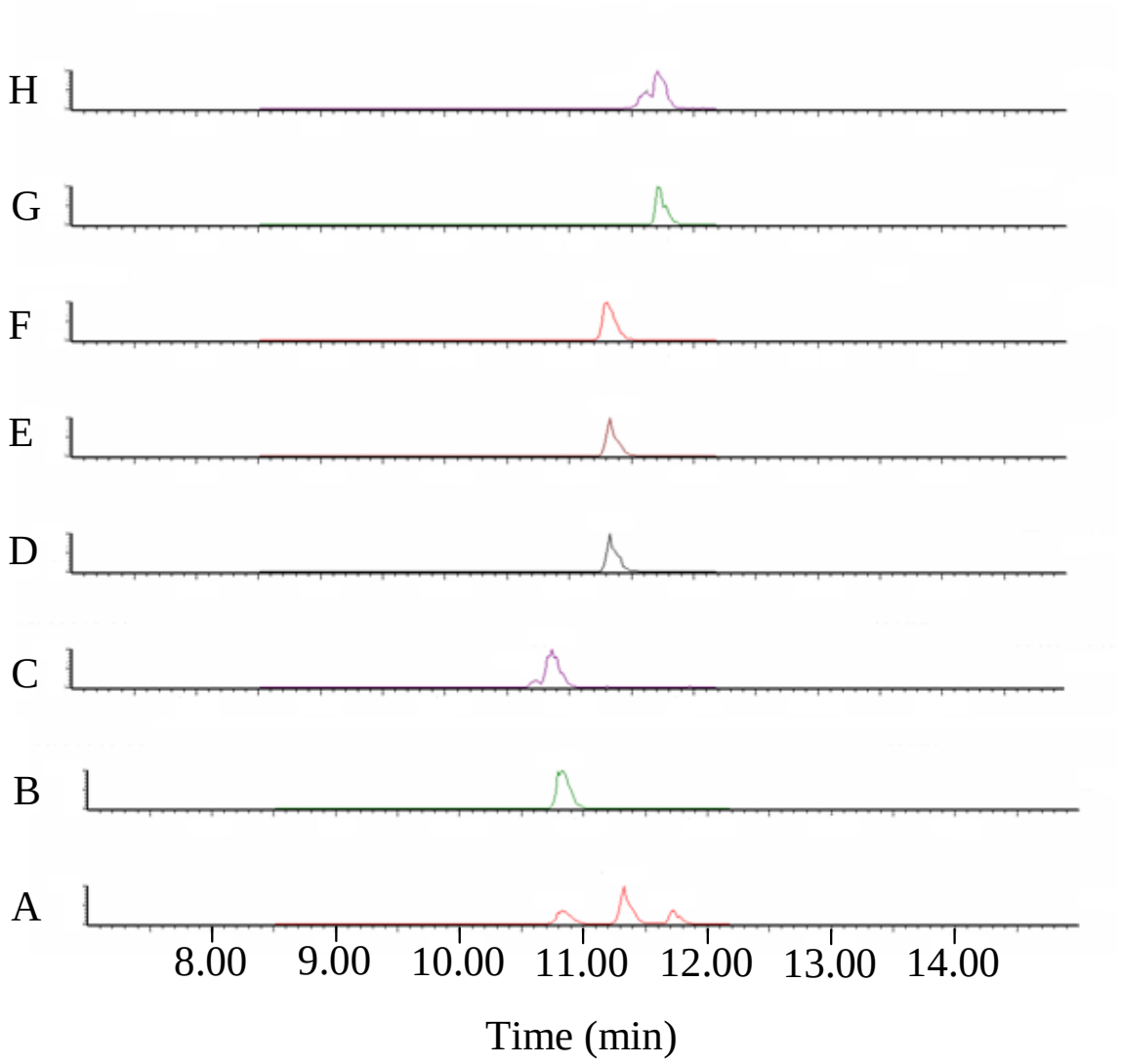

Figure 7.2: Individual chromatograms of the characteristic MS/MS transitions detected by function #3, during a PFC standard mixture injection. Chromatograms: TIC of function #3 (A), PFHpA (B), PFHxS (C), PFOA (D), ^{13}C-PFOA (E), THPFOS (F), PFNA (G), PFOS (H).

7.2.5 Data Analysis

In order to validate this method, procedural blanks (400 mL of Milli-Q water) and procedural recovery samples (400 mL of Milli-Q water, spiked with 160 μL of a 50 ppb PFC standard mixture) were extracted and analyzed concurrently with the waste water samples. The data analysis for all blank, recovery, and waste water samples was performed using the MassLynx software. Calibration curves for the PFCs where assembled based on detector response (peak area) versus concentrations of external standards. The external standards where injected at six different concentrations (2, 10, 50, 200, 1000, 20000 ng L^{-1}). The concentrations of the target PFCs in all the water samples were quantified via comparison to these external calibration curves.

7.3 Results and Discussion

Over the course of this study, 28 individual PFCs were identified and quantitated in procedural blank, recovery, and waste water samples. Recoveries for these known PFCs ranged from 81 – 117 % for perfluoroalkyl sulfonates, 75 – 133 % for perfluoroalkyl carboxylic acids, and 64 – 112 % for fluorooctane sulfonamides and alcohols. Concentrations of these known PFCs in the blank samples were below the limit of quantification (LOQ), with the exception for perfluorobutyric acid (PFBA). The LOQ was determined from the lowest standard concentration within ± 20 % relative standard deviation from the calibration curve. Upon analysis of the waste water extracts, PFOS, perfluorooctanoic acid (PFOA), and PFBA were the only PFCs detected at concentrations above their LOQ on a consistent basis in the diluted samples. As such, only these three PFCs are discussed in further detail in the following sections. A summary of

characteristic MS/MS transitions, LOQ, limit of detection (LOD), and slopes and R^2 values of the calibration curves for all the PFCs is located in Table 7.2.

7.3.1 Detection of Perfluorooctane Sulfonate

As stated in Section 7.2.5, the concentrations of the target PFCs in the water samples were quantified based on comparison of peak areas to calibration curves constructed from external standards. For brevity, the individual chromatograms of PFOS from injections of water samples and a 1.0 ppb PFC standard mixture are shown in Figure 7.3. In comparing the chromatograms of water samples and PFC standard mixtures, shifts in peak retention times of the target PFCs were observed. However, the general peak shape was maintained. Base on these observations, the peak area for each target PFC was determined based on peak shape and peak retention time. The calibration curve and the residue graph (used to determine the LOQ) for PFOS are shown in Figure 7.4. From Figure 7.4, a linear relationship between the peak area and concentration of PFOS is observed, where the R^2 value is 0.9999 (Table 7.2). PFOS had a LOQ of 10 ng L^{-1} and % recovery of 103 ± 12 (where % recovery is an average of six recovery samples). The PFOS concentration results, corrected for dilution factor, are summarized in Figure 7.5. On the day prior to production (J23), concentrations ranged from 4.0 – 13 μg L^{-1} in the first treatment tank (A0 – A3), 65 – 265 ng L^{-1} in the second treatment tank (B0 – B3), and 205 – 250 ng L^{-1} in the adjacent stream (G1 – G2). On the first day of PFOS production (J24), concentrations in the first treatment tank increased dramatically, as high as 520 μg L^{-1}, but decreased on the second (J25) and third (J26) production days to 5.5 – 41 μg L^{-1}.

Table 7.2: Summary of calibration curve slope and R^2 values, characteristic MS/MS transitions, limit of quantification (LOQ), and limit of detection (LOD).

PFCs	F#	Slope (intercept)	R^2	Transition (m/z)	LOQ (ng L^{-1})	LOD (ng L^{-1})
Perfluoroalkyl sulfonates (PFAS):						
PFEtS	1	5.21 (33)	0.9997	198.80 → 79.80	50	8
PFPrS	1	8.41 (35)	0.9996	248.90 → 79.60	10	1
PFBS	2	6.94 (0.0)	0.9979	298.70 → 79.70	50	1
PFHxS	3	6.94 (4.5)	0.9985	398.70 → 79.70	50	1
PFOS	3	6.11 (0.0)	0.9999	498.60 → 79.70	10	1
THPFOS	3	8.35 (0.0)	0.9999	426.70 → 406.70	200	0.5
Perfluoroalkyl carboxylic acids (PFCA):						
PFBA	1	20.2 (804)	0.9994	212.80 → 168.80	50	7
PFPeA	2	23.2 (-61)	0.9992	262.80 → 218.70	50	1
PFHxA	2	20.6 (0.0)	0.9975	312.80 → 268.80	50	0.5
PFHpA	3	25.7 (46)	0.9990	362.80 → 318.80	10	1
PFOA	3	30.0 (0.0)	0.9927	413.00 → 368.70	50	2
PFNA	3	17.3 (22)	0.9994	462.70 → 418.80	50	0.8
PFDA	4	15.0 (28)	0.9933	512.80 → 468.80	200	0.4
PFUnDA	4	19.8 (0.0)	0.9955	563.00 → 519.00	50	0.7
PFDoDA	4	17.7 (0.0)	0.9976	612.70 → 568.80	50	0.7
PFTeDA	5	16.1 (0.0)	0.9976	712.90 → 669.00	10	1
PFHxDA	5	9.17 (0.0)	0.9973	812.90 → 769.30	50	1
PFODA	5	9.01 (41)	0.9999	912.90 → 869.00	10	7
^{13}C-PFOA	3	28.2 (0.0)	0.9990	414.90 → 369.90	10	2
Fluorinated telomer alcohols and carboxylic acids (FTOH and FTCA):						
8:2 FTOH	5	0.15 (11)	0.9936	463.00 → 354.80	200	100
10:2 FTOH	5	0.09 (0.0)	0.9841	563.50 → 455.10	200	100
7:1 FTOH	5	0.16 (19)	0.9569	398.90 → 218.90	200	40
10:1 FTOH	5	1.64 (0.0)	0.9966	549.00 → 369.00	200	10
8:2 FTCA	4	1.66 (0.0)	0.9762	477.00 → 393.00	50	2
8:2 FTUCA	4	41.9 (0.0)	0.9991	457.00 → 393.00	50	0.4
Fluorooctane sulfonamides (FOSA):						
PFOSA	5	30.0 (0.0)	0.9996	497.70 → 77.70	10	0.5
N-EtFOSAA	4	4.80 (0.0)	0.9993	583.90 → 418.70	200	10
N-EtFOSA	5	30.9 (0.0)	0.9994	525.90 → 168.90	2	0.3

F#... Detection function number.

Figure 7.3

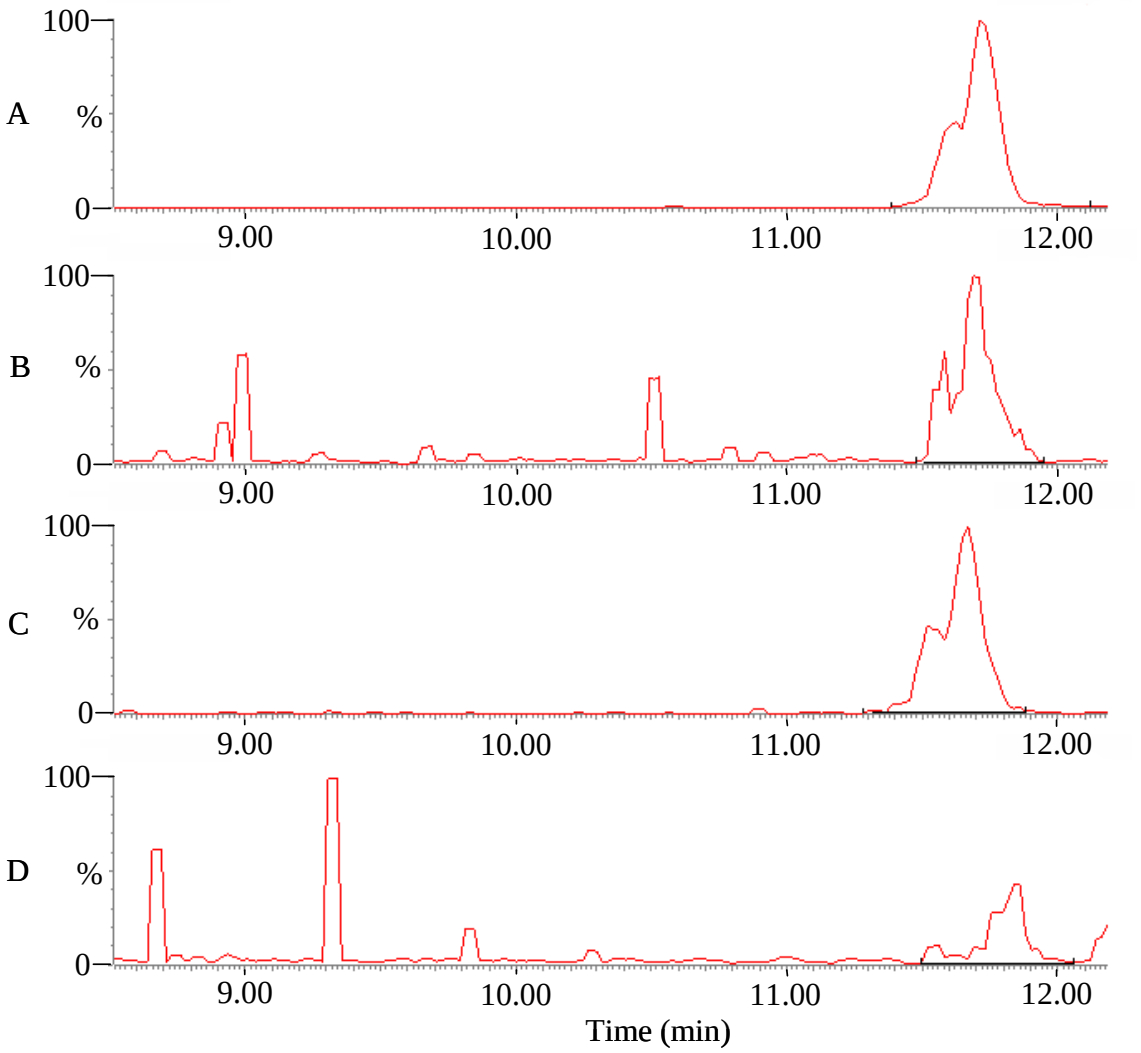

Figure 7.3: Individual chromatograms of PFOS from injections of PFC standard mixture and water samples taken during the second day of PFOS production. Chromatograms: 1.0 ppb PFC standard mixture (A), water sample from adjacent stream site G (B), water sample from second treatment tank B (C), water sample from first treatment tank A (D).

Figure 7.4

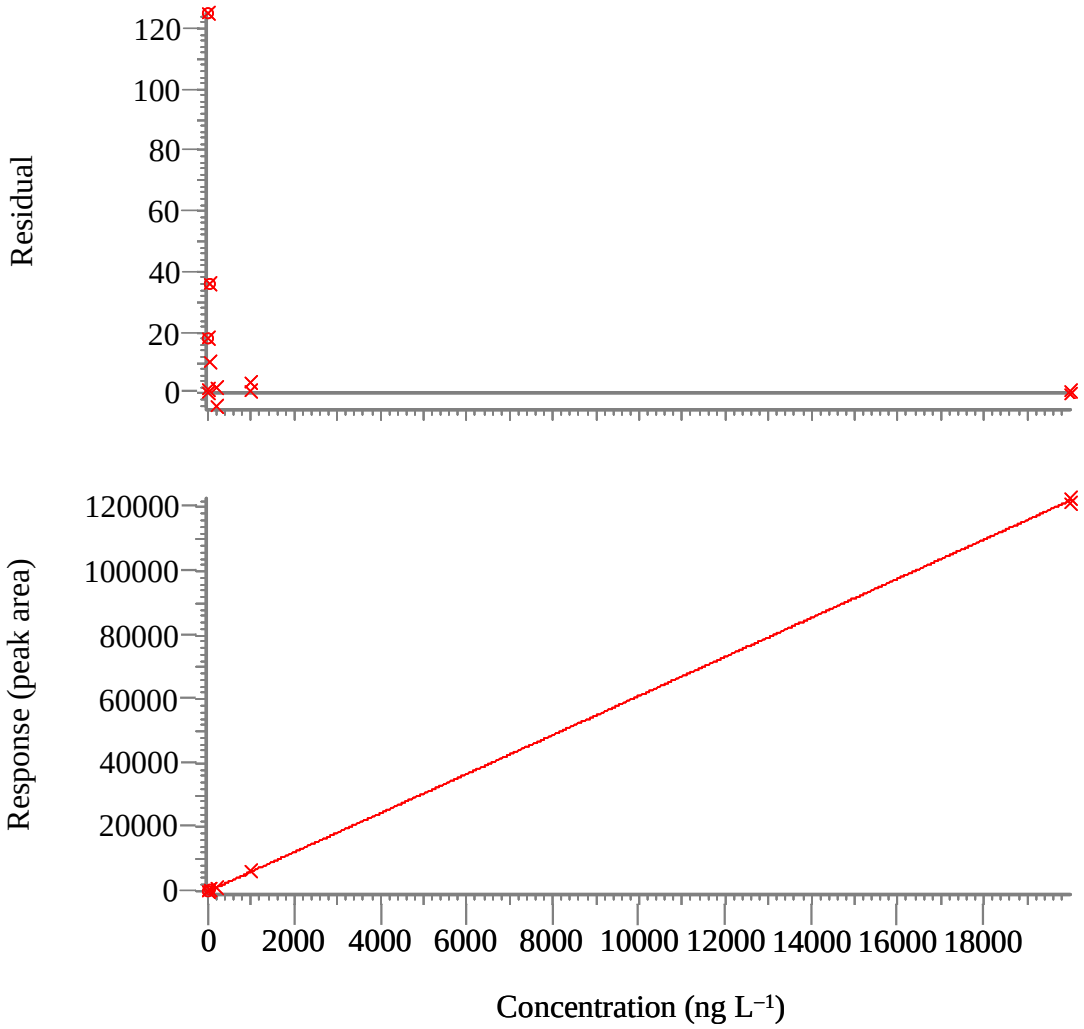

Figure 7.4: External calibration curve (bottom graph) and residue graph (top) for PFOS.

Figure 7.5: Concentration (ng L^{-1}) of PFOS in two waste water treatment tanks (sites A0 – A3 and B0 – B3), as well as in an adjacent stream into which the waste water was discharged (sites G1 – G2). Samples were collected one day prior to production (J23■) and three subsequent days during production of PFOS (J24■ – J25■ J26■).

Figure 7.5

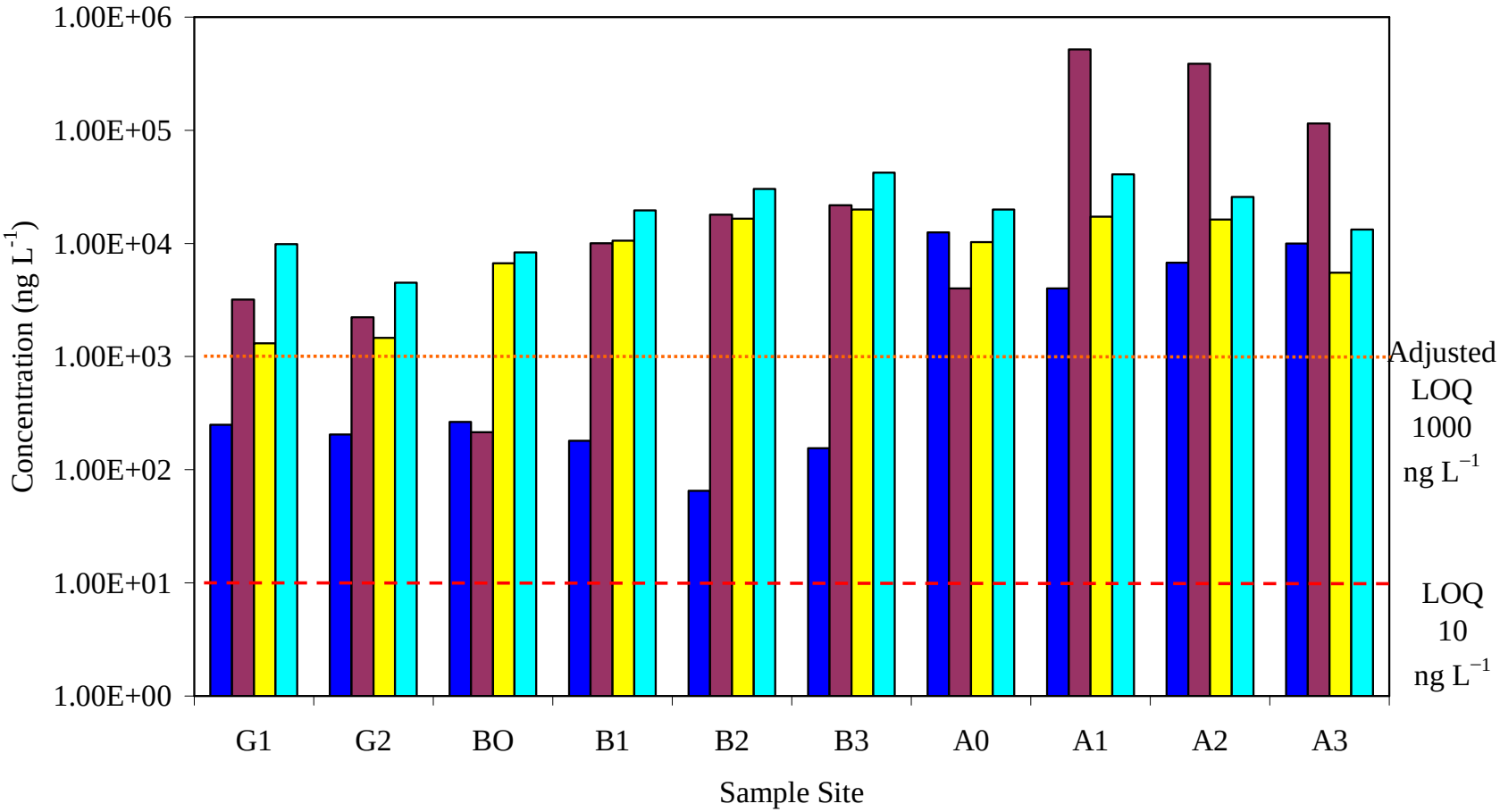
1.00E+06
1.00E+05
1.00E+04
1.00E+03
1.00E+02
1.00E+01
1.00E+00
Concentration (ng L-1)
Adjusted LOQ 1000 ng L−1
LOQ 10 ng L−1
G1
G2
BO
B1
B2
B3
A0
A1
A2
A3
Sample Site

Concentrations in the second treatment tank also increased during production (in comparison to J23), but remained relatively constant over all three production days (J24 – J26) at 6.7 – 42 μg L^{-1}. The PFOS concentrations in the first treatment tank (A0 – A3), on the second and third production days, were similar to that in the second treatment tank (B0 – B3) over all three production days. Finally, in the adjacent stream into which the effluent was discharged (G1 – G2), PFOS concentration levels generally increased from 2.2 – 3.2 μg L^{-1} on the first production day to 4.5 – 9.9 μg L^{-1} on the third production day. The PFOS concentration levels in the stream were 10- to 50-fold higher during production (J24 – J26) than prior to production (J23, 205 – 250 ng L^{-1}). All concentration levels, once corrected for dilution, were significantly larger than the LOQ, which was 10 ng L^{-1}. An adjusted LOQ for PFOS was determined by multiplying the LOQ by a factor of 100. Only the sites G1 –G2 and B0 – B3 on the day prior to PFOS production, and the B0 site on the first day of production, had PFOS concentration levels below this adjusted LOQ.

7.3.2 Detection of Perfluorooctanoic Acid

The calibration curve and the residue graph (used to determine the LOQ) for PFOS are shown in Figure 7.6. From Figure 7.6, a linear relationship between the peak area and concentration of PFOA is observed, where the R^2 value is 0.9927 (Table 7.2). PFOA had a LOQ of 50 ng L^{-1} and % recovery of 108 ± 7 (where % recovery is an average of six recovery samples).

Figure 7.6

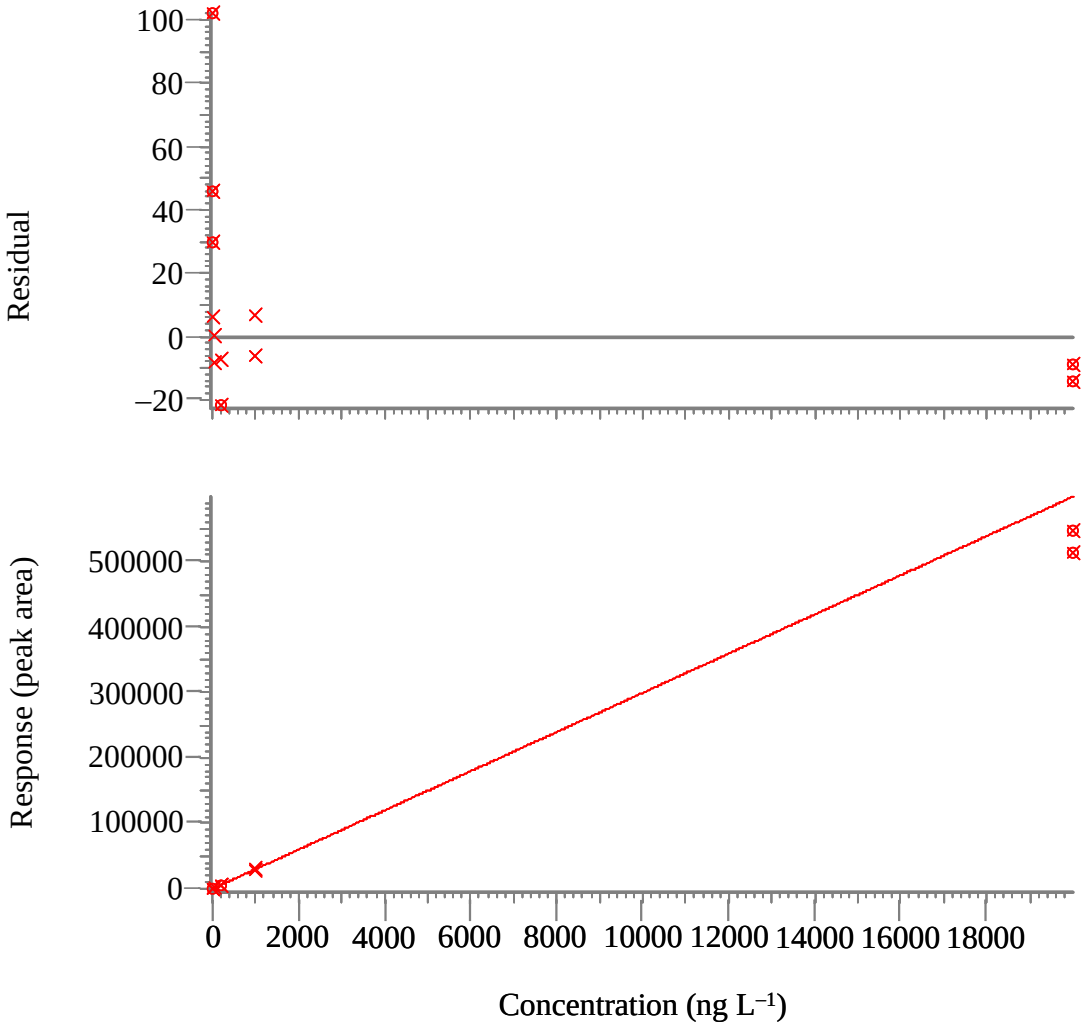

Figure 7.6: External calibration curve (bottom graph) and residue graph (top) for PFOA.

The PFOA concentration results, corrected for dilution factor, are summarized in Figure 7.7. On the day prior to production (J23), concentrations ranged from 25 – 48 μg L^{-1} in the first treatment tank (A0 – A3), 180 – 520 ng L^{-1} in the second treatment tank (B0 – B3), and 345 – 600 ng L^{-1} in the adjacent stream (G1 – G2). On the first day of PFOS production (J24), the concentrations of PFOA in the first treatment tank increased dramatically, as high as 532 μg L^{-1}, but decreased on the second (J25) and third (J26) production days to 27 – 57 μg L^{-1}. Concentrations in the second treatment tank also increased during production (in comparison to J23), but remained relatively constant over all three production days at 1.4 – 5.0 μg L^{-1}. The PFOA concentrations in the first treatment tank (A0 – A3) were consistently an order of magnitude higher than in the second treatment tank (B0 – B3) over all three production days. Finally, in the adjacent stream into which the effluent was discharged (G1 – G2), PFOA concentration levels remained relatively constant at 1.6 – 2.8 μg L^{-1} over all three production days. The PFOA concentration levels in the stream were 2- to 5-fold higher during production (J24 – J26) than prior to production (J23, 345 – 600 ng L^{-1}) in of PFOS. All concentration levels, once corrected for dilution, were significantly larger than the LOQ, which was 50 ng L^{-1}. An adjusted LOQ for PFOA was determined by multiplying the LOQ by a factor of 100. All sites had PFOA concentration levels below this adjusted LOQ, with the exception of sites A0 – A3.

Figure 7.7: Concentration (ng L^{-1}) of PFOA in two waste water treatment tanks (sites A0 – A3 and B0 – B3), as well as in an adjacent stream into which the waste water was discharged (sites G1 – G2). Samples were collected one day prior to production (J23■) and three subsequent days during production of PFOA (J24■ – J25■ – J26■).

Figure 7.7

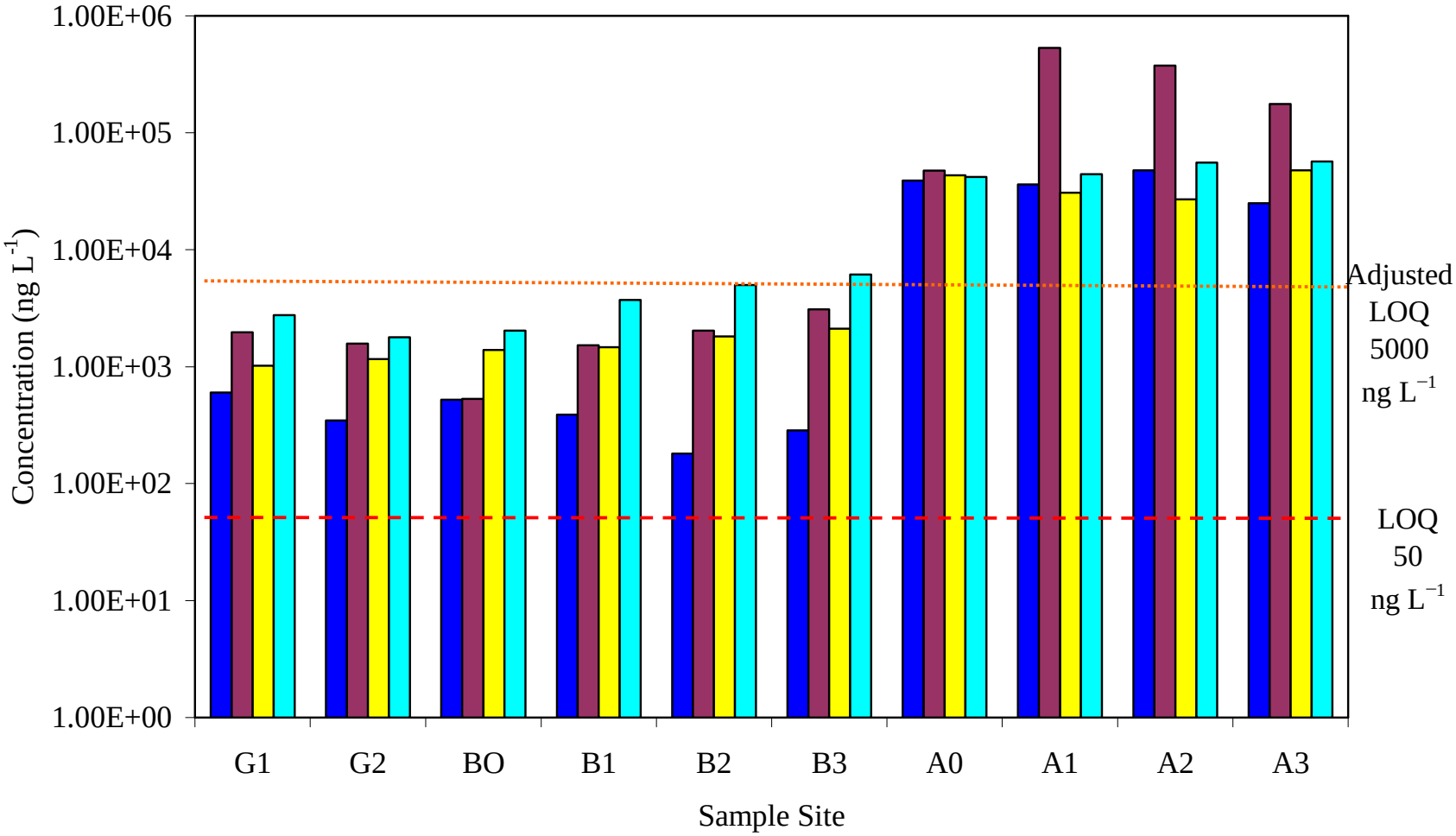
1.00E+06
1.00E+05
1.00E+04
1.00E+03
1.00E+02
1.00E+01
1.00E+00
Concentration (ng L-1)
G1
G2
BO
B1
B2
B3
A0
A1
A2
A3
Sample Site
Adjusted LOQ 5000 ng L−1
LOQ 50 ng L−1

7.3.3 Detection of Perfluorobutyric Acid

The calibration curve and the residue graph (used to determine the LOQ) for PFBA are shown in Figure 7.8. From Figure 7.8, a linear relationship between the peak area and concentration of PFOS is observed, where the R^2 value is 0.9994 (Table 7.2). PFBA had a LOQ of 50 ng L^{-1} and % recovery of 122 ± 4 (where % recovery is an average of six recovery samples).

The results for PFBA are not shown here. Generally, the PFBA concentrations in the waste water extracts were similar to those found in the blanks (5.3 – 13.4 μg L^{-1}). It was therefore concluded that PFBA is a contaminant in the current procedure. Further studies will be necessary to identify and eliminate the source of this contamination or, if not possible, to provide statistically reliable quantitation of PFBA in the blank.

Figure 7.8

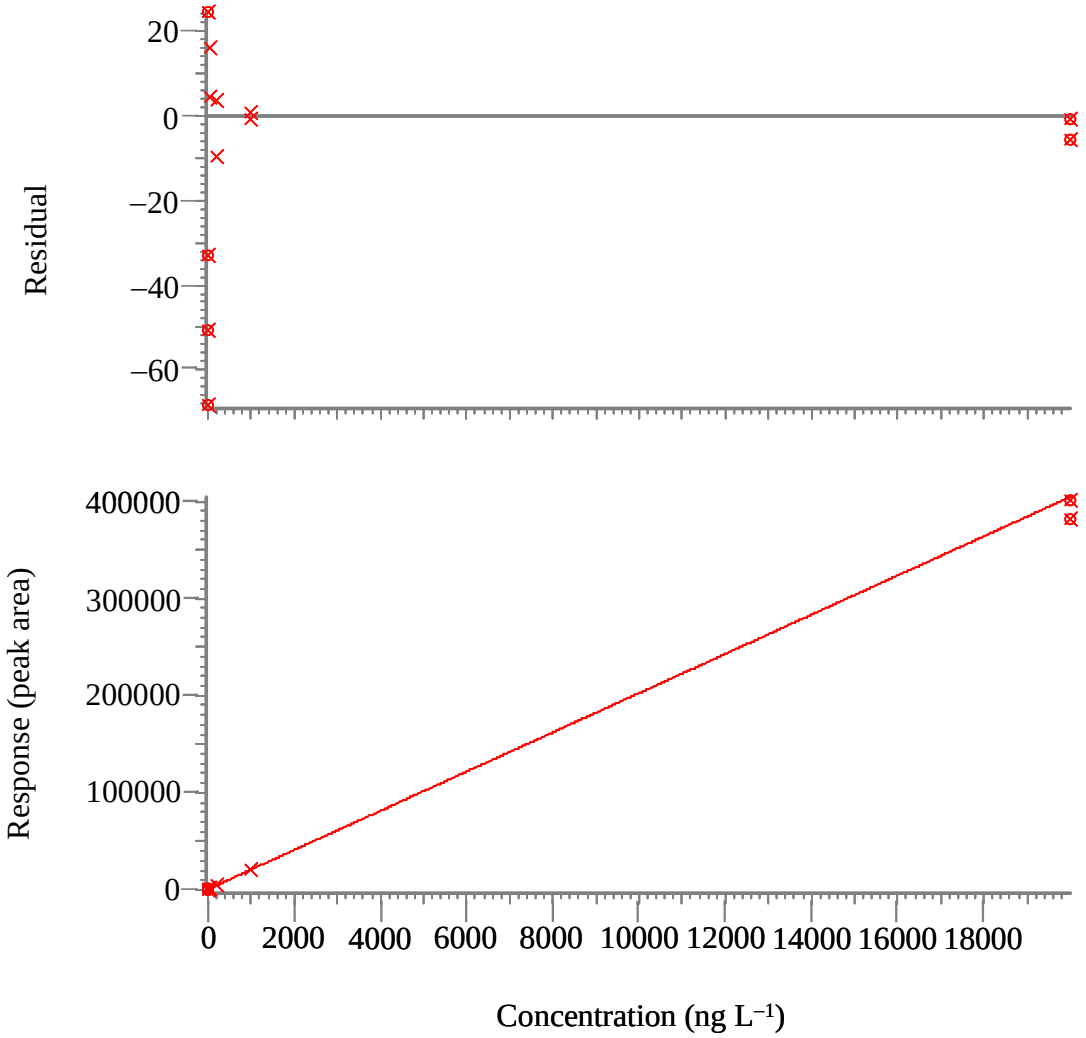

Figure 7.8: External calibration curve (bottom graph) and residue graph (top) for PFBA.

7.4 Summary

During this study, a specially modified LC-MS/MS system was used to detect and quantify the concentrations of known PFCs in water samples, which were sampled from two treatment tanks of a perfluorinated surfactant manufacturer and an adjacent stream into which the waste water was discharged into. Concentrations for most of the known PFCs were consistently below the LOQ in the diluted extraction samples, with the exception of PFOS, PFOA, and PFBA. Concentrations of PFOS and PFOA were generally higher during the days of perfluorinated surfactant production than the day prior to production. In the adjacent stream, PFOS and PFOA concentrations were also higher during the days of perfluorinated surfactant production than the day prior to production. However, the PFOS and PFOA concentrations in the stream were either less than or equal to the concentrations in the second treatment tank.

Concentrations of PFBA in the water samples were detected at the same levels as in the blank samples. This suggests that PFBA is currently a contaminant. As the use of PFBA in industry increases, further work in identifying and eliminating PFBA contamination in blank samples needs to be pursued, so that PBFA concentrations can be reliably quantified in water samples. This technique is robust, reliable, and fast (with a sample run time of 20 minutes). As more PFC standards are made available, this technique will allow for the reliable quantation of PFCs in water samples, which can have great impact on issues in regulating perfluorinated surfactants.

REFERENCES

7.5 References

[1] B.D. Key, R.D. Howell, C.S. Criddle; Environ. Sci. Technol. 31 (1997) 2445-2454.

[2] R.E. Banks, B.E. Smart, J.C. Tatlow; Organofluorine Chemistry: Principles and Commercial Applications; Plenum Press: New York, NY, 1994.

[3] J.P. Giesy, K. Kannan; Environ. Sci. Technol. 36 (2002) 146A-152A.

[4] E. Kissa, Fluorinated Surfactants: Synthesis, Properties, and Applications, Marcel Dekker, New York, NY, 1994.

[5] R.E. Banks, B.E. Smart, J.C. Tatlow, Organofluorine Chemistry: Principles and Commercial Applications, Plenum Press, New York, NY, 1994.

[6] R. Renner, Environ. Sci. Technol. 42 (2008) 648-650.

[7] J.R. Parsons, M. Saez, J. Dolfing, P. deVoogt, Environ Contamination Toxicology 196 (2008) 53-71.

[8] R. Renner, Environ. Sci. Technol. 40 (2006) 4.

[9] M.H. Russell, W.R. Berti, B. Szostek, R.C. Buck, Environ. Sci. Technol. 42 (2008) 800-807.

[10] E. Pramauro, E. Pelizzetti, Comprehensive Analytical Chemistry: Surfactants in Analytical Chemistry – Applications of Organized Amphiphilic Media, vol. 31, ed. by S.G. Weber, Elsevier Science B.V., Amsterdam, The Netherlands, 1996.

[11] M.K. So, N. Yamashita, S. Taniyasu, Q. Jiang, J.P. Giesy, K. Chen, T.K.S. Lam, Environ. Sci. Technol. 40, (2006) 2924-2929.

[12] N. Yamashita, K. Kannan, S. Taniyasu, Y. Horii, T. Okazawa, G. Petrick, T. Gamo, Environ. Sci. Technol. 38 (2004) 5522-5528.

CHAPTER 8: CONCLUSIONS AND FUTURE DIRECTIONS

Although perfluorinated surfactants (PFSs) have been utilized since the 1950s, it is only over the past decade that the number of peer-reviewed publications related to them has dramatically increased. However, the majority of this literature remains focused on either detection in the environment, toxicological effects in biota, or the sources/fates in the environment. While several studies have investigated the solubilization of organic pollutants by PFSs, virtually no investigations have been made into the transport effects of PFSs on co-contaminants in the environment. Through understanding of these transport effects, information can be gained about how the PFSs interact with various organic pollutants in the environment. This information can be utilized in models of risk assessment (e.g. contamination at spill sites) or as a basis for remediation techniques.

The research performed in this dissertation has sought to provide information to fill in this gap in knowledge. Based upon the experimental methods utilized, information pertaining to the transport effects of PFSs on organic pollutants in a model groundwater system was obtained through the use of reversed-phase liquid chromatography.

8.1 Experimental Methods

Chapter 2 details the experimental methods used to study the transport effects of PFSs on organic pollutants in a flow-through groundwater system, as well as identify various properties of the surfactants (i.e. critical micelle concentration and aggregation number). Reversed-phase liquid chromatography (RPLC) is utilized as a model for a flow-through groundwater system, with the resultant retention factors used to elucidate transport effects.

The main limitation of using RPLC to model a groundwater system is that several properties of traditional RPLC stationary phases do not resemble those of various soils. These differences in properties (i.e. carbon content and surface area) can lead to retention values (e.g. retention factors and equilibrium constants) and transport effects unrepresentative of a groundwater system. To overcome this limitation, a stationary phase with properties that more closely resembled those of soil was chosen. The pellicular stationary phase used in this research had a lower carbon content and surface area (0.39 %, 6.0 m^2 g^{-1}, respectively), than traditional octadecylsilica stationary phases used in RPLC (12 – 18 %, 200 – 400 m^2 g^{-1}, respectively), which fell within the typical range (0.11 – 6.09 %, 1.07 – 54.0 m^2 g^{-1}, respectively) for various matrices (e.g. soils, sediments, and suspended solids). The lower carbon content of the pellicular stationary phase allows for the elution of hydrophobic solutes (i.e. polycyclic aromatic hydrocarbons) in aqueous mobile phases, which are traditionally highly retained in RPLC systems, thus providing a more complete elucidation of transport effects. The lower carbon content also results in shorter retention times, allowing for a faster overall RPLC experimental procedure.

Another contributing factor to the transport effects of PFSs on organic pollutants is the critical micelle concentration (CMC) of each surfactant. As new PFSs are developed, an understanding of their CMC is necessary. As demonstrated in Chapter 2, a conductivity method based on the use of capillary electrophoresis (CE) identified an experimental CMC for sodium dodecyl sulfate (SDS) within 4.0 % error of the reported literature value. Alternatively, when this method was applied to the perfluorinated surfactant, lithium perfluorooctane sulfonate (LiPFOS), a CMC could not be determined.

However, the results did suggest the possible formation of dimers or trimers prior to the formation of micelles, at concentrations below the CMC. The possible formation of dimers or trimers is also supported by the system peak results in Chapter 6. The use of system peaks is an indirect method that uses retention factors of system peaks to elucidate surfactant interaction within the system. In addition, differences in surfactant isotherms are observed indirectly through differences in the chromatographic profile of the surfactants. The interaction of dimers or trimers with the stationary phase (or soil) can change the surface chemistry, thus changing the transport of organic pollutants within a groundwater system.

Experiments in Chapters 2 and 6 sought to provide information on the transport of the surfactants in the experimental system (i.e. a model groundwater system). A series of experiments beyond those presented within Chapters 2 and 6 is needed to further describe the interactions of PFSs within a model groundwater system. One experiment should evaluate the direct adsorption of different PFSs to various stationary phases over a range of surfactant concentrations. For this experiment, the batch equilibration method could be utilized to determine the mass of surfactant adsorbed per unit mass of stationary phase. The main limitations using this method would be the need for large quantities of stationary phase packing material and the long equilibration times.

A second experiment should evaluate the direct transport of PFSs in the model groundwater system, using RPLC with mass spectrometry detection. The retention factors determined from the injection of aqueous PFS solutions in a pure water mobile phase would give information on the direct transport of PFSs within the experimental system. Limitations of this type of study might be long retention times of the surfactants

(leading to long experimental analysis) and the need for stationary phases that closely resemble soil.

8.2 Transport Effects on Neutral Organic Pollutants

Chapters 3 and 4 detail the transport effects of model surfactants (e.g. SDS and LiPFOS) on a series of neutral substituted benzene compounds and polycyclic aromatic hydrocarbons (PAHs), using aqueous surfactant mobile phases both above and below their CMC. In both Chapters 3 and 4, the elution order exhibited by the model pollutants implies that their transport is dominated by the partition mechanism; with the addition of a surfactant acting to either enhance or deter overall transport.

As shown in Chapter 3, increasing the concentration of PFSs above the CMC increased the overall transport of a neutral organic pollutant in a groundwater system. However, pollutant transport decreased as the number, size, and polarizability of halogen substituents increased. In terms of PAHs, transport decreased as the ring number increased. Non-polar organic pollutants displayed greater interaction with hydrocarbon surfactants (HCSs) than PFSs, resulting in diminished transport effects for PFSs when compared to HCSs. The inclusion of fluorine as a substituent caused the model pollutant to have a greater affinity for PFSs than HCSs.

As shown in Chapter 4, the addition of a surfactant, below its CMC, will have a differing and noteworthy contribution to the transport effects of organic pollutants. Increasing the concentration of PFSs below the CMC increased the overall transport of neutral organic pollutants in a groundwater system. However, pollutant transport decreased with increasing concentrations of HCSs below the CMC. As surfactants are added to a system devoid of surfactants, the surfactant monomers adsorb to the stationary

phase (or soil). The adsorption of HCS monomers caused the stationary phase to become more hydrophobic. This hydrophobic environment leads to decreased transport of non-polar neutral organic pollutants, due to interaction between the pollutant and the HCS monomers adsorbed onto the stationary phase. However, the adsorption of PFS monomers caused the stationary phase to become both more hydrophobic and lipophobic. This environment leads to increased transport of non-polar neutral organic pollutants, due to less interaction between the pollutant and PFS monomers adsorbed onto the stationary phase. However, fluorinated pollutants experience decreased transport due to greater interactions with adsorbed PFS monomers on the stationary phase.

A series of experiments in addition to those presented in Chapters 3 – 4 is needed to completely identify the transport effects of PFSs on neutral organic pollutants. These experiments should evaluate the transport effects caused by varying different aspects (e.g. head group) of the perfluorinated surfactant utilized in RPLC. By systematically varying the perfluorinated surfactant utilized, and observing the retention values, a more complete understanding of the transport effects of PFSs on neutral organic pollutants in a groundwater system can be obtained, both above and below the CMC.

8.3 Transport Effects on Ionic Organic Pollutants

Chapter 5 details the transport effects of model anionic surfactants (i.e. SDS and LiPFOS), below their CMC, on a series of cationic aromatic amines. The overall elution order exhibited by the amines implies that their transport can be explained via a partition mechanism. However, the addition of the surfactants introduces transport effects due to ion-pairing and ion interaction mechanisms. In accordance with ion-pairing chromatography, the transport of the cationic pollutants greatly decreased as the

concentration of the anionic surfactant increased. As the concentration of surfactant in the mobile phase increased, there was a corresponding increase in the amount of surfactant monomers adsorbed on the stationary phase. The cationic amines interacted with the adsorbed surfactant monomers, were highly retained on the stationary phase, and exhibited decreased transport.

A series of experiments beyond those presented in Chapter 5 is needed to expand upon the transport effects of perfluorinated surfactants on cationic pollutants in a groundwater system. The first experiment should evaluate the transport effects caused by varying the head group of the perfluorinated surfactants. Sulfonates ($-SO_3^-$) and carboxylates ($-COO^-$) are the head groups of the most commonly utilized PFSs. The head groups of lesser utilized PFSs include sulfates ($-OSO_3^-$), phosphates ($-OP(OR)_2O^-$), and sulfonamides ($-SO_2NR^-$). While fluorinated telomer alcohols ($-OH$) are precursors to PFSs, their inclusion in an RPLC study would be impractical due to their high volatility. The PFS utilized in this research contained a sulfonate head group. For a more complete understanding of transport effects, a RPLC study using a PFS with a carboxylate head group should be conducted and compared to the results presented here.

A second experiment should evaluate what changes in mobile phase composition will have on the transport effects of anionic perfluorinated surfactants on cationic pollutants. As stated in Section 5.3.2, since the cationic aromatic amines were highly retained in aqueous surfactant mobile phases, an organic co-solvent (i.e. methanol) was added to the mobile phases in order to facilitate elution of the amines. It has been reported in literature [1,2], that the pK_a of substituted anilines vary depending on the

solvent. A study that determines the pK_a of the substituted anilines in various methanol/water solutions would provide information regarding the protonation state of the amines, and would contribute greatly to an understanding of the interactions between the cationic amines and adsorbed surfactant monomers utilized in this research.

8.4 Future Directions

Based on the research presented in this dissertation, there still remain several noteworthy areas of investigation. The following sections (Sections 8.4.1 – 8.4.3) give a brief overview of those areas of study.

8.4.1 Transport Effects of Short-Chain Perfluorinated Surfactants

Due to their thermal and chemical stability, long-chain PFSs tend to be more resistant to environmental degradation, and thus tend to bioaccumulate. As such, the development [3] and use of short-chain PFSs (i.e. carbon chain lengths less than 6) have been on the rise, as they are believed to undergo environmental degradation more readily.

A series of experiments could be performed to evaluate the transport effects on organic pollutants caused by varying the chain length of the surfactant utilized in RPLC. As stated previously, the model perfluorinated surfactant used in this research was a long-chain surfactant, consisting of eight carbons. A series of aqueous PFSs mobile phases, both above and below the CMC, could be used to elucidate what effect varying the chain length between $C_4 – C_6$ would have on pollutant transport in a groundwater system. As the chain length decreases, the solubility in water will increase, thus having a direct impact on transport of organic pollutants. As the chain length decreases, the CMC of the surfactant increases, thus the transport effects below the CMC become more important. In addition, a shorter chain surfactant monomer will have less interaction with the

stationary phase (e.g. soil). This decreased interaction will lead to less adsorbed surfactants, and increased transport effects on cationic pollutants (in comparison to a longer chain surfactant).

8.4.2 Transport Effects of Mixed Surfactant Solutions

In some applications the use of a single surfactant is unsuitable, and there is a need for a binary mixture of surfactants. The binary mixture can accomplish applications that neither surfactant can perform alone. The binary mixture can enter the environment in a similar fashion as the individual surfactants, and thus contribute to the overall transport of environmental co-contaminants. A secondary means of developing a binary mixture is through the mixing of separate surfactants, released into the environment as waste. It therefore stands to reason that binary mixtures of surfactants already exist within the environment to varying degrees. Thus the effects of a binary mixture of surfactants on the environmental transport of persistent organic pollutants need to be investigated.

In a review by Noriaki Funasaki, the topic of whether hydrocarbon and fluorocarbon surfactants mix either completely or partially is discussed [4]. Due to the differences in chemical and physical properties of hydrocarbon and fluorocarbon surfactants, the mixing of HCSs with PFSs is believed to be nonideal. In a study conducted by Barthélémy et al., ^{19}F-NMR and UV-visible absorbance spectroscopy were utilized to determine the miscibility of surfactant mixtures as a function of total surfactant concentration over a range of hydrocarbon-fluorocarbon ratios [5]. Both the ^{19}F-NMR and UV-visible absorbance results identified three distinct regions. The first region takes place below the CMC of both surfactants. It consists of the surfactants existing as

monomers. The latter two regions are defined by the differences in the CMC values of the surfactants. The second region takes place above the CMC of one surfactant (i.e. PFS) but below that of the other (i.e. HCS). It consists of micelles enriched by the lower CMC surfactant and monomers of both surfactants. The third region takes place above the CMC of both surfactants. It consists of two types of micelles (one enriched by PFS and the other by HCS) and monomers of both surfactants. Since the micelle is a dynamic system, and monomers move between it and the bulk solution, a micelle can contain monomers of both surfactants. It has also been suggested that a single mixed micelle can form when the CMCs of the pure surfactants are within a factor of 3 of each other [6]. However, if the surfactants are completely immiscible (i.e. no mixing of the surfactant monomers in the micelle), then the micelle will only contain monomers of an individual surfactant. The formation of these various regions may have little or no effect on transport or may lead to synergistic transport effects on co-pollutants [6]. The synergistic effect on the solubilization of PAHs by mixed micellar surfactant solutions (i.e. anionic hydrocarbon/nonionic hydrocarbon) has been reported in the literature [7].

A series of experiments could be performed to evaluate the transport effects of a mixed surfactant solution on organic pollutants. The transport effects could be elucidated based on changes in pollutant retention factors, as a function of total surfactant concentration over a range of perfluorinated/hydrocarbon surfactant ratios. The use of RPLC, in conjunction with data from either ^{19}F-NMR or UV-visible absorbance studies, would provide this information. Several aqueous mobile phases, consisting of a common type of binary surfactant mixture (i.e. anionic perfluorinated/anionic hydrocarbon or anionic perfluorinated/nonionic hydrocarbon), should be tested. By identifying the extent

to which binary mixtures effect the transport of organic pollutants, parameters can be developed to increase the ability of environmental modeling systems to better model sites where mixed surfactant contamination is a high possibility. Alternatively, the information could be used in groundwater remediation techniques, in order to tailor a pumping solution to effectively remove particular organic pollutants.

8.4.3 Transport Effects of a Perfluorinated Stationary Phase

In the environment, hydrocarbon surfactants can adsorb onto the surface of soil, presenting a new surface to organic pollutants that has different chemical and physical properties compared to the native soil. This phenomenon would also apply to fluorocarbon surfactants (i.e. PFSs) as well. In RPLC, fluorocarbon surfactant monomers will adsorb onto the stationary phase, thus forming a new stationary phase.

In order to gain a greater understanding of transport effects that adsorbed fluorocarbon surfactants have on organic pollutants, a series of experiments need to be performed. The first experiment should evaluate the retention of model neutral organic pollutants in a RPLC system utilizing various commercially available fluorinated stationary phases, with pure water as the mobile phase. Commercially available fluorinated stationary phases have been previously used in literature [8-11], as well as in various liquid chromatography applications [12]. The most common types of fluorinated stationary phases either consist of a partially fluorinated alkyl chain, a chain ending with a perfluorophenyl group, or a perfluorinated linear alkyl chain. The perfluorinated linear alkyl phase could be used as the stationary phase in a RPLC system, and the retention values can be compared to the results presented in Chapters 3 – 5. The perfluorinated linear alkyl stationary phase has a C_6 chain length with the particles being 5.0 µm in

diameter, having a 300 Å pore size, 5.0 % carbon content, and 100 $m^2 g^{-1}$ surface area. This would more closely resemble soil with a complete surface coverage of perfluorinated surfactant monomers. In addition, the properties of this stationary phase are comparable to the stationary phase used to perform the research in this dissertation (Section 8.1), thus allowing for a direct comparison of transport effects.

A second experiment could evaluate the retention of model organic pollutants in a RPLC system with a perfluorinated stationary phase, while utilizing aqueous surfactant solutions as the mobile phase. Aqueous HCS and PFS solutions similar to those utilized in Chapters 3 – 5 could be used for this type of study. This study would provide information into the interactions of the pollutants between the surfactant mobile phase and the perfluorinated stationary phase. This type of experiment would most likely provide the closes approximation of the transport effects experienced by organic pollutants in a groundwater system containing perfluorinated surfactants or a mixture of perfluorinated and hydrocarbon surfactants.

REFERENCES

8.5 References

[1] T.V Kashik, B.V. Prokop'ev, G.V. Rassolova, S.M. Ponomareva, Russ. Chem. B+ 20 (1971) 1847-1850.

[2] H.C. Brown, D.H. McDaniel, O. Häfliger, Ed. By E.A. Braude, F.C. Nachod, Determination of Organic Structures by Physical Methods, Academic Press, New York, 1955.

[3] M. Terrazas, R. Dams, Speciality Chemicals Magazine 24 (2004) 19-21.

[4] N. Funasaki, Surf. Sci. Series 46 (1992) 145-188.

[5] P. Barthélémy, V. Tomao, J. Selb, Y. Chaudier, B. Pucci, Langmuir 18 (2002) 2557-2563.

[6] T.J. Connolly, V.C. Reinsborough, X. Xiang, Aust. J. Chem. 45 (1992) 769-775.

[7] L. Zhu, S. Feng, Chemosphere 53 (2003) 459-467.

[8] P. Varughese, M.E. Gangoda, R.K. Gilpin, J. Chromat. Sci. 26 (1988) 401-405.

[9] H.Y. Aboul-Enein, V. Serignese, Anal. Chim. Acta 319 (1996) 187-190.

[10] I. De Miguel, A. Roueche, D. Betbeder, J. Chromatogr. A 840 (1999) 31-38.

[11] K. Jinno, H. Nakamura, Chromatographia 39 (1994) 285-293.

[12] W. Zhang, J. Fluorine Chem. 129 (2008) 910-919.